

Spring 1990

# Nonproportionally Loaded Steel Beam-Columns and Flexibly-Connected Nonsway Frames

Siva Prasad Darbhamulla  
*Old Dominion University*

Follow this and additional works at: [https://digitalcommons.odu.edu/cee\\_etds](https://digitalcommons.odu.edu/cee_etds)

 Part of the [Applied Mechanics Commons](#), and the [Civil Engineering Commons](#)

---

## Recommended Citation

Darbhamulla, Siva P. "Nonproportionally Loaded Steel Beam-Columns and Flexibly-Connected Nonsway Frames" (1990). Doctor of Philosophy (PhD), dissertation, Civil/Environmental Engineering, Old Dominion University, DOI: 10.25777/w8yp-0b85  
[https://digitalcommons.odu.edu/cee\\_etds/92](https://digitalcommons.odu.edu/cee_etds/92)

This Dissertation is brought to you for free and open access by the Civil & Environmental Engineering at ODU Digital Commons. It has been accepted for inclusion in Civil & Environmental Engineering Theses & Dissertations by an authorized administrator of ODU Digital Commons. For more information, please contact [digitalcommons@odu.edu](mailto:digitalcommons@odu.edu).

**NONPROPORTIONALLY LOADED STEEL BEAM-COLUMNS  
AND FLEXIBLY-CONNECTED NONSWAY FRAMES**

By

Siva Prasad Darbhamulla

B. E., May 1977, Andhra University, Visakhapatnam, India  
M. Tech., August 1979, Indian Institute of Technology, Kanpur, India

A Dissertation Submitted to the Faculty of  
Old Dominion University in Partial Fulfillment  
of the Requirements for the Degree of

DOCTOR OF PHILOSOPHY

CIVIL ENGINEERING

OLD DOMINION UNIVERSITY

May 1990

Approved by

\_\_\_\_\_  
Dr. Zia Razzaq, Chairman

\_\_\_\_\_  
Dr. J. Mark Dorrepaal

\_\_\_\_\_  
Dr. Duc T. Nguyen

\_\_\_\_\_  
Dr. R. Prabhakaran

# NONPROPORTIONALLY LOADED STEEL BEAM-COLUMNS AND FLEXIBLY-CONNECTED NONSWAY FRAMES

Siva Prasad Darbhamulla  
Old Dominion University  
Advisor: Dr. Zia Razzaq

## Abstract

A theoretical study of the inelastic stability of nonproportionally loaded steel beam-columns and flexibly-connected frames is conducted. Specifically, solution techniques are formulated to predict the nonlinear behavior of cross sections, spatial beam-columns, and nonsway plane frames under the combined influence of imperfections, flexible connections, and nonproportional loads. A set of new inelastic slope-deflection equations for imperfect members are derived and their use illustrated through in-depth studies of flexibly-connected portal and two-bay two-story frames. These equations are derived from a system of nonlinear ordinary differential equations. The member studies are carried out using a second-order finite-difference solution to a set of nonlinear equilibrium equations, and coupled to a tangent stiffness procedure for cross sections. The majority of the theoretical studies are carried out on a conventional sequential computer. Efficient concurrent computational algorithms are also presented for biaxial bending and column stability problems. Results are obtained using a multiprocessor computer known as the *Finite*

*Element Machine.* A critical appraisal of the conventional tangent modulus approach is presented in light of the analysis which includes elastic unloading of the material. It is found that the tangent modulus approach results in a fictitious ductile behavior. Furthermore, it is also realized that there is a dramatic difference in the nonlinear behavior between the proportionally and nonproportionally loaded structures. It is also observed that the proportionally loaded structures lead to rather unconservative peak loads. Additionally, members as integral parts of a frame may exhibit significantly different load-deformation behavior as compared to that of isolated members. The study on members and frames shows that nonproportional loads have a significant effect on their behavior and strength.

**This research is dedicated to  
my parents Jayalaxmi and Rama Linga Sastry**

## **Acknowledgement**

The author wishes to thank Dr. Zia Razzaq for the technical and moral support throughout this research. The appreciation is also extended to Dr. J. Mark Dorrepaal, Dr. Duc T. Nguyen, Dr. R. Prabhakaran, and Dr. Leon R. L. Wang for their participation and advise at various stages of this endeavor. Special thanks are due to my wife, Jan, for providing moral support and transforming the manuscript into this report. Appreciation is also extended to Ms. Sue C. Smith and Ms. Mary G. Carmone for their help with the preparation of this report.

The support from the faculty and my colleague graduate students of Civil Engineering Department is also recognized. The help form the Computer center of Old Dominion University is acknowledged.

## TABLE OF CONTENTS

<b>List of Tables</b>		vii
<b>List of Figures</b>		ix
<b>Nomenclature</b>		xiii
<b>1.0 INTRODUCTION</b>		
1.1 Introduction		1
1.2 Literature Review		2
1.3 Definition of Problems		4
1.4 Objectives and Scope		5
1.5 Assumptions and Conditions		6
<b>2.0 CROSS-SECTIONAL ANALYSIS</b>		
2.1 Equilibrium Equations		7
2.2 Concurrent Processing for Cross-Sectional Analysis		10
2.3 Nonproportionally Loaded Sections		12
<b>3.0 BIAXIALLY IMPERFECT COLUMNS</b>		
3.1 Theoretical Formulation		14
3.2 Concurrent Computing Solution		18
3.3 Numerical Study		19
<b>4.0 IMPERFECT BEAM-COLUMNS</b>		
4.1 Theoretical Formulation		22
4.1.1 Equilibrium Equations		22
4.1.2 End Restraint Conditions		24
4.2 Load Paths		25
4.2.1 Uniaxially Loaded Beam-Columns		25
4.2.2 Biaxially Loaded Beam-Columns		26
4.3 Solution Procedure		27

4.4	Numerical Study	29
4.4.1	Modeling of End Restraints	29
4.4.2	Behavior of Uniaxially Loaded I-Section Beam-Columns	32
4.4.3	Behavior of Biaxially Loaded I-Section Beam-Columns	34
4.4.4	Behavior of Biaxially Loaded Rectangular Tubular Beam-Columns	35
4.4.5	Critique on Tangent Modulus Approach	37
<b>5.0</b>	<b>FLEXIBLY-CONNECTED PLANE NONSWAY FRAMES</b>	
5.1	Theoretical Formulation	39
5.1.1	Inelastic Slope-Deflection Equations for Imperfect Beam-Column	39
5.1.2	Equilibrium and Compatibility for Flexible Connections	43
5.1.3	Analysis of Flexibly-Connected Imperfect Frames	45
	5.1.3.1 Portal Frame	45
	5.1.3.2 Two-Bay Two-Story Frame	47
5.2	Load Paths and Combinations	48
	5.2.1 Load Paths	48
	5.2.2 Load Combinations	49
5.3	Solution Procedure	49
5.4	Numerical Study	51
	5.4.1 Equivalent Structural Model	52
	5.4.2 Portal Frame Behavior	53
	5.4.3 Two-Bay Two-Story Frame Behavior	57
<b>6.0</b>	<b>CONCLUSIONS AND FUTURE RESEARCH</b>	
6.1	Conclusions	61
	6.1.1 Concurrent Computing	62
	6.1.2 Beam-Columns	63
	6.1.3 Frame Studies	65
6.2	Future Research	68
	<b>References</b>	69
	<b>Tables</b>	74
	<b>Figures</b>	92



<b>Appendix A Tangent Stiffness Method</b>	153
<b>Appendix B Finite Element Machine</b>	157
<b>Appendix C Inelastic Load and Moment Parameters</b>	161
<b>Appendix D External and Plastic Load Vectors</b>	162
<b>Appendix E Computer Program NONPRFRM</b>	164

## LIST OF TABLES

<u>TABLE</u>	<u>PAGE</u>
1. Concurrent processing efficiencies for hollow square section with $\gamma = 1.000$	74
2. Computational time on concurrent processors	75
3. Concurrent processing efficiencies for hollow square section with $\gamma = \gamma_{1s}$ to $\gamma_{8s}$	76
4. Concurrent processing efficiencies for hollow rectangular section with $\gamma = \gamma_{1r}$ to $\gamma_{8r}$	76
5. Peak loads of hollow square and rectangular columns	77
6. Execution times on concurrent processors for columns CN1 and CN5	78
7. Computational speedup factors and efficiencies for hollow square columns	79
8. Computational speedup factors and efficiencies for hollow rectangular columns	80
9. Summary of beam-column strength for various connection models	81
10. Maximum beam-column loads for various load paths and elastic restraints	82
11. Maximum beam-column loads for various load paths and elastic-plastic restraints ( $k_{a2}$ ; $m_{plastic} = 100$ in-kips)	82
12. Maximum external loads for uniaxially loaded imperfect beam-columns with partial rotational equal end restraints and various load paths (W8x31)	83

13. Comparison of predicted and previously published maximum loads for pinned-end beam-columns with biaxially eccentric load	84
14. Maximum external loads for biaxially loaded imperfect beam-columns with partial rotational equal end restraints and various load paths (L=12ft.; W8X31)	84
15. Maximum external nonproportional biaxial loads for partially restrained imperfect beam-column BC2 with hollow square section ( $k=k_{a2}$ )	85
16. Maximum external nonproportional biaxial loads for partially restrained imperfect beam-column BC3 with hollow square section ( $k=k_{a3}$ )	85
17. Maximum external nonproportional biaxial loads for partially restrained imperfect beam-column BC4 with hollow rectangular section ( $k=k_{a2}$ )	86
18. Maximum external nonproportional biaxial loads for partially restrained imperfect beam-column BC5 with hollow rectangular section ( $k=k_{a3}$ )	87
19. Equivalent structural model analysis results	88
20. Portal frame analysis results for FR1 through FR4 with FL1 through FL4	89
21. Portal frame analysis results for FR1, FR2, FR5, and FR6 with FL1 through FL4	90
22. Two-bay two-story frame analysis results for FR7 and FR8 with FL5 through FL6	91

## LIST OF FIGURES

<b><u>FIGURE</u></b>	<b><u>PAGE</u></b>
1. Discretized hollow rectangular and I-shaped sections subjected to axial load and biaxial bending moments	92
2. Typical residual stress patterns of cross sections	93
3. Material stress-strain relationships	94
4. Cross-sectional moment-curvature relationship	95
5. Yield surface	96
6. Speedup curves for moment-curvature relations for hollow square section	97
7. Moment-curvature relationships about x axis for hollow square section	98
8. Moment-curvature relationships about y axis for hollow square section	99
9. Yield surface contours for hollow square section	100
10. Moment-curvature relationships about x axis for hollow rectangular section	101
11. Moment-curvature relationships about y axis for hollow rectangular section	102
12. Yield surface contours for hollow rectangular section	103
13. Speedup curves for generation of yield surface for hollow square section	104
14. Speedup curves for generation of yield surface for hollow rectangular section	105

15. Various load paths for nonproportional loading	106
16. $\bar{m}_x$ - $\bar{\phi}_x$ relationship for a nonproportionally loaded I-section	107
17. $\bar{m}_y$ - $\bar{\phi}_y$ relationship for a nonproportionally loaded I-section	107
18. $p$ - $\bar{\epsilon}_0$ relationship for a nonproportionally loaded I-section	108
19. Imperfect column with biaxial partial restraints	109
20. Flowchart of the concurrent processing	110
21. Load versus midspan deflection for columns CN2 and CN6	111
22. Speedup factor versus number of processors relationship	112
23. Imperfect beam-column with biaxial restraints	113
24. Connection moment-rotation relationships	114
25. Linear and bilinear approximations of connection $m$ - $\theta$ curve for column analysis	115
26. Elastic-plastic and trilinear approximations of connection $m$ - $\theta$ curve for column analysis	116
27. Linear and bilinear approximations of connection $m$ - $\theta$ curve for beam-column analysis	117
28. Elastic-plastic and trilinear approximations of connection $m$ - $\theta$ curve for beam-column analysis	118
29. Interaction curves for uniaxially loaded partially restrained beam-column 4	119
30. Interaction curves for biaxially loaded partially restrained beam-column 8	120
31. Interaction curves for biaxially loaded partially restrained imperfect beam-column BC3 for load paths NP5 and NP6	121
32. Stiffness degradation curves for beam-column BC3 with load paths NP5 and NP6 and axial load $p=0.75$	122
33. Interaction curves for biaxially loaded partially restrained imperfect beam-column BC5 for load paths NP7 and NP8	123

34.	Stiffness degradation curves for beam-column BC5 with load paths NP7 and NP8 and axial load $p=0.75$	124
35.	Load versus midspan displacement relationships for BC0	125
36.	Stiffness degradation curves for BC0	126
37.	Beam-column	127
38.	Typical frame joint	128
39.	Imperfect portal frame	129
40.	Equivalent structural model for portal frame	130
41.	Flexibly-connected imperfect two-bay two-story frame	131
42.	Load-moment relationships	132
43.	Load-deflection relationships	133
44.	Stiffness degradation curves	134
45.	Axial load versus joint rotation relationship for portal frame FR2 and frame loading FL3 with NP9	135
46.	Stiffness degradation curve for portal frame FR2 and frame loading FL3 with NP9	136
47.	Axial load versus joint rotation relationship for portal frame FR2 and frame loading FL3 with NP10 and NP11	137
48.	Stiffness degradation curve for portal frame FR2 and frame loading FL3 with NP10 and NP11	138
49.	Axial load versus midspan displacement relationship for a column of the frame FR2 and loading FL3 with NP9	139
50.	Stiffness degradation curve for a column of the frame FR2 and loading FL3 with NP9	140
51.	Axial load versus midspan displacement relationship for a column of the frame FR2 and loading FL3 with NP10 and NP11	141

52.	Stiffness degradation curve for a column of the frame FR2 and loading FL3 with NP10 and NP11	142
53.	$p-\bar{m}$ interaction for frame FR2	143
54.	Axial load versus joint rotation relationship for two-bay two-story frame FR8 and frame loading FL8 with NP9	144
55.	Stiffness degradation curve for two-bay two-story frame FR8 and frame loading FL8 with NP9	145
56.	Axial load versus joint rotation relationship for two-bay two-story frame FR8 and frame loading FL8 with NP10 and NP11	146
57.	Stiffness degradation curve for two-bay two-story frame FR8 and frame loading FL8 with NP10 and NP11	147
58.	Axial load versus midspan displacement relationship for a column of the frame FR8 and loading FL8 with NP9	148
59.	Stiffness degradation curve for a column of the frame FR8 and loading FL8 with NP9	149
60.	Axial load versus midspan displacement relationship for a column of frame FR8 and loading FL8 with NP10 and NP11	150
61.	Stiffness degradation curve for a column of the frame FR8 and loading FL8 with NP10 and NP11	151
62.	$p-\bar{m}$ interaction for frame FR8	152

## NOMENCLATURE

A	Area
BC	Beam-column
C	Stability coefficient
C1, C2,...	Equivalent model designation
CN	Centrally loaded column designation
D	Dimensionless determinant, Depth of the cross section
E	Young's modulus
E1, E2, E3	Equivalent model frames
FL	Load combination for frame
FR	Frame Designation
I	Moment of inertia
L	Length
LC	Load condition for columns
M	Applied moment
N	Total nodes
NP	Nonproportional load designation
P	Applied axial load
Q	Member stiffness at a node .



## NOMENCLATURE - Cont'd

S	Stability coefficient
U	Total midspan displacement in minor axis plane
V	Total midspan displacement in major axis plane
$dA, \Delta A_i$	Elemental area
i	Processor number
j	Finite-difference node
k	Connection spring stiffness
m	Connection moment
$\bar{m}$	Dimensionless moment
p	Dimensionless axial load
$q_{ij}$	Cross-sectional inelastic properties
$s_1$	Speedup
t	Computational time
u	Displacement in minor axis plane
$u_{0i}$	Midspan amplitude of initial crookedness
v	Displacement in major axis plane
$v_{0i}$	Midspan amplitude of initial crookedness
$\gamma$	Moment ratio
$\delta P$	Incremental axial load
$\epsilon$	Normal strain
$\epsilon_0$	Axial strain

## NOMENCLATURE - Cont'd

$\epsilon_r$	Residual strain
$\bar{\epsilon}$	Dimensionless strain
$\epsilon_y$	Yield strain
$\eta$	Efficiency
$\phi$	Curvature
$\bar{\phi}$	Dimensionless Curvature
$\sigma$	Normal stress
$\sigma_{rc}, \sigma_{rt}$	Residual compressive and tensile stresses, respectively
$\sigma_y$	Yield stress
$\theta$	Rotation
$\zeta$	Proportionality constant
$\{F\}$	Load vector
$[K]$	Member global stiffness matrix
$[K_t]$	Cross-sectional tangent stiffness matrix
$\{M\}$	Moment vector
$[S]$	Inelastic slope-deflection properties matrix
$\{f\}$	Cross-sectional dimensionless load vector
$\{\alpha\}$	Tolerance vector
$[\beta]$	Coefficient matrix
$\{\Delta\}$	Member displacement vector
$\{\delta\}$	Cross-sectional dimensionless deformation vector

## NOMENCLATURE - Cont'd

$\{\theta\}$  Rotational deformations vector

## 1. INTRODUCTION

### 1.1 Introduction

Practical structural steel members and frames are imperfect, seldom possess ideal pinned or rigid joints, and may not be subjected to proportional loads. Previous studies have been devoted to an understanding of the effects of initial imperfections and flexible connections on the response of individual members subjected to proportional loads. In comparison, little research has been carried out on the influence of nonproportional loads on response of steel members and frames. The combined influence of imperfections, flexible connections, and nonproportional loading on the behavior and strength of such structures has not been studied.

Mathematically, the afore-mentioned inelastic behavior problems can be reduced to a system of materially nonlinear ordinary differential equations. Closed-form solutions to these equations are not possible since the coefficients of the governing differential equations vary with the level of external loads and also with the dependent variables, namely, the deformations. Over the past two decades, numerical solutions for specific cases of inelastic problems have been devised for implementation on sequential computers. Rigorous analysis is quite complex and time-consuming even for relatively *simple* structures. With the advent of parallel computers, efficient solutions to these problems appear to be possible. However, no such studies have been conducted by any investigators for inelastic analysis.

Parallel computing derives its name from the fact that in a parallel computer, there are a number of mini-computers or processors connected in parallel through an inter-processor communication network. The name *concurrent processing* is also used in the literature instead of *parallel computing*. Elasto-plastic problems appear to be suitable for solution on parallel computers. For example, the process of enforcing equilibrium conditions at several locations within the domain of a structure may be carried out concurrently.

The primary aim of this dissertation is to present an analysis of nonproportionally loaded practical steel members and frames. Sequential algorithms are devised for a majority of the problems, however, representative parallel algorithms are also included to explore the feasibility of using concurrent solution procedures.

## **1.2 Literature Review**

Long after the famous work of Euler (2) on column stability, Engesser (1) realized, in 1895, that metal columns of intermediate length may fail before the elastic buckling load is attained, that is by inelastic instability. Consequently, Engesser suggested the use of a reduced modulus approach for evaluating the inelastic strength of such members. The experimental results, however, were not in good agreement with this theory. In 1947, this controversy was resolved by Shanley (3) in a set of carefully controlled column experiments. Shanley suggested that the tangent modulus should be used instead of the reduced modulus and that it would result in a better prediction of the test results.

In 1961, Galambos and Ketter (11), Ketter (12), and Ketter and Prasad (13) analyzed the inelastic behavior of beam-columns with simple ends based on the tangent modulus theory. A few years later, Lu and Kamalvand (22) investigated beam-columns with fixed-ended supports. A number of other investigations were carried out (4,5,7,11-13,16,19,21,22,23,27,30,34,38-40,50,51,53-56) to understand the behavior of these members. Recently, Razzaq and Calash (51,54) presented a rigorous investigation of column behavior with partial restraints and biaxial initial crookedness. Other studies have explained partly the effects of residual stresses (4,6,12,13,38-40,51,54,56), end restraints (38,39,42,46,50,51,54,56), and initial crookedness (28,32,38,51,54,56) on member response. Some theoretical and experimental studies are carried out by Razzaq and McVinnie (45,55) on nonproportionally loaded pin-ended beam-columns with biaxial bending.

In 1957, Driscoll (8) conducted studies on the plastic behavior of frames. Galambos (10) considered the effects of the base fixity on frame behavior. Saap (14), Citipitioglu (15), McVinnie (18), Korn (20) and many other researchers (17,26,28,29,32,37,41,42,44,46,56) studied the behavior of various types of frames. Most of the frames studied were rigid-jointed. In a recent study, Aackroyd (37) adopted proportional loading and secant modulus theory to investigate Type 2 connection frames. Also, the study did not include the influence of initial crookedness of members in the frames.

The conventional sequential computers have been used for most of the past investigations. Parallel computers on the other hand, are fairly recent (33,35,36). In the early 1980s, NASA Langley Research Center developed a parallel computer

(47), called *The Finite Element Machine (FEM)*, designed specifically for numerical and finite element analysis of structures. A description of the FEM is given in Appendix B. The application of parallel computers has centered mainly around the development of algorithms for solving simultaneous linear equations such as those resulting from elastic finite element formulations (36,48).

A review of the existing literature shows that a study of structures with initial imperfections and flexible connections is needed when subjected to nonproportional loads. In addition, the validity of the tangent modulus approach needs to be evaluated critically. Also, no parallel solutions to inelastic problems have been published in the past.

The primary emphasis of this dissertation is on a rigorous study of the influence of nonproportional loads on the strength and behavior of steel beam-columns and plane frames.

### **1.3 Definition of Problems**

The main thrust of this dissertation is on a rigorous study of the influence of nonproportional loads on the inelastic response of steel beam-columns and plane frames. The influence of imperfections and flexible connections on the strength and behavior of these structures is also investigated. The analyses are based on an equilibrium approach which leads to a system of materially nonlinear ordinary differential equations with appropriate boundary conditions.

The analysis is performed using a finite-difference technique combined with an iterative solution procedure incorporating material unloading. A complete system of inelastic slope-deflection equations is also derived and used for the

nonproportionally loaded inelastic frames. The suitability of parallel computing is investigated through the inelastic analysis of cross sections and biaxially imperfect columns. The main computational work, however, is conducted on a sequential computer.

#### **1.4 Objectives and Scope**

The principal objectives of this study are to:

1. Study the effectiveness of concurrent computing for inelastic analysis of proportionally loaded cross sections.
2. Study the effect of material unloading on the response of cross sections when loaded nonproportionally.
3. Conduct concurrent analysis of biaxially imperfect and centrally loaded columns using the Finite Element Machine.
4. Identify suitable moment-rotation connection models for use in the analysis of beam-columns.
5. Investigate the behavior of beam-columns with uniaxial and biaxial nonproportional loads
6. Study flexibly-connected, imperfect, planar, nonsway frames subjected to nonproportional loads.

For member-level studies, both I-shaped and hollow rectangular sections are used. The development of inelastic slope-deflection analysis is demonstrated through detailed studies of a portal frame, and a two-bay two-story plane frame each subjected to a variety of load paths. The method presented, however, is fairly



general and can be adopted for the analysis of other types of nonsway plane frames.

### **1.5 Assumptions and Conditions**

The following basic assumptions and conditions are adopted in the analysis:

1. Displacements are small.
2. Member shortening is neglected.
3. Shear deformations are neglected.
4. No local buckling takes place.
5. Only axial and bending equilibrium conditions are considered.
6. The material stress-strain relationship is elastic-perfectly-plastic, with material elastic unloading.

## 2. CROSS-SECTIONAL ANALYSIS

A study of the effectiveness of concurrent computing for the inelastic analysis of biaxially loaded cross sections is given herein. The results are obtained utilizing Finite Element Machine. Also, the effect of nonproportional loading on the inelastic response of a cross section is investigated using a sequential computer. The analysis is based on the tangent stiffness procedure described in Reference 34.

### 2.1 Equilibrium Equations

Figure 1 shows discretized hollow rectangular, and I-shaped sections. The rectangular hollow section has a width  $B$ , a depth  $D$ , and a wall thickness  $t$ . The I-section has a flange width  $B$  and thickness  $t_f$ , an overall depth  $D$ , and a web thickness  $t_w$ . The loading consists of an axial load  $P$  applied perpendicular to the  $xy$ -plane and bending moments  $M_x$  and  $M_y$  about the  $x$  and  $y$  axes, respectively. The normal strain,  $\epsilon$ , at a point  $(x,y)$  of a cross section is expressed as:

$$\epsilon = \epsilon_0 - \phi_y x + \phi_x y + \epsilon_r \quad (1)$$

in which  $\epsilon_0$  is the average axial strain;  $\phi_x$  and  $\phi_y$  are the bending curvatures about the  $x$  and  $y$  axes, respectively; and  $\epsilon_r$  is the residual strain. The residual stress patterns used in this study are shown in Figure 2(a) and 2(b). Figures 3(a) and 3(b) show the  $\sigma$ - $\epsilon$  relations with and without material unloading, respectively. In this

figure,  $\sigma_y$  is the normal yield stress,  $E$  is the Young's modulus, and  $\epsilon_y$  is the yield strain. The stress-strain relationship is assumed to be identical in tension and compression. In the rate form:

$$\dot{\sigma} = E_t \dot{\epsilon} \quad (2)$$

in which  $E_t$  equals  $E$  if the material is elastic or if it is experiencing elastic unloading; it equals zero if the material is plastic. The axial and the biaxial moment equilibrium equations of the cross section can be written as:

$$P = - \int_{Ae} \sigma_e dA - \int_{Ap} \sigma_y dA \quad (3)$$

$$M_x = \int_{Ae} \sigma_e y dA + \int_{Ap} \sigma_y y dA \quad (4)$$

$$M_y = - \int_{Ae} \sigma_e x dA - \int_{Ap} \sigma_y x dA \quad (5)$$

in which  $dA$  is an elemental area of the cross section, and  $\sigma$  is the normal stress on that area. The subscripts  $e$  and  $p$  refer to the elastic and plastic parts, respectively, of a partially plastified section;  $\int_A$  denotes cross-sectional integration. Thus, given an axial load  $P$ , and a pair of bending moments  $M_x$  and  $M_y$ , the strain distribution is found while following Equation 2. In other words, compatible  $\epsilon_0$ ,  $\phi_x$ , and  $\phi_y$  need be obtained which satisfy equilibrium for  $P$ ,  $M_x$ , and  $M_y$ . The cross-sectional dimensionless load and deformation vectors,  $\{f\}$  and  $\{\delta\}$ , can be expressed as follows:

$$\{f\} = \{ p \quad \bar{m}_x \quad \bar{m}_y \}^T \quad (6)$$

$$\{\delta\} = \{ \bar{\epsilon}_0 \quad \bar{\phi}_x \quad \bar{\phi}_y \}^T \quad (7)$$

in which  $T$  indicates the transpose of a vector, and the other terms are defined in Appendix A. The solution procedure involves starting at a known state and incrementally converging to the next state for which only  $\{f\}$  is known. The deformation vector  $\{\delta\}$  is determined by iteratively adjusting a cross-sectional tangent stiffness matrix,  $[K_t]$ , relating the increments in  $\{f\}$  and  $\{\delta\}$  through a rate equation of the type (34):

$$\dot{\{f\}} = [K_t] \dot{\{\delta\}} \quad (8)$$

whose components are defined in Appendix A. The process is repeated until the imbalance in the external loads and internal forces becomes zero or is within a tolerance. Once the  $\epsilon$  distribution is found, the internal resisting forces are evaluated by numerical summation over the discretized cross section shown in Figure 1. This is readily done by replacing the integrals in Equations 3-5 by summations, and  $dA$  by  $\Delta A_i$  as shown in Figure 1.

The cross-sectional stiffness characteristics can be represented in the form of a thrust-moment-curvature ( $p-\bar{m}-\bar{\phi}$ ) relationship as shown in Figure 4. The initial or the linearly elastic portion of this curve can be determined noniteratively. The elasto-plastic and nearly plastic regions shown in Figure 4 are determined iteratively. The curve in this figure represents a moment-curvature ( $\bar{m}-\bar{\phi}$ ) relationship while the axial thrust  $p$  is held constant. The determinant of the tangent stiffness matrix,  $|[K_t]|$ , approaches zero as the maximum moment-carrying capacity of the cross section is reached.

## 2.2 Concurrent Processing for Cross-Sectional Analysis

In this section, a concurrent processing study of biaxially loaded hollow rectangular sections is presented using a Finite Element Machine (FEM). Appendix B contains a brief description of this multiprocessor computer.

If a cross section is subjected to a pair of gradually increasing moment values  $\bar{m}_x$  and  $\bar{m}_y$  in the presence of an axial load  $p$ , the maximum moments obtained define a typical point, such as  $S$ , on the yield surface shown schematically in Figure 5. The quantities  $\bar{m}_x^*$  and  $\bar{m}_y^*$  in this figure represent the maximum moment capacities for a given axial load level,  $p$ . In this study, the ratio of the moments  $\bar{m}_y$  to  $\bar{m}_x$  is:

$$\gamma = \bar{m}_y / \bar{m}_x \quad (9)$$

is held constant. For a given value of  $\gamma$ , a contour RST as shown in Figure 5 is generated for various values of  $p$  such as for  $p_1, p_2, \dots$ . To generate the yield surface, several contours such as RST are developed for various  $\gamma$  values. The numerical studies are based on hollow square and hollow rectangular sections of sizes  $7 \times 7 \times 0.375$  in, and  $8 \times 6 \times 0.375$  in, respectively, are analyzed. Each wall of the section is divided into two layers with 20 elemental areas in each layer, thus providing a total of 160 elemental areas per section. The  $\bar{m}-\bar{\phi}$  curves and the contours of the yield surfaces for these sections are developed by using 1, 2, 4, and 8 processors of the FEM, and the computational efficiencies are evaluated.

Table 1 summarizes the concurrent processing results for the hollow square section with  $\gamma = 1.000$  for developing 8 different moment-curvature curves each corresponding to a different axial load value. First, the 8 moment-curvature curves are developed concurrently on 8 processors. The analysis is then repeated with 4,

2, and 1 processors, respectively. When 8 processors are employed, it is found that different processors took different lengths of computational time. The maximum computational time with 8, 4, 2, and 1 processors is recorded in Table 1. The speedup factor,  $s_i$ , in this table is evaluated as follows:

$$s_i = t_1 / t_i \quad (10)$$

in which  $t_1$  is the time taken by a single processor to generate all eight moment-curvature curves, and  $t_i$  is the maximum computational time obtained when  $i$  number of processors are employed. The efficiency of concurrent computation,  $\eta_i$ , is determined as follows:

$$\eta_i = 100 (s_i / i) \quad (11)$$

Speedup factors of 7.69, 3.96, and 1.99 are obtained for 8, 4, and 2 processors, respectively, and the corresponding efficiencies are 96.2, 98.9, and 99.8 percent. The actual relationship between the number of processors employed and the resulting speedup factors is shown in Figure 6. The linear theoretical maximum relationship is also shown in this figure for a direct comparison. Table 2 presents a summary of the computational times on concurrent processors for the square and rectangular sections. For the square section, 8 different  $\gamma$  values, designated by  $\gamma_{1s}$  through  $\gamma_{8s}$  in this table, are used to generate the yield surface. The specific values used are:

$$\begin{array}{lll} \gamma_{1s} = 1.000 & \gamma_{2s} = 0.875 & \gamma_{3s} = 0.750 \\ \gamma_{4s} = 0.625 & \gamma_{5s} = 0.500 & \gamma_{6s} = 0.375 \\ \gamma_{7s} = 0.250 & \gamma_{8s} = 0.000 & \end{array} \quad (12)$$

First, 8 processors are employed to generate concurrently 8 different families of moment-curvature relations. Each family of the curves is obtained for a specific value of  $\gamma$  defined from Equation 12. Figures 7 and 8 together represent a typical family of curves for  $\gamma = 0.625$  and  $p = 0.0$  to  $0.9$ . The process is repeated with 4, 2, and 1 processors using the  $\gamma$  values summarized in Table 2. The computational times obtained for various processors are given in this table. The maximum time taken for each analysis is identified in the parentheses. The  $\bar{m}_x^*$  versus  $\bar{m}_y^*$  interaction contours of the yield surface are shown in Figure 9. For the rectangular section, with eight  $\gamma$  values,  $\gamma_{r1}$  through  $\gamma_{r8}$  are:

$$\begin{array}{lll}
 \gamma_{1r} = 0.000 & \gamma_{2r} = 0.300 & \gamma_{3r} = 0.600 \\
 \gamma_{3r} = 0.900 & \gamma_{5r} = 1.111 & \gamma_{6r} = 1.667 \\
 \gamma_{7r} = 3.333 & \gamma_{8r} = \infty & 
 \end{array} \quad (13)$$

The results for this section are also summarized in Table 2, and shown graphically in Figures 10 through 12.

Table 3 summarizes the speedup factors and the efficiencies for the square section. The maximum computational times in Table 3 were identified previously in Table 2. Table 4 summarizes the rectangular section results. Figures 13 and 14 show these results graphically.

### 2.3 Nonproportionally Loaded Sections

The response of materially nonlinear sections is dependent upon the history of loading. In this section, an example of an I-section subjected to biaxial nonproportional loads is presented. The procedure, however is also applicable to

hollow rectangular sections. Referring to Figure 15, the load path OA represents proportional loading. The load path OFDA indicates a typical nonproportional loading in that the cross section is subjected to  $M_x$ , followed by  $M_y$ , and finally followed by P until the section capacity is reached. Since significant strain reversal may occur due to nonproportional loading, the  $\sigma$ - $\epsilon$  curve in Figure 3(a) with material elastic unloading is used. Here, a W 8x31 section with no residual stresses is analyzed and the results are compared to those of Chen and Atsuta (34). The section walls are divided into two layers of 12 elemental areas in each plate, providing a total of 72 elements for the entire cross section. The load path OFDA as shown in Figure 15 ia used. The section is first subjected to  $\bar{m}_x = 0.6$  (level F), followed by  $\bar{m}_y = 0.6$  (level D), and finally followed by p which eventually attains a value of 0.3 at the full section capacity. Figures 16 through 18 show the resulting  $\bar{m}_x$ - $\bar{\phi}_x$ ,  $\bar{m}_y$ - $\bar{\phi}_y$ , and p- $\epsilon_0$  relationships, respectively, and are in reasonable agreement with the curves of Reference 34. The deviation of the curves of Reference 34 from those given here is due to the piecewise-linear approach adopted in that reference. The type of cross-sectional analysis demonstrated here is incorporated in the beam-column and frame analyses.



### 3. BIAXIALLY IMPERFECT COLUMNS

A sequential computational inelastic analysis of centrally loaded columns with biaxial imperfections and partial rotational restraints has been given previously by Razzaq and Calash (54). No concurrent solution to this or any other inelastic problem has been published in the past. In this chapter, a concurrent solution procedure is shown and later implemented on the Finite Element Machine (FEM).

#### 3.1 Theoretical Formulation

An imperfect column BT of length  $L$ , and with partial biaxial end restraints is shown schematically in Figure 19. It is subjected to an axial thrust  $P$  gradually until the maximum capacity is reached. The rotational restraint stiffnesses  $k_{Bx}$ ,  $k_{By}$ ,  $k_{Tx}$ ,  $k_{Ty}$  simulate the bending resistance of the connections, or structural members framing into the column at the member ends. The subscripts B and T refer to the member ends as shown in Figure 19. The material of the column follows an idealized elastic-perfectly-plastic  $\sigma$ - $\epsilon$  relationship shown in Figure 3(b). The hollow rectangular section selected used here has an initial residual stress distribution as shown in Figure 2(b). The corners have a tensile residual stress of  $\sigma_{rt} = 0.5\sigma_y$  and the midpoints of all four walls have a compressive residual stress of  $\sigma_{rc} = -0.2\sigma_y$ . The residual stress distribution is piecewise-linear along the length of the walls of the section and uniform across the thickness (40).

The inelastic behavior of the column shown in Figure 19 is governed by the following materially nonlinear ordinary differential equations (54):

$$q_{11} \epsilon_0 + q_{12} u'' + q_{13} v'' - P_r - P_p = P \quad (14)$$

$$\begin{aligned} q_{21} \epsilon_0 + q_{22} u'' + q_{23} v'' - M_{yre} - M_{yp} + P (u_i + u) \\ = m_{By} + (z/L) (m_{Ty} - m_{By}) \end{aligned} \quad (15)$$

$$\begin{aligned} q_{31} \epsilon_0 + q_{32} u'' + q_{33} v'' - M_{xre} - M_{xp} + P (v_i + v) \\ = m_{Bx} + (z/L) (m_{Tx} - m_{Bx}) \end{aligned} \quad (16)$$

in which the primes designate differentiation relative to  $z$ ;  $u$  and  $v$  are the respective flexural displacements due to  $P$ , in the  $x$  and  $y$  directions;  $\epsilon_0$  is the average axial strain. The  $q_{ij}$  terms are the inelastic cross-sectional properties evaluated using the numerical procedure described in the preceding chapter. The terms  $P_r$ ,  $P_p$ ,  $M_{xre}$ ,  $M_{yre}$ ,  $M_{xp}$ , and  $M_{yp}$  are inelastic load and moment parameters defined in Reference 54 and summarized in Appendix C. As shown in Figure 19, the initial member crookedness in the  $x$  and  $y$  directions is taken as follows:

$$u_i = u_{0i} \sin \pi z/L \quad (17)$$

$$v_i = v_{0i} \sin \pi z/L \quad (18)$$

where  $u_{0i}$  and  $v_{0i}$  are the respective midspan amplitudes. The terms  $m_{Bx}$ ,  $m_{By}$ ,  $m_{Tx}$ , and  $m_{Ty}$  in Equations 15 and 16 represent end spring moments given by:

$$m = k \theta \quad (19)$$

in which the spring stiffness  $k$  is  $k_{Bx}$ ,  $k_{By}$ ,  $k_{Tx}$ , or  $k_{Ty}$ , and  $\theta$  is the corresponding

member end rotation. The geometric boundary conditions are given as follows:

$$u(0) = v(0) = u(L) = v(L) = 0 \quad (20)$$

At the global level, Equation 14 is enforced implicitly by first solving it for  $\epsilon_0$  explicitly and then substituting it into Equations 15 and 16. This results in the following two global equilibrium equations:

$$\begin{aligned} Q_{xx} u'' + Q_{xy} v'' - (M_{yre} - \mu_{yre}) - (M_{yp} - \mu_{yp}) + P (u_i + u - u_Q) \\ = m_{By} + (z/L) (m_{Ty} - m_{By}) \end{aligned} \quad (21)$$

$$\begin{aligned} Q_{yx} u'' + Q_{yy} v'' - (M_{xre} - \mu_{xre}) - (M_{xp} - \mu_{xp}) + P (v_i + v - v_Q) \\ = m_{Bx} + (z/L) (m_{Tx} - m_{Bx}) \end{aligned} \quad (22)$$

where:

$$Q_{xx} = q_{22} - (q_{12} q_{21} / q_{11}) \quad (23a)$$

$$Q_{xy} = q_{23} - (q_{13} q_{21} / q_{11}) \quad (23b)$$

$$Q_{yx} = q_{32} - (q_{12} q_{31} / q_{11}) \quad (23c)$$

$$Q_{yy} = q_{33} - (q_{13} q_{31} / q_{11}) \quad (23d)$$

$$\mu_{yre} = q_{21} P_r / q_{11} \quad (23e)$$

$$\mu_{yp} = q_{21} P_p / q_{11} \quad (23f)$$

$$\mu_{xre} = q_{31} P_r / q_{11} \quad (23g)$$

$$\mu_{xp} = q_{31} P_p / q_{11} \quad (23h)$$

$$u_Q = q_{21} / q_{11} \quad (23i)$$

$$v_Q = q_{31} / q_{11} \quad (23j)$$

The numerical procedure is based on a second-order central finite-difference scheme (43) applied to Equations 21 and 22 at N equidistant nodes over [O, L], and invoking Equation 20. This results in:

$$Q_{xxj} ( u_{j-1}-2u_j+u_{j+1} )/h^2 + Q_{xyj} ( v_{j-1}-2v_j+v_{j+1} )/h^2 - ( M_{yre}^{-\mu_{yre}} )_j - ( M_{yp}^{-\mu_{yp}} )_j + P ( u_i+u-u_Q )_j = m_{By} + (z_j/L)( m_{Ty}-m_{By} ) \quad (24)$$

$$Q_{yyj} ( u_{j-1}-2u_j+u_{j+1} )/h^2 + Q_{xyj} ( v_{j-1}-2v_j+v_{j+1} )/h^2 - ( M_{xre}^{-\mu_{xre}} )_j - ( M_{xp}^{-\mu_{xp}} )_j + P ( v_i+v-v_Q )_j = m_{Bx} + (z_j/L)( m_{Tx}-m_{Bx} ) \quad (25)$$

where the spring moments in Equations 24 and 25 are:

$$m_{Bx} = k_{Bx} ( v_1-v_{-1} )/2h \quad (26)$$

$$m_{Tx} = -k_{Tx} ( v_{N+1}-v_{N-1} )/2h \quad (27)$$

$$m_{By} = k_{By} ( u_1-u_{-1} )/2h \quad (28)$$

$$m_{Ty} = -k_{Ty} ( u_{N+1}-u_{N-1} )/2h \quad (29)$$

Applying Equations 25 and 26 at all N nodes leads to following equilibrium equations in the matrix form:

$$[K] \{ \Delta \} = \{ F \} + \{ F \}_p \quad (30)$$

In this equation, [K] is the global stiffness matrix of the order 2Nx2N. The vector {Δ} contains lateral displacements as follows:

$$\{ \Delta \}^T = \{ u_{-1} \ v_{-1} \ u_1 \ v_1 \ u_2 \ v_2 \ u_3 \ v_3 \ \dots \ u_j \ v_j \ \dots \ u_{N-3} \ v_{N-3} \ u_{N-3} \ v_{N-3} \ u_{N-3} \ v_{N-3} \ u_{N-3} \ v_{N-3} \ } \quad (31)$$

The external and plastic force vectors, {F} and {F}<sub>p</sub>, are given in Appendix D.

Equation 30 is nonlinear since  $[K]$ ,  $\{F\}$ , and  $\{F\}_p$  depend on  $\{\Delta\}$ . Therefore, an iterative scheme is adopted in which the global stiffness matrix is updated and inverted at each iteration level. Also, a convergence study showed that it was sufficient to take  $N = 8$ .

### 3.2 Concurrent Computing Solution

A concurrent procedure is devised for the solution of Equation 30, based on a master-assistant processor configuration. The assembly of Equation 30 is assigned to the master processor, whereas the computation of  $q_{ij}$  terms and the inelastic load and moment load parameters is assigned to the assistant processors. A flow chart of the concurrent procedure implemented on the FEM is shown in Figure 20. The double-headed pointers in the flow chart indicate the interprocessor communication flow. The concurrent procedure is summarized as follows:

1. Input the section properties into the master and assistant processors.
2. Compute elastic properties for the  $N$  cross sections concurrently on all assistant processors and send this information to the master processor to assemble  $[K]$  and evaluate the initial determinant  $|[K]|$ .
3. Specify a small axial load,  $P = P_1$  in the master processor and solve Equation 30 for  $\{\Delta\}$ .
4. Synchronize all processors for communication.
5. Broadcast to the assistant processors the value of  $P$  and the necessary components of  $\{\Delta\}$  generated by the master processor.
6. Compute  $q_{ij}$  and the inelastic load and moment parameters for the  $N$  cross sections concurrently on the assistant processors using the tangent stiffness

procedure, and send the computed properties to the master processor in an asynchronous communication mode.

7. Assemble  $[K]$ ,  $\{F\}$ , and  $\{F\}_p$  in the master processor and solve Equation 30 to update  $\{\Delta\}$ .
8. Check for the convergence of  $\{\Delta\}$ . If convergence is not achieved, go to step 4.
9. If column becomes unstable ( $|[K]| \rightarrow 0$ ), stop the execution on the master processor after setting a flag, and go to step 11.
10. Set  $P = P_1 + \delta P$ , where  $\delta P$  is a small load increment, and go to step 4.
11. Stop execution on assistant processors and the master processor.

In step 6, an asynchronous communication mode is used since the various assistant processors do not necessarily complete their computations at the same instant. Furthermore, the asynchronous communication facilitates the assistant processors to send information as and when it becomes available.

### 3.3 Numerical Study

The effectiveness of the concurrent procedure is evaluated by analyzing eight sample column problems designated CN1 through CN8. Columns CN1-CN4 have a 7.0x7.0x0.375 in. hollow square section, while CN5-CN8 have an 8.0x6.0x0.375 in. hollow rectangular section. Three different  $k$  values are used in Equation 19, namely,  $k_1 = 0.0$  in-kip/rad,  $k_2 = 5,397$  in-kip/rad, and  $k_3 = 15.0 \times 10^{15}$  in-kip/rad. Here,  $k_1$  simulates pinned condition,  $k_2$  the bending resistance of a 5.0x5.0x0.1875 in. hollow square restraint beam of 12 ft. length, and  $k_3$  a nearly fixed condition. The columns are provided with equal end restraints about the  $x$  and  $y$  axes at the

top and bottom ends except for columns CN5 and CN8, which have unequal end restraints. The  $k$  values of these two columns are defined as  $k_{Bx} = k_1$ ;  $k_{By} = k_3$ ;  $k_{Tx} = k_2$ ;  $k_{Ty} = k_3$ . Imperfections are taken in the form of residual stresses as shown in Figure 2 and out-of-straightness given by Equations 17 and 18 with  $u_{0i} = v_{0i} = L/1,000$ . Sample load-deflection curves for columns CN2 and CN6 are shown in Figure 21, in which  $U$  and  $V$  represent the total midspan lateral deflections given by:

$$U = u_{0i} + u(L/2) \quad (32)$$

$$V = v_{0i} + v(L/2) \quad (33)$$

Table 5 summarizes the column peak loads for CN1-CN8. The quantity  $p_{max}$  in this table represents the maximum value of  $p$ ; that is, the column load-carrying capacity. The concurrent computing procedure is implemented on 2, 3, 5, and 9 processors and execution times are obtained to evaluate computational efficiencies. The number of processors includes both the master and the assistant processors. Table 6 summarizes the execution times on concurrent processors for the hollow square column CN1 and the hollow rectangular column CN5. The  $t_i$  values used for the speedup,  $s_i$ , and the efficiency,  $\eta_i$ , calculations are enclosed in parentheses. When 9 processors are used to analyze column CN1, the sum of the individual processor execution times is 9574.360 sec. Similarly, the sums for 5, 3, and 2 processors are 7199.466, 5972.540, and 6578.309 sec., respectively. The lowest of these sums is adopted as the estimated execution time on a single processor as recorded at the bottom of Table 6. Table 7 gives the speedup factors and

efficiencies for hollow square columns. As the number of processors increase,  $\eta_i$  decreases except when 2 processors are employed. The reduction in  $\eta_i$  with two processors is due to the loss of asynchronous communication advantage present when 3 or more processors are employed. This loss is attributable to the sequential computation of cross-sectional data on a single assistant processor. Furthermore, as the number of processors increase, the distribution of computational work among the assistant processors tends to become nonuniform. This is due to an unequal number of iterations required in the assistant processors in carrying out the tangent stiffness procedure. Similar results for hollow rectangular columns are given in Table 8. Corresponding to the results in Tables 7 and 8 for columns CN2 and CN6, the relationships between the speedup factor and the number of processors are shown in Figure 22, along with the theoretical maximum speedup.

A review of the numerical study carried out in this investigation indicate that the algorithm developed for the concurrent computing analysis of inelastic structural members is quite efficient, and the application of the new generation multiprocessor computers promise a great reduction in CPU time required for the analyses.



## 4. IMPERFECT BEAM-COLUMNS

The effect of nonproportional uniaxial and biaxial loads on the behavior of partially restrained nonsway imperfect beam-columns is studied. Adequate models for representing the connection moment-rotation curves are studied and used in the beam-column analysis. Both hollow rectangular and I-sections are considered. A critical evaluation of the tangent modulus approach is also conducted. In Chapter 5, this procedure modified and utilized for the analysis of plane nonsway frames.

### 4.1 Theoretical Formulation

#### 4.1.1 Equilibrium Equations

A biaxially imperfect and partially restrained beam-column, BT, of Length  $L$  is shown in Figure 23. It is subjected to an axial load  $P$ , and biaxial end moments  $M_{Bx}$ ,  $M_{By}$ ,  $M_{Tx}$ , and  $M_{Ty}$ . The partial restraint stiffnesses  $k_{Bx}$ ,  $k_{By}$ ,  $k_{Tx}$ , and  $k_{Ty}$  simulate the bending resistance of the flexible connections or structural members framing into the member ends. The material of the beam-column may follow the stress-strain relationship shown in Figure 3(a) or 3(b).

Equations 14-16 modified to include the applied end moments take the form:

$$q_{11} \epsilon_0 + q_{12} u'' + q_{13} v'' - P_r - P_p = P \quad (34)$$

$$q_{21} \epsilon_0 + q_{22} u'' + q_{23} v'' - M_{yre} - M_{yp} + P (u_i + u) \\ = m_{By} + (z/L) (m_{Ty} - m_{By}) - M_{By} - (z/L) (M_{Ty} - M_{By}) \quad (35)$$

$$\begin{aligned}
q_{31} \epsilon_0 + q_{32} u'' + q_{33} v'' - M_{xre} - M_{xp} + P (v_i + v) \\
= m_{Bx} + (z/L) (m_{Tx} - m_{Bx}) - M_{Bx} - (z/L) (M_{Tx} - M_{Bx}) \quad (36)
\end{aligned}$$

The initial crookedness of the member in the x and y directions, indicated in Figure 23 is governed by Equations 17 and 18. Equations 34-36 are also utilized to predict the behavior of uniaxially loaded members. The minor axis analysis is conducted by utilizing Equations 34 and 35 only and by setting  $v_i = 0$ , and  $M_{Bx} = M_{Tx} = 0$ . Similarly, the major axis analysis is carried out by utilizing Equations 34 and 36 only and by setting  $u_i = 0$ , and  $M_{By} = M_{Ty} = 0$ .

In the above-mentioned analysis,  $\epsilon_0$  is eliminated from Equations 35 and 36 by using Equation 34. The resulting differential equations with u and v as the dependent variables are then solved for using a second-order central finite-difference scheme (43). This results in the following member equilibrium equations:

$$[K] \{\Delta\} = \{M\} \quad (37a)$$

in which:

$$\{M\} = \{F\} + \{F\}_p + \{M\}_a \quad (37b)$$

where  $[K]$ ,  $\{\Delta\}$ ,  $\{F\}$ , and  $\{F\}_p$  are defined in the preceding chapter and  $\{M\}_a$  is the applied end moment vector. In the elastic range,  $[K]$ ,  $\{F\}$ , and  $\{M\}_a$  are explicitly defined and  $\{F\}_p$  is zero, whence, Equation 37(a) can be solved directly. In the inelastic range, however, the coefficients in  $[K]$  and the components of vector  $\{F\}_p$  become dependent upon the inelastic cross-sectional properties at various nodes along the member length.

#### 4.1.2 End Restraint Conditions

Past studies (9,24,31) indicate that beam-column connections exhibit nonlinear moment-rotation characteristics. Recently, Chen and Lui (53), and Razzaq and Calash (54) studied the effects of partial end restraints on member behavior. These and similar other studies (34,38,39,50,51) indicated that the flexible connections have a significant influence on member behavior. Figure 24 shows a typical moment-rotation,  $m-\theta$ , curve with an idealized piecewise-linear model of a connection. Chen and Lui (53) used  $m-\theta$  models defined by spline curves with optimization techniques to define the coefficients of these splines. While their method represents the connection response accurately, the procedure is cumbersome for practical use. Razzaq and Calash (54) in their study used practical piecewise-linear connection models typically shown in Figure 24. In order to identify suitable piecewise-linear connection characteristics, various models shown in Figures 25 through 28 are investigated. Specifically, linear, bilinear, and trilinear models are considered.

The moments  $m_{Bx}$ ,  $m_{By}$ ,  $m_{Tx}$ , and  $m_{Ty}$  in Equations 35 and 36 are dependent upon the moment-rotation  $m-\theta$  characteristics of a connection. For a linear  $m-\theta$  relationship, the spring moment follows line OA in Figure 24, and is given by:

$$m = k_a \theta ; \quad |m| \geq 0 \quad (38)$$

For a bilinear relationship, the spring moment follows path OAB in Figure 24. Thus:

$$m = k_a \theta ; \quad |m| \leq |m_a|$$

$$m = m_a + k_b (\theta - \theta_a) ; \quad |m| > |m_a| \quad (39)$$

in which  $m_a$  is the *knee* moment at  $\theta = \theta_a$  indicated in Figure 24. The spring stiffness is reduced to  $k_b$  past  $m_a$ . A trilinear connection  $m$ - $\theta$  is shown as the dashed line OABC in Figure 24 for which:

$$\begin{aligned} m &= k_a \theta ; & |m| &\leq |m_a| \\ m &= m_a + k_b (\theta - \theta_a) ; & |m_a| < |m| &\leq |m_b| \\ m &= m_b + k_c (\theta - \theta_b) ; & |m| &> |m_b| \end{aligned} \quad (40)$$

where  $m_a$  and  $m_b$  correspond to  $\theta_a$  and  $\theta_b$ . The connection stiffness in the tertiary range is  $k_c$ , as shown in Figure 24.

The  $m$  expressions given in this section are used for the spring moments  $m_{Bx}$ ,  $m_{By}$ ,  $m_{Tx}$  and  $m_{Ty}$  which appear in Equations 35 and 36.

## 4.2 Load Paths

Two different load paths are adopted for uniaxially loaded beam-columns, and are defined in Section 4.2.1. For biaxially loaded beam-columns, six different load paths are used, and are outlined in Section 4.2.2.

### 4.2.1 Uniaxially Loaded Beam-Columns

Referring to Figure 15, two different load paths designated as NP1 and NP2 are adopted for uniaxially loaded beam-columns and are defined as follows:

NP1: The axial load  $P$  is applied first incrementally and held constant, followed by gradually increasing equal end moments until the load-carrying capacity of the

member is reached. This corresponds to the load path OGB for member minor axis analysis, or OGC for member major axis analysis.

NP2: The equal end moments corresponding to the load-carrying capacity obtained in NP1 are applied first incrementally and held constant, followed by a gradually increasing axial load P until the member collapse occurs. This corresponds to load paths OEB or OFC for member minor and major axis analyses, respectively.

#### 4.2.2 Biaxially Loaded Beam-Columns

Referring to Figure 15, six different load paths designated as NP3 through NP8 are used for biaxially loaded beam-columns as defined below:

NP3: The axial load P is applied first incrementally and held constant, followed by  $M_x$  and  $M_y$  simultaneously, until the member collapses. The moment ratio is held constant and taken as follows:

$$M_x / M_y = r_x / r_y \quad (41)$$

where  $r_x$  and  $r_y$  are major and minor axis radii of gyration. This load path corresponds to OGA.

NP4: The moments  $M_x$  and  $M_y$  are applied proportionally following Equation 41, until the peak moment values from NP3 are attained, followed by P until collapse occurs. NP4 corresponds to load path ODA.

NP5: The axial load P of the same magnitude as in NP3 is applied first,  $M_x$  achieved in NP3 is applied next, followed by  $M_y$  until collapse occurs. NP5 corresponds to load path OGCA.

NP6: This load path is the reverse of NP5 in that  $M_y$  achieved in NP3 is applied

first, followed by  $M_x$  achieved in NP3, and finally followed by P until collapse occurs. NP6 corresponds to load path OEDA.

NP7: The axial load P of the same magnitude as in NP3 is applied first,  $M_y$  achieved in NP3 is applied next, followed by  $M_x$  until collapse occurs. This corresponds to load path OGBA.

NP8: This load path is the reverse of NP7 in that  $M_x$  achieved in NP3 is applied first, followed by  $M_y$  achieved in NP3, and finally followed by P until collapse occurs. NP8 corresponds to load path OFDA.

When hollow square section members are analyzed, NP7 and NP8 are redundant and correspond, respectively, to NP5 and NP6, owing to the double symmetry of the section.

### 4.3 Solution Procedure

The following sequential computing procedure is used for solving Equation 37(a) iteratively:

1. Evaluate initial cross-sectional properties at N nodes to assemble the initial global beam-column stiffness matrix [K] in Equation 37(a).
2. Specify small external loads and formulate  $\{M\}_1$  using Equation 37(b).
3. Solve for the deformation vector  $\{\Delta\}$  in Equation 37(a).
4. Compute the external nodal forces  $\{f\}_1$  and deformations  $\{\delta\}_1$  defined in Equations 6 and 7, respectively, in the elastic range corresponding to  $\{M\}_1$ .
5. Increase  $\{M\}$  to  $\{M\}_2 = \{M\}_1 + \{\delta M\}$ , in which  $\{\delta M\}$  is the resultant increment load vector. Solve Equation 37(a) for  $\{\Delta\}$ , and compute external force vectors  $\{f\}_2$  corresponding to  $\{M\}_2$ .

6. Using  $\{f\}_2$  vectors and the tangent stiffness procedure (34), compute  $[K_t]$  in Equation 8 for all cross sections.
7. Solve for an updated  $\{\Delta\}$  after assembling  $[K]$ ,  $\{F\}$ , and  $\{F\}_p$  utilizing the cross-sectional properties obtained in Step 6.
8. With the  $\{\Delta\}$  in Step 7, formulate the load vector  $\{M\}_3$ .
9. If  $|\{M\}_3 - \{M\}_2| \leq \{\alpha\}$ , where  $\{\alpha\}$  is the tolerance vector composed with load limits of 0.01% of the member yield-load capacity, go to Step 11.
10. Set  $\{M\}_1 = \{M\}_2$ ;  $\{f\}_1 = \{f\}_2$ ;  $\{M\}_2 = \{M\}_3$ , and go to Step 6.
11. Set  $\{M\}_1 = \{M\}_3$ ;  $\{f\}_1 = \{f\}_3$ , and repeat Steps 5-10 until the maximum load-carrying capacity of the beam-column is reached.

The procedure described herein is carried out using constant load increments throughout the elastic range. In the inelastic range, these load increments are successively reduced to avoid severe imbalance between the external and internal forces. The maximum load is obtained within 0.0002 times the cross-sectional yield capacity. Also, based on a convergence study, a total 15 nodes for I-section members and 11 nodes for hollow rectangular members over  $[0,L]$  is found to be sufficient. The cross-sectional analysis in Step 5 is conducted using two layers of 50 discrete elemental areas in each wall of an I-section, providing 100 equal-area elements per plate, and two layers of 24 discrete elemental areas in each wall of a hollow rectangular section, providing 48 equal area elements per plate.

## 4.4 Numerical Study

### 4.4.1 Modeling of End Restraints

Two different connection  $m$ - $\theta$  relationships given in References 24 and 53 are used for conducting a modeling study of the beam-column end restraints. A set of five piecewise-linear models is used for each connection type. These are shown in Figures 25 through 28. Figures 25 and 26 show the idealized  $m$ - $\theta$  models designated a1 through f1 for the first connection data (23) and are described as follows:

- a1: Linear approximation obtained by drawing a tangent to the nonlinear  $m$ - $\theta$  curve at the origin. The slope of the tangent is  $k_a = 42,135$  in-kip/rad.
- b1: Bilinear approximation based on tangents drawn at the origin and from the highest given point on the nonlinear  $m$ - $\theta$  curve. The respective initial and secondary connection stiffnesses are  $k_a = 42,135$  in-kip/rad, and  $k_b = 2,431$  in-kip/rad. The connection moment at the transition point where the two tangents meet is  $m_a = 316$  in-kips.
- c1: Bilinear approximation obtained by drawing a pair of secants to the nonlinear  $m$ - $\theta$  curve. Here,  $k_a = 31,580$  in-kip/rad;  $k_b = 3,115$  in-kip/rad;  $m_a = 300$  in-kips.
- d1: Bilinear *lower bound* approximation with the first straight line drawn from the origin to an intermediate point on the nonlinear  $m$ - $\theta$  curve, and the second line drawn by connecting the transition point to the highest available point on the  $m$ - $\theta$  curve. Here,  $k_a = 27,000$  in-kip/rad;  $k_b = 3,167$  in-kip/rad;  $m_a = 270$  in-kips.
- e1: Elastic-plastic approximation with two secants, with  $k_a = 30,385$  in-kip/rad;  $k_b$



= 0 in-kip/rad;  $m_a = 395$  in-kips.

f1: Trilinear approximation with two tangents as in b1 with the intermediate region represented by a secant to the nonlinear  $m-\theta$  curve. Here,  $k_a = 42,135$  in-kip/rad;  $k_b = 6,667$  in-kip/rad;  $k_c = 2,431$  in-kip/rad; at the transition where the first tangent and secant meet,  $m_a = 200$  in-kips; at the transition where the secant and the second tangent meet,  $m_b = 350$  in-kips.

Similarly, Figures 27 and 28 show the idealized  $m-\theta$  models designated as a2 through f2, for the second connection data (53). These are defined as follows:

a2:  $k_a = 24,000$  in-kip/rad.

b2:  $k_a = 24,000$  in-kip/rad;  $k_b = 1,286$  in-kip/rad;  $m_a = 100$  in-kips.

c2:  $k_a = 17,778$  in-kip/rad;  $k_b = 2,195$  in-kip/rad;  $m_a = 80$  in-kips.

d2:  $k_a = 13,333$  in-kip/rad;  $k_b = 2,368$  in-kip/rad;  $m_a = 80$  in-kips.

e2:  $k_a = 17,778$  in-kip/rad;  $k_b = 0$  in-kip/rad;  $m_a = 100$  in-kips.

f2:  $k_a = 24,000$  in-kip/rad;  $k_b = 3,583$  in-kip/rad;  $k_c = 1,286$  in-kip/rad;  $m_a = 70$  in-kips;  $m_b = 115$  in-kips.

For the numerical study, a W 8x31 section of 15 ft. length, is considered. Each of the amplitudes  $u_{0i}$  and  $v_{0i}$  are taken as  $L/1000$ . The material of the member is assumed to follow the  $\sigma-\epsilon$  relationship shown in Figure 3(b). When the residual stresses are present, the distribution in Figure 2(a) is used. First, a centrally loaded column with biaxial crookedness is analyzed using the six  $m-\theta$  models a1 through f1. The individual studies relative to the minor and major axes showed no significant effect of  $m-\theta$  relationships on the column peak loads. The end spring moments developed (18 in-kips to 141 in-kips) were considerably less than  $m_a$  value

when models a1 through f1 are used. Also, the major axis analysis is less sensitive to the various  $m-\theta$  models.

The effect of various  $m-\theta$  models on uniaxially loaded beam-column response is studied with  $u_{0i} = L/100,000$ . The beam-column is subjected to an axial load,  $P$ , and an end moment,  $M_{Ty}$ , at the member top, in a proportional manner such that the ratio between  $P$  and  $M_{Ty}$  is 2.25. At  $z = 0$ , a pinned condition is used, whereas, a partial rotational end restraint is provided at  $z = L$  to simulate the subassembly used in Reference 53. The results for this special case are compared to those in Reference 53. Table 9 summarizes the dimensionless peak loads,  $p_{max}$ , corresponding to the connection models a2 through f2.

The predicted end rotations show that with restraints b2, c2 and d2, the beam-columns collapse as soon as the top end spring attempts to develop a moment greater than  $m_a$ . The elastic-plastic restraint e2 allows the spring to rotate additionally even after the attainment of the plastic spring moment (100 in-kips). The beam-column with trilinear restraint f2 reached its peak load while the spring moment was between  $m_a$  and  $m_b$ . Thus, the third linear range of the  $m-\theta$  relation was not activated. The significant observation which is made from this table is that regardless of the type of connection modeling used, the peak load varied in a small range from 0.64 to 0.71. In fact, the lower bound model d2 gave the same peak load as the bilinear portion of the trilinear model f2. The peak load obtained by Chen and Lui (53) is 0.64 comparing favorably with these results. Thus, for the type of connections used herein, a simple linear or at most a bilinear connection  $m-\theta$  model is adequate. The results also indicate that the strength of these members is not

highly sensitive to the connection modeling.

#### 4.4.2 Behavior of Uniaxially Loaded I-Section Beam-Columns

The effect of nonproportional loads on the behavior of a 12 ft. long uniaxially crooked beam-column with equal end restraints is presented in this section. A W 8x31 section is used, with and without residual stresses. When the residual stresses are present, they are the type shown in Figure 2(b). The material of the beam-column follows the stress-strain law shown in Figure 3(a). The following initial spring stiffnesses are adopted:

$$k_{a1} = 0 \text{ in-kip/rad (Pinned-Condition)}$$

$$k_{a2} = 13,333 \text{ in-kip/rad}$$

$$k_{a3} = 24,000 \text{ in-kip/rad}$$

Additionally, the behavior of the beam-column with elastic-plastic end springs is also investigated wherein  $k_{a2}$  is adopted as the initial spring stiffness until the spring moment reaches the plastic limit value of  $m_a = 100$  in-kips.

The following load conditions designated as LC1 through LC4 and associated with load paths NP1 and NP2 are used for the beam-column study:

LC1: Corresponding to the load path NP1, a relatively large axial load is applied first incrementally and held constant, followed by gradually increasing the equal end moments until the member collapses.

LC2: The maximum end moments corresponding to the load condition LC1 are applied first incrementally and held constant, followed by a gradually increasing the axial load until the member collapses, thus following load path NP2.

LC3: Corresponding to the load path NP2, relatively large equal end moments are applied first incrementally and held constant, followed by gradually increasing the axial load until the member collapses.

LC4: The maximum axial load corresponding to the load condition LC3 is applied first incrementally and held constant, followed by gradually increasing equal end moments until the member collapses thus following the load path NP1.

The beam-column peak loads obtained for the major and minor axis analyses using LC1 through LC4 are summarized in Table 10. The maximum loads for the major axis are nearly the same, suggesting that the load paths have no significant effect on the member strength. However, when the beam-column is loaded about its minor axis, the maximum loads are found to be load path dependent. Furthermore, LC1 and LC2 provide nearly the same peak loads, while LC3 and LC4 exhibit a substantial difference in the maximum loads. In the absence of initial residual stresses,  $\bar{m}$  for LC3 is 19.7% greater than that for LC4 when the spring stiffness is  $k_{a3}$ . This difference is 10.5% when initial residual stresses are included.

The behavior of a beam-column with elastic-plastic restraints defined by  $k_{a2}$ , and  $m_a = 100$  in-kips is also investigated. Table 11 summarizes the maximum loads for various load paths and load conditions when these restraints are used. The results in this table indicate that the maximum loads are not load path dependent in the presence of elastic-plastic restraints.

Since the above-mentioned results indicated that the minor axis analysis is load path dependent when linear end restraints are present, additional minor axis analyses were carried out on beam-columns with  $L=8, 12,$  and  $16$  ft., and  $k = k_{a2}$  or  $k_{a3}$ .

Load paths NP1 and NP2 are again adopted in this analysis. For each beam-column different load levels are used to define an interaction curve between  $p$  and  $\bar{m}_y$ . The results obtained are summarized in Table 12 for beam-columns numbered 1 through 6. A graphical presentation of the interaction loads for beam-column 4 is given in Figure 29. The interaction peak loads obtained by using the stress-strain law given in Figure 3(b), neglecting the elastic unloading (tangent modulus), is also shown in this figure. For  $p = 0.0$  to  $0.45$ , the tangent modulus curve gives unconservative moment estimates. This phenomenon is also observed in beam-columns 2 and 6.

#### 4.4.3 Behavior of Biaxially Loaded I-Section Beam-Columns

Biaxially loaded I-section beam-columns may experience twist in addition to bending. However, past experimental and theoretical studies (21,25) indicate that such open sections with a width to depth ratio of nearly one experience negligibly small twist. Since the section adopted for the present study meets this condition, twisting is therefore neglected. This assumption was found to be valid through a comparison of the results from the present analysis to those in References 21 and 25 for pinned beam-columns subjected to proportional loads. Table 13 shows this comparison. The maximum loads are clearly in good agreement.

In order to investigate nonproportional load effects on biaxially loaded beam-column behavior, a 12 ft. long W 8x31 section member with elastic partial restraints is used. Various nonproportional load paths are adopted and the member response obtained. The cross section possesses residual stresses as shown in Figure 2(b). Two different end restraint stiffnesses,  $k = k_{a2}$  or  $k_{a3}$  are used and the beam-

columns are subjected to load path NP3 or NP4. The results from this study are reported in Table 14. For beam-column numbered 8, Figure 30 shows an interaction diagram between  $p$  and the dimensionless minor axis maximum moment,  $\bar{m}_y^*$ . The figure also shows the tangent modulus curve. A comparison of these curves indicates that the tangent modulus peak loads are unconservative. A load path dependency is obviously present in the nonproportionally loaded I-section beam-columns.

#### 4.4.4 Behavior of Biaxially Loaded Rectangular Tubular Beam-Columns

A relatively limited amount of research has been conducted in the past on rectangular tubular beam-columns subjected to nonproportional loads. Razzaq and McVinnie (55) conducted inelastic analysis and experiments on biaxially loaded pinned-end members subject to nonproportional loads. In this section, the behavior of rectangular tubular imperfect beam-columns subjected to different load paths defined as NP3 through NP8 are presented. For the rectangular tubular section, the torsional effects are negligible (55) and ignored.

For the beam-column studied, the length is taken as 12 ft. Each of the initial midspan amplitude in Equations 17 and 18 is taken as  $L/1000$ . Hollow square,  $7 \times 7 \times 0.375$  in., and rectangular,  $8 \times 6 \times 0.375$  in. sections are used for the beam-columns studied herein. The material stress-strain law in Figure 3(a) is used. The initial residual stresses in Figure 2(a) are adopted. For each beam-column, identical rotational restraints are used at both ends about the  $x$  and  $y$  axes, that is:

$$k = k_{Bx} = k_{By} = k_{Tx} = k_{Ty} \quad (42)$$

For the numerical study conducted, the  $k$  values defined in Section 4.4.2 are used.

The following five types of beam-columns designated as BC1 through BC5 are studied:

BC1: hollow square section with  $k = k_{a1}$

BC2: hollow square section with  $k = k_{a2}$

BC3: hollow square section with  $k = k_{a3}$

BC4: hollow rectangular section with  $k = k_{a2}$

BC5: hollow rectangular section with  $k = k_{a3}$

For the beam-column BC1 with pinned boundaries, NP3 through NP8 provided practically the same maximum loads. For the beam-columns BC2 through BC5, however, significant load path dependence is found for certain load combinations. The results obtained for BC2-BC5 are summarized in Tables 15 through 18. Figure 31 compares the interaction curves for BC3 with load paths NP5 and NP6. Figure 32 shows the stiffness degradation curves for BC3 with an axial load level of 0.75, in which  $D$  is the dimensionless determinant of the global tangent stiffness matrix for the entire member, and is calculated as:

$$D = |[K]|_{\text{current}} / |[K]|_{\text{initial}} \quad (43)$$

where *current* represents the determinant of  $[K]$  at the given load level, and *initial* refers to the determinant at the zero load level. From Figure 32(a), it is noticed that in case of NP5,  $p = 0.75$  is applied first, followed by  $\bar{m}_x$ , however, the member collapsed at a moment value  $\bar{m}_x = 0.39$  which is less than that found in NP3. As a result, the moment  $\bar{m}_y$  could not be applied for NP5. This is evident from Figure 32(c) in which the curve for NP5 is absent.

The stiffness degradation curve in Figure 32(b) for NP5 shows *valleys* in the form of near-abrupt changes in  $D$  indicating as if the beam-column suddenly loses a considerable stiffness followed by an immediate gain with a small variation in the loads. The studies herein are based on adopting a total of 196 elemental areas for each of the eleven nodes along the member length. When the number of elemental areas was increased to 560 or more, the first of the two valleys disappeared but this did not affect the peak loads. However, it was found for some other cases reported in Tables 15 through 18 that the number and shape of these valleys could both decrease or increase, with an increase in the number of elemental areas. Fortunately, these valleys did not alter the peak loads by more than 2%. From these observations, it appears that such valleys in stiffness degradation curves are a result of redistribution of stresses. Figures 33 and 34 show the curves for BC5 with load paths NP7 and NP8. Here again, the load path dependence has a significant effect on the member strength. Thus, the behavior and strength of hollow square and rectangular section nonsway beam-columns with imperfections and partial end restraints is found to be significantly influenced by nonproportional loads. This dependence disappears only for certain load combinations, or for the special case of pinned boundaries.

#### **4.4.5 Critique on Tangent Modulus Approach**

The analyses in the preceding sections explained the influence of load paths on the beam-column behavior. Specific studies are also compared with the tangent modulus analysis. Presented herein is an investigation of the effect of  $\sigma$ - $\epsilon$  relationships shown in Figures 3(a) and 3(b) on the response of a proportionally



loaded imperfect beam-column. The member is 15 ft. long with a W 8x31 section, having equal elastic partial end restraints with  $k = k_{a2}$ . The residual stresses used are shown in Figure 2(b). Also, a proportionality constant of 1.0 is used between the axial load and the equal end moments.

The beam-column response is represented in the form of axial load versus lateral displacement relationship in Figure 35. Also, stiffness degradation curves for the analyses are given in Figure 36. An observation of the load-displacement relationship in Figure 35 suggests that the beam-column exhibits a near plateau behavior when the tangent modulus approach is used. This is also associated with relatively large displacements near the collapse load. In contrast, the analysis associated with the material elastic unloading indicates that the structure possesses a lesser degree of *ductility*, that is, the displacements near the peak load are smaller compared to those from the tangent modulus approach. The tangent modulus method neglects the redistribution of stresses along the member length, thus resulting in *fictitious* strains and *fictitious* ductile behavior. The analysis including material unloading, on the other hand, considers localized strain reversals. The effect of localized strain reversals is observed in Figure 36 as indicated by the *valleys* in the in the stiffness degradation curves.

## 5. FLEXIBLY-CONNECTED PLANE NONSWAY FRAMES

A theoretical investigation of the effect of nonproportional loads on the behavior of flexibly-connected nonsway plane imperfect frames is presented in this chapter. The solution procedure used in Chapter 4 is modified to formulate inelastic slope-deflection equations for an imperfect beam-column, and adopted for plane frame analysis. The use of these equations is illustrated through detailed studies of a portal frame and a two-bay two-story frame.

### 5.1 Theoretical Formulation

#### 5.1.1 Inelastic Slope-Deflection Equations for Imperfect Beam-Column

For a prismatic beam-column subjected to loads  $P$ ,  $M_B$  and  $M_T$  as shown in Figure 37, the slope-deflection equations have the following well-known (23) form:

$$M_b = (EI/L) (C\theta_B + S\theta_T) \quad (44)$$

$$M_T = (EI/L) (S\theta_B + C\theta_T) \quad (45)$$

in which  $C$  and  $S$  are stability coefficients, and  $\theta_B$  and  $\theta_T$  are end slopes. Equations 44 and 45 are obviously valid only for elastic members with no imperfections. In this section, a set of new slope-deflection equations are formulated which account for inelastic action, initial crookedness, and residual stresses.

Equation 37(a) can be written in the following partitioned form:

$$\begin{bmatrix} \mathbf{K}_{11} & \mathbf{K}_{12} \\ \mathbf{K}_{21} & \mathbf{K}_{22} \end{bmatrix} \begin{Bmatrix} \Delta_1 \\ \Delta_2 \end{Bmatrix} = \begin{Bmatrix} \mathbf{F}_1 \\ \mathbf{F}_2 \end{Bmatrix} + \begin{Bmatrix} \mathbf{F}_{p1} \\ \mathbf{F}_{p2} \end{Bmatrix} + \begin{Bmatrix} \mathbf{M}_1 \\ \mathbf{M}_2 \end{Bmatrix} \quad (46a)$$

in which  $\{\Delta_1\}$  is defined as:

$$\{\Delta_1\}^T = \{u_{-1} \ u_1 \ u_{N-1} \ u_{N+1}\} \quad \text{or} \quad \{v_{-1} \ v_1 \ v_{N-1} \ v_{N+1}\} \quad (46b)$$

for minor/major axis analysis;  $\{\Delta_2\}$  is the interior nodes displacement vector defined as:

$$\{\Delta_1\}^T = \{u_2 \ u_3 \ \dots \ u_j \ \dots \ u_{N-3} \ u_{N-2}\} \quad \text{or} \quad \{v_2 \ v_3 \ \dots \ v_j \ \dots \ v_{N-3} \ v_{N-2}\} \quad (46c)$$

for minor or major axis. Expanding Equation 46(a):

$$[\mathbf{K}_{11}] \{\Delta_1\} + [\mathbf{K}_{12}] \{\Delta_2\} = \{\mathbf{F}_1\} + \{\mathbf{F}_{p1}\} + \{\mathbf{M}_1\} \quad (47a)$$

$$[\mathbf{K}_{21}] \{\Delta_1\} + [\mathbf{K}_{22}] \{\Delta_2\} = \{\mathbf{F}_2\} + \{\mathbf{F}_{p2}\} + \{\mathbf{M}_2\} \quad (47b)$$

Solving Equation 47(b) for  $\{\Delta_2\}$ :

$$\{\Delta_2\} = [\mathbf{K}_{22}]^{-1} (-[\mathbf{K}_{21}] \{\Delta_1\} + \{\mathbf{F}_2\} + \{\mathbf{F}_{p2}\} + \{\mathbf{M}_2\})$$

Substituting  $\{\Delta_2\}$  into Equation 47(a) gives:

$$[\mathbf{K}_r] \{\Delta_1\} = \{\mathbf{F}_r\} + \{\mathbf{F}_{pr}\} + \{\mathbf{M}_r\} \quad (48)$$

in which:

$$[\mathbf{K}_r] = [\mathbf{K}_{11}] - [\mathbf{K}_{12}] [\mathbf{K}_{22}]^{-1} [\mathbf{K}_{21}]$$

$$\{\mathbf{F}_r\} = \{\mathbf{F}_1\} - [\mathbf{K}_{22}]^{-1} \{\mathbf{F}_2\}$$

$$\{F_{pr}\} = \{F_{p1}\} - [K_{22}]^{-1} \{F_{p2}\} \text{ and}$$

$$\{M_r\} = \{M_1\} - [K_{22}]^{-1} \{M_2\}$$

The load vector  $\{M_r\}$  in Equation 48 may be decomposed and written as:

$$\{M_r\} = [\beta] \{M_a\} \quad (49)$$

where:

$$\{M_a\} = \{M_B \ M_T\}^T \quad (50)$$

and  $[\beta]$  is a coefficient matrix. From Equations 48 and 49:

$$\{\Delta_1\} = [K_r]^{-1} (\{F_f\} + \{F_{pr}\} + [\beta] \{M_a\}) \quad (51)$$

Equation 51 can be rewritten as follows:

$$\{\Delta_1\} = [F] \{M_a\} + \{\delta_f\} + \{\delta_p\} \quad (52)$$

where:

$$[F] = [K_r]^{-1} [\beta]$$

$$\{\delta_f\} = [K_r]^{-1} \{F_f\}$$

$$\{\delta_p\} = [K_r]^{-1} \{F_{pr}\}$$

Relative to the beam-column minor axis, Equation 52 can be written in the following expanded form:

$$\begin{Bmatrix} u_{-1} \\ \bar{u}_1 \\ u_{N-1} \\ u_{N+1} \end{Bmatrix} = \begin{bmatrix} F_{11} & F_{12} \\ F_{21} & F_{22} \\ F_{31} & F_{32} \\ F_{41} & F_{42} \end{bmatrix} \begin{matrix} M_B \\ \\ M_T \\ \end{matrix} + \begin{Bmatrix} \delta_{f1} \\ \delta_{f2} \\ \delta_{f3} \\ \delta_{f4} \end{Bmatrix} + \begin{Bmatrix} \delta_{p1} \\ \delta_{p2} \\ \delta_{p3} \\ \delta_{p4} \end{Bmatrix} \quad (53)$$

Using Equation 53, the beam-column end slopes can be computed as follows:

$$\begin{Bmatrix} \theta_B \\ \theta_T \end{Bmatrix} = \begin{bmatrix} R_{BB} & R_{BT} \\ R_{TB} & R_{TT} \end{bmatrix} \begin{Bmatrix} M_B \\ M_T \end{Bmatrix} + \begin{Bmatrix} \theta_{fB} \\ \theta_{fT} \end{Bmatrix} + \begin{Bmatrix} \theta_{pB} \\ \theta_{pT} \end{Bmatrix} \quad (54)$$

in which:

$$\theta_B = (u_1 - u_{.1})/2h \quad (55a)$$

$$\theta_T = (u_{N+1} - u_{N-1})/2h \quad (55b)$$

$$R_{BB} = (F_{21} - F_{11})/2h \quad (55c)$$

$$R_{BT} = (F_{22} - F_{12})/2h \quad (55d)$$

$$R_{TB} = (F_{41} - F_{31})/2h \quad (55e)$$

$$R_{TT} = (F_{42} - F_{32})/2h \quad (55f)$$

$$\theta_{fB} = (\delta_{f2} - \delta_{f1})/2h \quad (55g)$$

$$\theta_{fT} = (\delta_{f4} - \delta_{f3})/2h \quad (55h)$$

$$\theta_{pB} = (\delta_{p2} - \delta_{p1})/2h \quad (55i)$$

$$\theta_{pB} = (\delta_{p4} - \delta_{p3})/2h \quad (55j)$$

where  $h$  is the member panel length. The beam-column end moments  $M_B$  and  $M_T$  are obtained from Equation 54 as:

$$\begin{Bmatrix} M_B \\ M_T \end{Bmatrix} = \begin{bmatrix} S_{BB}^{\lambda_B} & S_{BT}^{\lambda_T} \\ S_{TB}^{\lambda_B} & S_{TT}^{\lambda_T} \end{bmatrix} \begin{Bmatrix} \theta_B \\ \theta_T \end{Bmatrix} - \begin{Bmatrix} M_{pB} \\ M_{pT} \end{Bmatrix} - \begin{Bmatrix} M_{fB} \\ M_{fT} \end{Bmatrix} \quad (56)$$

in which:

$$\begin{Bmatrix} M_{fB} \\ M_{fT} \end{Bmatrix} = \begin{bmatrix} R_{BB} & R_{BT} \\ R_{TB} & R_{TT} \end{bmatrix}^{-1} \begin{Bmatrix} \theta_{fB} \\ \theta_{fT} \end{Bmatrix}$$

$$\begin{Bmatrix} M_{pB} \\ M_{pT} \end{Bmatrix} = \begin{bmatrix} R_{BB} & R_{BT} \\ R_{TB} & R_{TT} \end{bmatrix}^{-1} \begin{Bmatrix} \theta_{pB} \\ \theta_{pT} \end{Bmatrix}$$

Equation 56 represents modified slope-deflection matrix equation for an inelastic beam-column, and are hereafter referred to as *inelastic slope-deflection* equations.

This equation can be written in the following simplified form:

$$\{M_a\} = [S] \{\theta\} - \{M_f\} - \{M_p\} \quad (57)$$

where [S] is the beam-column tangent stiffness matrix;  $\{M_f\}$  and  $\{M_p\}$  are the load vectors resulting from the so-called *p-δ effects* and partial plastification. Equation 57 is derived relative to the member minor axis. A similar equation can also be derived for the major axis using the same procedure.

### 5.1.2 Equilibrium and Compatibility for Flexible-Connections

Initially it appears that the presence of flexible beam-column end connections may be accounted for in frame analysis as follows. If the effect of the connections is included in the [S] matrix of Equation 57, it poses a problem in satisfying the rotational compatibility condition correctly at member to spring junction when the spring stiffness is relatively large. For example, if very stiff rotational springs are associated with a girder, an incorrect inelastic *converged* deflected shape of the girder results while performing the member-level analysis owing to the fact that the springs tend to nearly fix the member end rotationally. Needless to say, a very stiff spring at a connection should not necessarily result in a zero connection rotation in a frame.

To circumvent the above-mentioned difficulty, the flexible end connection is simulated as a two-noded member of zero length. This is explained by means of a typical joint as shown in Figure 38. Three members numbered 1, 2, and 3 in this figure are connected at a joint J through flexible connections with stiffnesses  $k_{T1}$ ,  $k_{B2}$ , and  $k_{T3}$ . The joint J is subjected to a bending moment M. The end nodes of members 1, 2, and 3 are  $T_1$ ,  $B_2$ , and  $T_3$ , respectively. The connection lengths  $T_1J$ ,  $B_2J$ , and  $T_3J$  are each taken as zero. Equation 57 applied at  $T_1$ ,  $B_2$ , and  $T_3$ , without including the effect of the spring in the [S] matrix, results in the following inelastic equations:

$$M_{T1} = S_{TB,1} \theta_{B1} + S_{TT,1} \theta_{T1} - M_{fT1} - M_{pT1} \quad (58a)$$

$$M_{B1} = S_{BB,2} \theta_{B2} + S_{BT,2} \theta_{T2} - M_{fB2} - M_{pB2} \quad (58b)$$

$$M_{T1} = S_{TB,3} \theta_{B3} + S_{TT,3} \theta_{T3} - M_{fT3} - M_{pT3} \quad (58c)$$

The equilibrium equation at nodes  $T_1$ ,  $B_2$ ,  $T_3$ , and J can be written as:

$$M_{T1} + k_{T1} (\theta_{T1} - \theta_J) = 0 \quad (59a)$$

$$M_{B2} + k_{B2} (\theta_{B2} - \theta_J) = 0 \quad (59b)$$

$$M_{T3} + k_{T3} (\theta_{T3} - \theta_J) = 0 \quad (59c)$$

$$M + k_{T1} (\theta_{T1} - \theta_J) + k_{B2} (\theta_{B2} - \theta_J) + k_{T3} (\theta_{T3} - \theta_J) = 0 \quad (59d)$$

In these equations,  $\theta_{T1}$ ,  $\theta_{B2}$ , and  $\theta_{T3}$  are the member end rotations, and  $\theta_J$  is the joint rotation. Equations 59(a) through 59(d) also satisfy the rotational compatibility condition. It is necessary to point out that Equations 59(a) through 59(d) need to be employed carefully when relatively stiff springs are present.

### 5.1.3 Analysis of Flexibly-Connected Imperfect Frame

#### 5.1.3.1 Portal Frame

Figure 39 shows a schematic diagram of a flexibly-connected nonsway plane portal frame. The frame consists of two columns AB and CD of equal length  $L_c$  and a girder BC of length  $L_b$ . The columns are partially restrained elastically at supports A and D and are joined to the girder at B and C. The beam-to-column connections at B and C are represented by rotational springs. The members in the portal frame are imperfect with the column out-of-straightness defined by Equation 17 and the girder out-of-straightness defined by Equation 18. The columns AB and CD are oriented to bend about their minor axis while the girder BC bends about its major axis. The frame is subjected to axial loads,  $P_3$  and  $P_6$ , and bending moments,  $M_3$  and  $M_6$  at specified joints nonproportionally. In this dissertation, numerical examples of frames with I-section members are presented. However, the computer programs developed can also be used for frames with rectangular hollow section members. A sample portal frame having symmetric geometry and loading can be modeled and analyzed as an equivalent beam-column. For example, setting  $P_3 = P_6 = P$ ;  $M_3 = M_6 = M$ , and taking  $+u_i$  for the member AB in Figure 39, an equivalent model as shown in Figure 40 can be deduced for the left half of the frame. This modeling is valid only if the girder BC is elastic and carries negligibly small axial load throughout the load history. Under these conditions, the equivalent spring stiffness,  $k_e$ , at B of the model is given by:

$$k_e = 2EI_g/L_g [1/(1+2EI_g/kL_g)] \quad (60)$$



where  $g$  refers to the girder. This equivalent model allows a direct use of the beam-column analysis procedure given in Chapter 4.

For a frame which cannot be modeled in the manner described above due to geometric or loading asymmetry, the detailed inelastic slope-deflection equations in Section 5.1.1 must be utilized for each member of the frame. For the frame in Figure 39, Equation 57 applied to each member gives:

$$M_{23} = S_{22} \theta_2 + S_{23} \theta_3 - M_{f23} - M_{p23} \quad (61a)$$

$$M_{32} = S_{32} \theta_2 + S_{33} \theta_3 - M_{f32} - M_{p32} \quad (61b)$$

$$M_{45} = S_{44} \theta_4 + S_{45} \theta_5 - M_{f45} - M_{p45} \quad (61c)$$

$$M_{54} = S_{54} \theta_4 + S_{55} \theta_5 - M_{f54} - M_{p54} \quad (61d)$$

$$M_{67} = S_{66} \theta_6 + S_{67} \theta_7 - M_{f67} - M_{p67} \quad (61e)$$

$$M_{76} = S_{76} \theta_7 + S_{77} \theta_7 - M_{f76} - M_{p76} \quad (61f)$$

Also, the following joint equilibrium and compatibility conditions must be enforced:

$$M_{23} + k (\theta_2 - \theta_1) = 0 \quad (62a)$$

$$M_{45} + k (\theta_4 - \theta_3) = 0 \quad (62b)$$

$$M_{54} + k (\theta_5 - \theta_6) = 0 \quad (62c)$$

$$M_{76} + k (\theta_7 - \theta_8) = 0 \quad (62d)$$

$$M_{32} + k (\theta_3 - \theta_4) + M_3 = 0 \quad (62e)$$

$$M_{67} + k (\theta_6 - \theta_7) - M_6 = 0 \quad (62f)$$

It should be noted that Equation 62(e) and 62(f) are the total joint equilibrium equations. The geometric boundary conditions are:

$$\theta_1 = \theta_8 = 0 \quad (63)$$

that is, there is no rotational settlement of ground supports at A and D. Upon substitution of Equations 61(a) through 61(f) and 63, Equations 62(a) through 62(f) can be written in the following matrix form:

$$[K_G] \{\theta_G\} = \{M_{fG}\} + \{M_{pG}\} + \{M_G\} \quad (64)$$

Here the subscript G is used to emphasize that this is a global frame equilibrium equation. Equation 64 is solved for  $\{\theta_G\}$  iteratively for the frame response prediction. The vector  $\{M_{fG}\}$  has terms like  $M_{f23}$ ,  $M_{f32}$ , . . . of Equations 61(a), 61(b), . . . , and are dependent upon the axial load P and the member displacements. The vector  $\{M_{pG}\}$  has terms like  $M_{p23}$ ,  $M_{p32}$ , . . . of Equations 61(a), 61(b), . . . , and are dependent upon the internal plastic force parameters. The vector  $\{M_G\}$  contains the externally applied joint moments and includes terms like  $M_3$  and  $M_6$  of Equations 62(e) and 62(f).

### 5.1.3.2 Two-Bay Two-Story Frame

A schematic diagram of an imperfect two-bay two-story nonsway frame is given in Figure 41. The frame consists of three continuous columns loaded relative to their minor axis, and four girders loaded about their major axis. Each member of the frame has a length L. The beam-to-column connections are simulated as elastic springs with a constant rotational stiffness k. The frame is subjected to joint loading consisting of axial loads, P, and/or bending moments, M. Following a procedure similar to that presented in Section 5.1.3.1, the governing equilibrium equations for

this problem can be obtained in the form given by Equation 64.

## 5.2 Load Paths and Combinations

### 5.2.1 Load Paths

With reference to Figure 15, following load paths are used for the numerical study presented in Section 5.4:

NP9: Both  $p$  and  $\bar{m}$  are applied simultaneously in a proportional manner with a proportionality constant,  $\zeta$ , defined as:

$$\zeta = \bar{m}/p \quad (65)$$

NP9 corresponds to the path OB.

NP10: An axial load  $p = p^*$  is applied first, followed by both  $p$  and  $\bar{m}$  applied simultaneously, satisfying the relationship:

$$p = \bar{m} + p^* \quad (66)$$

NP10 corresponds to the path OHB.

NP11: Both  $p$  and  $\bar{m}$  are applied simultaneously in a proportional manner, as in Equation 65, until  $\bar{m}$  reaches the ultimate value obtained in NP10. This is followed by an increase in the axial load  $p$  while holding  $\bar{m}$  constant. NP11 corresponds to the path OIB.

The loads are incremented until the load-carrying capacity of the structure is reached. When load path NP9 is used, the analysis is carried out following the stress-strain laws given in Figures 3(a) as well as 3(b) for a critical view on the tangent modulus approach which neglects elastic unloading.

### 5.2.2 Load Combinations

Unlike for a single member, the portal and two-bay two-story frames can be subjected to various load combinations due to the presence of a number of joints. The following load combinations are utilized in the present study.

#### a. Portal frame

Referring to Figure 39:

FL1: An axial load  $P_3 = P$ , and a *counterclockwise* bending moment  $M_3 = M$  are used while keeping  $P_6 = M_6 = 0$ .

FL2: Same loading as FL1, except that the bending moment  $M_3 = M$  is applied *clockwise*.

FL3: In addition to the loads in FL1,  $P_3 = P$  and  $M_3 = M$  are used.

FL4: The same loading condition as in FL3 is used, except that  $M_3$  and  $M_6$  are reversed in direction.

#### b. Two-bay two-story frame

Referring to Figure 41:

FL5:  $P$  and  $M$  are applied at joint A only.

FL6: The loading is the same as in FL5, except that  $M$  is *clockwise*.

FL7: All the loads shown at the joints A through F are applied.

FL8: The loading is the same as in FL7, except that the direction of  $M$  is reversed.

### 5.3 Solution Procedure

Equation 64 is materially nonlinear since the stiffness matrix  $[K_G]$  and the moment vectors  $\{M_{rG}\}$  and  $\{M_{pG}\}$  are dependent upon the deformation vector  $\{\theta_G\}$ . The following iterative scheme is devised to predict the load-deformation

response of the frame:

1. Evaluate the initial elastic properties for each member and deduce Equation 57 for each member.
2. Assemble global stiffness matrix  $[K_G]$  in equation 64.
3. Prescribe small loads and formulate the load vectors  $\{M_{fG}\}$  and  $\{M_{pG}\}$  in Equation 64.
4. Solve Equation 64 for a set of deformations  $\{\theta_G\}$ .
5. Compute the member end moment vectors  $\{M_a\}$  using Equation 57. Next, determine the member end actions using simple statics, and formulate the load vector  $\{M\} = \{M\}_i$  in Equation 37(a). Here,  $i$  refers to the iteration number.
6. Analyze the members with  $\{M\}_i$  individually using the procedure given in Chapter 4, and compute the converged member stiffness matrices  $[K]$  in Equation 37(a).
7. Update the inelastic slope-deflection Equation 57 for each member, reassemble  $[K_G]$ ,  $\{M_{fG}\}$  and  $\{M_{pG}\}$ , and update  $\{\theta_G\}$  using Equation 64.
8. Recompute the member end moment vectors  $\{M_a\}$  using Equation 57, and update  $\{M\} = \{M\}_{i+1}$  in Equation 37(a).
9. If  $|\{M\}_{i+1} - \{M\}_i| \leq \{\alpha\}$ , where  $\{\alpha\}$  is the tolerance taken as 0.01%, go to Step 11.
10. Set  $\{M\}_i = \{M\}_{i+1}$ , and go to Step 6.
11. If  $|[K_G]| \rightarrow 0$ , go to Step 13.
12. Increase (or change) the external loads, that is,  $P$  and/or  $M$ , update the load vectors  $\{M_{fG}\}$  and  $\{M_{pG}\}$  in Equation 64, and go to Step 4.

### 13. Stop.

The solution procedure described herein is programmed on a sequential computer using FORTRAN and named NONPRFRM. A listing of this computer program is included in Appendix E.

## 5.4 Numerical Study

To gain an in-depth understanding of the behavior of the nonsway plane frames referred to in Section 5.1.2, an extensive numerical study is conducted using the solution procedures described in Chapter 4 and Section 5.3. Since the number of variables is quite large, the material properties and the dimensions of the members are fixed. Each beam-column is a W 8x31 section loaded about its minor axis. Each girder, however is a S 12x31.8 section loaded about its major axis. The length of each member is taken as 15 ft. The frame is A36 steel, that is, with  $E = 29,000$  ksi,  $\sigma_y = 36$  ksi, and following the  $\sigma$ - $\epsilon$  relationship of either Figure 3(a) or 3(b). The following two magnitudes of the initial crookedness amplitudes are used for the beam-columns:

$$u_{01} = L/1000 \quad (67)$$

$$u_{02} = L/100,000 \quad (68)$$

Similarly, the initial crookedness amplitudes for the girders are:

$$v_{01} = L/1000 \quad (69)$$

$$v_{02} = L/100,000 \quad (70)$$

Each connection behaves elastically with a stiffness  $k = 13,333$  in-kip/rad. A linear moment-rotation relationship is adopted since the beam-column behavioral study in Chapter 4 indicated that this type of connection provides significant load path

dependency.

#### 5.4.1 Equivalent Structural Model

This section contains the outcome of a numerical study of the portal frame in Figure 39 and its equivalent structural model in Figure 40 under the symmetry conditions described in Section 5.1.2. Referring to Figure 40, three types of equivalent structures E1, E2, and E3 with  $u_{0i}$  values in Equation 17 given by  $+u_{01}$ ,  $-u_{01}$ , and  $+u_{02}$ , respectively, are considered. A total of 16 equivalent models designated as C1 through C16 are considered to investigate the influence of load paths NP9, NP10, and NP11 on their behavior. The stress-strain relationship shown in Figure 3(a) is adopted for all of the cases except for C14 and C16 for which the relationship ignoring material unloading shown in Figure 3(b) is used. The maximum axial load,  $p_{\max}$ , and the maximum applied moment,  $\bar{m}_{\max}$ , as found from the analysis are given in Table 19.

Figures 42 through 44 present some of the key results of the study graphically. Figure 42 exhibits the dimensionless load versus applied moment ( $p$ - $m$ ) relationships for the three load paths NP9, NP10, and NP11 and the cases C1, C2, C13, and C14 for E1. With NP10,  $p_{\max}$  and  $\bar{m}_{\max}$  are found to be 0.84, and 0.33, respectively, for case C1. With NP11,  $\bar{m}_{\max}$  and  $p_{\max}$  are found to be 0.33, and 0.86, respectively, for C2. With NP9, the case C13 based on  $\sigma$ - $\epsilon$  relationship in Figure 3(a) provides a somewhat greater maximum load-carrying capacity than that for C14 with  $\sigma$ - $\epsilon$  relationship in Figure 3(b). Also, the maximum moments obtained for the cases C1 and C2 are found to be significantly less than those obtained for C13 and C14. For example, case C13 provides a moment capacity of 0.80 which is 0.47 in excess of that

for C1 while the axial loads do not differ significantly.

Figure 43 shows dimensionless load versus column midheight deflection ( $p\bar{u}_c$ ) relationships for the cases C1, C2, C13, and C14 of frame E1. The deflection is nondimensionalized by one half the member flange width. The  $p\bar{u}_c$  responses obtained for the cases C1 and C2 with NP10 and NP11, respectively, indicate that the deflections are positive throughout the history of loading. However, the deflections changed their sign during the loading for the cases C13 and C14 with NP9, since the end moments had a more dominant effect as compared with the so-called P-delta effect.

Figure 44 shows stiffness degradation curves corresponding to the cases C1, C2, C13, and C14. In this figure,  $D$  is the dimensionless determinant defined in Equation 43. The  $D$ - $p$  curves for the cases C1, C2, and C13 in Figure 44 show *valleys* in the form of rapid changes in  $D$  indicating that considerable strain reversal is present in the structure. Similar findings were also observed for beam-column studies in Chapter 4. Such valleys, however, are not observed for the case C14 since the material unloading is not included.

#### **5.4.2 Portal Frame Behavior**

The portal frame shown in Figure 39 is first analyzed numerically under various load histories. Later, extensive additional computer runs were made to generate load-moment interaction curves. The load combinations FL1 through FL4 with the load paths NP9 through NP11 described in Section 5.2 are utilized to analyze 6 types of portal frames with various configurations of the initial crookedness. These frames are designated as FR1 through FR6 and are described below:



- FR1: All of the members AB, BC, and CD are nearly perfect, with  $u_{0i}$  in Equation 17 given by  $u_{02}$  in Equation 68 for members AB and CD, and with  $v_{0i}$  in Equation 18 given by  $v_{02}$  in Equation 70 for member BC. The  $u_i$  for members AB and CD is as shown in Figure 39 while  $v_i$  for member BC is opposite to that shown in this figure.
- FR2: The members AB and CD are initially crooked as shown in Figure 39 with the midspan amplitudes equal to  $u_{01}$  in Equation 67, and  $v_i$  for BC is opposite to the direction shown in this figure with its midspan amplitude given by Equation 69.
- FR3: The member AB is nearly perfect as for the frame FR1, with  $u_{0i} = u_{02}$ , and the members BC and CD are initially crooked as for the frame FR2.
- FR4: The members AB and BC are initially crooked as in FR2, and the member CD is nearly perfect as for the frame FR1.
- FR5: The member AB is initially crooked as in FR2, the member CD is initially crooked in the direction opposite to that indicated in Figure 39, with  $u_{0i} = u_{01}$  in Equation 67, and the member BC is initially crooked as for the frame FR2.
- FR6: The configuration of this frame is the same as FR5, except that the lateral support at C is replaced by a support at B.

The frame FR6 is analyzed in order to gain an insight into the nature of the induced girder axial load and its effect on the frame behavior. The parametric study conducted thus encompasses the frames FR1 through FR6 and the frame loadings FL1 through FL4 for the load paths NP9, NP10, and NP11. For NP10,  $p^*$

in Equation 65 is taken as 0.5.

The numerical results for frames FR1 through FR6 are summarized in Tables 20 and 21. The peak loads obtained for the frames FR1 through FR4 with FL1 and FL2 following the three load paths NP9, NP10, and NP11 are given in Table 20. The results clearly indicate that the nonproportional load paths NP10 and NP11 result in substantially different maximum load-carrying capacities as compared to that resulting from the proportional load path NP9. For the frame FR2 with FL1, for example, the load paths NP10 and NP11 result in practically the same peak loads,  $p_{\max} = 0.71$  and  $\bar{m}_{\max} = 0.21$ , whereas NP9 results in  $p_{\max} = 0.64$  and  $\bar{m}_{\max} = 0.64$ . Similar observations are also made for other frames included in this table.

Table 21 summarizes the maximum loads for frames FR1, FR2, FR5, and FR6 for FL3 and FL4 with NP9 through NP11. It should be noted that the structural model used in Section 5.4.1 is equivalent to the frames FR1 and FR2 for the load combinations FL3 and FL4. The peak loads for FR1 with NP10 and NP11 in Table 21 are found to be practically the same as those for the equivalent structural models C9 through C12 in Table 19. Also, the peak loads for the frame FR2 with load paths NP10 and NP11 are fairly similar to those obtained for the cases C1 through C8. However, the maximum loads for the cases C13 through C16 are somewhat greater than those for the frame FR2 with the load path NP9. This discrepancy is attributed to the *softening* effect of the induced axial compression in the girder. This means that a somewhat over-estimated value of  $k_e$  is used in the equivalent structural model.

Figures 45 through 53 present the key results obtained for the portal frame FR2 with the load combination FL3. The overall frame behavior is presented in Figures 45 through 48 and the response of the beam-column AB of this frame is shown in Figures 49 through 52. The load-deformation response of the frame is represented by the dimensionless axial load,  $p$ , versus the joint rotation,  $\theta_A$  relationship. When the proportional load path NP9 is used, the  $p$ - $\theta_A$  relations for FR2 based on the material curves of Figure 3(a) or 3(b) are nearly the same, as shown in Figure 45. The corresponding stiffness degradation curves are shown in Figure 46. It is interesting to note that the curve with the tangent modulus approach shows a significant loss of frame stiffness compared with that including material unloading. The members of the frame, with material elastic unloading included, experience considerable redistribution of stresses resulting in localized strain reversals.

Figures 47 and 48 show, respectively the  $p$ - $\theta_A$  and  $D$ - $p$  relationships for the frame FR2 with the load combination FL3 and subjected to the load paths NP10 and NP11. For NP10, the  $p$ - $\theta_A$  relation indicates a slight reduction in the joint rotation as the loads are increased. The probable cause of such a reduction in deformations may be explained as follows. Throughout the loading history of the frame, the beam-column AB exhibits a reverse curvature that is to say that it is bent in an *S-curve* because of the presence of the rotational restraints at the base of the frame. Also, the beam-column experiences substantial yielding as the loads reach the maximum load-carrying capacity of the frame. At this instant, the rotational restraints tend to cause a *snap-through* type of beam-column deformation, thus

elastically unloading the beam-column to gain enough strength to resist the snap-through type of deformations. Eventually, the structure fails due to the instability of beam-columns. Figure 51 showing the load-deformation response of the beam-column AB clearly substantiates these conclusions by indicating a reduction in the member displacements followed by further increase as the load is incremented.

The stiffness degradation curves for the frame FR2 with FL3 and the beam-column AB of this frame are shown in Figures 48 and 52, respectively. These curves exhibit the presence of substantial unloading in the form of *valleys*. Similar observations are also made in a number of the frame results.

To generate the interaction curve between  $p$  and  $\bar{m}$ , frame FR2 with load combination FL3 with the load path NP9 is considered. The following 9 different proportionality constants,  $\zeta$ , defined by Equation 65 are used for the analysis:

$$\begin{array}{lll}
 \zeta = 0.00 & \zeta = 0.25 & \zeta = 0.50 \\
 \zeta = 1.00 & \zeta = 2.00 & \zeta = 4.00 \\
 \zeta = 8.00 & \zeta = 20.00 & \zeta = \infty
 \end{array} \tag{71}$$

The results from the analysis are graphically represented by an interaction curve shown in Figure 53. The results from the numerical studies with the load paths NP10 and NP11 are also plotted in the form of data points. Figure 53 is noticed to predict frame maximum loads accurately. Within the parameters considered herein, this interaction curve forms an envelope to predict the strength of the frame FR2.

### 5.4.3 Two Bay Two-Story Frame Behavior

The two-bay two-story frame shown in Figure 41 is analyzed first for various

load histories, followed by extensive additional analyses to construct a load-moment interaction envelope. The following two different frames with prescribed initial crookedness configurations are used in the numerical study:

FR7: Frame with nearly perfect members, that is, each of the beam-column has  $u_{0i} = u_{02}$  given by Equation 68 and each of the girder has  $v_{0i} = v_{02}$  given by Equation 70 with all of the members initially curved as shown in Figure 41.

FR8: Frame with the Beam-columns ADG and CFI are initially crooked as shown in Figure 41 with each member having  $u_{0i} = u_{01}$  in Equation 67, and the girders are initially crooked as shown in this figure with each girder having  $v_{0i} = v_{01}$  as given in Equation 69.

The frames FR7 and FR8 are subjected to the four load combinations FL5 through FL8 and load paths NP9 through NP11 described in Section 5.2. In this study,  $p^* = 0.50$  is used in Equation 65 for load combinations FL5 and FL6, and  $p^* = 0.25$  is used for the loading combinations FL7 and FL8.

Table 22 presents a summary of the results obtained for the frames FR7 and FR8 with load combinations FL5 through FL8 when subjected to the proportional load path NP9, and the nonproportional load paths NP10 and NP11. A review of the maximum loads recorded in this table indicates that the load path NP9 predicts moment capacities unconservatively when compared to those obtained for the load paths NP10 and NP11. For example, for the frame FR8 with FL6, NP9 gives  $\bar{m}_{\max} = 0.68$ , whereas NP10 or NP11 predict  $\bar{m}_{\max} = 0.22$ . Similar differences in moment capacities is observed for all of the frames included in Table 22.

An examination of the computer output for the frame FR8 with load combination FL8 subjected to the load path NP11 indicated that the maximum load-carrying capacity of this frame is governed by the failure of the beam-column EH in contrast to a general expectation of a failure of either DG or FI in Figure 41. This unpredictable behavior is explained as follows. The computer output revealed that considerable yielding of the beam-columns DG and FI takes place when the inelastic action is initiated in the frame. Further change in the applied loads activate the nearly perfect beam-column EH to share somewhat of a greater load relative to the yielded beam-columns DG and FI. During such redistribution of loads, the beam-columns DG and FI experience material unloading thereby gaining some amount of stiffness. This material unloading is caused by the restraining effect offered by the member end partial rotational restraints. This process continues in the beam-columns DG and FI while the member EH begins to plastify. The restraining, however, is not felt by the beam-column EH since it is nearly straight, additionally, the symmetrical bending of the frame induces no significant bending moments on EH. Consequently, the beam-column EH is deprived of any possible material unloading while the members DG and FI continue to redistribute the internal loads. Finally, the beam-column EH becomes completely plastic resulting in the eventual collapse of the frame.

The results corresponding to those reported in Table 22 for FR8 with FL7 are shown graphically in Figures 54 through 62. A detailed study of these results indicate the two-bay two-story frame behavior to be consistent with that of the portal frame studies reported in Section 5.4.2. The interaction diagram for the frame FR8

with FL7 shown in Figure 62 is constructed by carrying out a number of frame analyses using the different values of the proportionality constants given from Equation 71. Here, the interaction curve is found to form an envelope closely predicting the maximum strength of the frame for various load paths.

## 6. CONCLUSIONS AND FUTURE RESEARCH

The main thrust of this investigation is on a rigorous analysis of the influence of nonproportional loads on the inelastic response of imperfect beam-columns and flexibly-connected steel nonsway plane frames. The analysis is performed using a finite-difference technique combined with an iterative solution procedure. A set of inelastic slope-deflection equations is derived and utilized for the frame analysis. The suitability of concurrent computing is investigated through inelastic analysis of cross sections and biaxially imperfect columns. The main computational work, however, is performed using the sequential computer.

A number of examples have been presented throughout this dissertation encompassing the above-mentioned inelastic problems. The cross-sectional and member studies include both I-sections and hollow rectangular sections. The frame studies are limited to I-section members to restrict the volume of research.

The conclusions drawn from this research are discussed in the following sections and appropriate recommendations for further research are made at the end.

### 6.1 Conclusions

To conveniently present the conclusions, the studies are grouped into three categories, namely, (i) Concurrent Computing Studies, (ii) Beam-Column Studies, and (iii) Frame Studies. Various conclusions drawn for each category are discussed



here.

### **6.1.1 Concurrent Computing**

The effectiveness of concurrent computing using the Finite Element Machine is studied and the corresponding conclusions are presented as follows:

#### **A. Cross-sectional analysis**

1. A maximum speedup factor of 7.69 is achieved on eight processors resulting in an efficiency of 96.1 per cent.
2. The minimum speedup factor for the study is found to be 7.09 on eight processors which corresponds to 88.6% efficiency.
3. The speedup factors increased as the number of processors are reduced. This is primarily due to an efficient distribution of computational load between the processors and also reduction in communication time between the processors.

#### **B. Column studies**

1. In general, the execution times required to analyze hollow rectangular columns (CN5-CN8) are greater than those for the hollow square columns (CN1-CN4). This difference in computational time is explained as follows. The hollow rectangular column began yielding at a lower load level due to the smaller bending resistance about the minor axis and resulted in a greater number of cycles for convergence in the nonlinear range compared to the hollow square column.
2. The speedup factors are found to be of the same order for both hollow square and rectangular columns although larger computational times are needed for

the latter ones.

3. The communication overhead needed is negligibly small since the analysis is dominated by extensive arithmetical computations on all processors. The development of the algorithm exploits the inherent quality of processors that are designed to be efficient computers. Therefore, algorithms which exploit this property will derive efficient speedups.
4. Generally, the computational time needed to analyze the structure increases with the degree of end fixity of the column.
5. The computational efficiency decreases as the number of processors increase, suggesting an optimal limit on the number of processors that may be employed.

In summary, the concurrent computing algorithms are found to be efficient to analyze this class of nonlinear problems.

### **6.1.2 Beam-Columns**

Specific studies on beam-columns include an investigation of the restraint modeling, and a behavioral study of uniaxially and biaxially loaded I-section beam-columns and biaxially loaded hollow rectangular section beam-columns subjected to various load paths. The following conclusions are drawn from the numerical studies:

#### **A. Restraint modeling effect on beam-columns**

1. The studies indicate that the end restraints can be practically modeled by a simple linear or at the most a bilinear moment-rotation relation.
2. The beam-column analyses predict that the strength of the members is not highly sensitive to the connection modeling.

3. When the connection possesses a relatively large stiffness, a simple linear model will provide accurate connection response.
  4. These models in general provide simple and accurate moment-rotations relationship for a connection spring.
- B. Nonproportionally loaded I-section beam-columns
1. The major axis response of beam-columns is not load path dependent for all practical purposes.
  2. The minor axis response of beam-columns is load path dependent when elastic rotational restraints are present.
  3. With elastic-plastic end restraints, the load paths provide nearly the same peak loads.
  4. For load paths NP1 and NP2, the load conditions LC1 and LC2 provide nearly the same peak loads, while load paths LC3 and LC4 exhibit a substantial difference for the minor axis loading when elastic restraints are present.
  5. A consideration of appropriate nonproportional loadings may provide greater allowable loads for beam-columns with elastic end restraints.
  6. Neglecting the effects of material unloading may lead to unconservative estimation of load-carrying capacity of beam-columns.
  7. A greater degree of unconservativeness results for the biaxially loaded beam-columns.
  8. Considerable redistribution of stresses takes place along the member length in the inelastic range.
  9. The study on beam-columns with proportional loads indicated that the tangent

modulus approach exhibits a *fictitious* ductile behavior of the member. Such fictitious ductility is not noticed in the experimental investigations.

C. Nonproportionally loaded hollow rectangular beam-columns:

1. Significant load dependence exists for biaxially loaded hollow rectangular beam-columns.
2. Critical combination of loadings in a load path may dramatically change the strength of the member in comparison to yet another the load path(s).
3. The load path dependence disappears only for certain load combinations, or for the special case of pinned boundaries.
4. Considerable material unloading is present and is indicated in the form of *valleys* in the stiffness degradation curves.
5. Substantially a greater number of cross-sectional elemental areas are required when the analysis includes material unloading.
6. The members analyzed using the tangent modulus approach exhibit a fictitious yield plateau in contrast to the relatively less ductile behavior observed in experimental investigations.

### 6.1.3 Frame Studies

The following conclusions are derived from the frame studies conducted in this research:

A. Equivalent structural model

1. The peak loads for imperfect structure are larger than those for the nearly perfect structural model when the applied moment causes deflection opposite

to the initial crookedness.

2. Nearly the same peak loads result for structural models subjected to load paths NP10 and NP11.
3. The strength of nonproportionally loaded equivalent structural model is substantially less than that of the proportionally loaded one.
4. There is a dramatic difference in the behavior between the nonproportionally loaded and the proportionally loaded structures.
5. In some cases, the equivalent structural model provided unconservative peak loads compared to the corresponding frame analyses results.

B. Portal and two-bay two-story frames

1. The inelastic slope-deflection equation method of frame analysis is found to be simple and practical.
2. The number of degrees of freedom involved for the global frame response prediction is quite small due to the inelastic slope-deflection method.
3. Specific case studies for the portal frame analyses compared with those of equivalent structural model indicated that the frame analysis procedures are reliable.
4. The effect of *P-delta* effects on girders is found to be significant for some of the portal frames analyzed.
5. The maximum load-carrying capacity of frames, in general, are found to be unconservative when tangent modulus approach was used.
7. For the frames considered, the girders in general exhibited elastic behavior.
8. The frame analyses using tangent modulus unloading of the material did not

exhibit a large yield plateau unlike in the case of individual member studies even when the tangent modulus approach is used.

9. Substantial redistribution of loads takes place in the inelastic range for the frames.
10. There is a significant difference in the behavior between the nonproportionally and proportionally loaded frames.
11. For portal frames, the failure in general is governed by the instability failure of the beam-columns.
12. When the lateral support location is altered in the frame as in FR6 relative to FR5, the girder experienced a tensile axial load indicating that the location of lateral support can alter the behavior of girders.
13. For two-bay two-story frames, the outer columns experienced considerable redistribution of stresses and the frame maximum loads are attained when the lower story central beam-column eventually failed due to inelastic instability, in contrast to the generally expected failure of the initially crooked outer beam-columns.
14. The interaction diagrams developed for the frames form a type of maximum load envelope which govern the maximum load-carrying capacity for these frames when subjected to various load paths.

The present study clearly indicates that the combined influence of nonproportional loads, imperfections, and flexible connections on the behavior and strength of structural members and frames is very significant. In general, proportionally loaded structures provided unconservative maximum loads for beam-

columns as well as frames. The inelastic slope-deflection equations developed for the frame analysis are found to efficient and simple for practical use.

## **6.2 Future Research**

Considering the scope of the present research the following recommendations are made for future investigations.

1. No verifiable data is available at present in the literature to experimentally corroborate the theoretical developments in this study. Therefore, experimental investigation of the structural behavior investigated herein will be a challenge in the future.
2. The inherent potential for parallelization of this theoretical formulation makes it a suitable candidate for application on concurrent computers.
3. The concept of the inelastic slope-deflection equations for beam-columns may be extended to investigate the behavior of sway frames.
4. Modifications of member equilibrium equations to include member loads in addition to the applied nodal loads will enhance the analytical capability of the computer program developed herein.
5. The theoretical formulations developed for plane frame analyses may be extended to study the behavior of space frames.
6. An experimental investigation of various load paths in real-life structures may be performed for use in the future research.
7. The torsional effects of the open section members may be incorporated into the present analysis to enhance its scope.

## REFERENCES

1. Engesser, F., *Schweizerische Bauzeitung*, Vol. 26, 1895.
2. Euler, L., "Elastic Curves," Translated and Annotated by Oldfather, W. A., Ellis, C. A., and Brown, D. M., 1933.
3. Shanley, F. R., "Inelastic Column Theory," *Journal of Aeronautical Sciences*, Vol. 14, 1947.
4. Osgood, W. R., "The Effect of Residual Stress on Column Strength," *Proceedings of First National Congress of Applied Mechanics*, June, 1951.
5. Duberg, J. E., and Wilder, T. W., "Inelastic Column Behavior," *NACA Technical Note*, No. 2267, Washington, D. C., January, 1951.
6. Huber, A. W., and Beedle, L. S., "Residual Stress and Compressive Strength of Steel," *The Welding Journal*, Vol. 33, December, 1954.
7. Ketter, R. L., "Stability of Beam-Columns above Elastic Limit," *Proceedings of ASCE*, Vol. 81, Separate No. 692, May, 1955.
8. Driscoll, G. C., and Beedle, L. S., "The Plastic Behavior of Structural Members and Frames," *The Welding Journal*, Vol. 36, No.6, June, 1957.
9. Munse, W. H., Bell, W. G., and Chesson, E., "Behavior of Riveted and Bolted Beam-to-Column Connections," *Journal of Structural Division*, ASCE, Vol. 85, March, 1959.
10. Galambos, T. V., "Influence of Partial Base-Fixity on Frame Stability," *Journal of the Structural Division*, ASCE, Vol. 86, No. ST5, May, 1960.
11. Galambos, T. V., and Ketter, R. L., "Columns Under Combined Bending and Thrust," *Transactions of ASCE*, Vol. 126, Part I, 1961.
12. Ketter, R. L., "Further Studies on the Strength of Beam-Columns," *Proceedings of ASCE*, Vol. 87, No. ST6, August, 1961.
13. Galambos, T. V., and Prasad, J., "Ultimate Strength Tables for Beam-Columns," *Welding Research Council Bulletin*, No. 78, June, 1962.



14. Saap, D. A., "Inelastic Stability of Rectangular Frames," *Ph. D. Dissertation*, University of Illinois, Urbana-Champaign, 1964.
15. Citipitioglu, E., "Stability of Rigid-Jointed Space Frames," *Ph. D. Dissertation*, Oklahoma State University, Oklahoma, 1965.
16. Dwyer, T. J., and Galambos, T. V., "Plastic Behavior of Tubular Beam-Columns," *Journal of the Structural Division*, ASCE, Vol. 91, No. ST4, August, 1965.
17. Driscoll, G. C., et al, "Plastic Design of Multi-Story Frames," *Fritz Engineering Laboratory Report*, No. 273.20, Lehigh University, Bethlehem, Pennsylvania, 1965.
18. McVinnie, W. W., "Elastic and Inelastic Buckling of an Orthogonal Space Frame," *Ph. D. Dissertation*, University of Illinois, Urbana-Champaign, 1966.
19. Culver, G. C., "Exact Solution of the Biaxial Bending," *Journal of the Structural Division*, ASCE, Vol. 92, No. ST2, April, 1966.
20. Korn, A., "The Elastic-Plastic Behavior of Multistory, Unbraced, Planar Frames," *Ph. D. Dissertation*, Washington University, St. Louis, Missouri, 1967.
21. Birnsteil, C., "Experiments on H-Columns Under Biaxial Bending," *Journal of the Structural Division*, ASCE, Vol. 94, No. ST10, October, 1968.
22. Lu, L. W., and Kamalvand, H., "Ultimate Strength of Laterally Loaded Columns," *Journal of the Structural Division*, ASCE, Vol. 94, No. ST6, June, 1968.
23. Galambos, T. V., *Structural Members and Frames*, Printice Hall, Inc./Englewood Cliffs, New Jersey, 1968.
24. Lewitt, C. S., Chesson, E., and Munse, W. H., "Restraint Characteristics of Flexible Rivetted and Bolted Beam-To-Column Connections," *Engineering Experiment Station Bulletin*, No. 500, University of Illinois at Urbana-Champaign, January, 1969.
25. Sharma, S. S., and Gaylord, E. H., "Strength of Steel Beam-Columns with Biaxially Eccentric Load," *Journal of the Structural Division*, ASCE, Vol. 95, No. ST12, December, 1969.
26. Romstad, K. M., and Subramanian, C. V., "Analysis of Frames with Partial Connection Rigidity," *Journal of the Structural Division*, ASCE, Vol. 96, No. ST11, November, 1970.
27. Gupta, S. P., and Agarwal, M. K., "Ultimate Strength of Beam-Column Hinged

- at Both Ends," *Journal of the Institute of Engineers (India)*, Civil Engineering Division, Vol. 54, Patr CI3, January, 1974.
28. Harung, H. S., Elektr Sveisning A/S, B. N., Miller, M. A., and Brotton, D. M., "Imperfections in Axially Loaded Plane Frames," *International Journal of Numerical Methods in Engineering*, Vol. 8, n4, 1974.
  29. Nair, R. S., "Overall Elastic Stability of Multistory Buildings," *Journal of the Structural Engineering*, ASCE, Vol. 101, n12, December, 1975.
  30. Wood, B. R., Beaulieu, D., and Adams, P. F., "Failure Aspects of Design by P-Delta Method," *Journal of Structural Engineering*, ASCE, Vol. 102, n3, March, 1976.
  31. Lispon, S. L., "Single-Angle Welded-Bolted Connections," *Journal of the Structural Division*, ASCE, Vol. 103, No. ST3, March, 1977.
  32. Simitzes, G. J., and Kunadis, A. N., "Nonlinear Buckling Analysis of Imperfection Sensitive Simple Frames," *International Colloquium on Stability of Structures Under Static and Dynamic Loads*, Washington, D. C., May, 1977.
  33. Hayashi, K., and Yokoyama, M., "Direct Simulation Of Engineering Problems With a Fast Array Computer," *Bulletin of the Japan Society of Mechanical Engineers*, Vol. 20, No. 149, 1977.
  34. Chen, W. F., and Atsuta, T., *Theory of Beam-Columns*, Vol. 2, McGraw-Hill, Inc., New York, 1977.
  35. Smith, B., "A Pipelined Shared Resource MIMD Computer," *Proceedings of 1978 International Conference on Parallel Processing*, August, 1978.
  36. Jordan, H., "A Special Purpose Architecture for Finite Element Analysis," *Proceedings of 1978 International Conference on Parallel Processing*, August, 1978.
  37. Ackroyd, M. H., "Nonlinear Inelastic Stability of Flexibly-Connected Plane Steel Frames," *Ph. D. Dissertation*, University of Colorado, Boulder, 1979.
  38. Razzaq, Z., Chang, J. G., and Kruger, P. K., "Initially Crooked Columns With Partial Restraints," *Annual Technical Session*, Structural Stability Research Council, New York, 1980.
  39. Chen, W. F., "End Restraint and Column Stability," *Journal of the Structural Division*, ASCE, Vol. 106, No. ST11, November, 1980.
  40. Balio, G., and Campanini, G., "Equivalent Bending Moments for Beam-Columns," *Journal of Constructional Steel Research*, Vol. 1, No. 3, May, 1981.

41. Rahimzadeh-Hanachi, J., "Nonlinear Elastic Frame Analysis by Finite Element," *Ph. D. Dissertation*, Michigan State University, Michigan, 1981.
42. Moncarz, P. D., and Gerstle, K. H., "Steel Frames With Nonlinear Connections," *Journal of Structural Engineering*, ASCE, Vol. 107, August, 1981.
43. Burden, R. L., Faires, J. D., and Reynolds, A. C., *Numerical Analysis*, Second Edition, Prindle, Weber & Schmidt, Massachusetts, 1981.
44. Stowan, S. H., "Nonlinear Collapse Load Analysis of Braced Frame Structures," *Ph. D. Dissertation*, Case Western University, Cleveland, 1982.
45. Razzaq, Z., and McVinnie, W. W., "Rectangular Tubular Steel Columns Loaded Biaxially," *Journal of Structural Mechanics*, ASCE, Vol. X, No. 4, 1982.
46. Marglichi, K., "Non-Rigid Frame Analysis," *Ph. D. Dissertation*, Washington State University, St. Louis, Missouri, 1982.
47. Storaasli, O. O., Peebles, S., Crockett, T. W., Kott, J. D., and Adams, L. M., "The Finite Element Machine: An Experiment in Parallel Processing," *Research in Structures and Solid Mechanics-1982*, NASA CP-2245, October, 1982.
48. Adams, L. M., "Iterative Algorithms for Large Sparse Linear Systems on Parallel Computers," *Ph. D. Dissertation*, University of Virginia, Charlottesville, 1982.
49. Jones, S. W., Kirby, P. A., and Nethercot, D. A., "Analysis of Frames With Semi-Rigid Connections - A State of the Art Report," *Journal of Constructional Steel Research*, Vol. 3, n2, 1983.
50. Razzaq, Z., "Restraint Effect on Steel Column Strength," *Journal of Structural Engineering*, ASCE, Vol. 109, No. 2, February, 1983.
51. Razzaq, Z., and Calash, A. Y., "Partially Restrained Columns With Biaxial Crookedness and Residual Stresses," *Structures Congress*, ASCE, Houston, Texas, October, 1983.
52. Leondorf, D., "Advanced Computer Architecture for Engineering Analysis and Design," *Ph. D. Dissertation*, University of Michigan, Ann Arbor, Michigan, 1983.
53. Chen, W. F., and Lui, E. M., "Columns With End Restraint and Bending in Load Resistance Design Factor," *Engineering Journal*, AISC, 3rd Quarter, Vol. 22, No. 3, 1985.
54. Razzaq, Z., and Calash, A. Y., "Imperfect Columns With Biaxial Partial

Restraints," *Journal of Structural Engineering*, ASCE, Vol. 111, No. 4, April, 1985.

55. Razzaq, Z., and McVinnie, W. W., "Theoretical and Experimental Behavior of Biaxially Loaded Inelastic Columns," *Journal of Structural Mechanics*, ASCE, Vol. 14, No. 3, March, 1986.
56. Galambos, T. V., *Guide to Stability Design Criteria for Metal Structures*, Fourth Edition, John Wiley and Sons, Inc., New York, N. Y., 1988.

Table 1. Concurrent processing results for hollow square section with  $\gamma = 1.000$

Number of processors	Maximum computational time (sec)	Speedup $s_i$	Efficiency $\eta_i$
8	312.853	7.69	96.1
4	608.171	3.96	99.0
2	1204.867	1.99	99.5
1	2405.829	---	---

Table 2. Computational time on concurrent processors

Number of processors	Square section		Rectangular section	
	Moment ratio $\gamma$	Computational time (sec)	Moment ratio $\gamma$	Computational time(sec)
8	$\gamma_{1s}$	1289.836	$\gamma_{1r}$	1289.817
	$\gamma_{2s}$	(1422.777)	$\gamma_{2r}$	(1419.233)
	$\gamma_{3s}$	1419.230	$\gamma_{3r}$	1333.203
	$\gamma_{4s}$	1398.955	$\gamma_{4r}$	1137.931
	$\gamma_{5s}$	1333.192	$\gamma_{5r}$	1253.166
	$\gamma_{6s}$	1273.721	$\gamma_{6r}$	1291.926
	$\gamma_{7s}$	1143.658	$\gamma_{7r}$	1261.039
	$\gamma_{8s}$	1102.597	$\gamma_{8r}$	1102.564
4	$\gamma_{1s}, \gamma_{3s}$	2701.822	$\gamma_{1r}, \gamma_{2s}$	(2715.432)
	$\gamma_{2s}, \gamma_{4s}$	(2823.155)	$\gamma_{3r}, \gamma_{4s}$	2471.114
	$\gamma_{5s}, \gamma_{7s}$	2471.129	$\gamma_{5r}, \gamma_{6s}$	2538.101
	$\gamma_{6s}, \gamma_{8s}$	2375.804	$\gamma_{7r}, \gamma_{8s}$	2362.757
2	$\gamma_{1s}, \gamma_{3s}, \gamma_{5s}, \gamma_{7s}$	(5197.993)	$\gamma_{1r}$ to $\gamma_{4s}$	(5172.083)
	$\gamma_{2s}, \gamma_{4s}, \gamma_{6s}, \gamma_{8s}$	5190.392	$\gamma_{5r}$ to $\gamma_{8s}$	4896.691
1	$\gamma_{1s}$ to $\gamma_{8s}$	10324.935	$\gamma_{1r}$ to $\gamma_{8s}$	10067.648

Table 3. Concurrent processing efficiencies for hollow square section with  $\gamma = \gamma_{1s}$  to  $\gamma_{8s}$

Number of processors	Maximum computational time (sec)	Speedup $s_i$	Efficiency $\eta_i$
8	1422.777	7.26	90.7
4	2823.155	3.66	91.5
2	5197.993	1.99	99.5
1	10,324.935	---	---

Table 4. Concurrent processing efficiencies for hollow rectangular section with  $\gamma = \gamma_{1r}$  to  $\gamma_{8r}$

Number of processors	Maximum computational time (sec)	Speedup $s_i$	Efficiency $\eta_i$
8	1419.233	7.09	88.6
4	2715.432	3.71	92.7
2	5172.083	1.95	97.5
1	10,067.648	---	---

Table 5. Peak loads of hollow square and rectangular columns

Hollow square section			Hollow rectangular section		
Column	Spring stiffness	$P_{max}$	Column	Spring stiffness	$P_{max}$
CN1	$k_1$	0.851	CN5	$k_1$	0.832
CN2	$k_1$	0.887	CN6	$k_1$	0.875
CN3	$k_1$	0.951	CN7	$k_1$	0.930
CN4	$k_1$	0.902	CN8	$k_1$	0.859

$$k^* (k_{Bx} = k_1, k_{Tx} = k_2, k_{By} = k_2, k_{Ty} = k_3)$$



Table 6. Execution times on concurrent processors for columns CN1 and CN5

Number of Processors	Number of cross sections per assistant processor	Executive time (sec)	
		Column CN1	Column CN5
9	1	1083.285	1319.343
		1082.937	1318.933
		1083.267	1319.327
		1083.283	1319.353
		1083.068	1319.089
		1083.244	1319.292
		1083.268	1319.325
		1083.185	1319.235
		(1088.823)	(1322.104)
5	2	(1442.337)	(1709.396)
		1441.870	1708.872
		1442.230	1709.380
		1442.284	1709.335
		1430.745	1694.345
3	4	(2002.951)	2250.632
		2002.196	(2349.794)
		1967.393	2306.682
2	8	3286.645	3842.815
		(3291.664)	(3848.343)
1	8	5272.540 <sup>a</sup>	6907.108 <sup>a</sup>

<sup>a</sup> Estimated times.

Table 7. Computational speedup factors and efficiencies for hollow square columns

Column	Spring stiffness	Number of processors	Maximum execution time (sec)	Speedup ( $s_i$ )	Efficiency ( $\eta_i$ )
CN1	$k_1$	9	1088.823	5.49	61.0
		5	1442.284	4.14	82.8
		3	2002.951	2.98	99.4
		2	3291.664	1.81	90.7
		1	5972.540	---	---
CN2	$k_2$	9	1527.131	5.89	65.4
		5	2090.294	4.30	86.1
		3	3017.470	2.98	99.4
		2	5084.405	1.77	88.5
		1	8994.377	---	---
CN3	$k_3$	9	988.095	5.15	57.3
		5	1270.900	4.01	80.2
		3	1780.100	2.86	95.4
		2	2837.310	1.79	89.8
		1	5093.126	---	---
CN4	$k^*$	9	1871.138	5.53	61.4
		5	2506.175	4.13	82.5
		3	3481.424	2.97	99.0
		2	5520.623	1.87	93.7
		1	10240.735	---	---

$k^*$  ( $k_{Bx} = k_1, k_{Tx} = k_2, k_{By} = k_2, k_{Ty} = k_3$ )

Table 8. Computational speedup factors and efficiencies for hollow rectangular columns

Column	Spring stiffness	Number of Processors	Maximum execution Time (sec)	Speedup (s <sub>i</sub> )	Efficiency (η <sub>i</sub> )
CN5	$k_1$	9	1322.104	5.22	58.0
		5	1709.396	4.04	80.8
		3	2350.632	2.94	97.9
		2	3848.343	1.79	89.7
		1	6907.108	---	---
CN6	$k_2$	9	1700.910	5.65	62.8
		5	2245.908	4.28	85.6
		3	3219.390	2.98	99.4
		2	5398.389	1.78	89.0
		1	9609.606	---	---
CN7	$k_3$	9	4386.441	5.67	63.0
		5	5911.918	4.21	84.2
		3	8332.422	2.99	99.6
		2	13880.841	1.79	89.7
		1	24887.504	---	---
CN8	$k'$	9	4570.608	5.61	62.3
		5	6040.994	4.24	84.8
		3	8555.816	2.99	99.6
		2	14147.350	1.81	90.6
		1	25619.272	---	---

$$k' (k_{Bx} = k_1, k_{Tx} = k_2, k_{By} = k_2, k_{Ty} = k_3)$$

Table 9. Summary of beam-column strength for various connection models

Restraint type	$P_{max}$	Spring moment
a2	0.71	124.23
b2	0.69	95.92
c2	0.66	79.89
d2	0.64	79.85
e2	0.67	100.00
f2	0.64	72.00

\*in inch-kip units

Table 10. Maximum beam-column loads for various load paths and elastic restraints

$r$	Spring stiffness	Load	Major axis		Minor axis		Major axis		Minor axis	
			LC1	LC2	LC1	LC2	LC3	LC4	LC3	LC4
0.0	$k_{a3}$	p	0.950	0.952	0.935	0.910	0.426	0.426	0.290	0.290
		$\bar{m}$	0.021	0.021	0.182	0.182	1.200	1.160	4.600	3.842
-0.3	$k_{a1}$	p	0.710	0.710	0.625	0.625	0.166	0.166	0.261	0.261
		$\bar{m}$	0.192	0.192	0.086	0.086	0.900	0.901	0.850	0.849
-0.3	$k_{a2}$	p	0.750	0.761	0.800	0.731	0.321	0.321	0.075	0.075
		$\bar{m}$	0.275	0.275	0.675	0.675	1.050	1.084	3.400	3.343
-0.3	$k_{a3}$	p	0.800	0.798	0.850	0.856	0.377	0.377	0.311	0.311
		$\bar{m}$	0.313	0.313	0.543	0.543	1.200	1.202	4.600	4.163

Table 11. Maximum beam-column loads for various load paths and elastic-plastic restraints ( $k_{a2}$ ;  $m_{plastic} = 100$  in-kips)

Bending axis	Load	LC1	LC2	LC3	LC4
Major	p	0.800	0.800	0.168	0.168
	$\bar{m}$	0.198	0.198	1.000	1.000
Minor	p	0.800	0.799	0.150	0.150
	$\bar{m}$	0.159	0.159	1.400	1.499

Table 12. Maximum external loads for uniaxially loaded imperfect beam-columns with partial rotational equal end restraints and various load paths (W8X31)

Beam-Column	Length (ft.)	Spring Stiffness	Load Path	Maximum External Loads					
				$\frac{p}{\bar{m}}$					
1	8	$k_{\alpha}$	NP2	$\frac{p}{\bar{m}}$	0.000 3.211	0.075 3.000	0.737 1.500	0.961 0.000	-- --
			NP1	$\frac{p}{\bar{m}}$	0.000 3.211	0.075 2.990	0.737 1.733	0.961 0.000	-- --
2	8	$k_{\alpha}$	NP2	$\frac{p}{\bar{m}}$	0.000 4.689	0.169 4.000	0.669 2.500	0.968 1.000	0.958 0.000
			NP1	$\frac{p}{\bar{m}}$	0.000 4.689	0.169 4.190	0.669 2.155	0.865 1.114	0.958 0.084
3	12	$k_{\alpha}$	NP2	$\frac{p}{\bar{m}}$	0.000 3.736	0.238 3.000	0.749 1.500	0.867 0.001	-- --
			NP1	$\frac{p}{\bar{m}}$	0.000 3.736	0.238 3.344	0.749 0.845	0.867 0.144	-- --
4	12	$k_{\alpha}$	NP2	$\frac{p}{\bar{m}}$	0.000 5.014	0.360 4.500	0.550 3.000	0.744 1.500	0.893 0.000
			NP1	$\frac{p}{\bar{m}}$	0.000 5.014	0.360 3.842	0.550 3.476	0.744 1.825	0.893 0.258
5	16	$k_{\alpha}$	NP2	$\frac{p}{\bar{m}}$	0.000 5.561	0.182 4.500	0.273 3.000	0.496 1.500	0.751 0.000
			NP1	$\frac{p}{\bar{m}}$	0.000 5.561	0.182 3.032	0.273 3.590	0.496 1.593	0.751 0.007
6	16	$k_{\alpha}$	NP2	$\frac{p}{\bar{m}}$	0.000 6.983	0.100 6.000	0.352 4.500	0.649 1.500	0.795 0.000
			NP1	$\frac{p}{\bar{m}}$	0.000 6.983	0.100 5.483	0.352 3.923	0.649 2.087	0.795 0.386

Table 13. Comparison of predicted and previously published maximum loads for pinned-end beam-columns with biaxially eccentric load

Reference Number	Cross Section	Length (in.)	Eccentricity $e_x$ (in.)	Eccentricity $e_y$ (in.)	p		$\frac{p \text{ Predicted}}{p \text{ Reference}}$
					Predicted	Reference	
21	H 6x6	96	1.61	2.78	0.426	0.421	1.01
21	H 5x5	120	2.38	2.51	0.284	0.297	0.96
25	W12x65	180	18.40	3.76	0.186	0.199	0.93
25	W12x65	270	18.40	3.76	0.167	0.169	0.99
25	W12x65	360	18.40	3.76	0.149	0.144	0.97

\*  $m_x = Pe_x/M_{Vx}$ ;  $m_y = Pe_y/M_{Vy}$

Table 14. Maximum external loads for biaxially loaded imperfect beam-columns with partial rotational equal end restraints and various load paths (L=12ft.; W8X31)

Beam-Column	Spring Stiffness	Load Path	Maximum External Loads					
			p	$m_x$	$m_y$			
7	$k_{x2}$	NP2	p	0.000	0.251	0.525	0.876	0.869
			$m_x$	1.078	0.864	0.405	0.070	0.000
			$m_y$	0.631	0.506	0.237	0.041	0.000
		NP1	p	0.000	0.250	0.500	0.750	0.869
			$m_x$	1.078	0.864	0.405	0.070	0.000
			$m_y$	0.631	0.506	0.237	0.041	0.000
8	$k_{x3}$	NP2	p	0.000	0.276	0.503	0.919	0.904
			$m_x$	1.255	0.952	0.471	0.039	0.000
			$m_y$	0.735	0.558	0.276	0.023	0.000
		NP1	p	0.000	0.250	0.500	0.780	0.904
			$m_x$	1.255	0.952	0.471	0.039	0.000
			$m_y$	0.735	0.558	0.276	0.023	0.000

Table 15. Maximum external nonproportional biaxial loads for partially restrained imperfect beam-column BC2 with hollow square section ( $k=k_{a2}$ )

Load case	Dimensionless Maximum Loads				
	$p$	0.25	0.50	0.75	0.93
NP3	$\bar{m}_x$	1.86	1.11	0.89	0.42
	$\bar{m}_y$	1.86	1.11	0.89	0.42
	$p$	0.00	0.27	0.50	0.77
NP4	$\bar{m}_x$	1.86	1.11	0.89	0.42
	$\bar{m}_y$	1.86	1.11	0.89	0.42
	$p$	0.00	0.27	0.50	0.77
NP5	$p$	0.00	0.25	0.50	0.75
	$\bar{m}_x$	1.86	1.11	0.89	0.31
	$\bar{m}_y$	0.24	1.17	0.39	0.00
NP6	$\bar{m}_y$	1.86	1.11	0.89	0.42
	$\bar{m}_x$	0.24	1.11	0.89	0.42
	$p$	0.00	0.30	0.51	0.77

Table 16. Maximum external nonproportional biaxial loads for partially restrained imperfect beam-column BC3 with hollow square section ( $k=k_{a3}$ )

Load case	Dimensionless Maximum Loads				
	$p$	0.25	0.50	0.75	0.94
NP3	$\bar{m}_x$	1.95	1.62	1.18	0.50
	$\bar{m}_y$	1.95	1.62	1.18	0.50
	$p$	0.00	0.35	0.44	0.76
NP4	$\bar{m}_x$	1.95	1.62	1.18	0.50
	$\bar{m}_y$	1.95	1.62	1.18	0.50
	$p$	0.00	0.35	0.44	0.76
NP5	$p$	0.00	0.25	0.50	0.75
	$\bar{m}_x$	1.95	1.62	1.18	0.39
	$\bar{m}_y$	1.73	1.74	0.83	0.00
NP6	$\bar{m}_y$	1.95	1.62	1.18	0.50
	$\bar{m}_x$	1.73	1.62	1.18	0.50
	$p$	0.00	0.21	0.44	0.76



Table 17. Maximum external nonproportional biaxial loads for partially restrained imperfect beam-column BC4 with hollow rectangular section ( $k=k_{a2}$ )

Load case		Dimensionless Maximum Loads				
NP3	$p$	0.00	0.25	0.50	0.75	0.91
	$\bar{m}_x$	2.02	1.19	0.75	0.32	0.00
	$\bar{m}_y$	2.14	1.26	0.80	0.34	0.00
NP4	$\bar{m}_x$	2.02	1.19	0.75	0.32	-
	$\bar{m}_y$	2.14	1.26	0.80	0.34	-
	$p$	0.05	0.40	0.45	0.78	-
NP5	$p$	0.00	0.25	0.50	0.75	-
	$\bar{m}_x$	2.14	1.19	0.75	0.32	-
	$\bar{m}_y$	0.99	1.18	1.02	0.30	-
NP6	$\bar{m}_y$	2.02	1.26	0.80	0.34	-
	$\bar{m}_x$	0.61	1.19	0.75	0.32	-
	$p$	0.00	0.39	0.46	0.78	-
NP7	$p$	0.00	0.25	0.50	0.75	-
	$\bar{m}_y$	2.02	1.26	0.80	0.29	-
	$\bar{m}_x$	0.61	0.97	0.60	0.00	-
NP8	$\bar{m}_x$	2.14	1.19	0.75	0.32	-
	$\bar{m}_y$	0.99	1.26	0.80	0.34	-
	$p$	0.00	0.26	0.45	0.78	-

Table 18 Maximum external nonproportional biaxial loads for partially restrained imperfect beam-column BC5 with hollow rectangular section ( $k = k_{a3}$ )

Load case		Dimensionless Maximum Loads				
NP3	p	0.00	0.25	0.50	0.75	0.93
	$\bar{m}_x$	1.95	1.43	1.04	0.35	0.00
	$\bar{m}_y$	2.07	1.52	1.11	0.37	0.00
NP4	$\bar{m}_x$	1.95	1.43	1.04	0.35	-
	$\bar{m}_y$	2.07	1.52	1.11	0.37	-
	p	0.02	0.34	0.48	0.75	-
NP5	p	0.00	0.25	0.50	0.75	-
	$\bar{m}_x$	1.95	1.43	1.04	0.35	-
	$\bar{m}_y$	3.69	1.84	0.98	0.47	-
NP6	$\bar{m}_y$	2.07	1.52	1.11	0.37	-
	$\bar{m}_x$	1.83	1.43	1.04	0.35	-
	p	0.00	0.38	0.49	0.75	-
NP7	p	0.00	0.25	0.50	0.75	-
	$\bar{m}_y$	2.07	1.52	1.11	0.37	-
	$\bar{m}_x$	1.83	1.66	1.34	0.00	-
NP8	$\bar{m}_x$	1.95	1.43	1.04	0.35	-
	$\bar{m}_y$	2.07	1.52	1.11	0.37	-
	p	0.38	0.39	0.49	0.75	-

Table 19. Equivalent structural model analysis results

Frame	Case Study	$u_0$	Sign of M	Load Path	$\sigma$ - $e$ Figure 3	$P_{\max}$	$\bar{m}_{\max}$
E1	C1	$+u_{01}$	+	NP10	(a)	0.83	+0.33
	C2	$+u_{01}$	+	NP11	(a)	0.86	+0.33
E1	C3	$+u_{01}$	-	NP10	(a)	0.74	-0.24
	C4	$+u_{01}$	-	NP11	(a)	0.75	0.24
E2	C5	$-u_{01}$	-	NP10	(a)	0.83	-0.33
	C6	$-u_{01}$	-	NP11	(a)	0.84	-0.33
E2	C7	$-u_{01}$	+	NP10	(a)	0.74	+0.24
	C8	$-u_{01}$	+	NP11	(a)	0.81	+0.24
E3	C9	$+u_{02}$	+	NP10	(a)	0.78	+0.28
	C10	$+u_{02}$	+	NP11	(a)	0.80	+0.28
E3	C11	$+u_{02}$	-	NP10	(a)	0.78	-0.28
	C12	$+u_{02}$	-	NP11	(a)	0.79	-0.28
E1	C13	$+u_{01}$	+	NP9	(a)	0.80	-0.80
	C14	$+u_{01}$	+	NP9	(b)	0.75	+0.75
E1	C15	$+u_{01}$	-	NP9	(a)	0.70	-0.70
	C16	$+u_{01}$	-	NP9	(b)	0.68	-0.68

Table 20. Portal frame analysis results for FR1, FR2, FR5, and FR6 with FL1 through FL4

Frame Type	Loading		Load path NP9	Maximum loads for Load path NP10	Load path NP11
FR1	FL1	$\frac{p_{max}}{m_{max}}$	0.67 0.67	0.75 0.25	0.75 0.25
	FL2	$\frac{p_{max}}{m_{max}}$	0.72 0.72	0.76 0.26	0.76 0.26
FR2	FL1	$\frac{p_{max}}{m_{max}}$	0.64 0.64	0.71 0.21	0.71 0.21
	FL2	$\frac{p_{max}}{m_{max}}$	0.71 0.71	0.82 0.32	0.84 0.32
FR3	FL1	$\frac{p_{max}}{m_{max}}$	0.67 0.67	0.75 0.25	0.75 0.25
	FL2	$\frac{p_{max}}{m_{max}}$	0.72 0.72	0.76 0.26	0.76 0.26
FR4	FL1	$\frac{p_{max}}{m_{max}}$	0.64 0.64	0.71 0.21	0.71 0.21
	FL2	$\frac{p_{max}}{m_{max}}$	0.71 0.71	0.82 0.32	0.84 0.32

Table 21. Portal frame analysis results for FR1, FR2, FR5, and FR6 with FL1 through FL4

Frame Type	Loading		Load path NP9	Maximum loads for Load path NP10	Load path NP11
FR1	FL3	$\frac{P_{max}}{m_{max}}$	0.67 0.67	0.75 0.25	0.75 0.25
	FL4	$\frac{P_{max}}{m_{max}}$	0.72 0.72	0.76 0.26	0.76 0.26
FR2	FL3	$\frac{P_{max}}{m_{max}}$	0.64 0.64	0.79 0.29	0.70 0.29
	FL4	$\frac{P_{max}}{m_{max}}$	0.71 0.71	0.83 0.33	0.84 0.33
FR5	FL3	$\frac{P_{max}}{m_{max}}$	0.64 0.64	0.66 0.16	0.72 0.16
	FL4	$\frac{P_{max}}{m_{max}}$	0.64 0.64	0.68 0.18	0.72 0.18
FR6	FL3	$\frac{P_{max}}{m_{max}}$	0.64 0.64	0.66 0.16	0.72 0.16
	FL4	$\frac{P_{max}}{m_{max}}$	0.64 0.64	0.68 0.18	0.72 0.18

Table 22. Two-bay two-story frame analysis results for FR7 and FR8 with FL5 through FL6

Frame Type	Loading		Load path NP9	Maximum loads for Load path NP10	Load path NP11
FR7	FL5	$\frac{P_{max}}{M_{max}}$	0.61 0.61	0.69 0.19	0.72 0.19
	FL6	$\frac{P_{max}}{M_{max}}$	0.63 0.63	0.71 0.21	0.71 0.21
FR8	FL5	$\frac{P_{max}}{M_{max}}$	0.59 0.59	0.66 0.16	0.66 0.16
	FL6	$\frac{P_{max}}{M_{max}}$	0.68 0.68	0.72 0.22	0.72 0.22
FR7	FL7	$\frac{P_{max}}{M_{max}}$	0.38 0.38	0.39 0.14	0.39 0.14
	FL8	$\frac{P_{max}}{M_{max}}$	0.38 0.38	0.39 0.14	0.39 0.14
FR8	FL7	$\frac{P_{max}}{M_{max}}$	0.36 0.36	0.38 0.13	0.39 0.13
	FL8	$\frac{P_{max}}{M_{max}}$	0.39 0.39	0.39 0.14	0.39 0.14

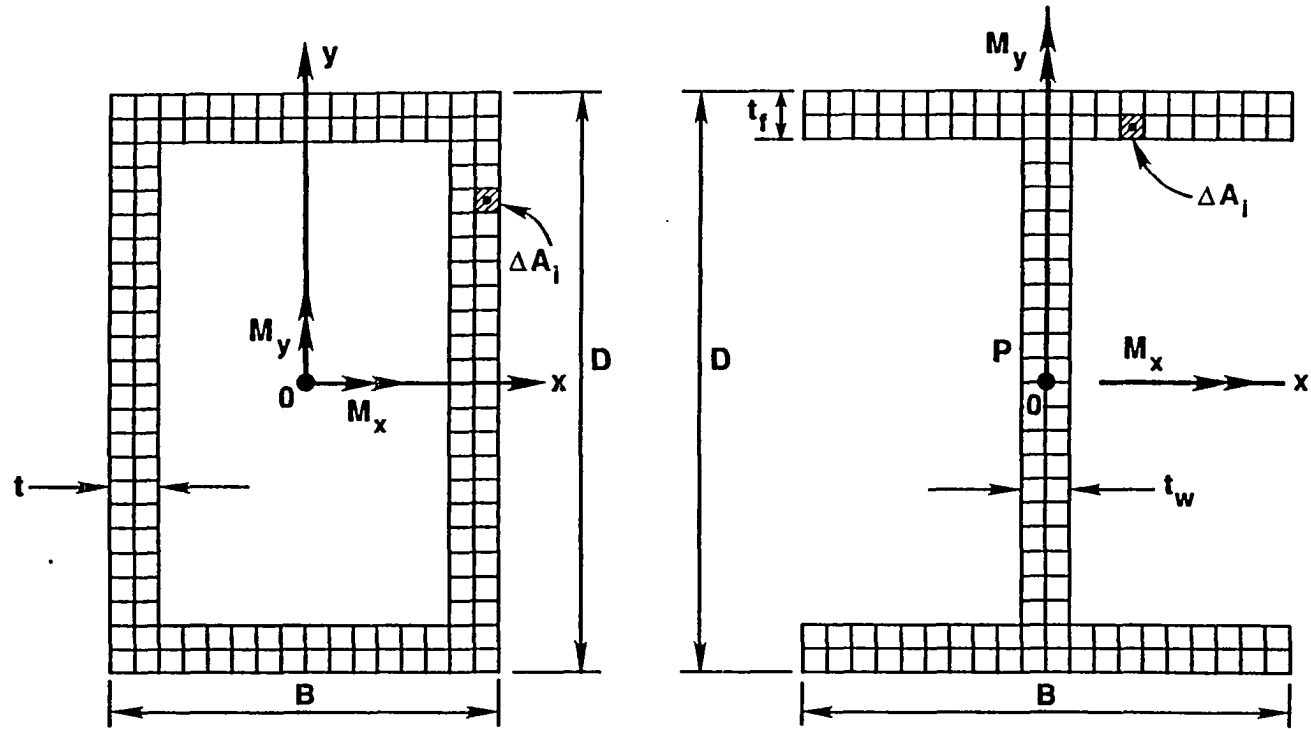


Figure 1. Discretized hollow rectangular and I-shaped sections subjected to axial load and biaxial bending moments

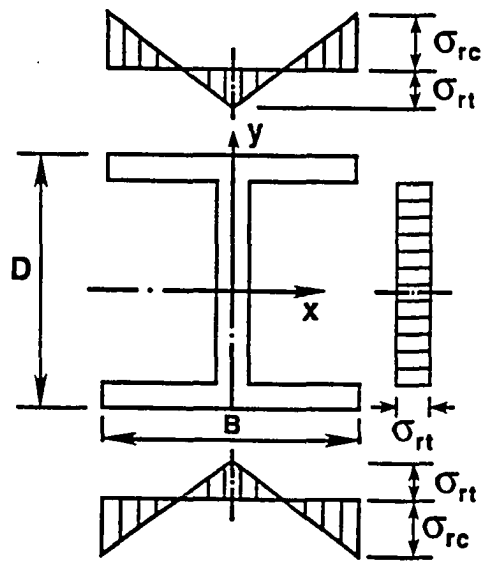
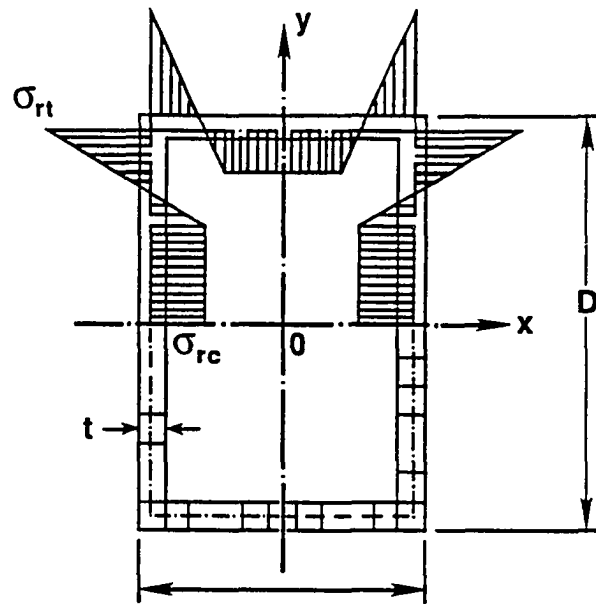
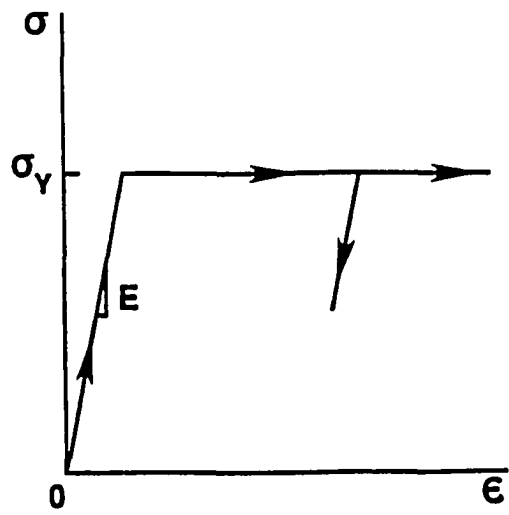
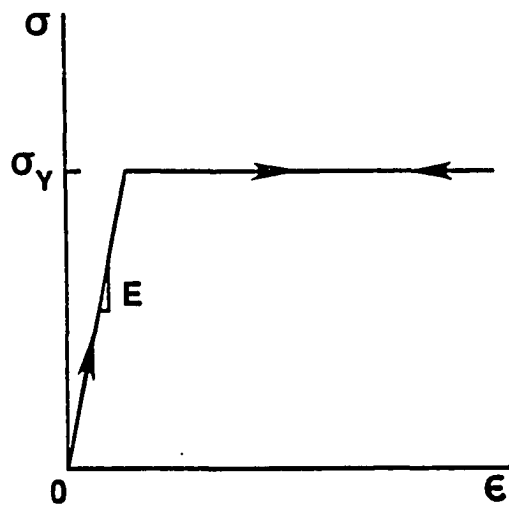


Figure 2. Typical residual stress patterns of cross sections





(a)



(b)

Figure 3. Material stress-strain relationships

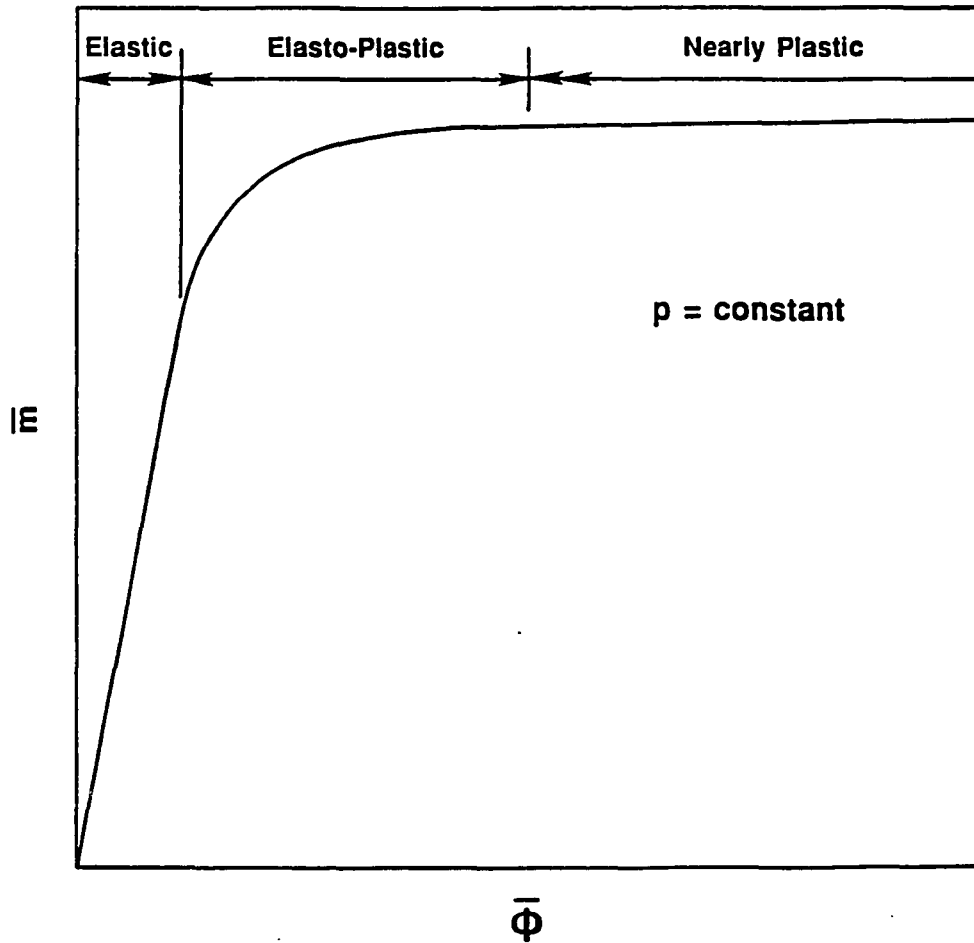


Figure 4. Cross-sectional moment-curvature relationship

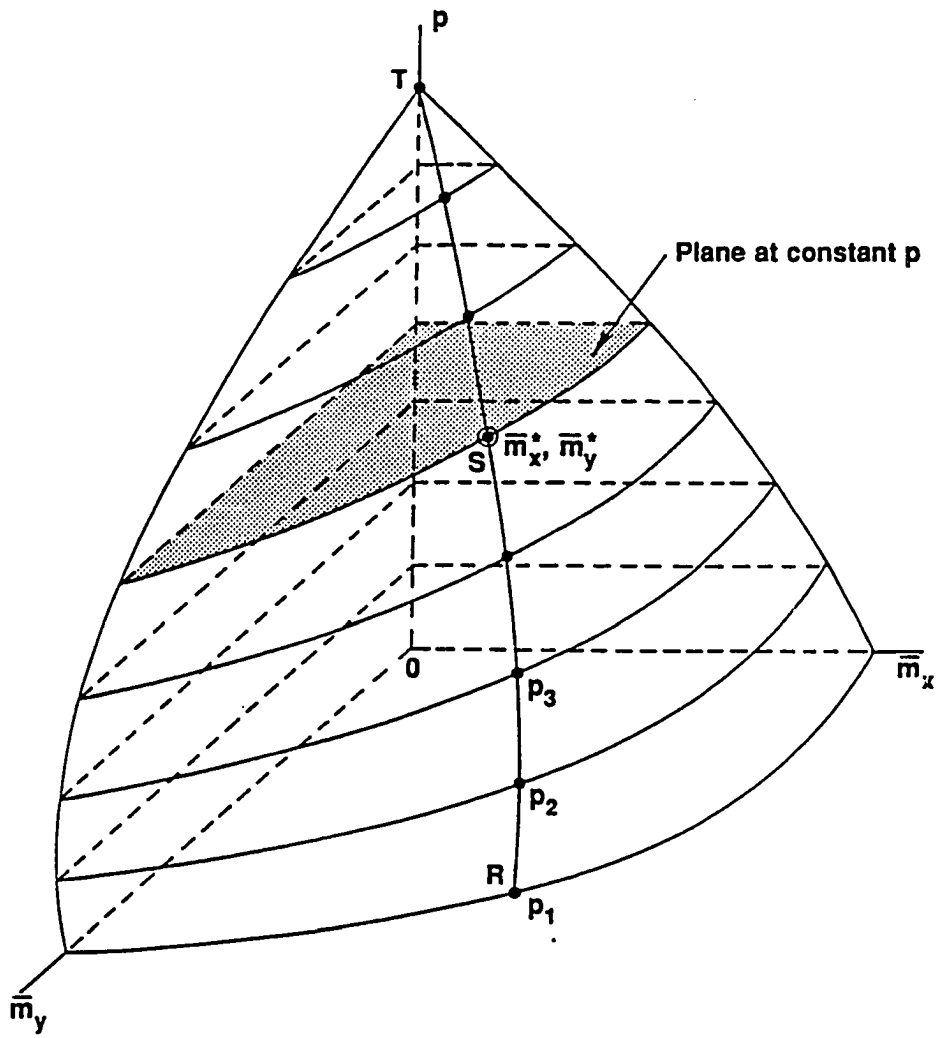


Figure 5. Yield surface

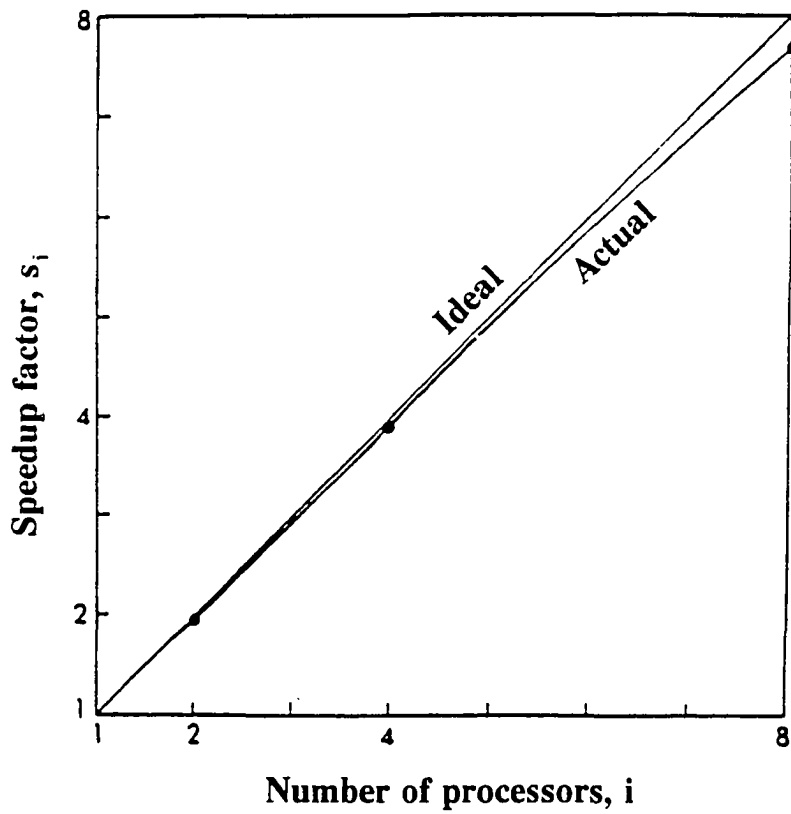


Figure 6. Speedup curves for moment-curvature relations for hollow square section

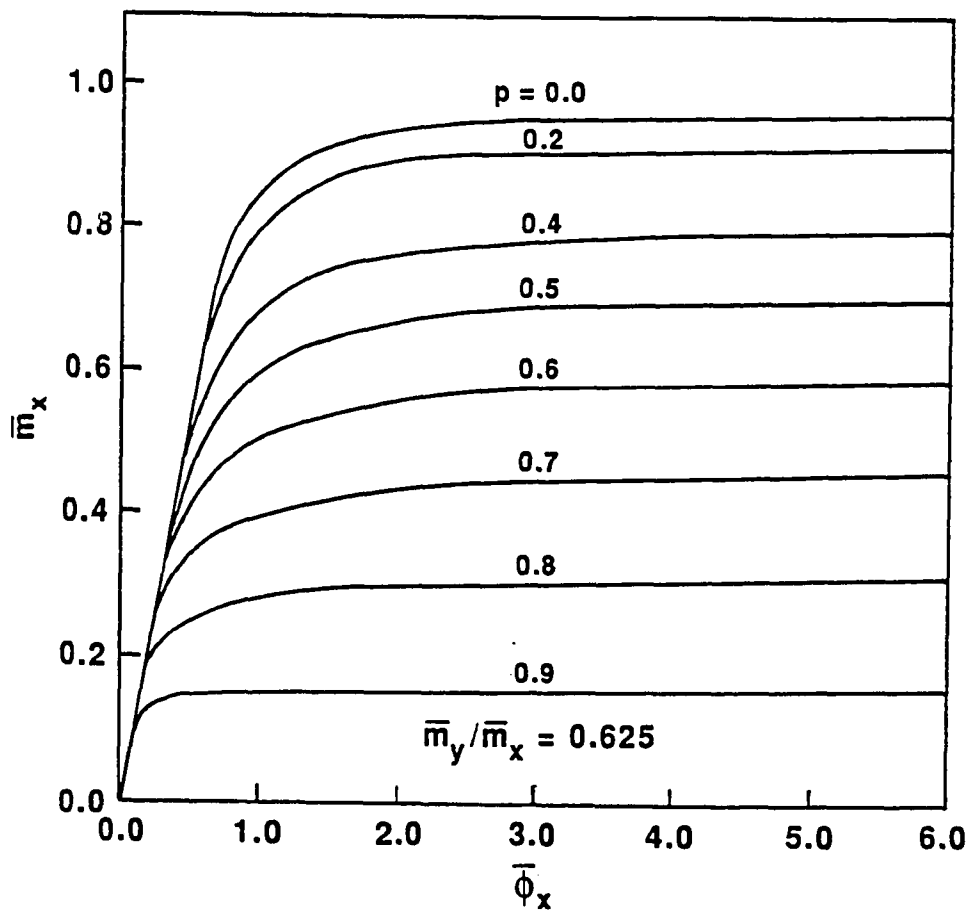


Figure 7. Moment-curvature relationships about x axis for hollow square section

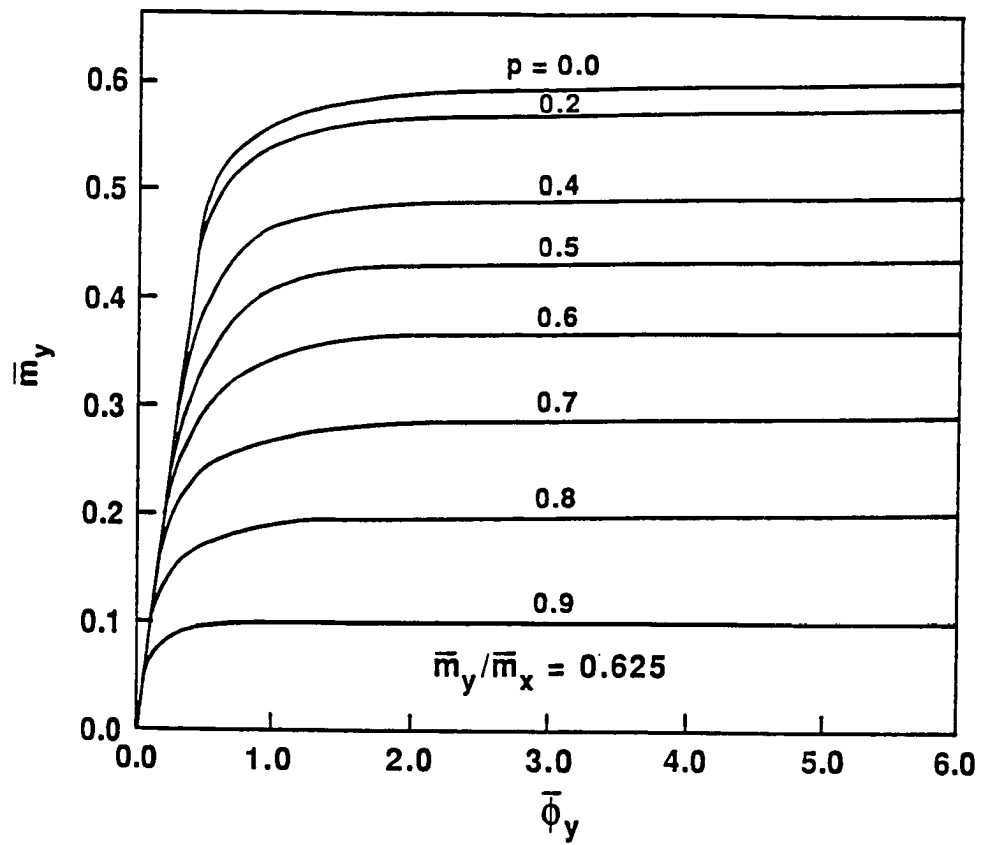


Figure 8. Moment-curvature relationships about y axis for hollow square section

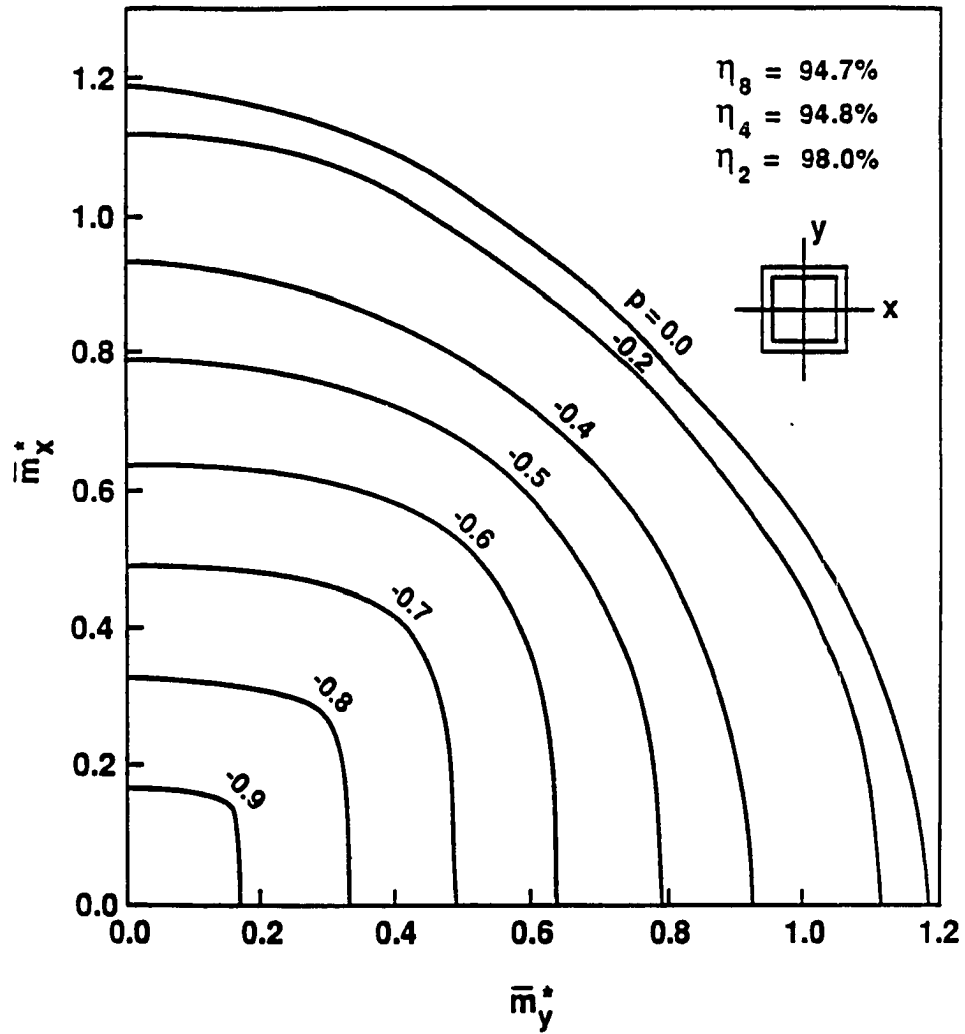


Figure 9. Yield surface contours for hollow square section

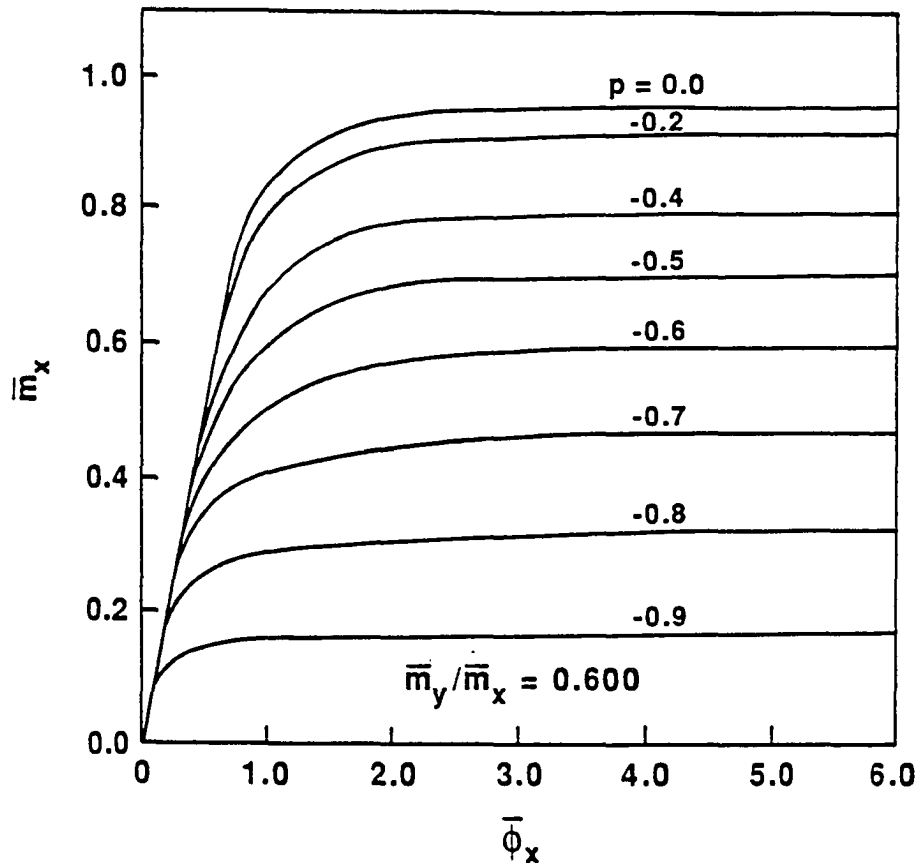


Figure 10. Moment-curvature relationships about x axis for hollow rectangular section



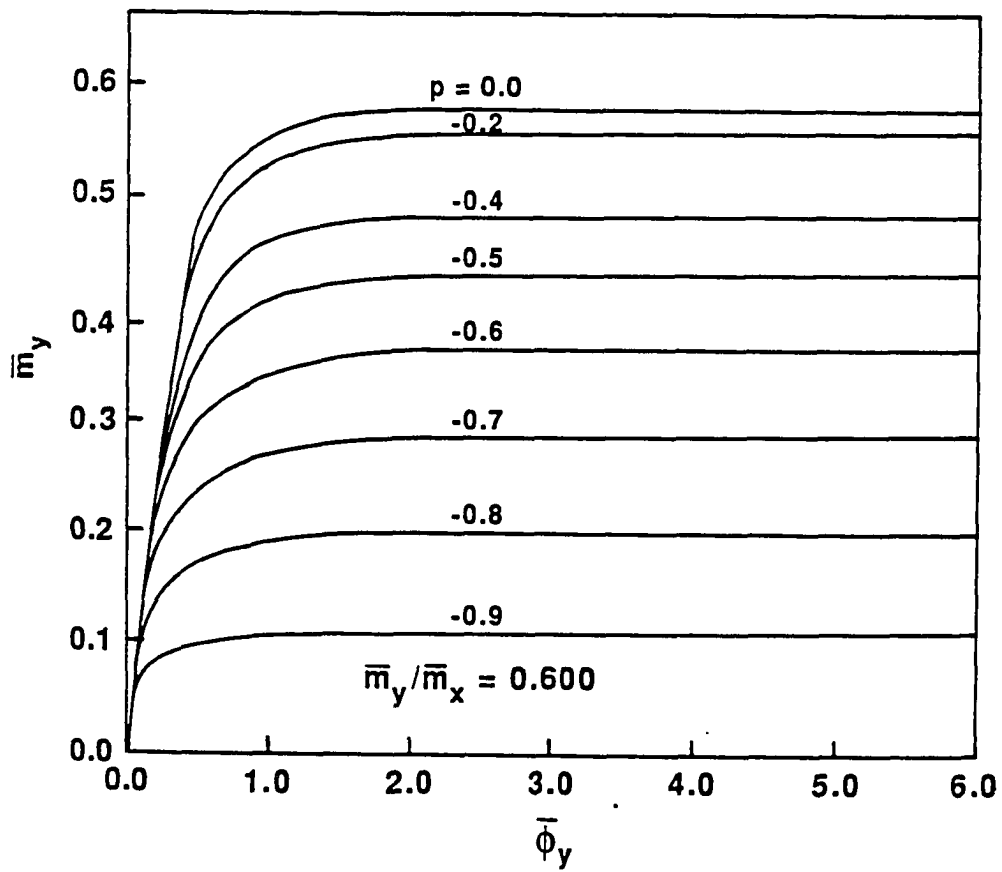


Figure 11. Moment-curvature relationships about y axis for hollow rectangular section

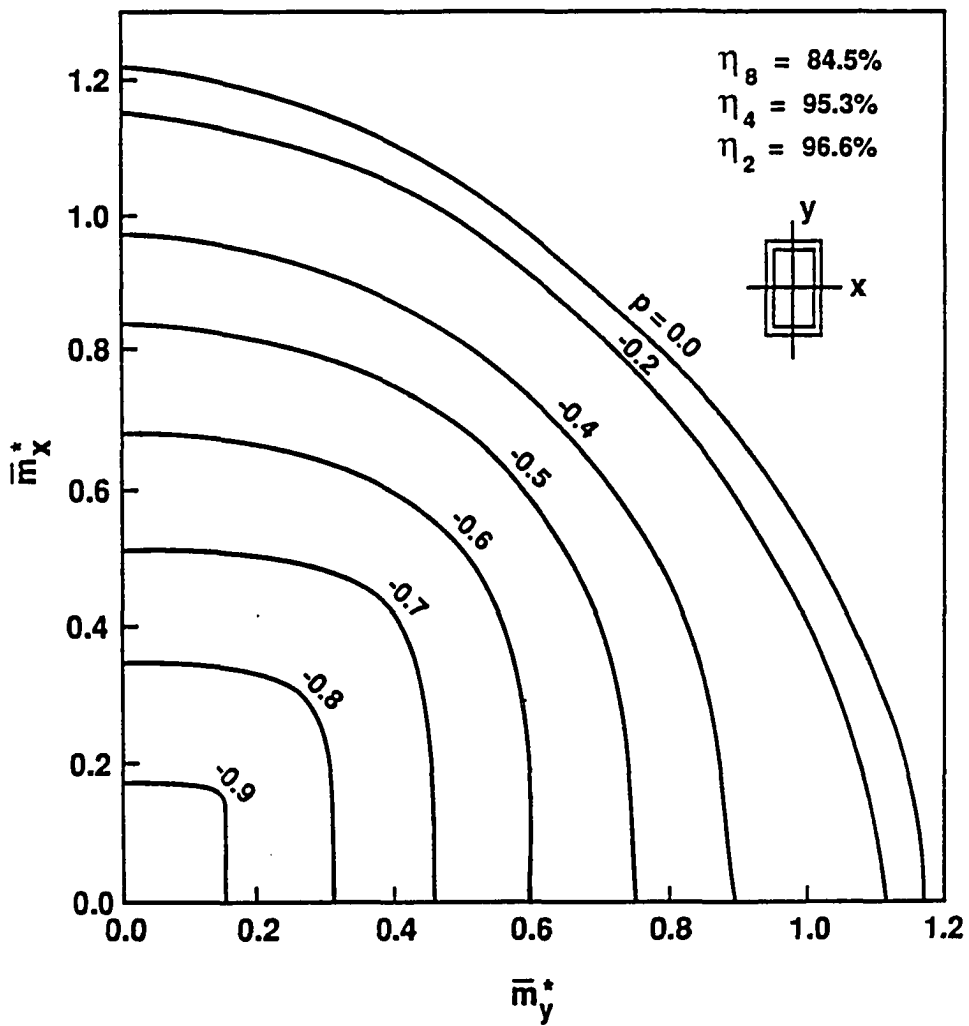


Figure 12. Yield surface contours for hollow rectangular section

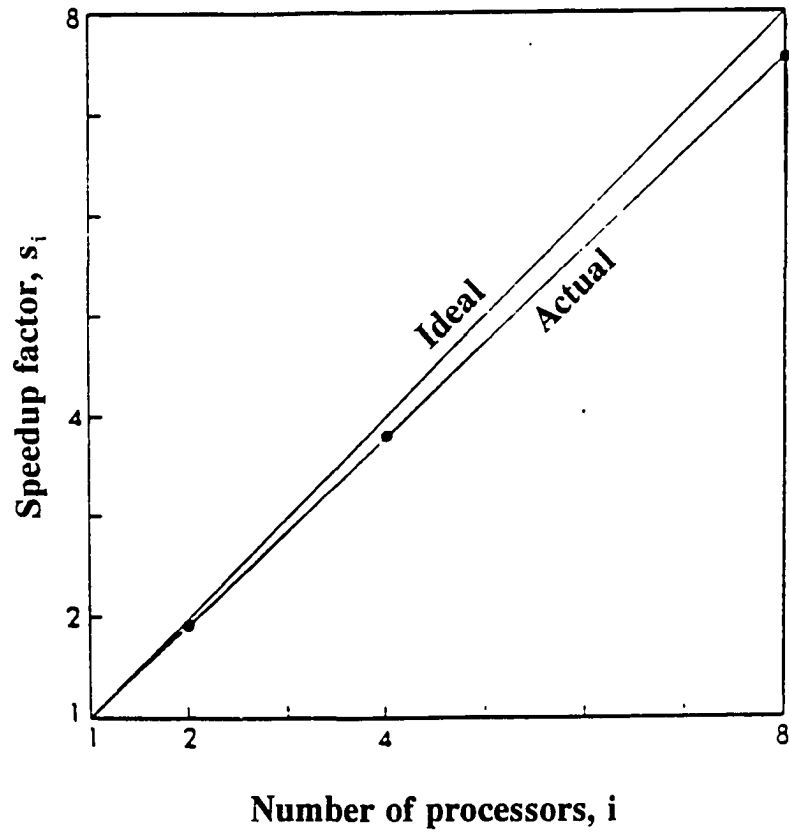


Figure 13. Speedup curves for generation of yield surface for hollow square section

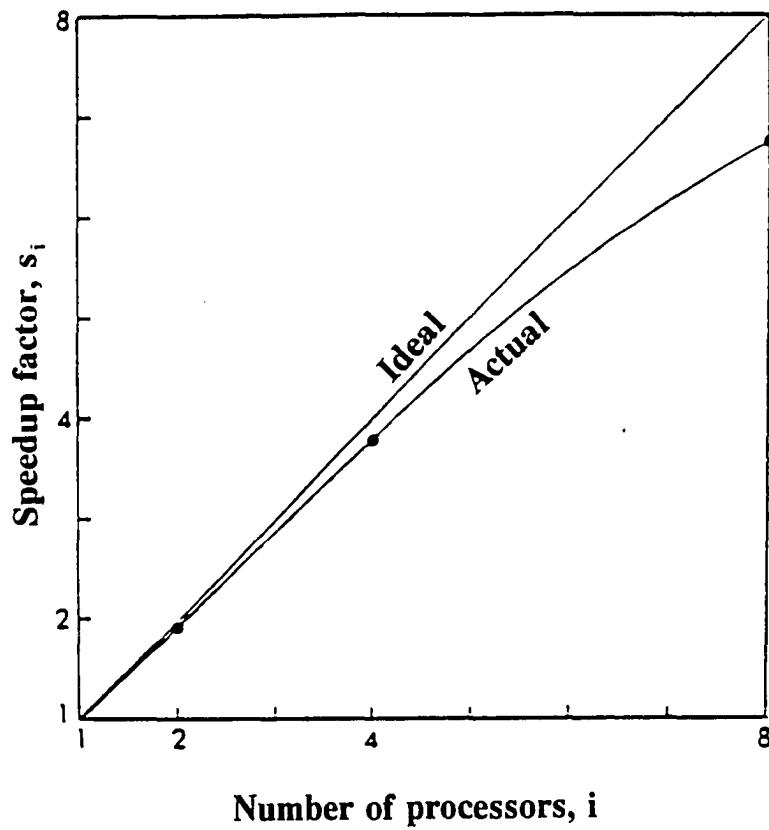


Figure 14. Speedup curves for generation of yield surface for hollow rectangular section

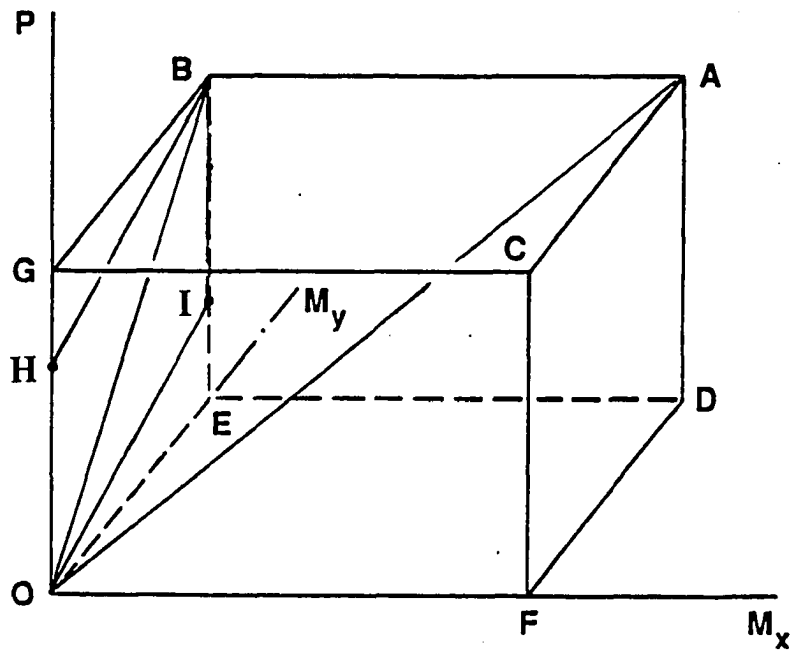


Figure 15. Various load paths for nonproportional loading

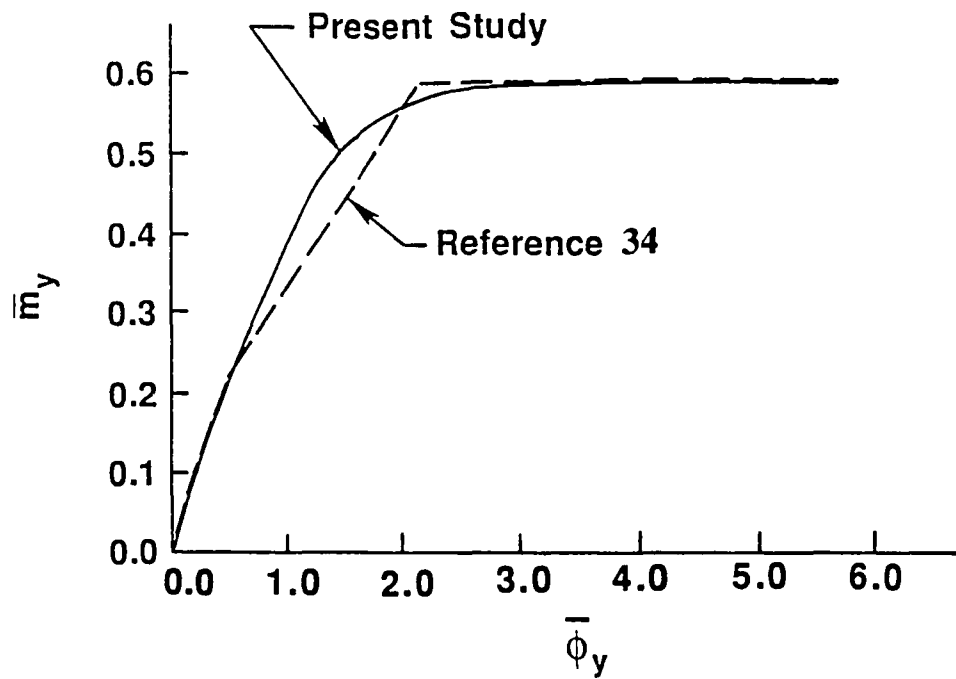


Figure 16.  $\bar{m}_y$ - $\bar{\phi}_y$  relationship for a nonproportionally loaded I-section

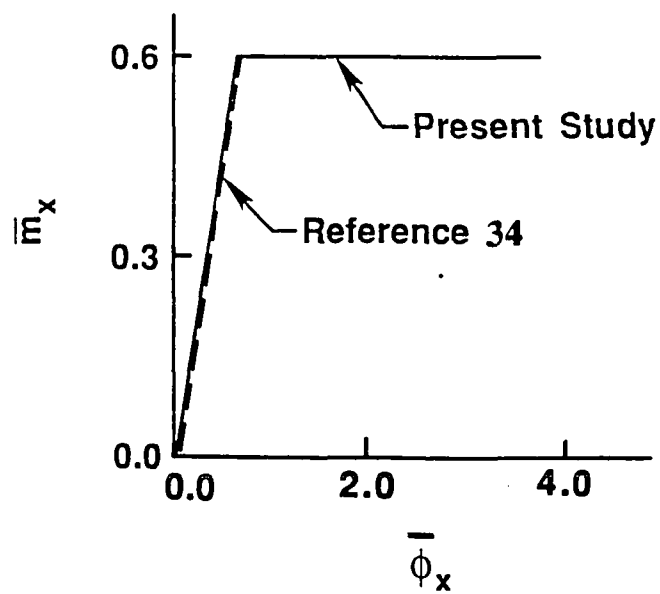


Figure 17.  $\bar{m}_x$ - $\bar{\phi}_x$  relationship for a nonproportionally loaded I-section

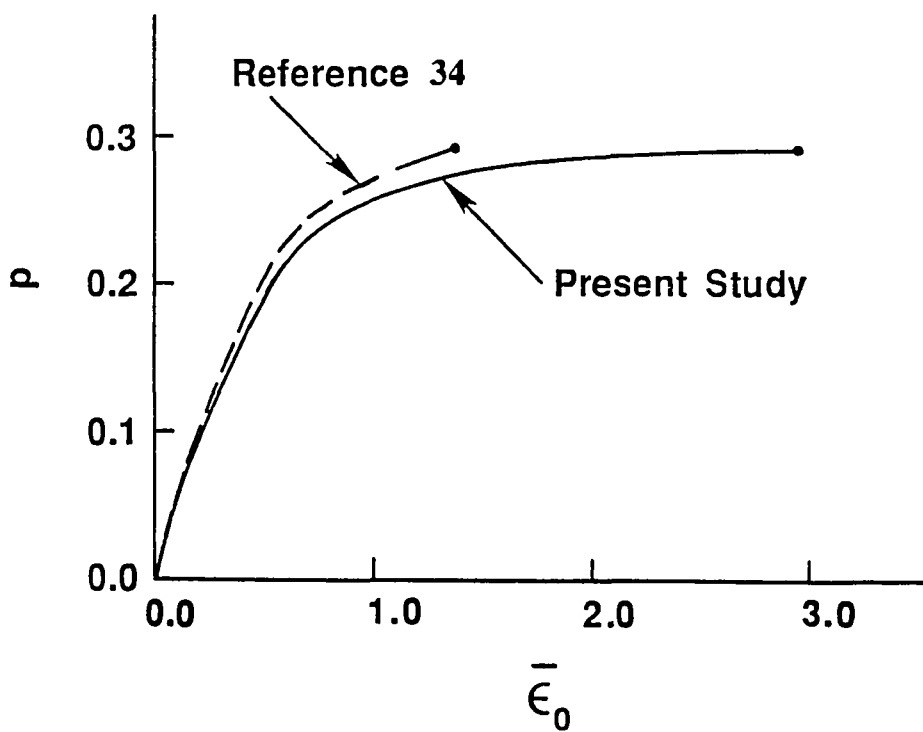


Figure 18.  $\rho$ - $\bar{\epsilon}_0$  relationship for a nonproportionally loaded I-section

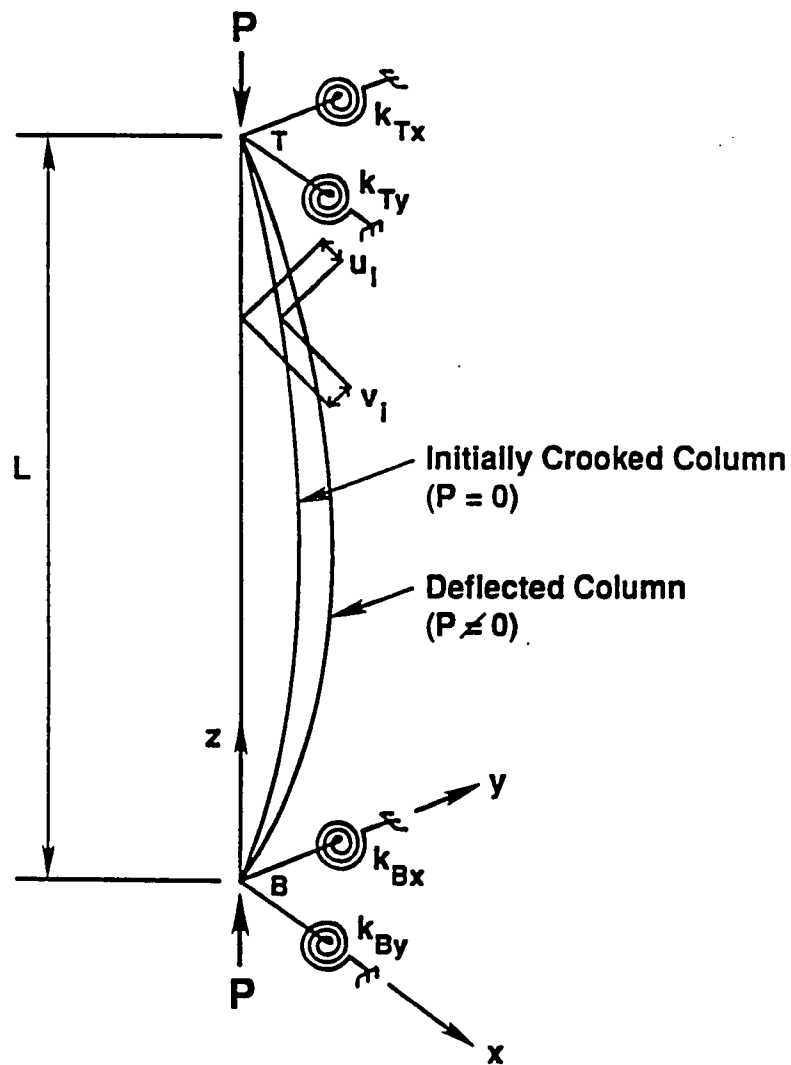


Figure 19. Imperfect column with biaxial partial restraints



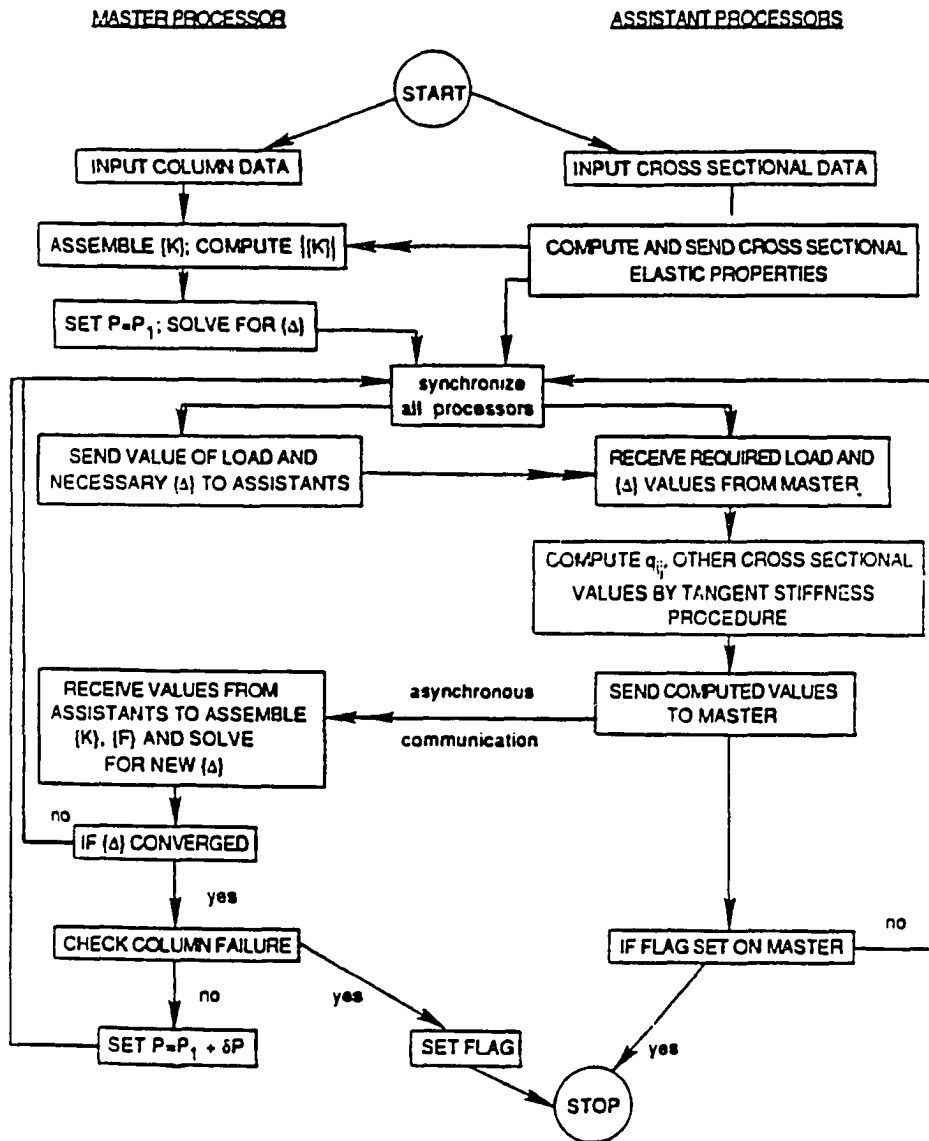


Figure 20. Flow chart of the concurrent processing

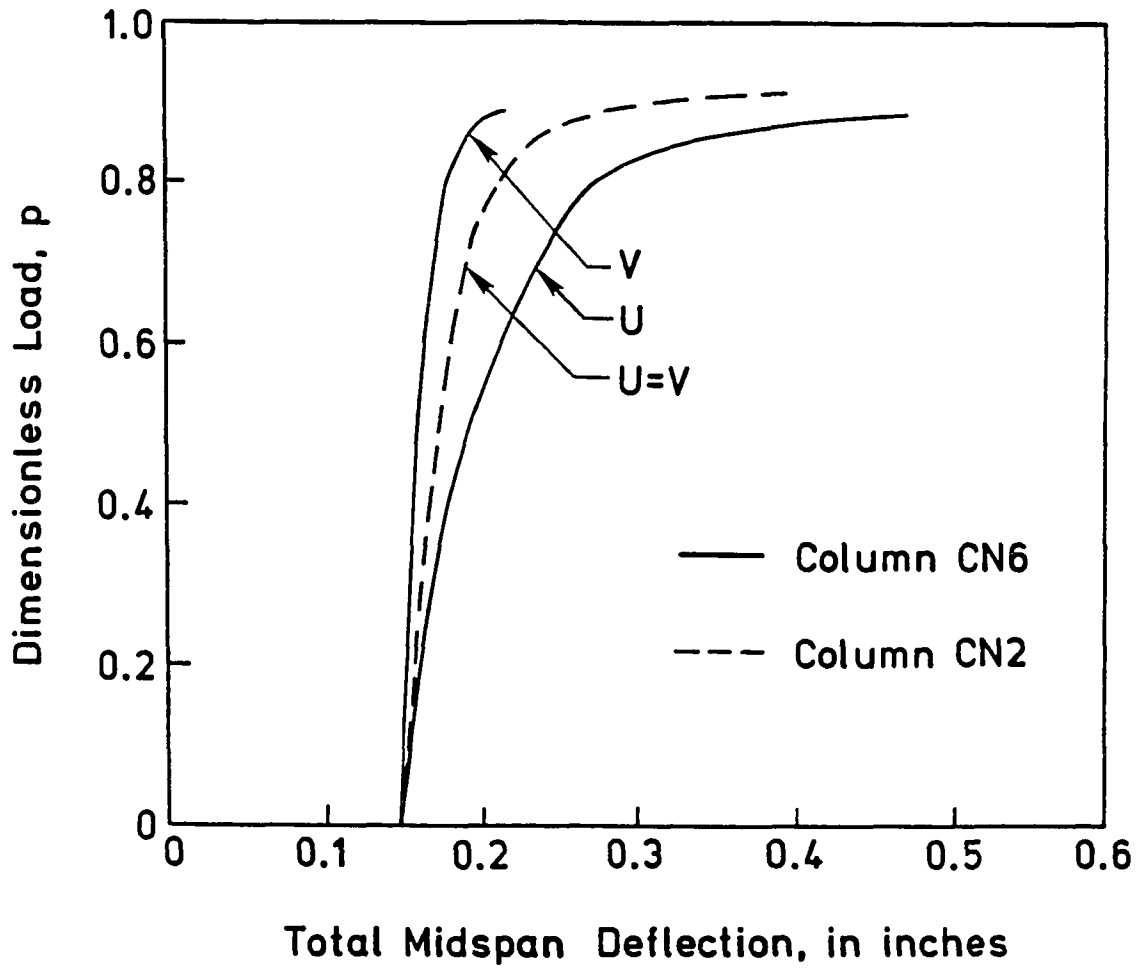


Figure 21. Load versus midspan deflection for columns CN2 and CN6

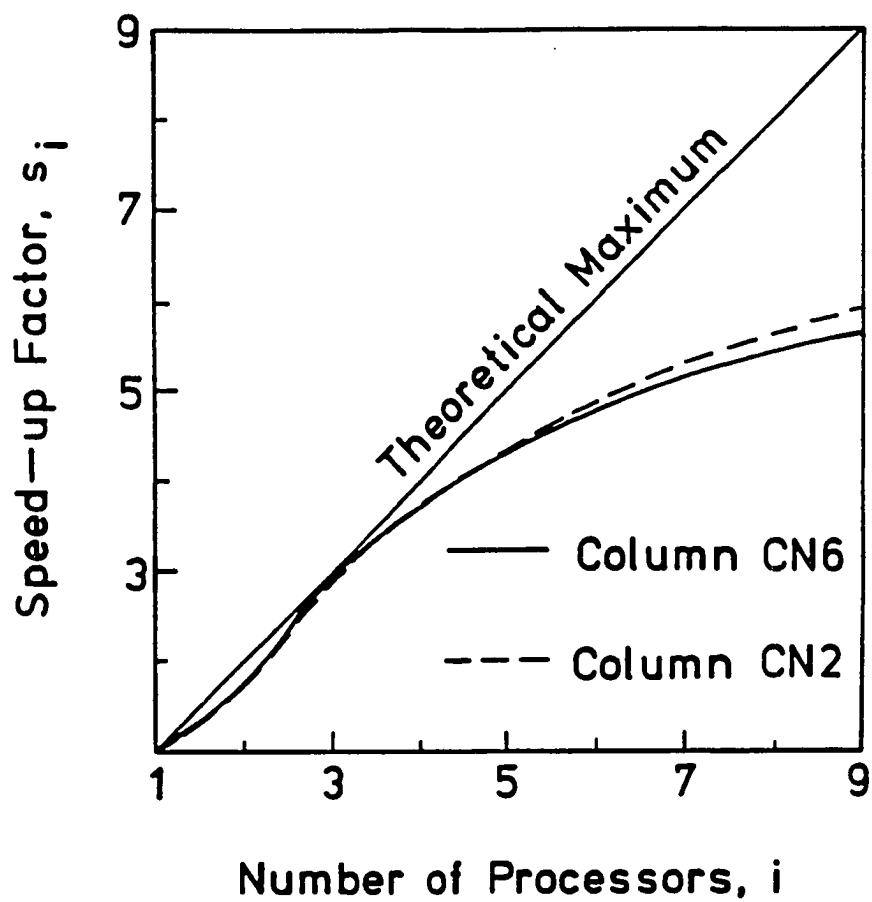


Figure 22. Speedup factor versus number of processors relationship

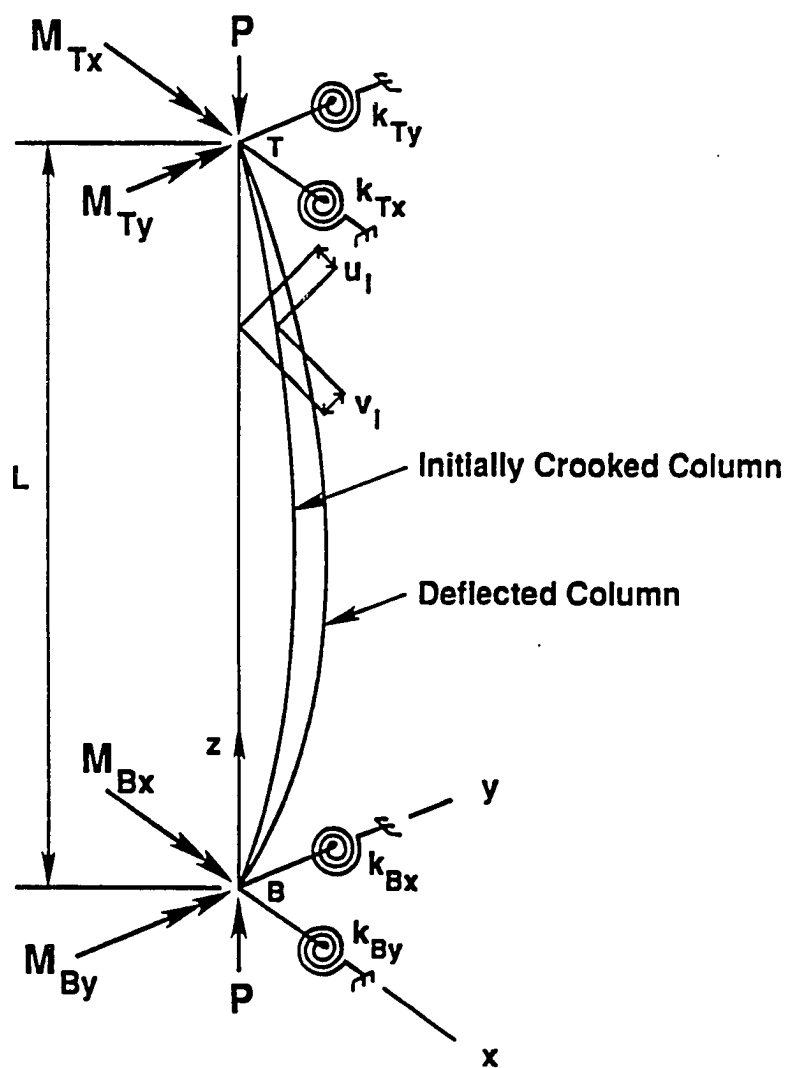


Figure 23. Imperfect beam-column with biaxial restraints

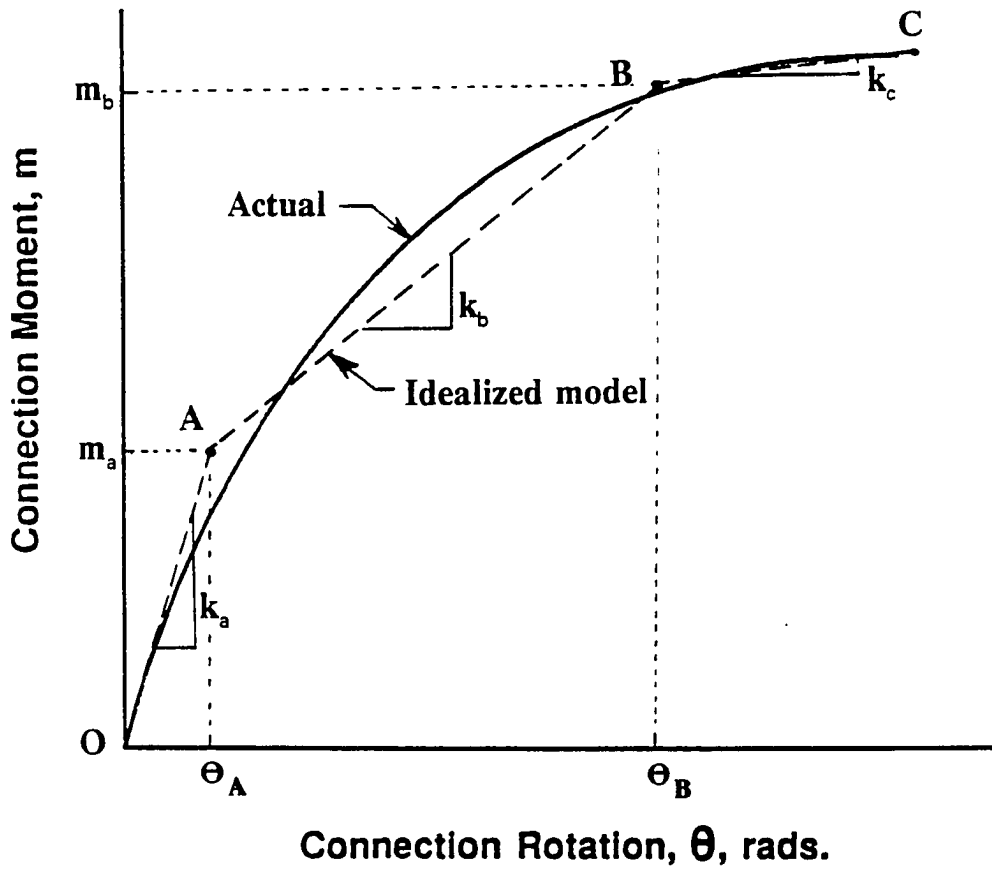


Figure 24. Connection moment-rotation relationships

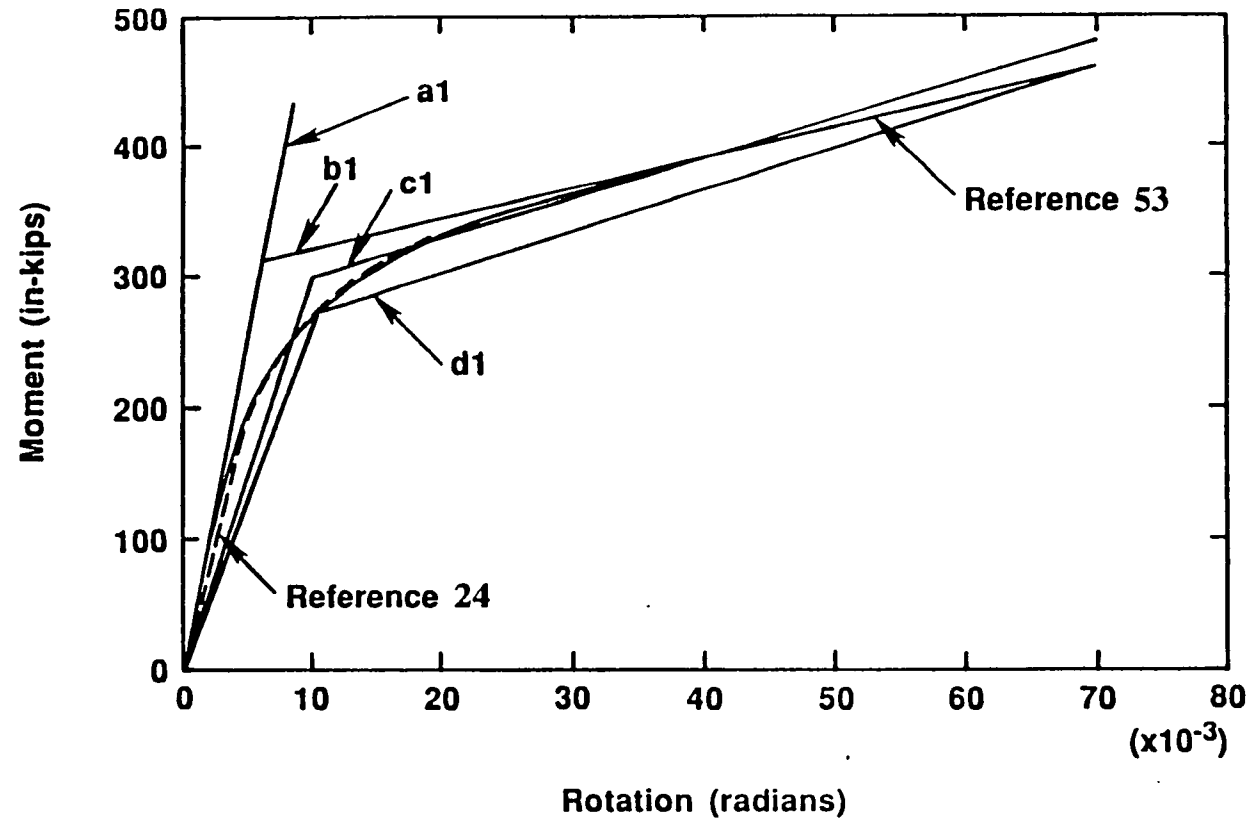


Figure 25. Linear and bilinear approximations of connection  $m-\theta$  curve for column analysis

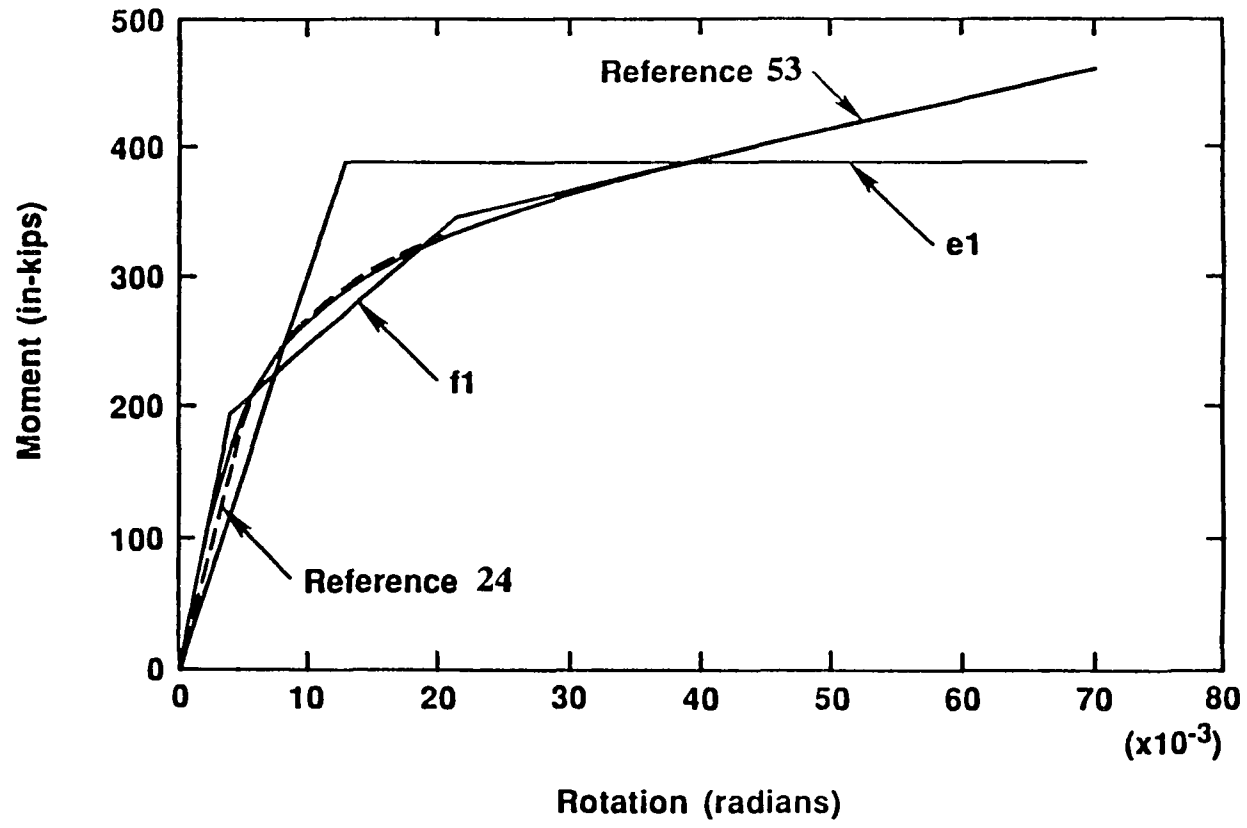


Figure 26. Elastic-plastic and trilinear approximations of connection  $m-\theta$  curve for column analysis

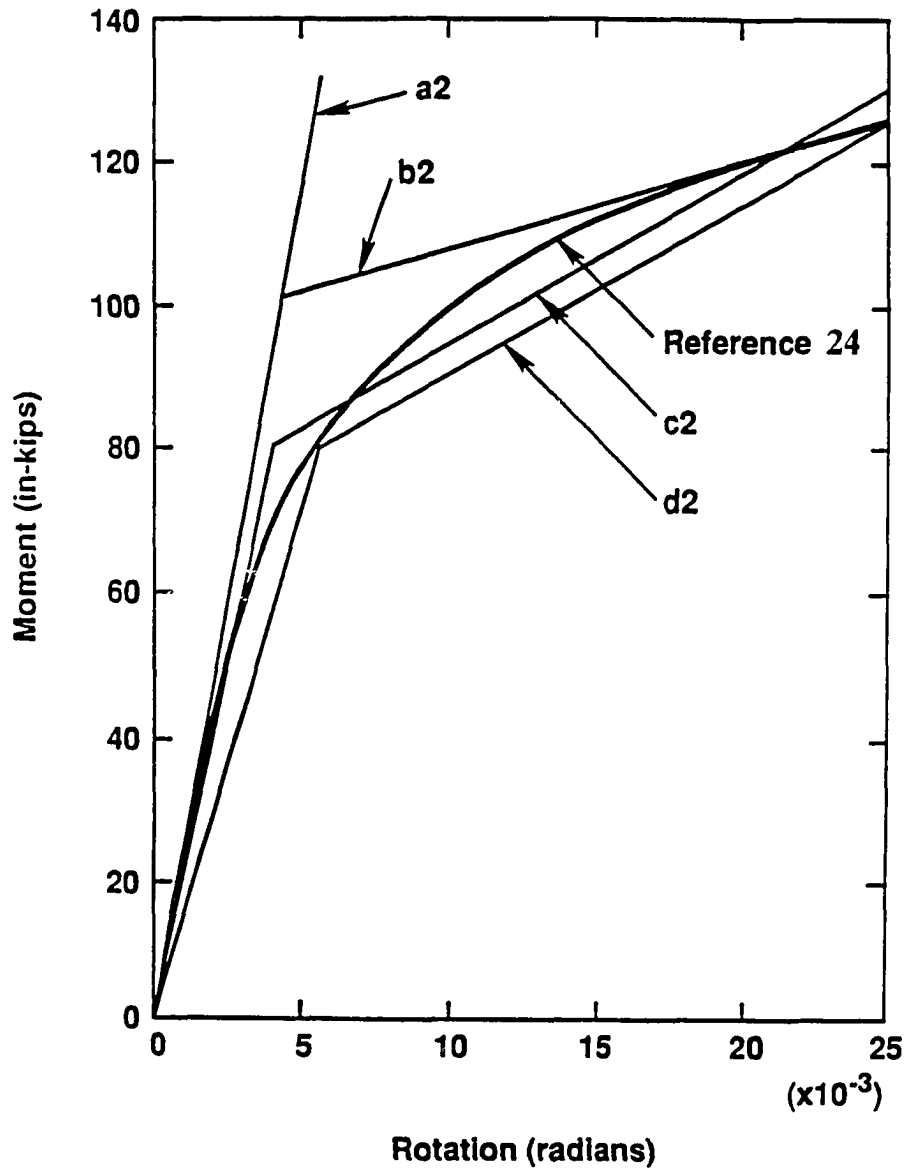


Figure 27. Linear and bilinear approximations of connection  $m-\theta$  curve for beam-column analysis



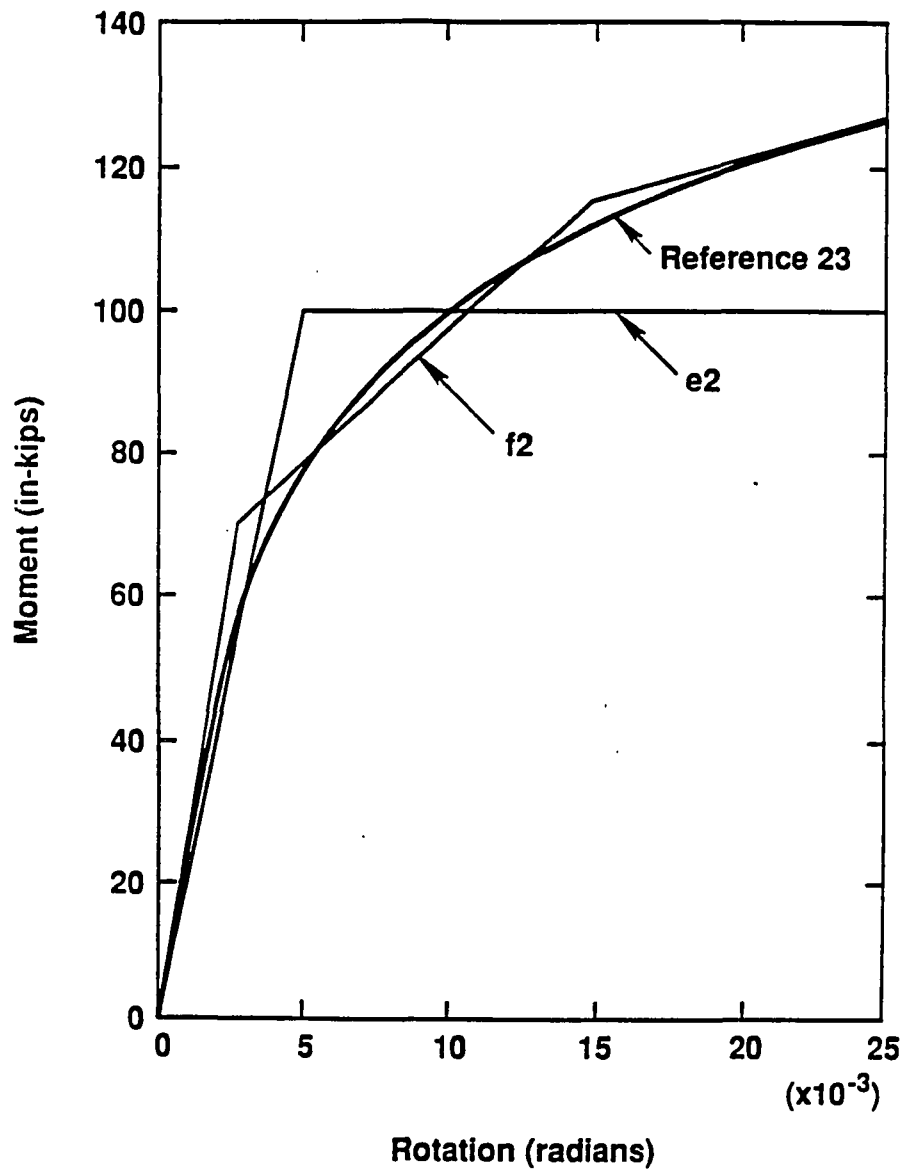


Figure 28. Elastic-plastic and trilinear approximations of connection  $m-\theta$  curve for beam-column analysis

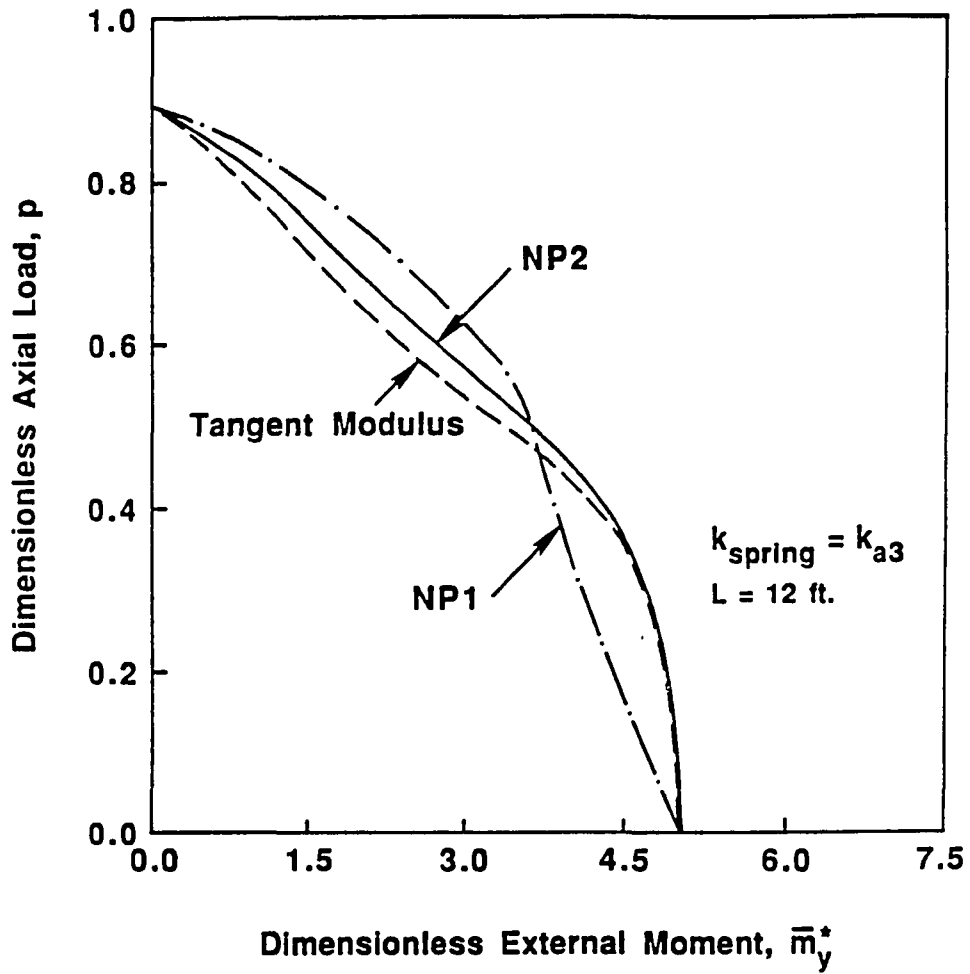


Figure 29. Interaction curves for uniaxially loaded partially restrained beam-column 4

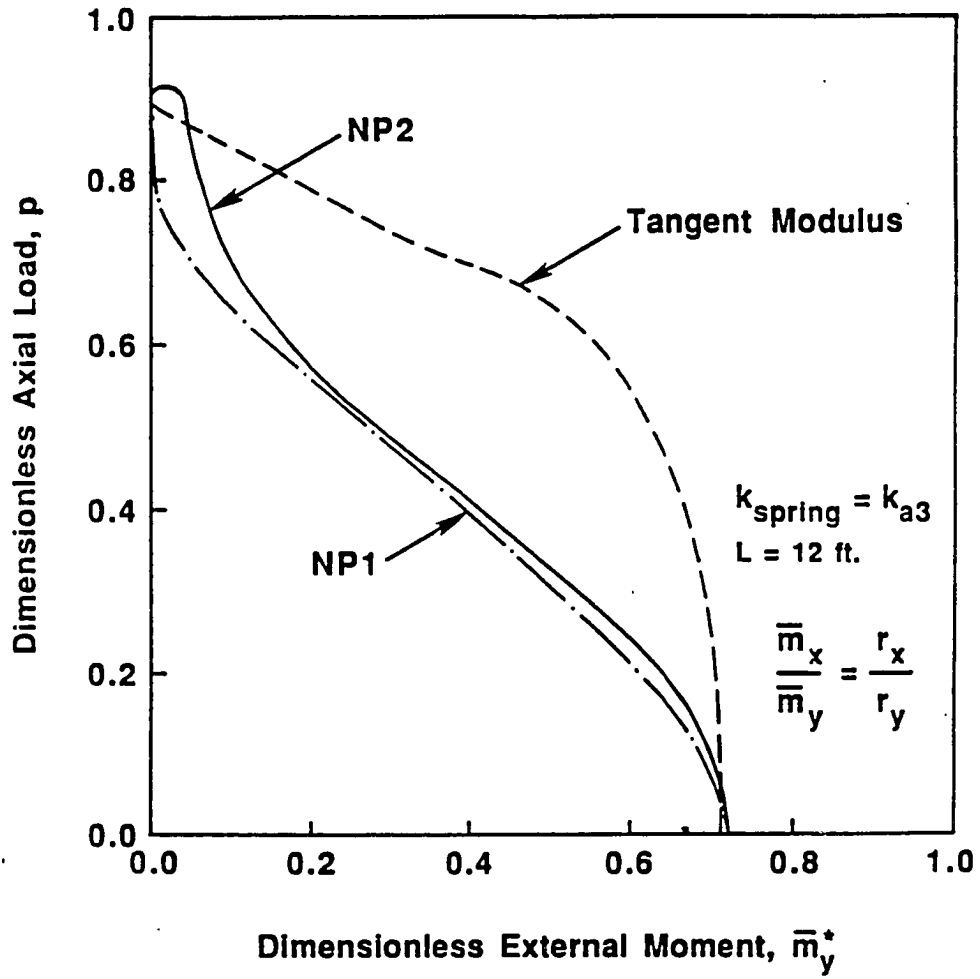


Figure 30. Interaction curves for biaxially loaded partially restrained beam-column 8

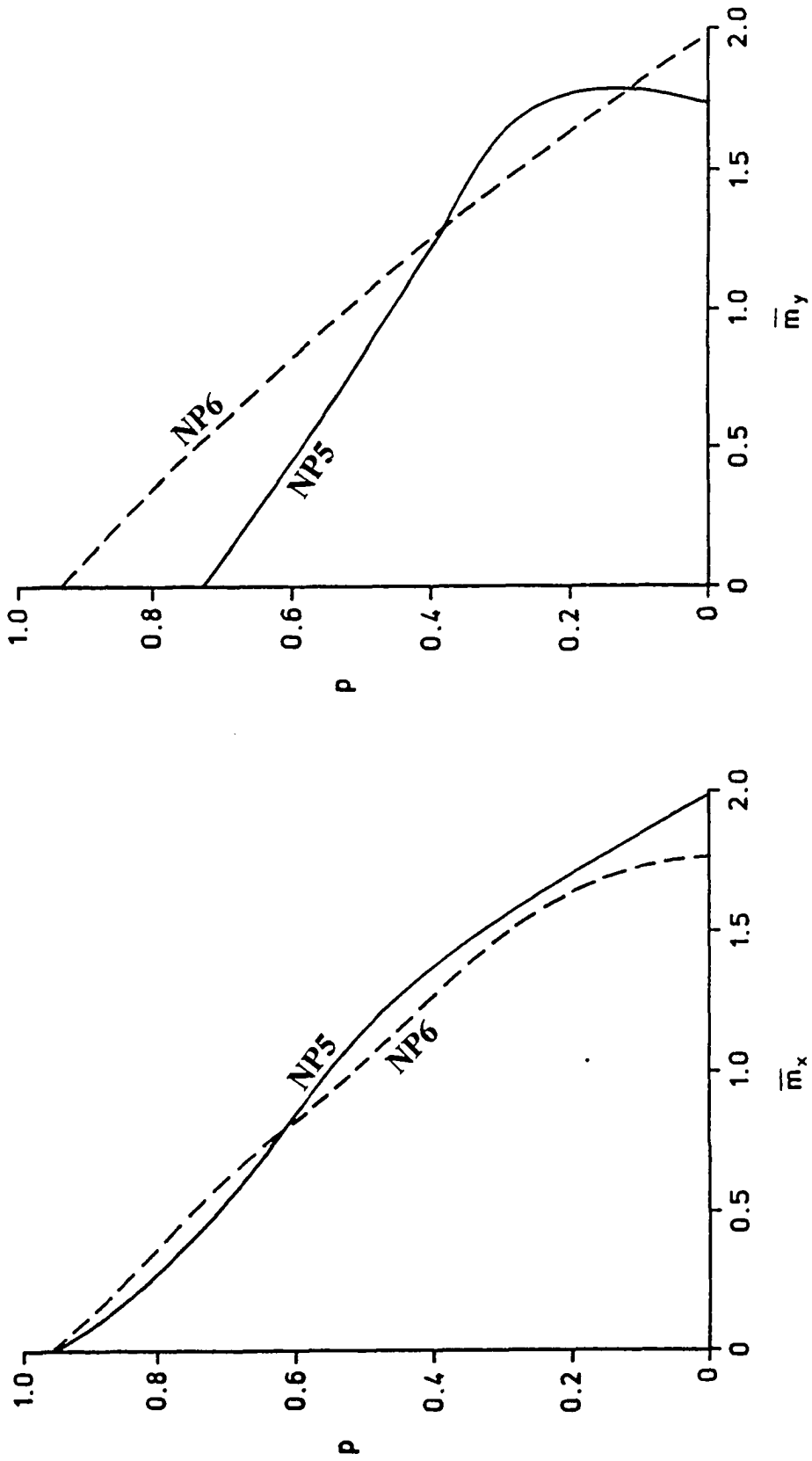


Figure 31. Interaction curves for biaxially loaded partially restrained imperfect beam-column BC3 for load paths NP5 and NP6 (a) (b)

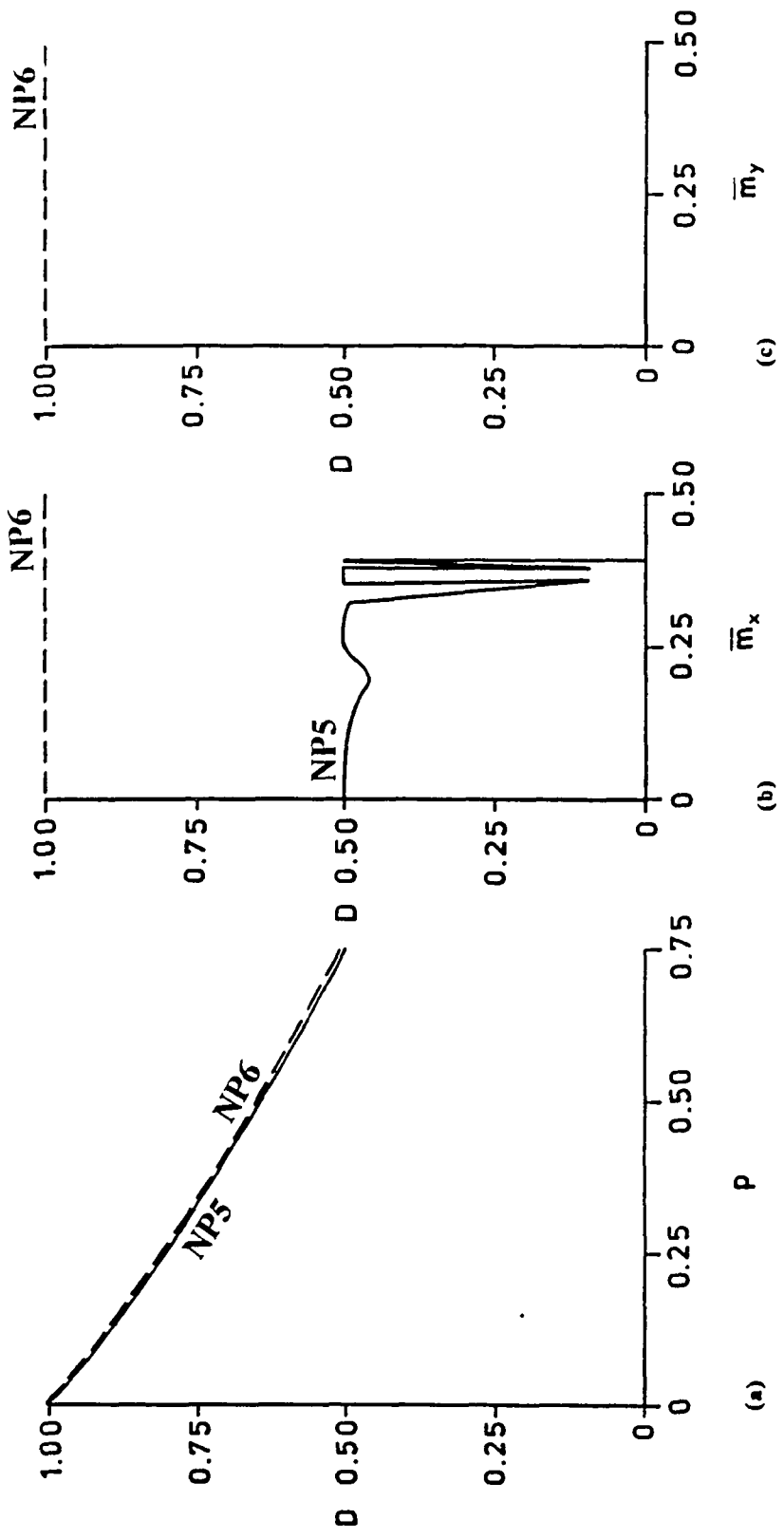
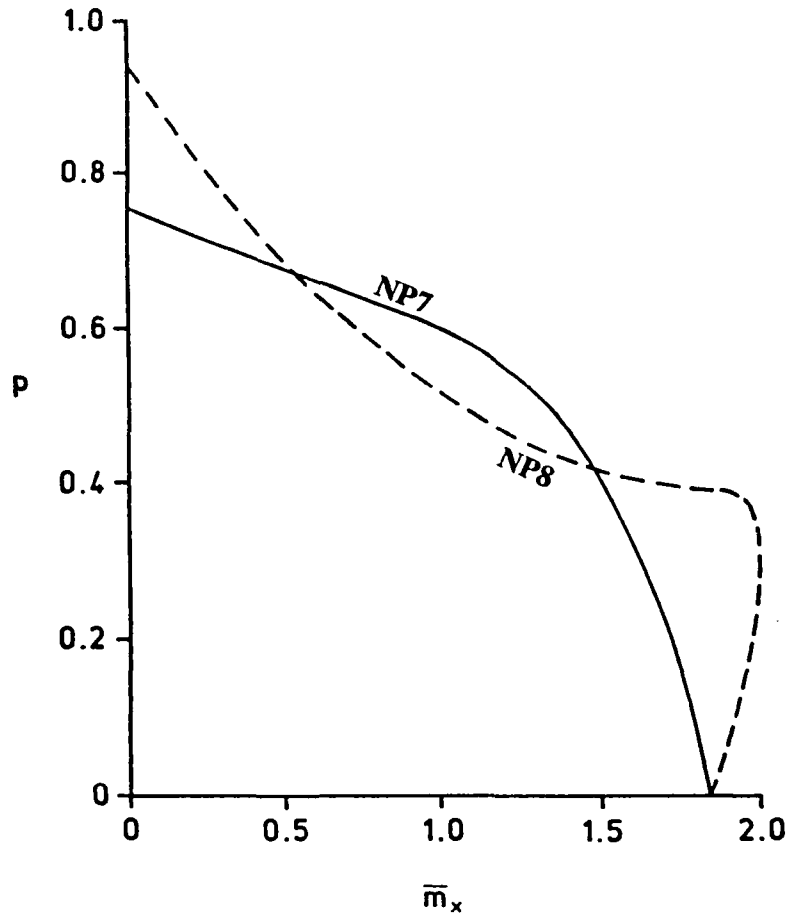
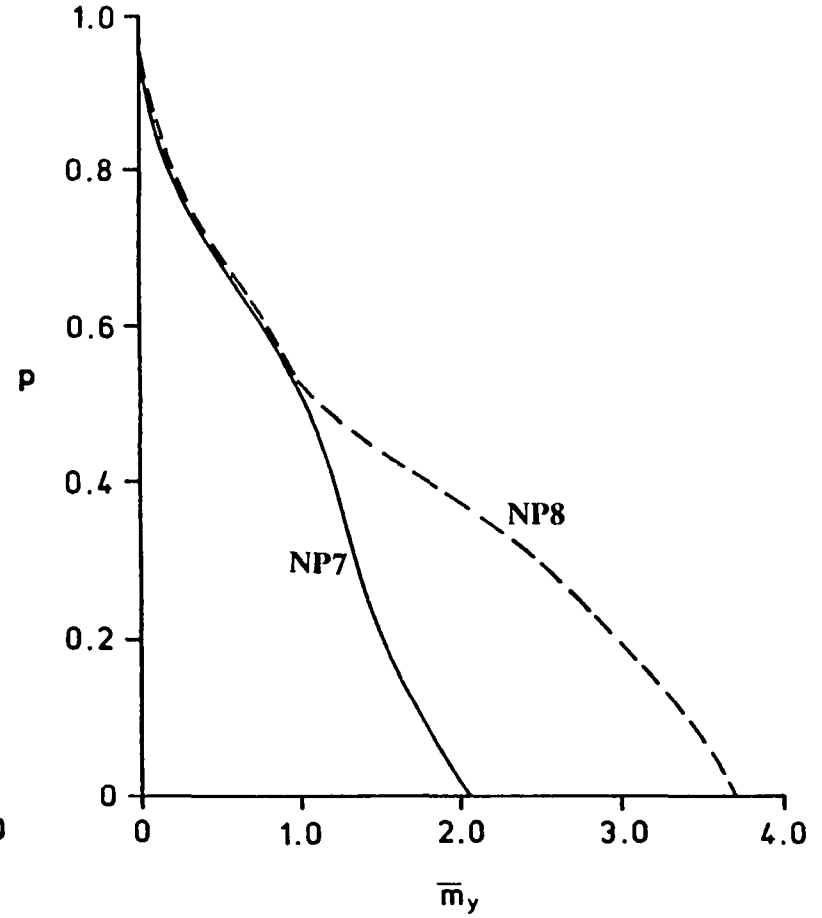


Figure 32. Stiffness degradation curves for beam-column BC3 with load paths NP5 and NP6 and axial load  $p=0.75$



(a)



(b)

Figure 33. Interaction curves for biaxially loaded partially restrained imperfect beam-column BC5 for load paths NP7 and NP8

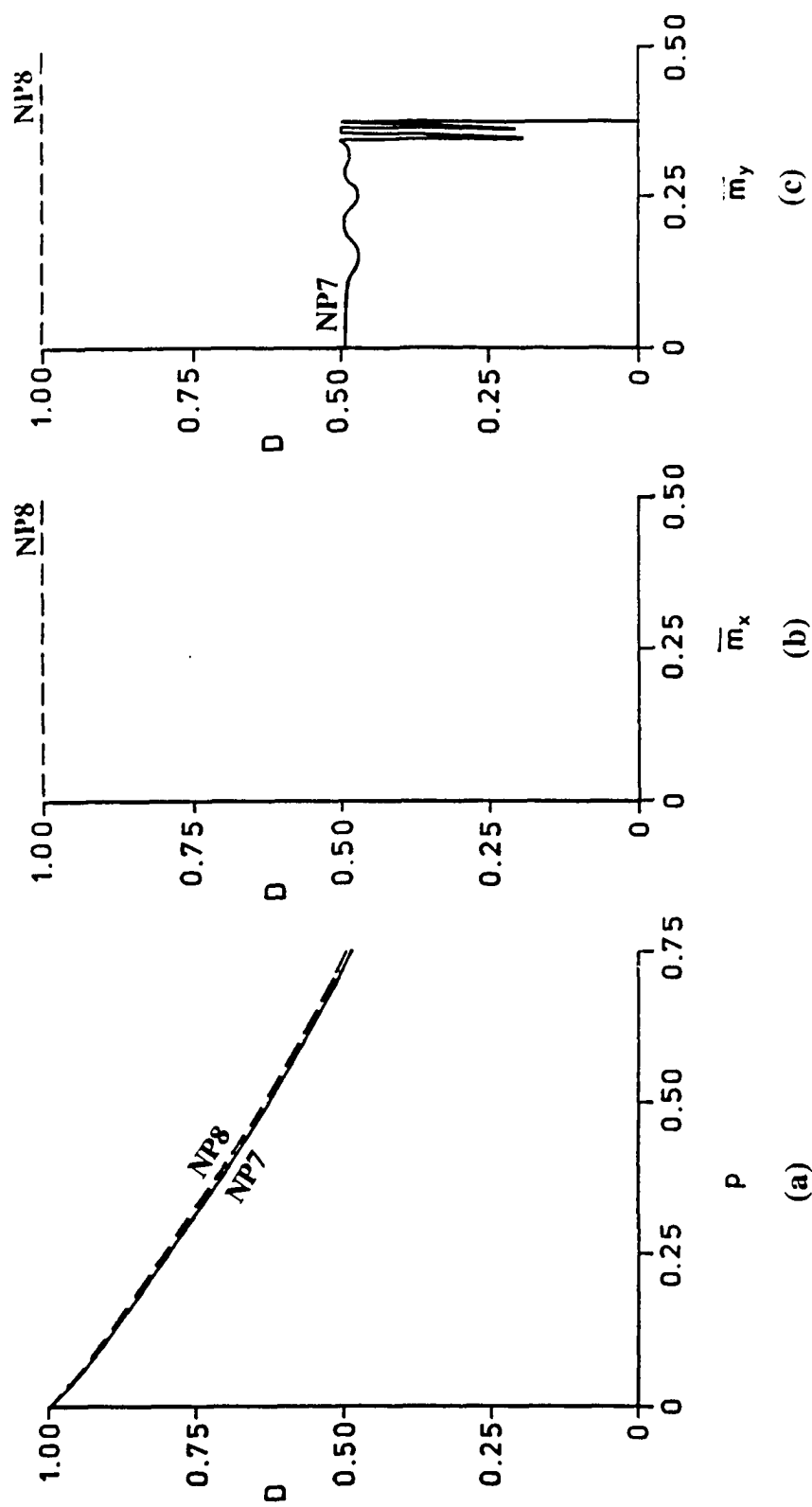


Figure 34. Stiffness degradation curves for beam-column BC5 with load paths NP7 and NP8 and axial load  $p=0.75$

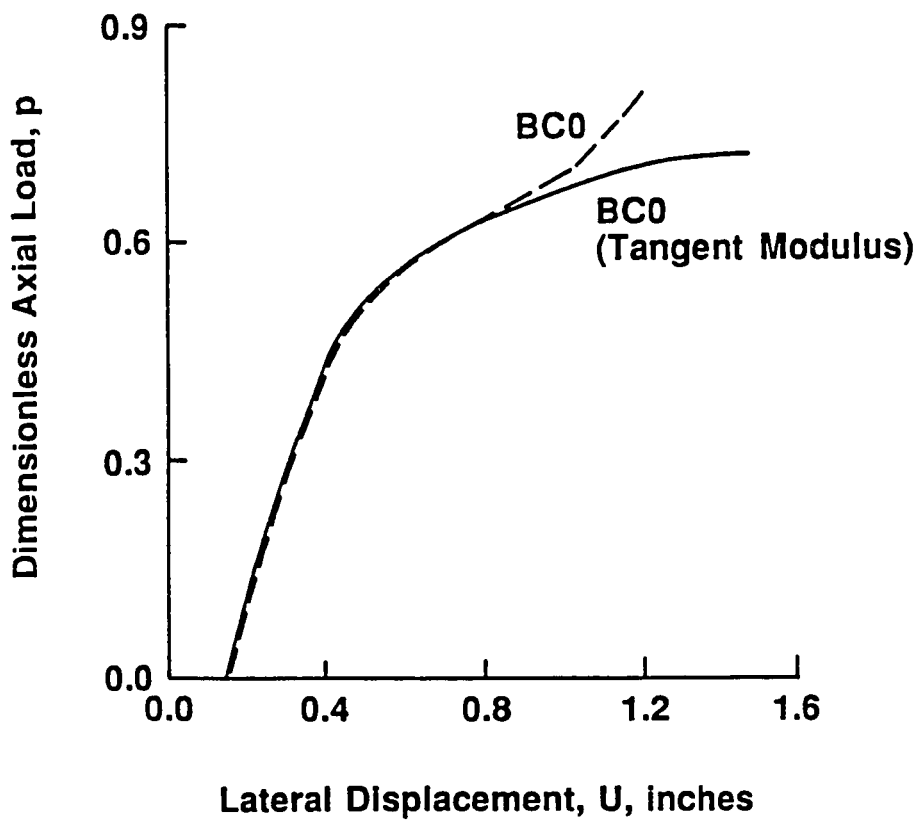


Figure 35. Load versus midspan displacement relationships for BC0



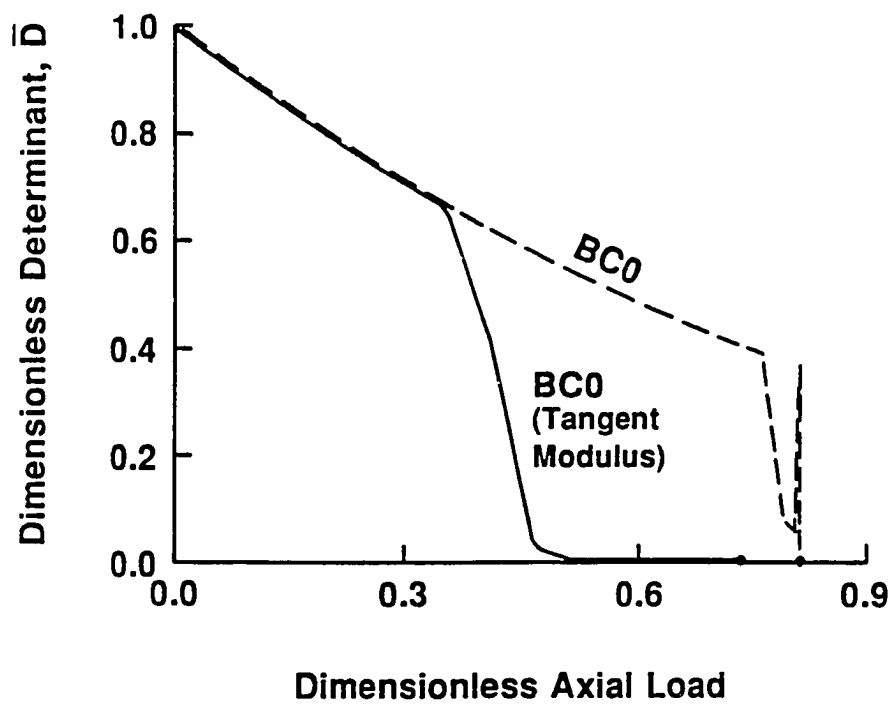


Figure 36. Stiffness degradation curves for BC0

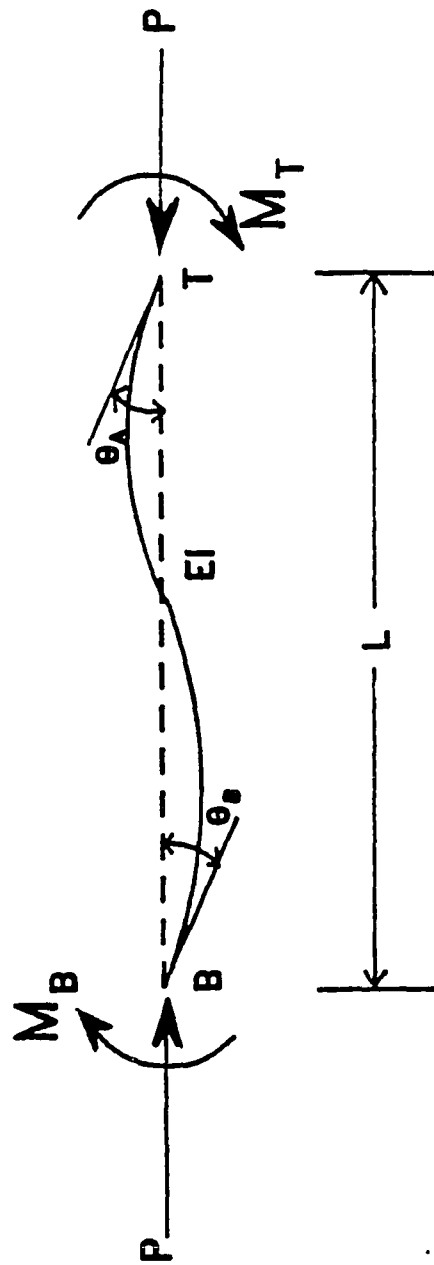


Figure 37. Beam-column

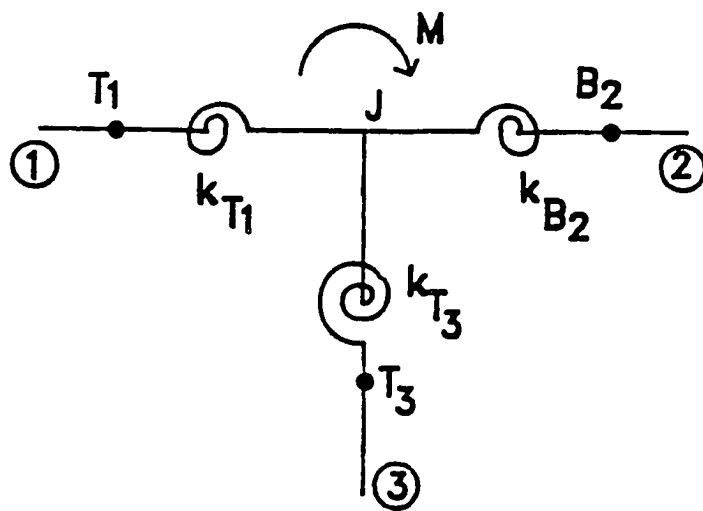


Figure 38. Typical frame joint

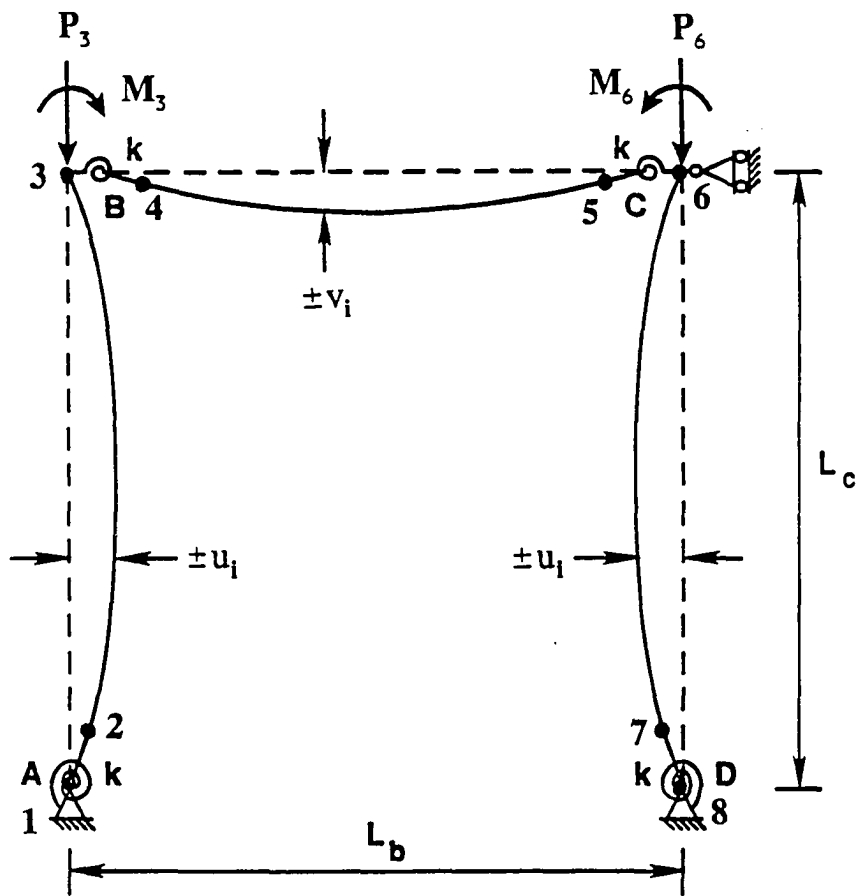


Figure 39. Imperfect portal frame

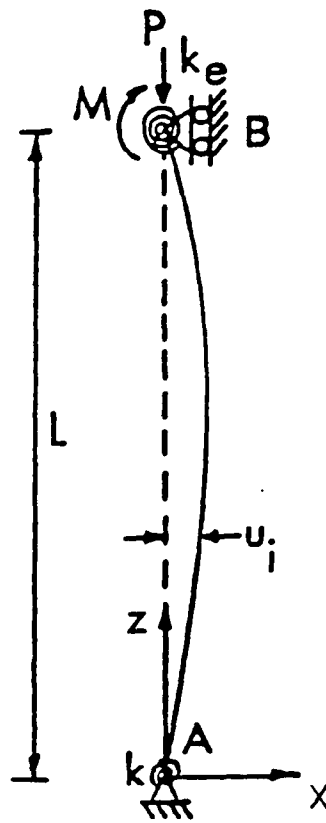


Figure 40. Equivalent structural model for portal frame

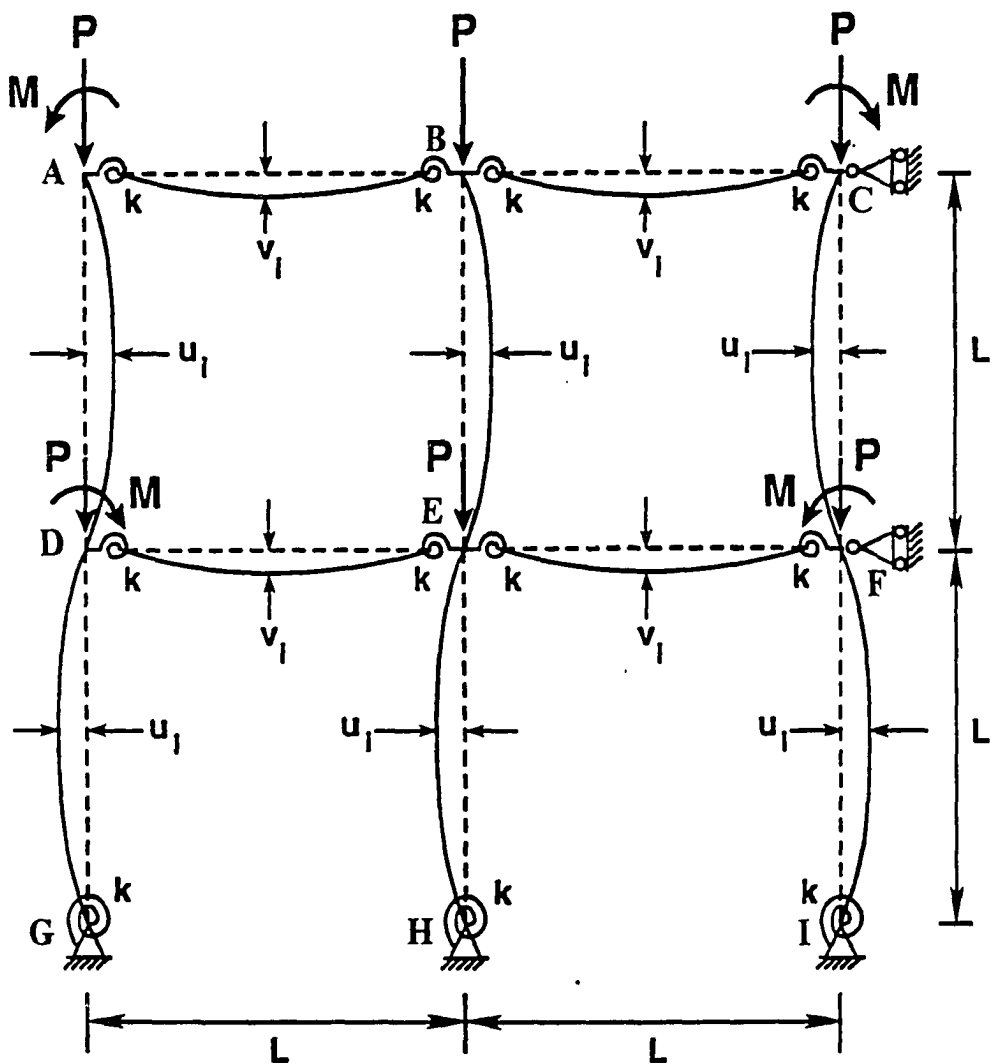


Figure 41. Flexibly-connected imperfect two-bay two-story frame

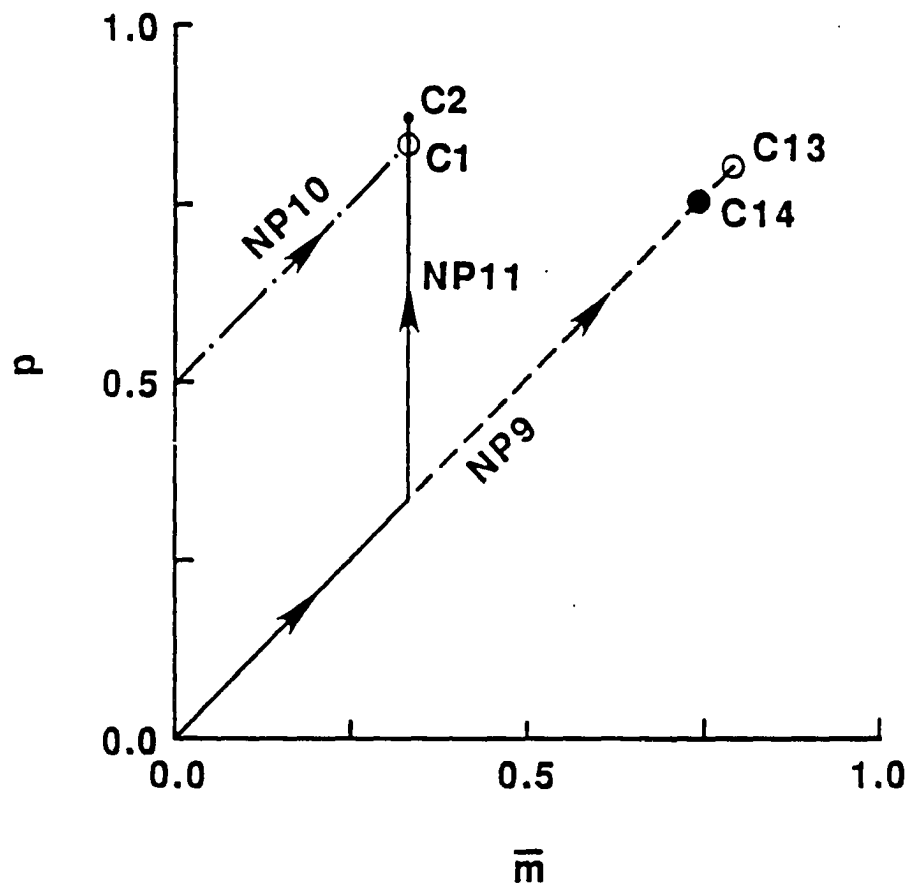


Figure 42. Load-moment relationships

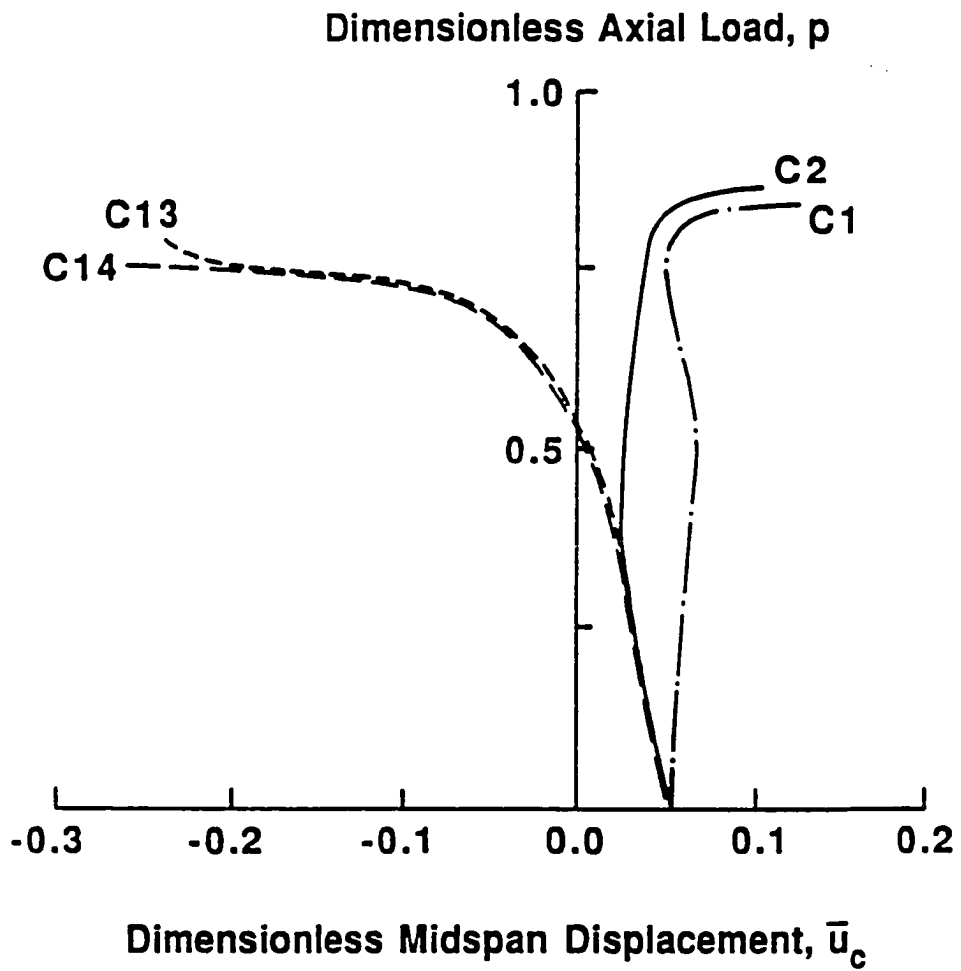
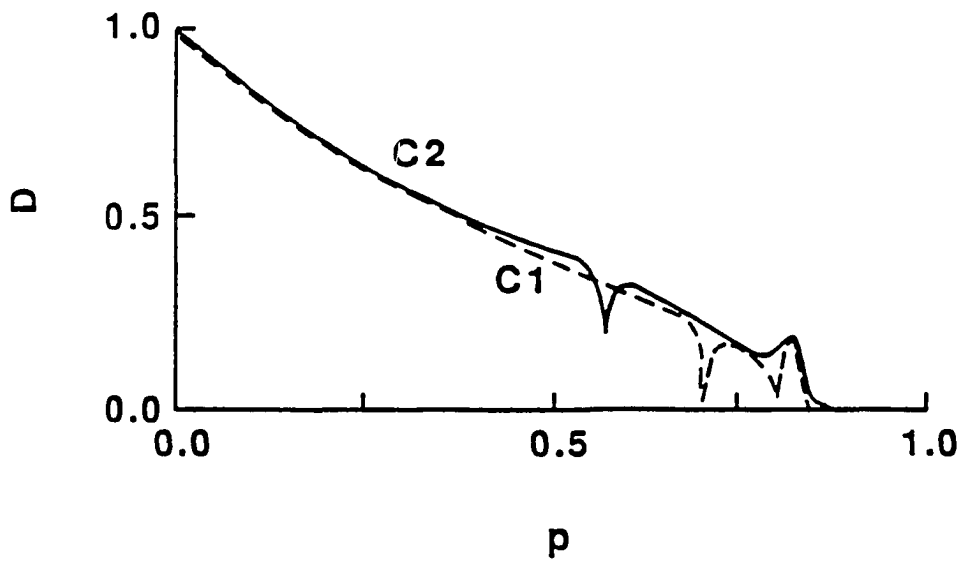
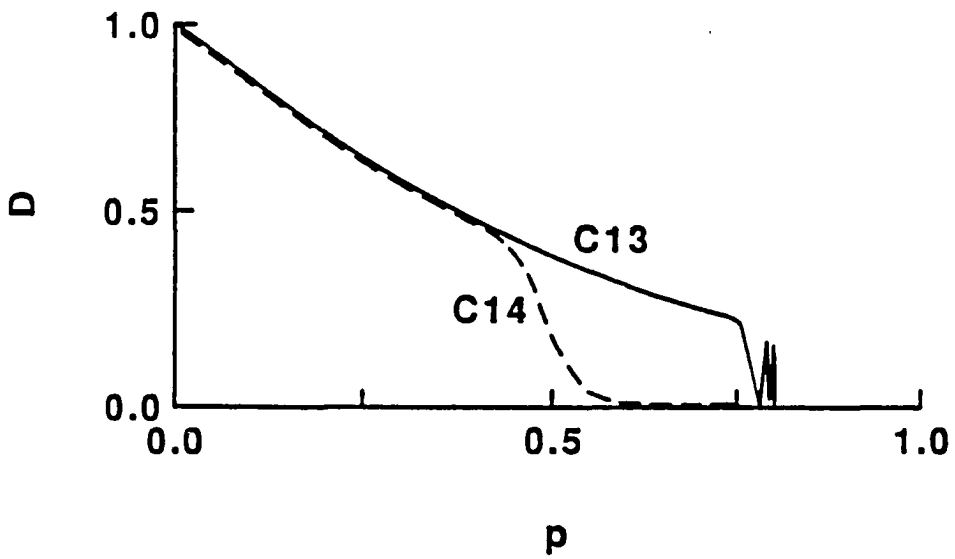


Figure 43. Load-deflection relationships





(a) Cases C1 and C2



(b) Cases C13 and C14

Figure 44. Stiffness degradation curves

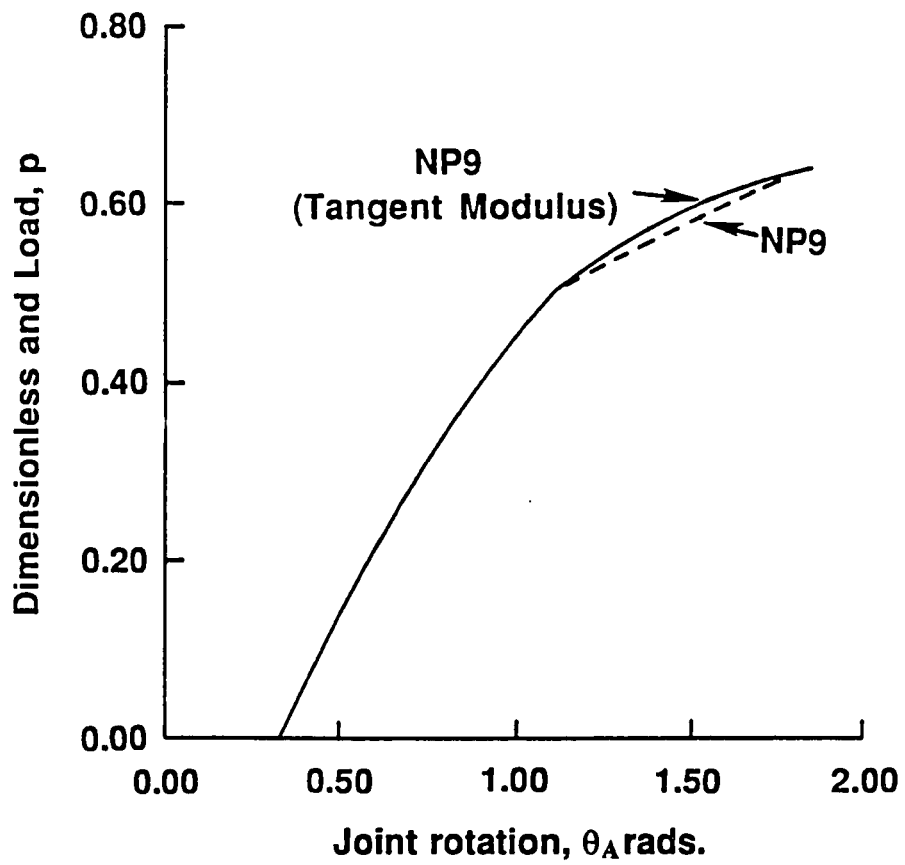


Figure 45. Axial load versus joint rotation relationship for portal frame FR2 and frame loading FL3 with NP9

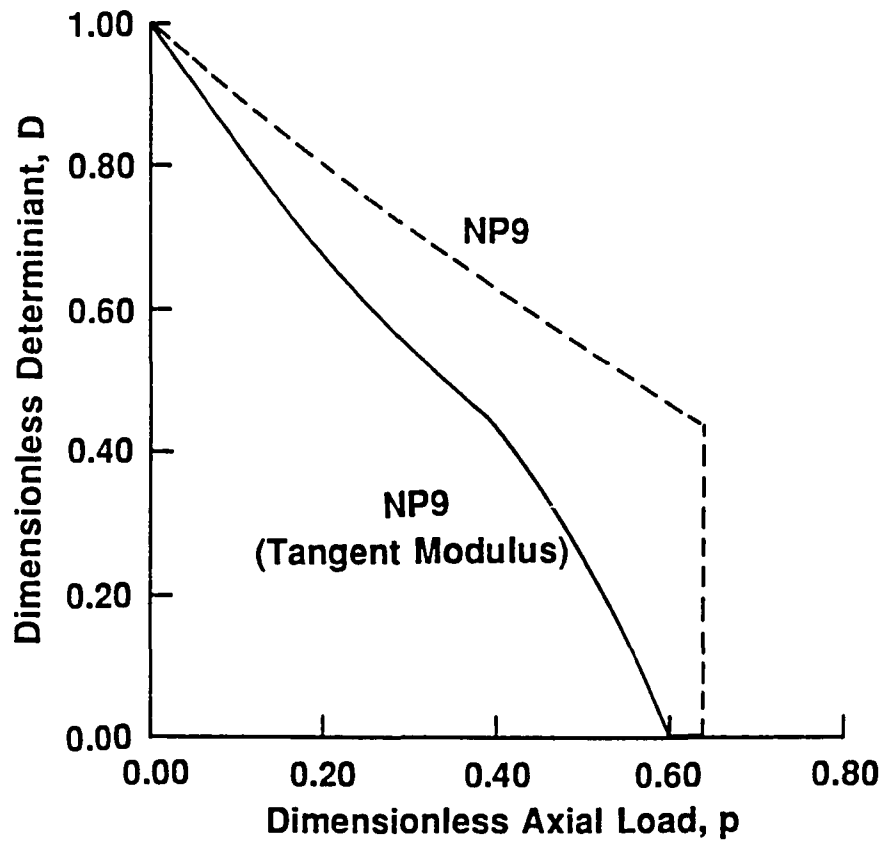


Figure 46. Stiffness degradation curve for portal frame FR2 and frame loading FL3 with NP9

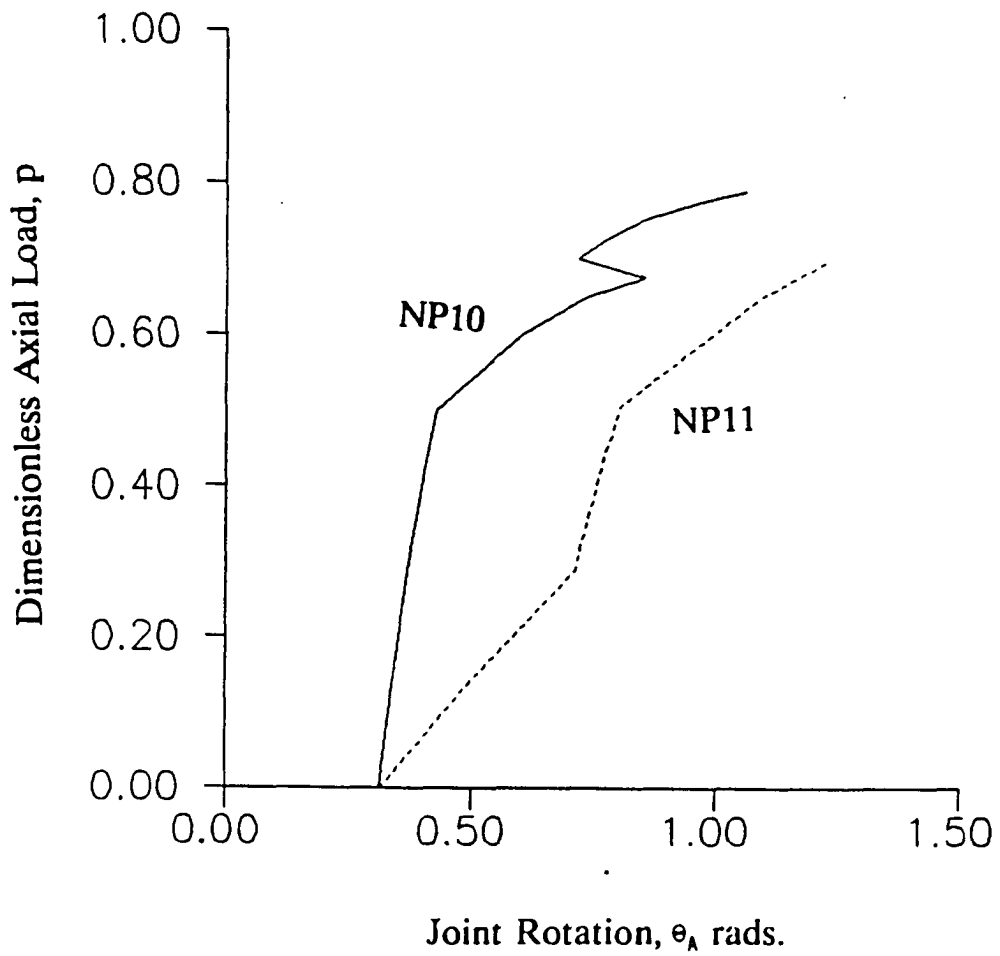


Figure 47. Axial load versus joint rotation relationship for portal frame FR2 and frame loading FL3 with NP10 and NP11

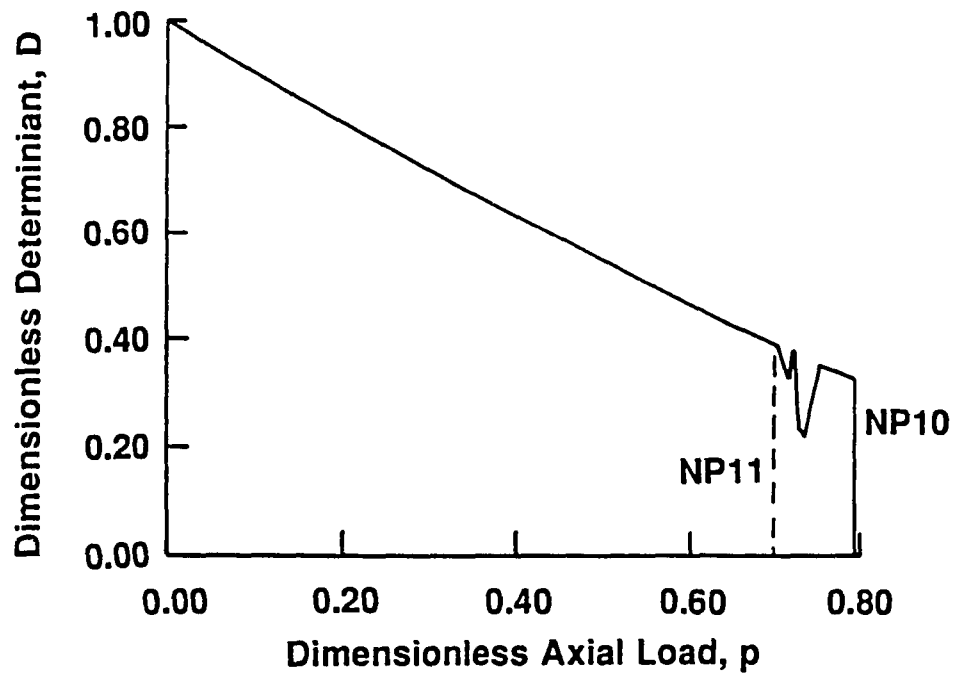


Figure 48. Stiffness degradation curve for portal frame FR2 and frame loading FL3 with NP10 and NP11

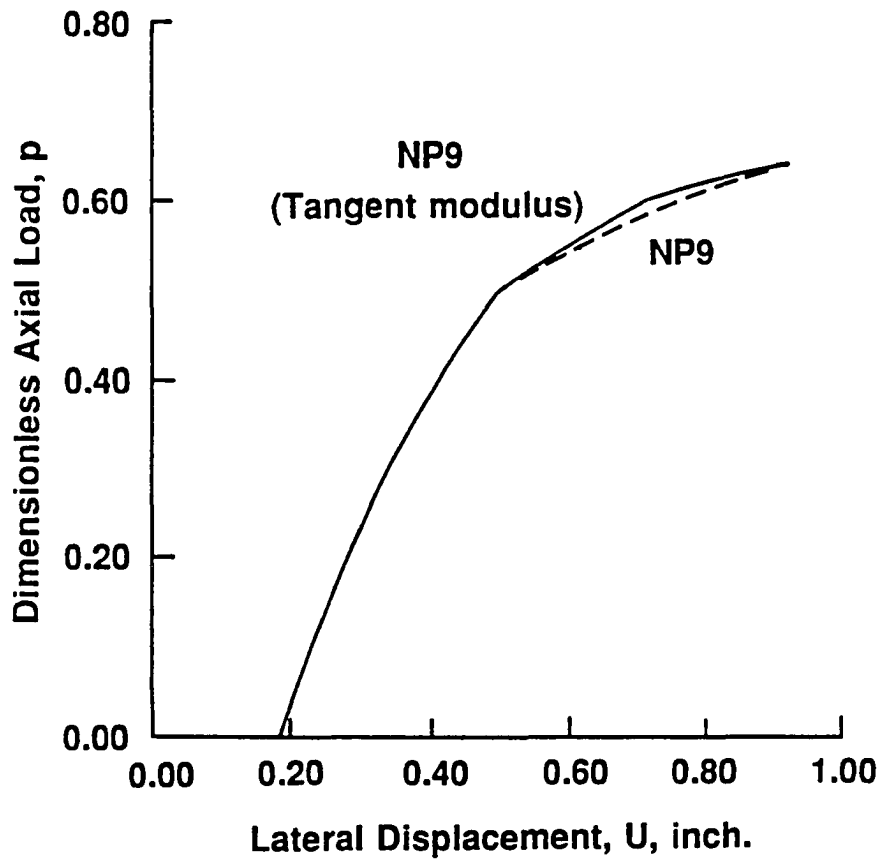


Figure 49. Axial load versus midspan displacement relationship for a column of the frame FR2 and loading FL3 with NP9

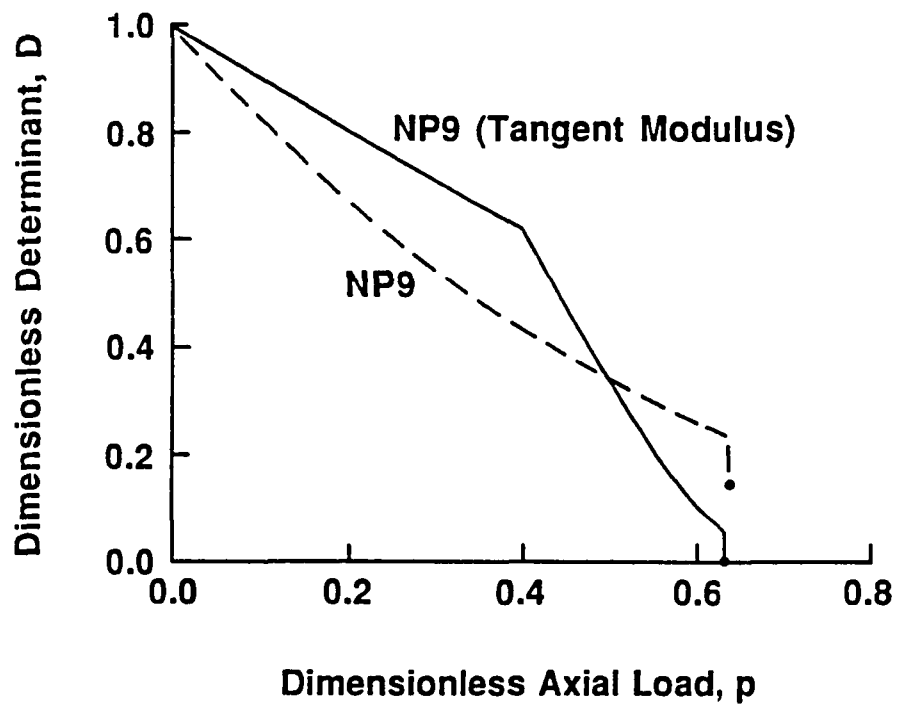


Figure 50. Stiffness degradation curve for a column of the frame FR2 and loading FL3 with NP9

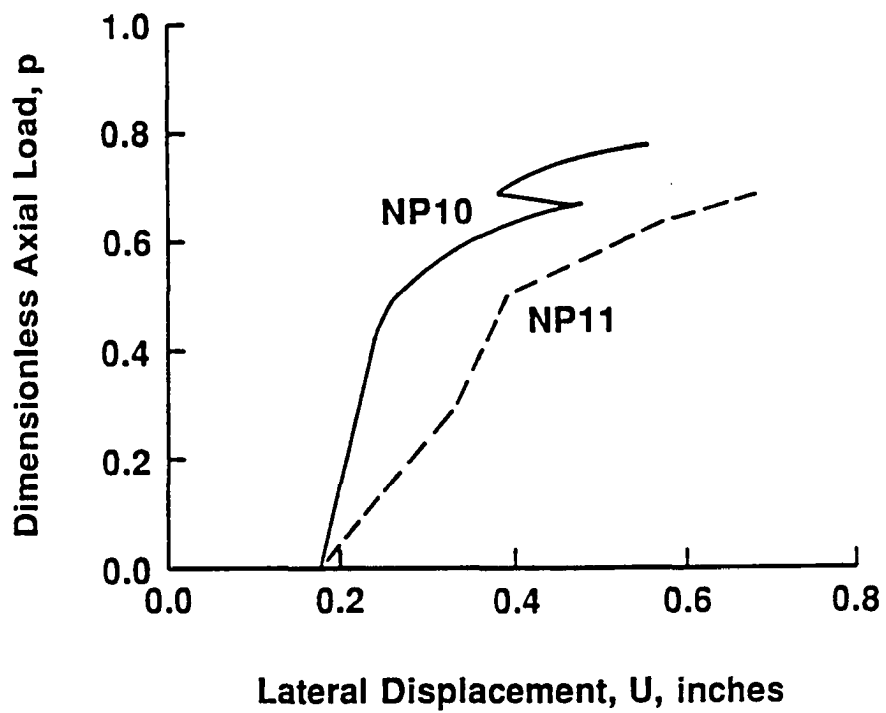


Figure 51. Axial load versus midspan displacement relationship for a column of the frame FR2 and loading FL3 with NP10 and NP11



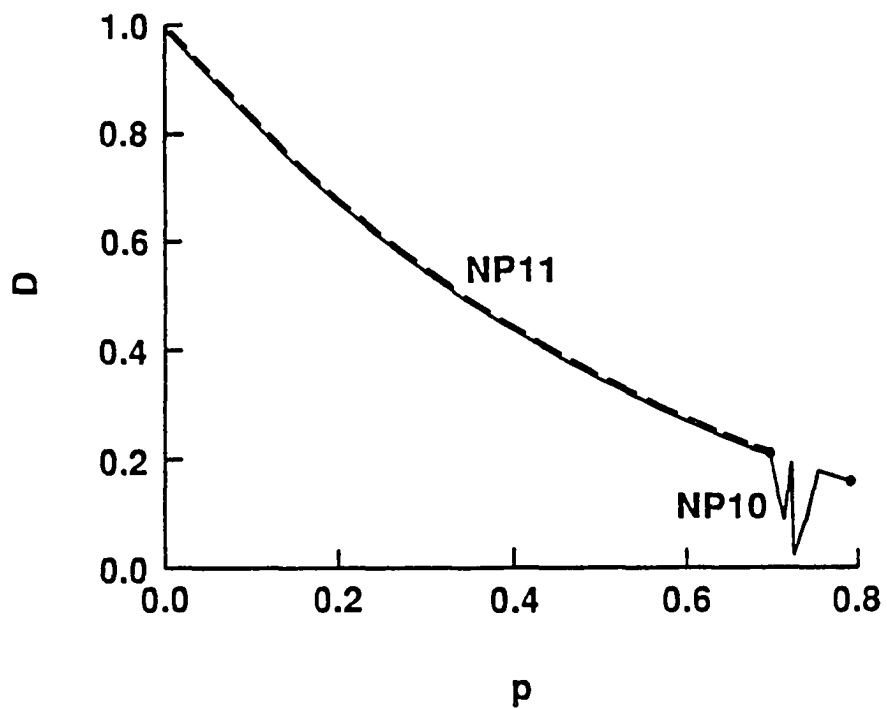


Figure 52. Stiffness degradation curve for a column of the frame FR2 and loading FL3 with NP10 and NP11

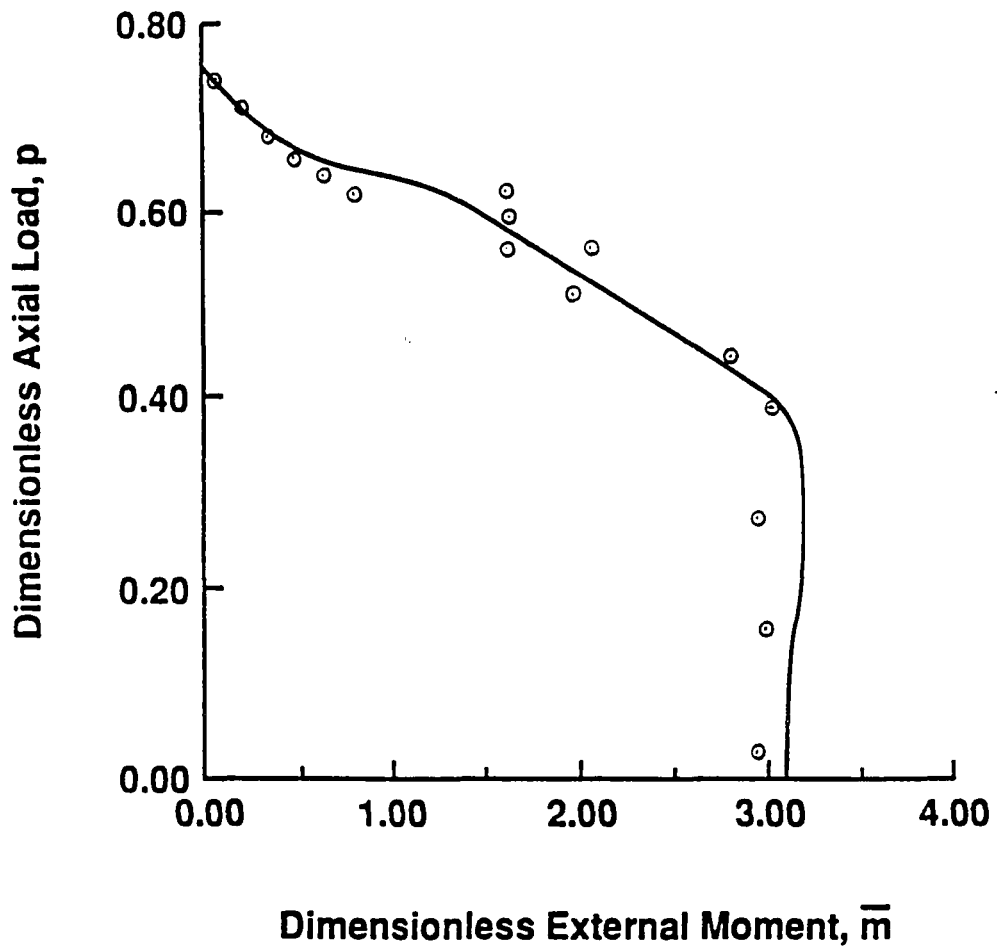


Figure 53.  $p$ - $\bar{m}$  interaction for frame FR2

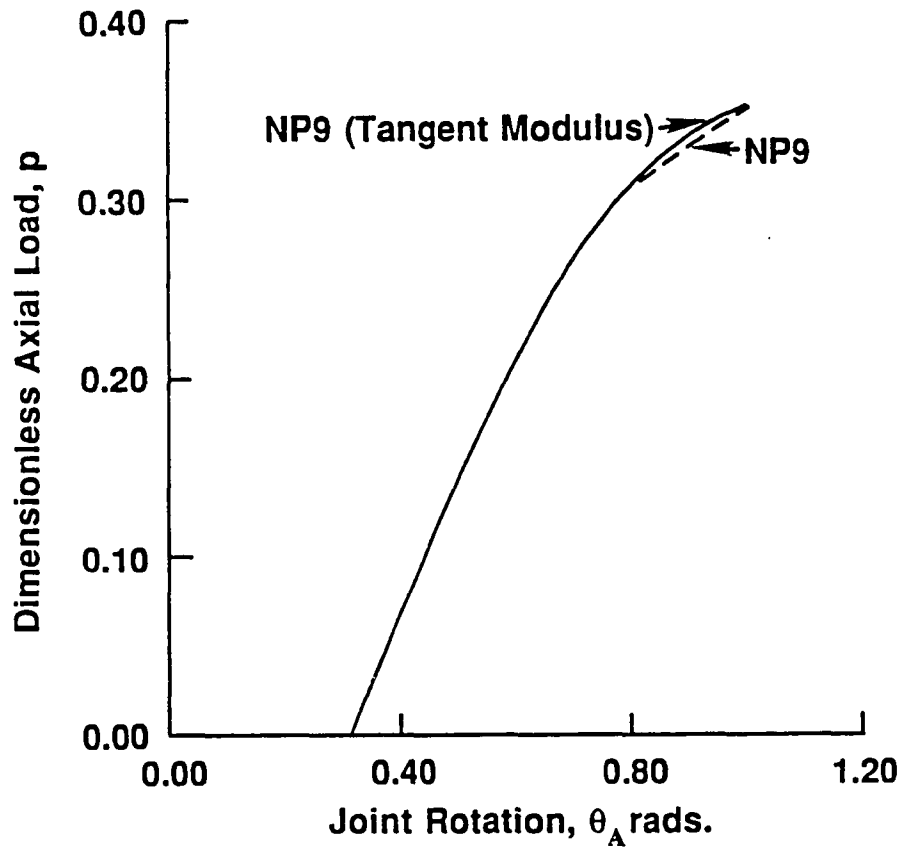


Figure 54. Axial load versus joint rotation relationship for two-bay two-story frame FR8 and frame loading FL8 with NP9

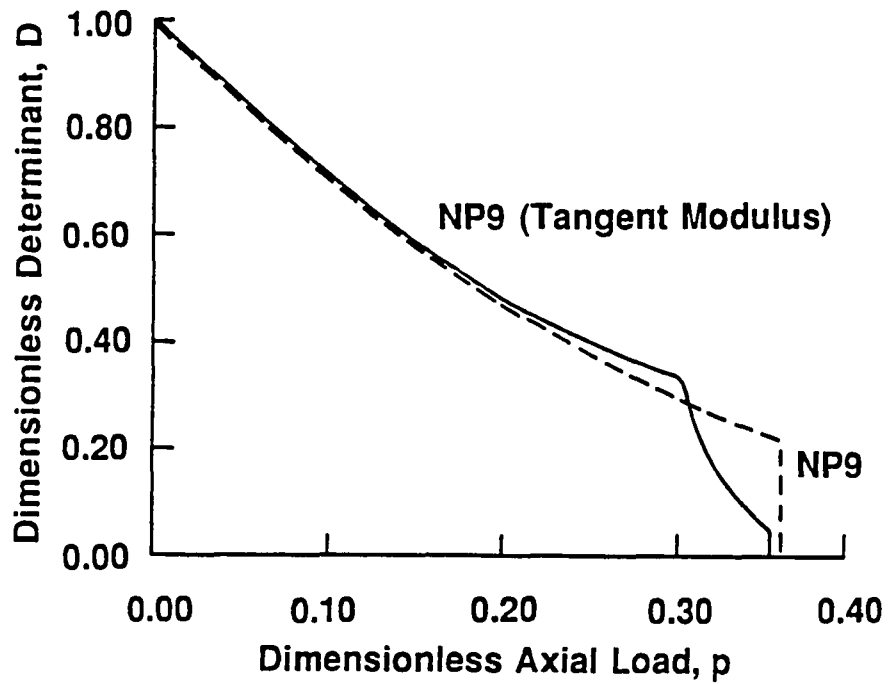


Figure 55. Stiffness degradation curve for two-bay two-story frame FR8 and frame loading FL8 with NP9

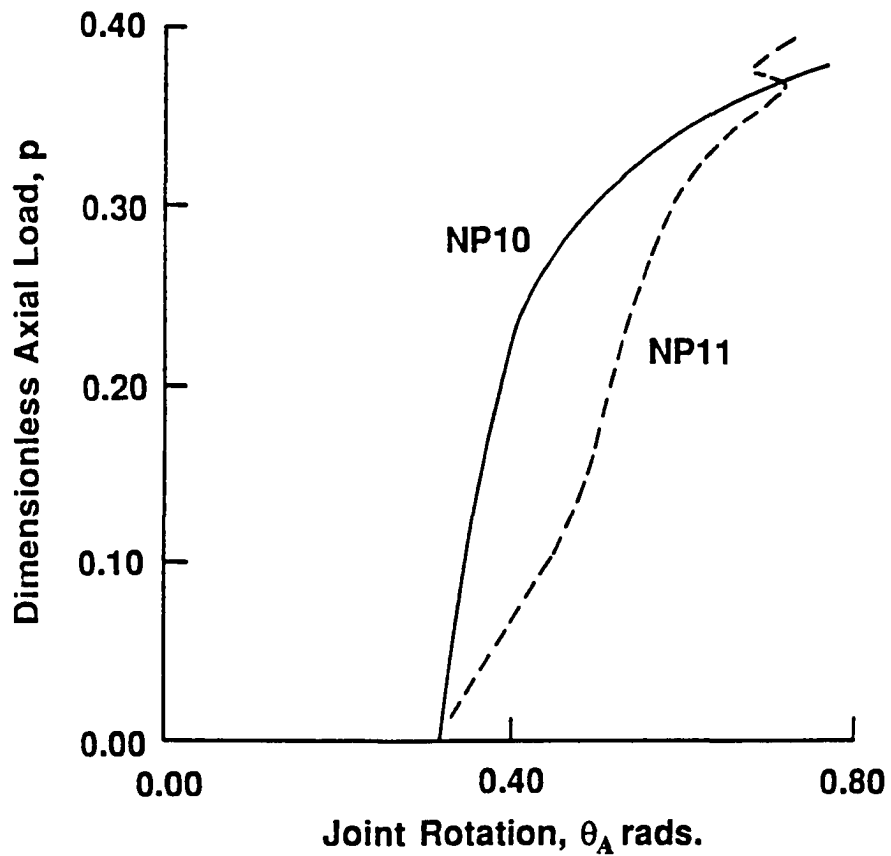


Figure 56. Axial load versus joint rotation relationship for two-bay two-story frame FR8 and frame loading FL8 with NP10 and NP11

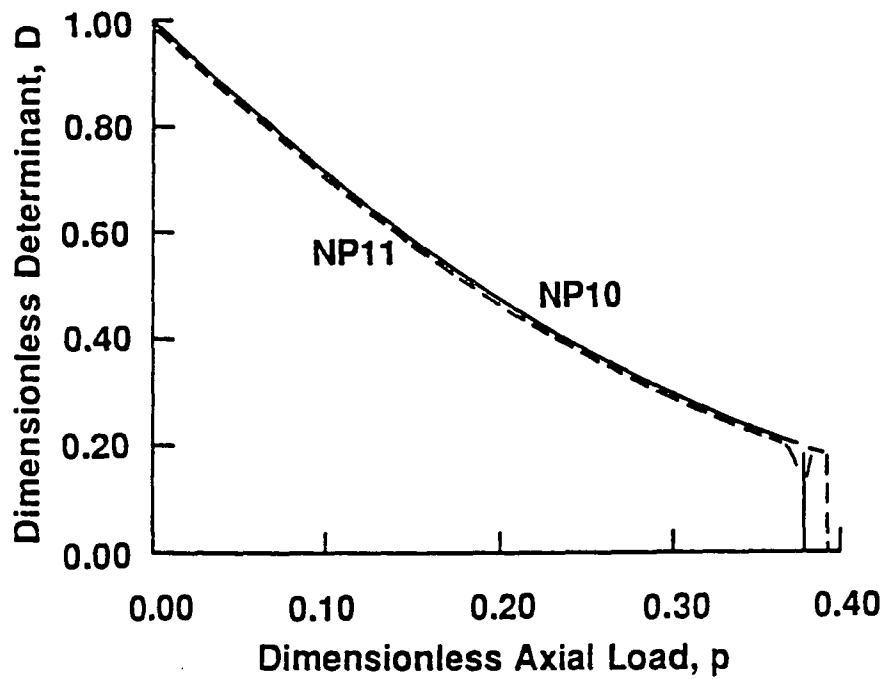


Figure 57. Stiffness degradation curve for two-bay two-story frame FR8 and frame loading FL8 with NP10 and NP11

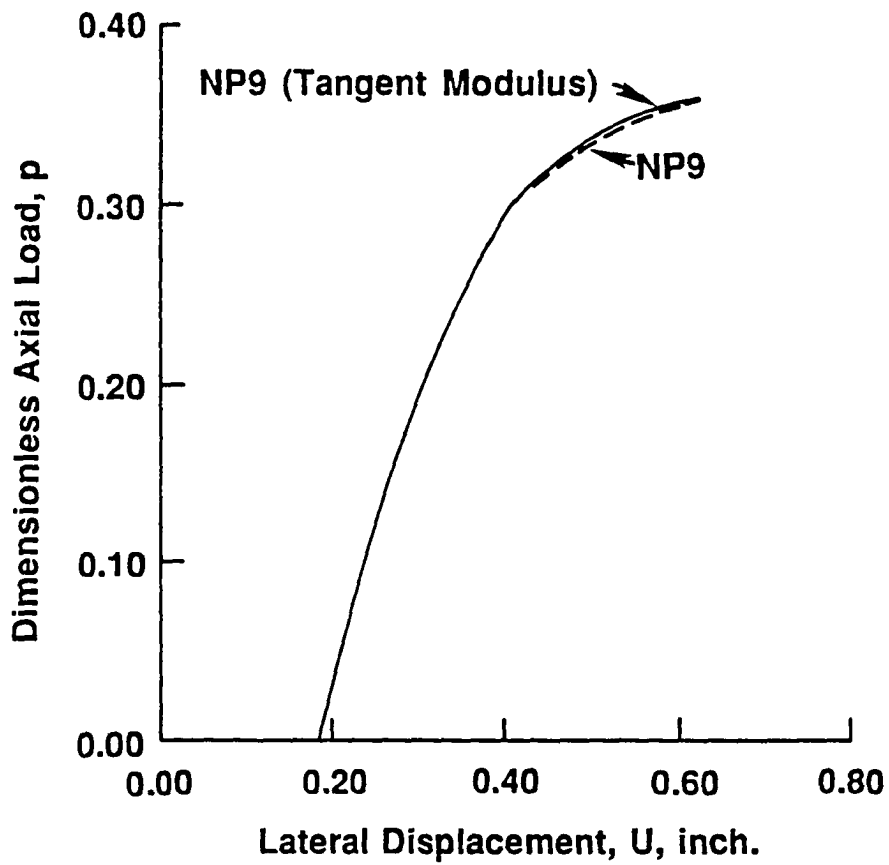


Figure 58. Axial load versus midspan displacement relationship for a column of the frame FR8 and loading FL8 with NP9

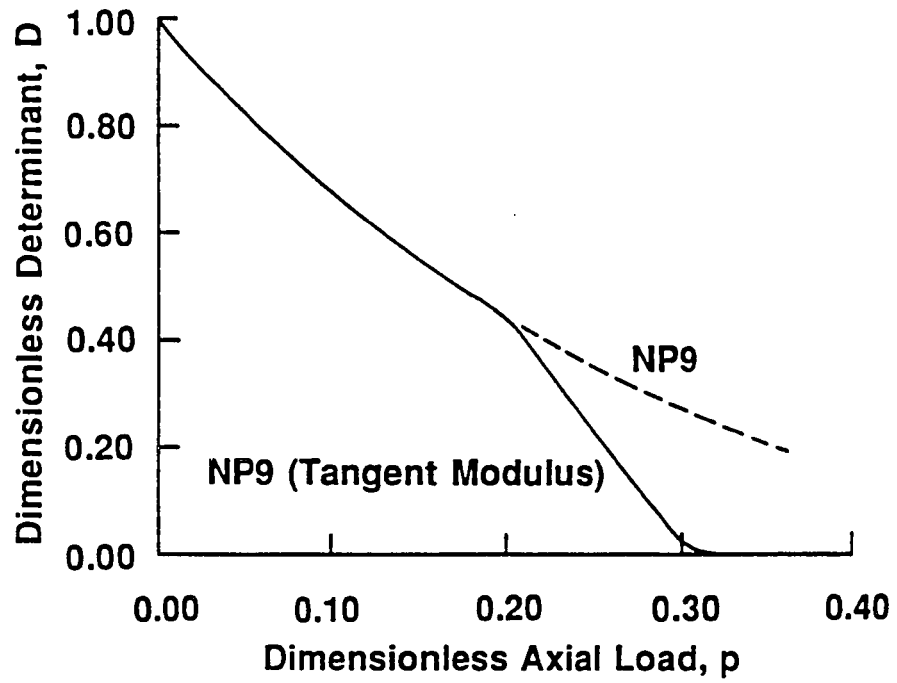


Figure 59. Stiffness degradation curve for a column of the frame FR8 and loading FL8 with NP9



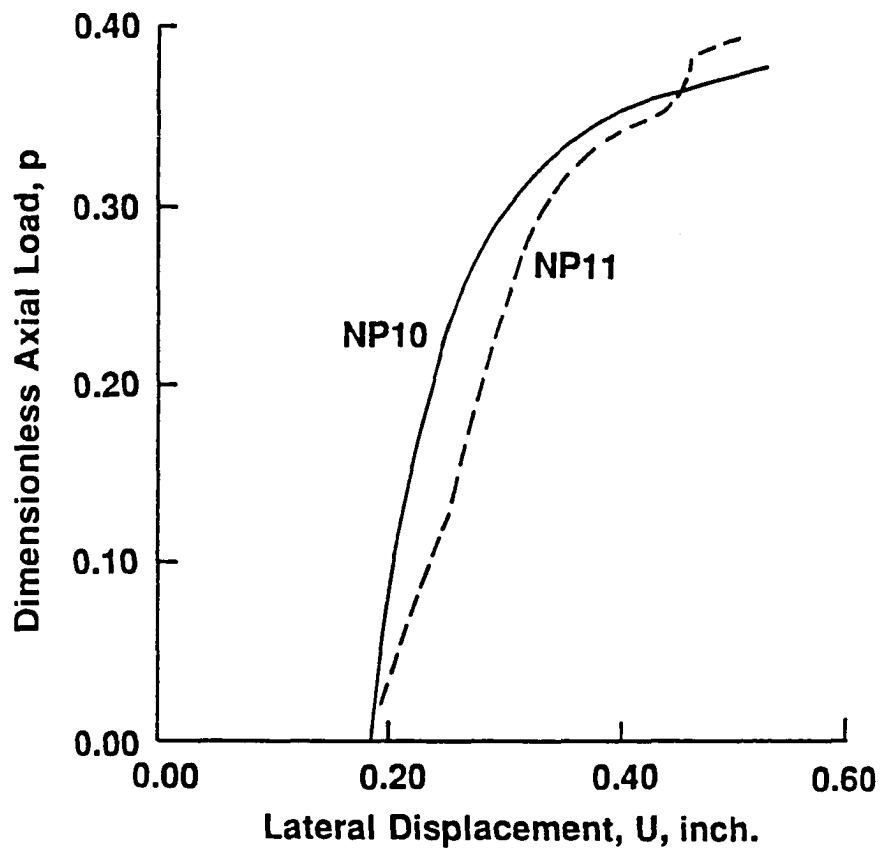


Figure 60. Axial load versus midspan displacement relationship for a column of frame FR8 and loading FL8 with NP10 and NP11

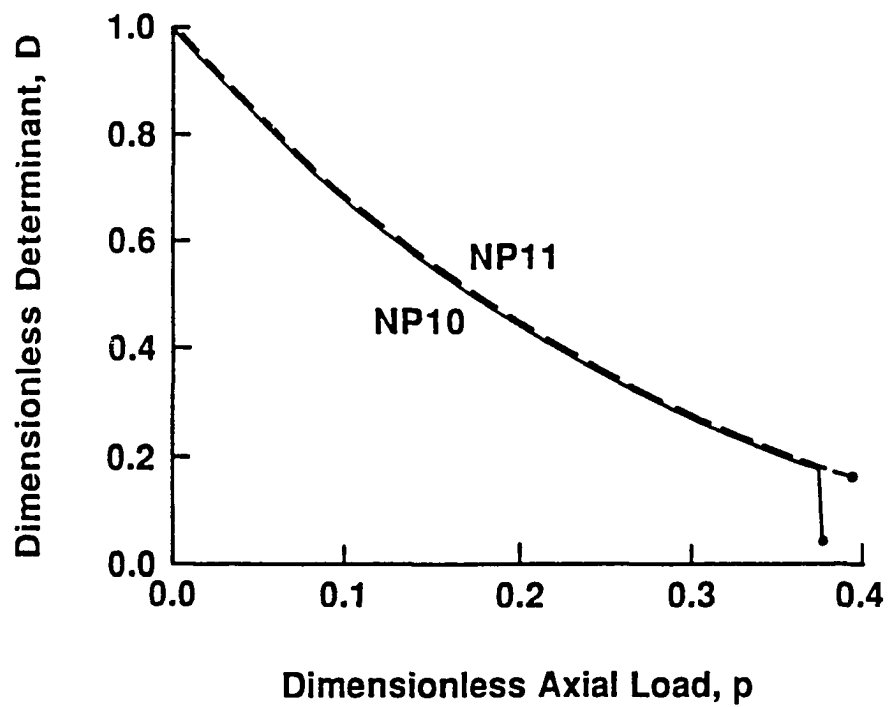


Figure 61. Stiffness degradation curve for a column of the frame FR8 and loading FL8 with NP10 and NP11

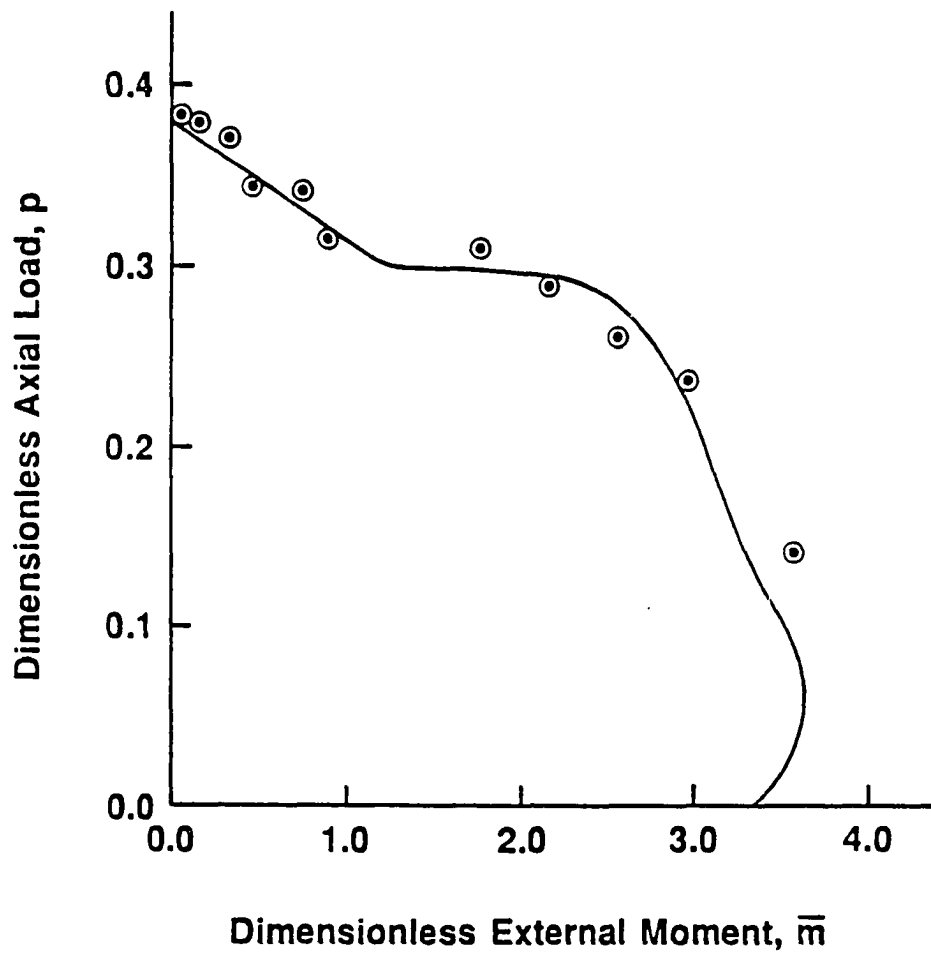


Figure 62.  $p$ - $\bar{m}$  interaction for frame FR8

## APPENDIX A

### Tangent Stiffness Method

The various terms and incremental equations for use in the tangent stiffness procedure for the problem shown in Figure 1 are summarized in this appendix. It can be shown that the dimensionless rate form of Equations 3-5 take the form of Equation 8, which can be written explicitly as follows:

$$\begin{Bmatrix} \dot{p} \\ \dot{m}_x \\ \dot{m}_y \end{Bmatrix} = \begin{bmatrix} q_{11} & q_{12} & q_{13} \\ q_{21} & q_{22} & q_{23} \\ q_{31} & q_{32} & q_{33} \end{bmatrix} \begin{Bmatrix} \dot{\bar{\epsilon}}_0 \\ \dot{\phi}_x \\ \dot{\phi}_y \end{Bmatrix} \quad (\text{A1})$$

$$q_{11} = \int \bar{E}_i \frac{da}{A} \quad (\text{A2})$$

$$q_{12} = \int \bar{E}_i \bar{y} \frac{da}{A} \quad (\text{A3})$$

$$q_{13} = - \int \bar{E}_i \bar{x} \frac{da}{A} \quad (\text{A4})$$

$$q_{21} = \int \bar{E}_i \bar{y} \frac{da}{I_x} \quad (\text{A5})$$

$$q_{22} = \int \bar{E}_t \bar{y}^2 \frac{da}{\bar{I}_x} \quad (\text{A6})$$

$$q_{23} = - \int \bar{E}_t \bar{x} \bar{y} \frac{da}{\bar{I}_x} \quad (\text{A7})$$

$$q_{31} = - \int \bar{E}_t \bar{x} \frac{da}{\bar{I}_y} \quad (\text{A8})$$

$$q_{32} = - \int \bar{E}_t \bar{x} \bar{y} \frac{da}{\bar{I}_y} \quad (\text{A9})$$

$$q_{33} = \int \bar{E}_t \bar{x}^2 \frac{da}{\bar{I}_y} \quad (\text{A10})$$

$$p = \frac{P}{A \sigma_y} \quad (\text{A11})$$

$$\bar{m}_x = \frac{M_x}{M_{yx}} \quad (\text{A12})$$

$$\bar{m}_y = \frac{M_y}{M_{yy}} \quad (\text{A13})$$

$$\bar{\epsilon}_0 = \frac{\epsilon_0}{\epsilon_y} \quad (\text{A14})$$

$$\bar{\phi}_x = \frac{\phi_x}{\phi_{yx}} \quad (\text{A15})$$

$$\bar{\phi}_y = \frac{\phi_y}{\phi_{yy}} \quad (\text{A16})$$

$$\bar{E}_y = \frac{E_t}{E} \quad (\text{A17})$$

$$da = d\bar{x} d\bar{y} \quad (\text{A18})$$

$$\bar{x} = \frac{x}{\frac{B}{2}} \quad (\text{A19})$$

$$\bar{y} = \frac{y}{\frac{D}{2}} \quad (\text{A20})$$

$$\bar{A} = \frac{4A}{BD} \quad (\text{A21})$$

$$\bar{I}_x = \frac{16I_x}{BD^3} \quad (\text{A22})$$

$$\bar{I}_y = \frac{16I_y}{B^3D} \quad (\text{A23})$$

$$M_{yx} = \frac{\sigma_y I_y}{\frac{D}{2}} \quad (\text{A24})$$

$$M_{yy} = \frac{\sigma_y I_y}{\frac{B}{2}} \quad (\text{A25})$$

$$\epsilon_y = \frac{\sigma_y}{E} \quad (\text{A26})$$

$$\phi_{yx} = \frac{\varepsilon_y}{2} \tag{A27}$$

$$\phi_{yy} = \frac{\varepsilon_y}{2} \tag{A28}$$

where  $A$  is the area of cross section, and  $I_x$  and  $I_y$  are the moments of inertia about the  $x$  and  $y$  axes, respectively. The integrals in Equations A2-A10 are evaluated by numerical summation over the discrete elemental areas shown in Figure 1.

## APPENDIX B

### The Finite Element Machine

The *Finite Element Machine* (47) is a special purpose computer having as a main component an array of interconnected microcomputers. In addition to the array processors, there is an input/output (I/O) processor that provides operator console control, mass storage, problem input, and printed output for the array. The I/O processor is a conventional minicomputer that has a high bandwidth connection directly to one of the processors of the array. Communications within the microprocessor array take place by way of word-oriented point-to-point communications channels and, to a lesser extent, by way of cooperative computation networks involving all microcomputers in the array. There is no common memory in the system.

The processors of the array and the I/O processor are based on the Texas Instruments (TI) 990 minicomputer/9900 microcomputer. The I/O processor is a TI 990/10 minicomputer and the array processors also called the modal processors, are based on the TI TMS 9900 single chip microprocessor. This also contains TMS 9901 programmable systems interface and TMS 9902 asynchronous communications controller configured as on the 990/100M board that is built around the chip. In



addition, microprocessors have 16 bit/word of dynamic random access memory (RAM) and a Am9512 floating point arithmetic unit. The CPU board also contains 16K bytes of erasable, programmable read-only memory, 32K bytes of dynamic read/write memory. The nodal processors are interconnected by four different hardware structures:

1. A network of local communication links
2. A time multiplexed global bus
3. Cooperative signaling flag networks
4. A cooperative sum/maximum computation network

An overall block diagram of the finite element machine is shown in Figure B. The FEM system software is designed such that the controller serves as a host for the array. Thus, the controller is in charge of the overall system. Activities on the array are initiated and terminated by commands issued from the controller. These commands may be either directed to individual processors or broadcast to all of them through the global bus, as appropriate. Additionally, the controller supports program development, file storage, and pre- and postprocessing of data. The controller does not participate in execution of parallel application programs to facilitate uniform array monitoring. The system software is augmented by additional software for parallel computing. A set of about 40 programs known collectively as FEM array control software (FACS) implements the controller's portion of initialization, data management, program control, debugging, and postprocessing functions for the array. The FACS programs, invoked by system command interpreter (SCI) commands, serve as the interface between the user and the array.

Each array processor is installed with an operating system called Nodal Exec and a PASCAL language subroutine library, PASLIB. The Nodal Exec is divided into two major sections. One section provides services typical of most operating systems such as memory management, process control, low-level I/O and communication routines, timers, and interrupt handlers. The other section contains a set of command routines that carry out functions requested by the controller. Application programs are down-loaded onto the array processors for execution. These programs are regular sequential programs written in PASCAL language and each program is individual to a single processor. PASLIB allows the application programs to be parallelized. It also provides subroutines for communication between processes, I/O to and from the controller, timing, processor identification, flat settings, and floating-point operations. The parallelization is achieved by an appropriate design of algorithms suitable to the architecture of the FEM.

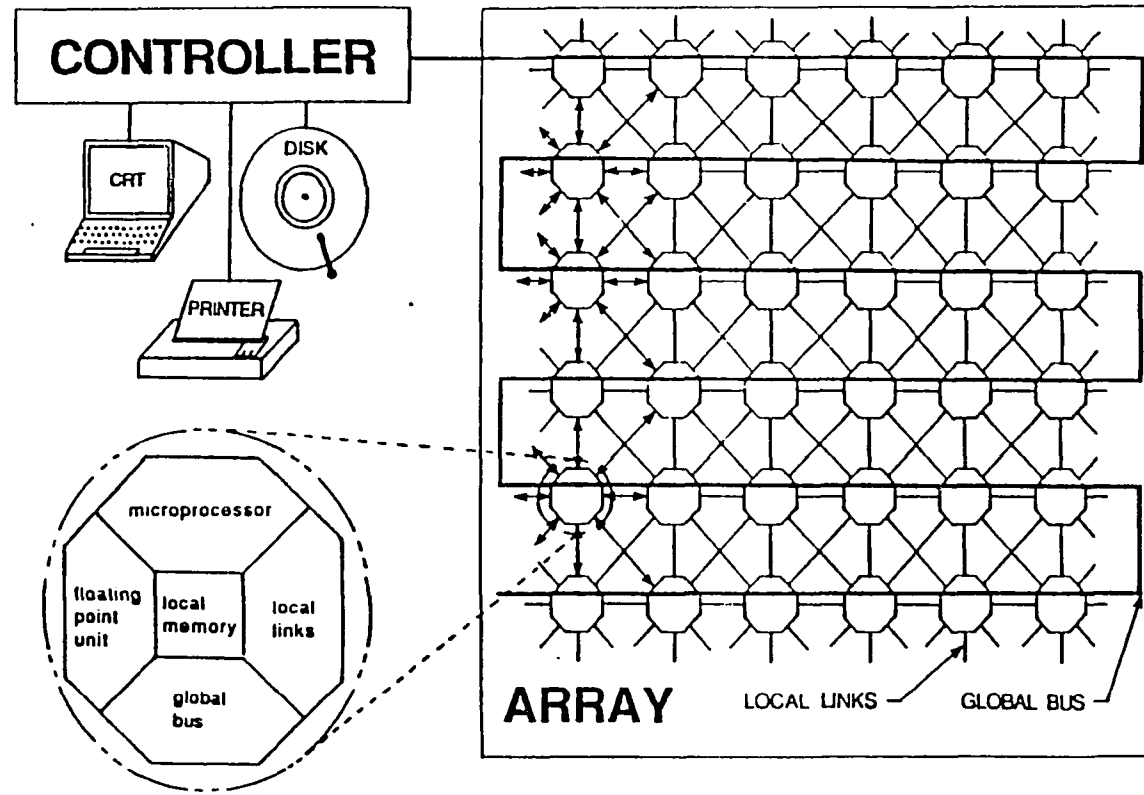


Figure B. Finite element machine block diagram

## APPENDIX C

### Inelastic Load and Moment Parameters

The inelastic load and moment parameters used in Equations 14 - 16 are defined as follows:

$$P_r = \int_{Ae} \sigma_r dA \quad (C1)$$

$$P_p = \int_{Ap} \sigma_y dA \quad (C2)$$

$$M_{xre} = \int_{Ae} \sigma_r y dA \quad (C3)$$

$$M_{yre} = \int_{Ae} \sigma_r x dA \quad (C4)$$

$$M_{xpe} = \int_{Ap} \sigma_y y dA \quad (C5)$$

$$M_{ype} = \int_{Ap} \sigma_y x dA \quad (C6)$$

The above integrals are evaluated numerically by summing over the discretized cross sections of the type shown in Figure 1.

## APPENDIX D

### External and Plastic Load Vectors

The external force vector,  $\{F\}$ , in Equation 30 is defined as follows:

$$\{F\} = \left\{ \begin{array}{l} (M_{yre} - yre)_0 + P u_{Q0} \\ (M_{xre} - xre)_0 + P v_{Q0} \\ (M_{yre} - yre)_1 + P (u_Q - u_i)_1 \\ (M_{xre} - xre)_1 + P (v_Q - v_i)_1 \\ (M_{yre} - yre)_2 + P (u_Q - u_i)_2 \\ (M_{xre} - xre)_2 + P (v_Q - v_i)_2 \\ \cdot \\ \cdot \\ (M_{yre} - yre)_j + P (u_Q - u_i)_j \\ (M_{xre} - xre)_j + P (v_Q - v_i)_j \\ \cdot \\ \cdot \\ (M_{yre} - yre)_{N-2} + P (u_Q - u_i)_{N-2} \\ (M_{xre} - xre)_{N-2} + P (v_Q - v_i)_{N-2} \\ (M_{yre} - yre)_{N-1} + P (u_Q - u_i)_{N-1} \\ (M_{xre} - xre)_{N-1} + P (v_Q - v_i)_{N-1} \\ (M_{yre} - yre)_N + P u_{QN} \\ (M_{xre} - xre)_N + P v_{QN} \end{array} \right\} \quad (D1)$$

Also, the plastic load vector,  $\{F\}_p$  in Equation 30 is given by:

$$\{F\}_p = \begin{Bmatrix} (M_{yp} - \mu_{yp})_0 \\ (M_{xp} - \mu_{xp})_0 \\ (M_{yp} - \mu_{yp})_1 \\ (M_{xp} - \mu_{xp})_1 \\ \cdot \\ \cdot \\ \cdot \\ \cdot \\ (M_{yp} - \mu_{yp})_j \\ (M_{xp} - \mu_{xp})_j \\ \cdot \\ \cdot \\ \cdot \\ \cdot \\ (M_{yp} - \mu_{yp})_{N-1} \\ (M_{xp} - \mu_{xp})_{N-1} \\ (M_{yp} - \mu_{yp})_N \\ (M_{xp} - \mu_{xp})_N \end{Bmatrix} \quad (D2)$$

**APPENDIX E**

**Computer Program NONPRFRM**







FILE: NONPRFRM FORTRAN A OLD DOMINION UNIVERSITY

```

FBM=0.0
MEM=1
MARCH=1
DO 5 M=1,NUMMEM
CALL READIM(M)
CALL GBL2LCL(M)
PB=0.0
BB=0.0
BBY=0.0
BT=0.0
CALL MEMBER(M)
IF (MARCH.EQ.-1) GOTO 100
J=MEMREF(M,1)
J=MEMREF(M,2)
IF (MEMID(M).EQ.1) GOTO 6
S1=EKG(1,1)*BMFCTR(M)
S2=EKG(1,3)*BMFCTR(M)
S3=EKG(3,1)*BMFCTR(M)
S4=EKG(3,3)*BMFCTR(M)
F1=ERP(1)*BMFCTR(M)
F2=ERP(3)*BMFCTR(M)
GOTO 7
6
CONTINUE
S1=EKG(2,2)*BMFCTR(M)
S2=EKG(2,4)*BMFCTR(M)
S3=EKG(4,2)*BMFCTR(M)
S4=EKG(4,4)*BMFCTR(M)
F1=ERP(2)*BMFCTR(M)
F2=ERP(4)*BMFCTR(M)
CONTINUE
7
CALL GBLSTIF(1,J,S1,S2,S3,S4,F1,F2,GBLK,GBLP,MEQ)
DO 6) K=1,NSPR
I=KREF(K,1)
J=KREF(K,2)
S1=SPRK(K)
S2=SPRK(K)
S3=SPRK(K)
S4=SPRK(K)
F1=0.0
F2=0.0
CALL GBLSTIF(1,J,S1,S2,S3,S4,F1,F2,GBLK,GBLP,MEQ)
CONTINUE
61
CALL SOLVE(GBLK,GBLP,GBLDEL,GBLDET,MEQ,0)
IF (GBLDET.LE.TOL2) GOTO 100
FDET=GBLDET
GBLDET=GBLDET/FDET
WRITE(1,*) 'FDET=',FDET
DO 10 I=1,MEQ
DELOD(I)=GBLDEL(I)
POLD(I)=GBLP(I)
POLD(I)=GBLP(I)
CONTINUE
10

```

FILE: NONPRFRM FORTRAN A OLD DOMINION UNIVERSITY

```

MEMRY=1
CALL COPY(+)
ICLK=0
35
CONTINUE
LOOP=1
MARCH=1
MEM=1
FBMD=FBMD+PBINC
FBMD=FBMD+BRINC
IF (ICLK.EQ.1) GOTO 11
IF (DABS(FBMD).GT.PLA) FBMD=PLM
CONTINUE
11
IF (ICLK.EQ.2) GOTO 13
IF (DABS(FBMD).GT.BMLM) FBMD=BMLM
CONTINUE
13
FBM=FBMD+BFCTR(I)
FBA=FBMD+BFCTR(I)
DO 45 I=1,MODES
BM(I)=FBA+BRROT(I)
CONTINUE
45
DO 16 I=1,NUMMEM
FP(I)=FBM+FPID(I)
CONTINUE
46
DO 26 J=1,MEQ
GBLP(I)=BM(I)
DO 26 J=1,MEQ
GBLK(I,J)=0.0
26
CALL MELOAD(GBLDEL,MEQ)
DO 15 M=1,NUMMEM
CALL READIM(M)
CALL GBL2LCL(M)
PB=FP(M)/PFCTR(M)
BBY=BBM(M,1)/BMFCTR(M)
BBX=BBM(M,3)/BMFCTR(M)
BT=BBM(M,2)/BMFCTR(M)
BTA=BBM(M,4)/BMFCTR(M)
WRITE(1,*) 'CHECK ON DIMENSIONS'
C
IF (MEMID(M).EQ.0) WRITE(1,*)M,PB,BBY,BTX
C
IF (MEMID(M).EQ.1) WRITE(1,*)M,PB,BBX,BTA
CALL MEMBER(M)
MARCH=MEM
IF (MARCH.EQ.-1) GOTO 100
J=MEMREF(M,1)
J=MEMREF(M,2)
IF (MEMID(M).EQ.1) GOTO 16
S1=EKG(1,1)*BMFCTR(M)
S2=EKG(1,3)*BMFCTR(M)
S3=EKG(3,1)*BMFCTR(M)
S4=EKG(3,3)*BMFCTR(M)
F1=ERP(1)*BMFCTR(M)
F2=ERP(3)*BMFCTR(M)
GOTO 17

```

FILE: NONPRFM FORTRAN A OLD DOMINION UNIVERSITY

```

16 CONTINUE
S1=-EGK(2,2)*BMCTR(M)
S2=-EGK(2,4)*BMCTR(M)
S3=-EGK(4,2)*BMCTR(M)
S4=-EGK(4,4)*BMCTR(M)
F1=-ERP(2)*BMCTR(M)
F2=-ERP(4)*BMCTR(M)
17 CONTINUE
CALL GBLSTIF(1,J,S1,S2,S3,S4,F1,F2,GBLK,GBLP,MEQ)
CONTINUE
15 DO 60 N=1,NSPR
I=REF(K,1)
J=REF(K,2)
S1=SPRK(I)
S2=SPRK(J)
S3=SPRK(N)
S4=SPRK(K)
F1=0.0
F2=0.0
CALL GBLSTIF(1,J,S1,S2,S3,S4,F1,F2,GBLK,GBLP,MEQ)
CONTINUE
WRITE(1,*) ' GBLK AND GBLP '
C DO 20 I=1,MEQ
C WRITE(1,*) (GBLK(I,J),J=1,MEQ), ' ; ',GBLP(I)
C800 FORMAT(1X,6(E15.8,3X),5X,E15.8)
C200 CONTINUE
DO 32 I=1,MEQ
POLD(I)=GBLP(I)
CONTINUE
32 CALL SOLVE(GBLK,GBLP,GBLDEL,GBLDET,MEQ,1)
GBLDET=GBLDET/FRDET
IF (GBLDET.LE.TOL2) GOTO 100
ID=0
WRITE(1,*) 'GBLP PREVIOUS AND PRESENT'
C DO 20 I=1,MEQ
C WRITE(1,*) I,POLD(I),POLD(I)
C IF (DABS(POLD(I))-POLD(I)).LE.TOL1) ID=ID+1
C POLD(I)=POLD(I)
C DELD(I)=GBLDEL(I)
C20 CONTINUE
IF (ID.NE.MEQ) GOTO 40
WRITE(1,*) '***** CONVERGED IN FRAMESUB *****'
WRITE(1,*) '***** CONVERGED IN FRAMESUB *****'
WRITE(1,*)
WRITE(1,*) P : BM : DET : FPBND,FPBND,GBLDET
DO 250 I=1,MUMMEM
WRITE(1,*) MEM=I, 'U-' : DT : OPM(I,1), 'V-' : DEFORM(I,2)
CONTINUE
WRITE(1,*)
250 DO 251 I=1,MEQ
WRITE(1,*) 'TETA',I,GBLDEL(I)
CONTINUE
251 WRITE(1,*)

```

FILE: NONPRFM FORTRAN A OLD DOMINION UNIVERSITY

```

NONO3160
NONO3170
NONO3180
NONO3190
NONO3200
NONO3210
NONO3220
NONO3230
NONO3240
NONO3250
NONO3260
NONO3270
NONO3280
NONO3290
NONO3300
NONO3310
NONO3320
NONO3330
NONO3340
NONO3350
NONO3360
NONO3370
NONO3380
NONO3390
NONO3400
NONO3410
NONO3420
NONO3430
NONO3440
NONO3450
NONO3460
NONO3470
NONO3480
NONO3490
NONO3500
NONO3510
NONO3520
NONO3530
NONO3540
NONO3550
NONO3560
NONO3570
NONO3580
NONO3590
NONO3600
NONO3610
NONO3620
NONO3630
NONO3640
NONO3650
NONO3660
NONO3670
NONO3680
NONO3690
NONO3700
NONO3710
NONO3720
NONO3730
NONO3740
NONO3750
NONO3760
NONO3770
NONO3780
NONO3790
NONO3800
NONO3810
NONO3820
NONO3830
NONO3840
NONO3850
NONO3860
NONO3870
NONO3880
NONO3890
NONO3900
NONO3910
NONO3920
NONO3930
NONO3940
NONO3950
NONO3960
NONO3970
NONO3980
NONO3990
NONO4000
NONO4010
NONO4020
NONO4030
NONO4040
NONO4050
NONO4060
NONO4070
NONO4080
NONO4090
NONO4100
NONO4110
NONO4120
NONO4130
NONO4140
NONO4150
NONO4160
NONO4170
NONO4180
NONO4190
NONO4200
NONO4210
NONO4220
NONO4230
NONO4240
NONO4250
NONO4260
NONO4270
NONO4280
NONO4290
NONO4300
NONO4310
NONO4320
NONO4330
NONO4340
NONO4350
NONO4360
NONO4370
NONO4380
NONO4390
NONO4400

```

FILE: MONPRFRM FORTRAN A OLD DOMINION UNIVERSITY

```

C      GBLK (1,1) = S1 + GBLK (1,1)
      IF (J.EQ.0) RETURN
      GBLK (1,1) = S2 + GBLK (1,1)
      GBLP (1,1) = F1 + GBLP (1,1)
      GBK (1,1) = S3 + GBK (1,1)
      CONTINUE
      GBK (J,J) = S4 + GBK (J,J)
      GBLP (J) = F2 + GBLP (J)
      RETURN
      END
C
C      SUBROUTINE MELOAD (GBLDEL,MEQ)
      IMPLICIT REAL*8 (A-H,O-Z)
      CHARACTER*4 CODE,LOAD,UNLD
      DIMENSION GBLDEL (MEQ)
      DIMENSION FS (10)
      *****
      COMMON/STRGBL/TSDM (10,15,400),TSDC (10,15,400),SIGM (10,15,400)
      I = SIGC (10,15,400)
      COMMON/DISGBL/DSM (10,30),DSC (10,30),DIM (10,30),DIC (10,30)
      COMMON/FRDP/DELOLO (17),POLR (17),DELOLC (17),POLDC (17)
      COMMON/SPRBL/MSK (10,3),MRY (10,3),TKX (10,3),TKY (10,3)
      I = TETA (10,2),TETA0 (10,2),TETA1 (10,2),TETA2 (10,2)
      COMMON/PROPGBL/ARMB (10),ARMA (10),ARY (10)
      I = ARMB (10),ARTRMB (10),ARTRMB (10),ARMB (10),ARYND (10)
      I = ARMB (10),REYND (10)
      COMMON/ADIRGBL/AD (10),AD (10),XTF (10),XTW (10),XEBW (10),XEBT (10)
      I = XEOP (10),XEDT (10)
      COMMON/CRKGBL/SAL (10),SSEGL (10),SUNIT (10),SUNIT (10),SUNIT (10)
      I = XRT (10),SUO (10,15),SVO (10,15),FRU (10),FRU (10),FRU (10)
      COMMON/MATGBL/XE (10),XSTGY (10),SEYBAR (10)
      COMMON/VALGBL/ARTRB (10),ARTRD (10),AYRCB (10),AYRCB (10)
      I = XC1 (10),XC2 (10),XCBB (10),XCBY (10),XCTA (10),XCTY (10)
      COMMON/DSCRGBL/MSSECS (10),MBX (10),MDR (10),MTBX (10),MTDX (10)
      I = MXX (10),MTX (10),MUMEL (10),LS (10)
      COMMON/KSKGBL/SKM (10,15,3),SKC (10,15,3)
      COMMON/FACBL/FAC (10,15,3),FAC (10,15,3)
      COMMON/DELGBL/DELM (10,15,3),DEL (10,15,3)
      COMMON/FLGGBL/LUNLDM (10,15,400),LUNLDC (10,15,400)
      COMMON/CONST/P1
      COMMON/DEYGBL/DETI (10)
      COMMON/MSRGBL/SEGG (10,4,4),SERP (10,4,4),CEGP (10,4,4)
      COMMON/FRGEG/SPRK (8),MREF (8,2),MEMREF (10,2),MEARID (10),MEMADJ (10,3)
      *****
      COMMON/MSKCL/FGK (4,4),ERP (4)
      *****
      COMMON/STRCL/TSD (15,400),TSM (15,400),SIG (15,400)
      I = TSDK (15,400),SIGK (15,400)
      COMMON/DISLCL/DI (30),FFI (30)

```

FILE: MONPRFRM FORTRAN A OLD DOMINION UNIVERSITY

```

      COMMON/SPRCL/BLX (3),BY (3),TX (3),TY (3),TBA (2),TBY (2),TTX (2),TTY (2)
      COMMON/PROPLCL/AR,RIX,RIY,ARND,RIJND,RIYND,RAND,RYND,ZKND,ZYND
      COMMON/ADIMLCL/B,D,TE,TM,EBM,EBT,EDM,EDT
      COMMON/CRKCL/AL,SEGL,UMT,VINT,RC,RT,SIGRC,SIGRT
      I = VO (15),VO (15),TU,TV
      COMMON/MATLCL/E,SIGY,EYBAR
      COMMON/EVALLCL/ARTRB,ARTRD,YRCB,YRCD,C1,C2,CBK,CBY,CTA,CTY
      COMMON/DSCRCL/MSSEC,MB,MD,MTB,MTD,MK,MT,LL,MEL
      COMMON/MSKCL/SKM (15,3,3)
      COMMON/ALCL/FAC (15,3)
      COMMON/DELLCL/DELX (15,3)
      COMMON/FLGCL/LUNLD (15,400),LUNLDC (15,400)
      COMMON/FLAGS/CODE,LOAD,UNLD,MEW,MENTRY,LATFIX
      COMMON/TOL/TOL1,TOL2,TOL3,TOLL
      COMMON/DETLCL/DET
      *****
      COMMON/FRAME/NUMFER,MODES,MSPR,LPATH,MRESTR,MODFIX (17)
      COMMON/LDING/ALFAM,PIMC,PLIM,BMIME,BALIM,BAROT (17),FPID (10)
      COMMON/EXTSPR/SPRK1,SPRK2,SPRK3,SPRK4
      COMMON/LDADS/FPB,FBM
      COMMON/FCTRS/FCCTR (10),BMFCTR (10)
      *****
      COMMON/TETA/TETA (4)
      COMMON/CK/FLNK (3,4),FIMP (3,2)
      COMMON/BRKLOAD/BRM (10,4),FP (10),BM (17)
      COMMON/NEALDS/PB,BBX,BBY,BTX,BTY
      *****
      C-----
      C-- FIRST FIND END MOMENTS ON MEMBERS -----
      DD 10 I=1,NUMMEM
      DD 11 J=1,4
      BBM (I,J) = 0.0
      CONTINUE
      J = MEMREF (I,1)
      K = MEMREF (I,2)
      IF (MEMID (I),EQ.1) GOTO 15
      IF (MODFIX (J),EQ.1) .OR. MODFIX (K),EQ.2) GOTO 16
      BBM (I,1) = SEGG (1,1) * GBLDEL (J) + SEGN (1,1,3) * GBLDEL (K) + SERP (1,1)
      CONTINUE
      IF (MODFIX (K),EQ.1) .OR. MODFIX (K),EQ.2) GOTO 10
      BBM (I,2) = SEGG (1,3,1) * GBLDEL (J) + SEGG (1,3,3) * GBLDEL (K) + SERP (1,3)
      GOTO 10
      CONTINUE
      BBM (I,3) = SEGG (1,2,2) * GBLDEL (J) + SEGG (1,2,4) * GBLDEL (K) + SERP (1,2)
      BBM (I,4) = SEGG (1,4,2) * GBLDEL (J) + SEGG (1,4,4) * GBLDEL (K) + SERP (1,4)
      CONTINUE
      DD 40 I=1,NUMMEM
      DD 40 J=1,4
      BBM (I,J) = BBM (I,J) + BMFCTR (I)
      CONTINUE
      DD 20 I=1,NUMMEM
      IF (MEMID (I),EQ.0) F5 (I) = (BBM (I,1) + BBM (I,2)) / SAL (I)

```



FILE: NONPRFM FORTRAN A OLD DOMINION UNIVERSITY

```

40      POLDC(I)=POLD(I)
        DELODC(I)=DELOD(I)
        CONTINUE
        DD 30 M=1,NUMBER
        CALL READIN(M)
        DD 100 I=1,4
        CERP(M,I)=SERP(M,I)
        CEGR(M,I,J)=SEGR(M,I,J)
        CONTINUE
        DD 105 I=1,MSEC
        DO 105 J=1,MEL
        TSOC(M,I,J)=TSOM(M,I,J)
        S1GC(M,I,J)=SIGM(M,I,J)
        TUNLDC(M,I,J)=TUNLDM(M,I,J)
        CONTINUE
        DD 110 I=1,2*HNSCC
        DSC(M,I)=DSM(M,I)
        DIC(M,I)=DIM(M,I)
        CONTINUE
        DD 125 I=1,MSEC
        DO 125 J=1,3
        FAC(M,I,J)=FAM(M,I,J)
        DELC(M,I,J)=DELM(M,I,J)
        SKC(M,I,J,K)=SKM(M,I,J,K)
        CONTINUE
        DD 126 J=1,3
        RETURN
C
C
C
35      CONTINUE
        DD 11 I=1,MEL
        POLD(I)=POLDC(I)
        DELOD(I)=DELODC(I)
        CONTINUE
        DD 101 I=1,4
        CALL READIN(M)
        DD 101 J=1,4
        SERP(M,I)=CERP(M,I)
        SEGR(M,I,J)=CEGR(M,I,J)
        CONTINUE
        DD 105 I=1,MSEC
        DD 105 J=1,MEL
        TSOM(M,I,J)=TSOC(M,I,J)
        SIGM(M,I,J)=S1GC(M,I,J)
        TUNLDM(M,I,J)=TUNLDC(M,I,J)
        CONTINUE
        DD 111 I=1,2*HNSCC
        DSM(M,I)=DSC(M,I)
        DIM(M,I)=DIC(M,I)
        CONTINUE
        DD 126 J=1,3

```

FILE: NONPRFM FORTRAN A OLD DOMINION UNIVERSITY

```

FAM(M,I,J)=FAC(M,I,J)
DELM(M,I,J)=DELC(M,I,J)
DD 126 K=1,3
SKM(M,I,J,K)=SKC(M,I,J,K)
CONTINUE
CONTINUE
RETURN
END
C
C
C
SUBROUTINE MEMBER(MEM)
IMPLICIT REAL*8 (A-H,O-Z)
CHARACTER*4, CODE, LOAD, UNLD
DIMENSION PK(30),DS(30),F(30),FF(30)
C -----
C
COMMON/STRGBL/TSOM(10,15,400),TSOC(10,15,400),SIGM(10,15,400)
1,S1GC(10,15,400)
COMMON/D1SGBL/DSM(10,30),DSC(10,30),DIM(10,30),D1C(10,30)
COMMON/FROP/DELOD(17),POLD(17),DELODC(17),POLDC(17)
COMMON/SPRGLB/BAK(10,3),BKX(10,3),TKX(10,3),TKY(10,3)
1,TETBA(10,2),TETBY(10,2),TETTA(10,2),TETTY(10,2)
COMMON/PROPGBL/AR(10),ARI(10),ARIY(10)
1,ARND(10),ARIND(10),ARIYND(10),ARRND(10),ARYND(10)
2,ARZND(10),ARZYND(10)
COMMON/ADIMGBL/AR(10),AD(10),ATF(10),XEBW(10),XEBT(10)
1,XEDM(10),XEDT(10)
COMMON/CROKGBL/SAL(10),SSEGL(10),SVINT(10),SVINT(10),XRC(10)
1,XRT(10),SWO(10,15),SWO(10,15),FRTU(10),FRTV(10)
COMMON/MATGBL/HE(10),XSIGY(10),SEYBAR(10)
COMMON/MVALGBL/HRHTB(10),HRSTO(10),KYRCM(10),KYRCO(10)
1,XCI(10),XCT(10),XCBX(10),XCBY(10),XCTA(10),XCTY(10)
COMMON/OSERGBL/MSECS(10),MBA(10),MDX(10),MTBA(10),MTDX(10)
1,MKA(10),MTX(10),MUNEL(10),LS(10)
COMMON/ASRGBL/SRR(10,15,3),SRK(10,15,3)
COMMON/FAGBL/FAR(10,15,3),FAL(10,15,3)
COMMON/DEGLB/DELN(10,15,3),DELC(10,15,3)
COMMON/FLGGBL/TUNLDM(10,15,400),TUNLDC(10,15,400)
COMMON/CONST/P1
COMMON/DETGBL/DETI(10)
COMMON/MSKGBL/SEK(10,4,4),SERP(10,4,4),CEEK(10,4,4),CERP(10,4,4)
COMMON/FACED/SPRK(B),KREF(B,2),MEMREF(10,2),MEMID(10),MEMADJ(10,3)
COMMON/MSKCL/EGK(4,4),ERP(4)
COMMON/STRCLC/TSO(15,400),SIGX(15,400)
1,TSOX(15,400),SIGK(15,400)
COMMON/D1SCLC/BI(30),FFI(30)
COMMON/SPRCLC/BA(3),BY(3),TX(L),TY(L),TBX(2),TBY(2),TTA(2),TTY(2)
COMMON/PROPCLC/AR,RIX,RIY,ARMND,RIYND,RXND,RYND,ZXND,ZYND
COMMON/ADIMCLC/D,TF,TW,EBW,EBT,EDM,EDT
COMMON/CROKCLC/AL,SEGL,UINT,VINT,RC,RT,SIGRC,SIGRT

```

FILE: NONPRFRM FORTRAN A OLD DOMINION UNIVERSITY

```

1 .UO (15), V0 (15), TU, TV
COMMON/MATLCL/E, SIGY, EYBAR
COMMON/VALLCL/ARTB, ARTD, YRCD, C1, C2, CBR, CBY, CTA, CTY
COMMON/DSCRLC/INSEC, MB, MD, MTB, MTD, MK, MT, LL, MEL
COMMON/MSKLLC/SRR (15, 3)
COMMON/FALCL/FAK (15, 3)
COMMON/DELCL/DELX (15, 3)
COMMON/FLGCL/LUNLDM (15, 400)
COMMON/FLGCS/LOAD, UNLD, MEM, MENTRY, LATFIX
COMMON/TOL/TOL1, TOL2, TOL3, TOL4
COMMON/DETLCL/DET

C
C
COMMON/FRAME/NUMMEA, NODES, MSPR, LPATH, MRESTR, MODFIX (17)
COMMON/LDINC/ALFAR, P, IMC, PL, IA, BM, IME, BML, IA, BMRDT (17), FPID (10)
COMMON/EXTSPR/SPRKT1, SPRK2, SPRK3, SPRK4
COMMON/LOADS/FPB, FBM
COMMON/FCTRS/PFCTR (10), BMFCTR (10)

C
C
COMMON/TETA/TETA (4)
COMMON/BMLD/BBM (10, 4), FP (10), BM (17)
COMMON/GK/FIMK (3, 4), FIMP (3, 2)
COMMON/HEALDS/PB, BBA, BBT, BTA, BTY

C
COMMON/DEFORM/DEFORM (10, 2)

C
COMMON/TLOAD/GP (30), GL (30, 4), PK (30, 30)
COMMON/RESTR/AR, ARB, ARK, ARX, ARTX, ARTY
COMMON/XX/X1, X2, X3, X4
CALL COLUMN (MEN, LL, AR, DS, F, FF)
RETURN
END

C
C
SUBROUTINES START FROM THIS STAGE
IMPLICIT REAL*8 (A-H,O-Z)
CHARACTER*4 CODE, LOAD, UNLD
DIMENSION AK (M, M), DS (M), F (M), FF (M), COEF (14), DATA (4)
C
C
COMMON/STRGBL/TSOM (10, 15, 400), TSOC (10, 15, 400), SIGM (10, 15, 400)
1 .SIGC (10, 15, 400)
COMMON/DISEBL/DSM (10, 30), DSC (10, 30), DIM (10, 30), OLC (10, 30)
COMMON/ERRP/DELOD (17), POLD (17), POLDE (17), POLDE (17)
COMMON/SPRGL/BSK (10, 1), SKY (10, 3), LNA (10, 3), TKY (10, 3)
1 .TETB (10, 2), TETBT (10, 2), TETTX (10, 2), TETTY (10, 2)
COMMON/PROPGBL/FAK (10), ARTX (10), ARTY (10)
1 .KARND (10), XRIAND (10), ARTYND (10), XRAMD (10), ARYND (10)
2 .AZZND (10), RZYND (10)
COMMON/ADINGBL/AB (10), AD (10), XTF (10), XTW (10), XEBW (10), XEBT (10)
COMMON/RESTR/AR, ARB, ARK, ARX, ARTX, ARTY
1 .REB (10), REBT (10)
COMMON/CROKGBL/SAL (10), SSEGL (10), SVINT (10), SVINT (10), ARC (10)

```

FILE: NONPRFRM FORTRAN A OLD DOMINION UNIVERSITY

```

1 .ART (10), SUO (10, 15), SVO (10, 15), FRTV (10), FRTV (10)
COMMON/MATGBL/AE (10), ASIGY (10), SEYBAR (10)
COMMON/VALLCL/ARTB (10), ARTD (10), YRCD (10), YRCD (10), XACTY (10)
1 .XCI (10), XCI (10), XCBY (10), XCBY (10), XACTX (10), XACTY (10)
COMMON/DSCRBL/INSEC (10), MBR (10), MDR (10), MTBR (10), MTD (10)
1 .MKX (10), MTK (10), NUMEL (10), LLS (10)
COMMON/ASRGL/SRR (10, 15, 3), SRC (10, 15, 3)
COMMON/FACBL/FAK (10, 15, 3), FAC (10, 15, 3)
COMMON/DELGBL/DELX (10, 15, 3), DELC (10, 15, 3)
COMMON/FLGCL/LUNLDM (10, 15, 400), LUNLDC (10, 15, 400)
COMMON/COMST/PI
COMMON/DEYGBL/DEY (10)
COMMON/MSRGL/SECR (10, 4), SERP (10, 4), CEGK (10, 4, 4), CERP (10, 4)
COMMON/FREED/SPRKB (8), RREF (8, 2), MEMREF (10, 2), MEMID (10), MEMADJ (10, 3)
COMMON/MSKLLC/EGK (4, 4), ERP (4)

C
C
COMMON/STRCLC/TSO (15, 400), TSK (15, 400), SIG (15, 400)
1 .TSOK (15, 400), SIGR (15, 400)
COMMON/DISCLC/DI (30), FFI (30)
COMMON/SPRCLC/BA (3), BY (3), TA (3), TY (3), TBA (2), TBY (2), TTX (2), TTY (2)
COMMON/PROPLC/AR, ART, RIT, RY, ARND, RYND, RYND, RYND, ZRND, ZYND
COMMON/ADIMLC/B, D, TF, TW, EBW, EBT, EDW, EDT
COMMON/CROKLC/AL, SEGL, UIMT, VIMT, RC, RT, S, IGRC, SIGRT
1 .UO (15), V0 (15), TU, TV
COMMON/MATLCL/E, SIGY, EYBAR
COMMON/VALLCL/ARTB, ARTD, YRCD, C1, C2, CBR, CBY, CTA, CTY
COMMON/DSCRLC/INSEC, MB, MD, MTB, MTD, MK, MT, LL, MEL
COMMON/MSKLLC/SRR (15, 3)
COMMON/FALCL/FAK (15, 3)
COMMON/DELCL/DELX (15, 3)
COMMON/FLGCL/LUNLDM (15, 400), LUNLDC (15, 400)
COMMON/FLGCS/LOAD, UNLD, MEM, MENTRY, LATFIX
COMMON/TOL/TOL1, TOL2, TOL3, TOL4
COMMON/DETLCL/DET

C
C
COMMON/FRAME/NUMMEA, NODES, MSPR, LPATH, MRESTR, MODFIX (17)
COMMON/LDINC/ALFAR, P, IMC, PL, IA, BM, IME, BML, IA, BMRDT (17), FPID (10)
COMMON/EXTSPR/SPRKT1, SPRK2, SPRK3, SPRK4
COMMON/LOADS/FPB, FBM
COMMON/FCTRS/PFCTR (10), BMFCTR (10)

C
C
COMMON/TETA/TETA (4)
COMMON/BMLD/BBM (10, 4), FP (10), BM (17)
COMMON/GK/FIMK (3, 4), FIMP (3, 2)
COMMON/HEALDS/PB, BBA, BBT, BTA, BTY

C
COMMON/DEFORM/DEFORM (10, 2)

C
COMMON/TLOAD/GP (30), GL (30, 4), PK (30, 30)
COMMON/RESTR/AR, ARB, ARK, ARX, ARTX, ARTY
COMMON/XX/X1, X2, X3, X4
CALL COLUMN (MEN, LL, AR, DS, F, FF)
RETURN
END

C
C
SUBROUTINES START FROM THIS STAGE
IMPLICIT REAL*8 (A-H,O-Z)
CHARACTER*4 CODE, LOAD, UNLD
DIMENSION AK (M, M), DS (M), F (M), FF (M), COEF (14), DATA (4)
C
C
COMMON/STRGBL/TSOM (10, 15, 400), TSOC (10, 15, 400), SIGM (10, 15, 400)
1 .SIGC (10, 15, 400)
COMMON/DISEBL/DSM (10, 30), DSC (10, 30), DIM (10, 30), OLC (10, 30)
COMMON/ERRP/DELOD (17), POLD (17), POLDE (17), POLDE (17)
COMMON/SPRGL/BSK (10, 1), SKY (10, 3), LNA (10, 3), TKY (10, 3)
1 .TETB (10, 2), TETBT (10, 2), TETTX (10, 2), TETTY (10, 2)
COMMON/PROPGBL/FAK (10), ARTX (10), ARTY (10)
1 .KARND (10), XRIAND (10), ARTYND (10), XRAMD (10), ARYND (10)
2 .AZZND (10), RZYND (10)
COMMON/ADINGBL/AB (10), AD (10), XTF (10), XTW (10), XEBW (10), XEBT (10)
COMMON/RESTR/AR, ARB, ARK, ARX, ARTX, ARTY
1 .REB (10), REBT (10)
COMMON/CROKGBL/SAL (10), SSEGL (10), SVINT (10), SVINT (10), ARC (10)

```

FILE: NONPRFRM FORTRAN A OLD DOMINION UNIVERSITY

```

CC      WRITE(2,A) 'IN COLUMN WITH MEMBER',MEM
      DO 20 I=1,N
        DS(I)=DSM(MEM,I)
        DI(I)=DIM(MEM,I)
20      CONTINUE
        KLM=NSEC/2
        NUDLE=RELM*1
        NITER=0
100     CONTINUE
        DATA(1)=DS(4)-DS(2)
        DATA(2)=DS(N)-DS(N-2)
        DATA(3)=DS(3)-DS(1)
        DATA(4)=DS(N)-DS(N-3)
C----- ADDITIONS FOR TRILINEAR SPRINGS -----
C
      X1=DABS(TVADATA(1))
      X2=DABS(TVADATA(2))
      X3=DABS(TUADATA(3))
      X4=DABS(TUADATA(4))
      CALL RESTRK(X1,X2,X3,X4)
      Y2=TVARKRDATA(2)
      Y3=TUARKRDATA(3)
      Y4=TUARKRDATA(4)
      IF (X1.GT.TX(1)) Y1=Y1+(BX(1)-BK(2))*ATX(1)
      IF (X2.GT.TX(1)) Y2=Y2-(TX(1)-TX(2))*ATX(1)
      IF (X3.GT.TY(1)) Y3=Y3+(BY(1)-BY(2))*ATY(1)
      IF (X4.GT.TY(1)) Y4=Y4-(TY(1)-TY(2))*ATY(1)
      IF (X1.GT.TX(2)) Y1=Y1+(BX(2)-BK(1))*ATX(2)
      IF (X2.GT.TX(2)) Y2=Y2-(TX(2)-TX(1))*ATX(2)
      IF (X3.GT.TY(2)) Y3=Y3+(BY(2)-BY(1))*ATY(2)
      IF (X4.GT.TY(2)) Y4=Y4-(TY(2)-TY(1))*ATY(2)
      DATA(1)=CBRY1/TV
      DATA(2)=CBRY2/TV
      DATA(3)=CBRY3/TU
      DATA(4)=CBRY4/TU
      DO 30 I=1,M
        DO 30 J=1,M
          AK(I,J)=0.0
30      CONTINUE
      DO 40 I=1,NSEC
        I1=2*I-1
        JJ=2*I
        DO 41 J=1,3
          FAX(I,J)=FAX(MEM,I,J)
          DELX(I,J)=DELX(MEM,I,J)
          DO 41 K=1,3
            SKX(I,J,K)=SKX(MEM,I,J,K)
41          CONTINUE
          DO 42 J=1,NEL
            TSOX(I,J)=TSOX(MEM,I,J)
            SIGX(I,J)=SIGX(MEM,I,J)
            LUNLOX(I,J)=LUNLOX(MEM,I,J)
42          CONTINUE

```

FILE: NONPRFRM FORTRAN A OLD DOMINION UNIVERSITY

```

      CALL SELS(DATA,1,DS(1),DS(JJ),DS(JJ),COEF)
      IF (DET.LE.TOL2) GO TO 50
      CALL ASMBLE(I,AK,F,COEF,M,MSEC)
40      CONTINUE
      DO 410 I=1,M
        FF(I)=F(I)
        DD 410 JJ=1,M
        PK(11,JJ)=AK(11,JJ)
410     CONTINUE
      CALL SOLVE(AK,F,DS,DET,M,1)
      IF (INTRY.NE.0) GO TO 60
      IF (DET.LE.TOL2) GO TO 50
      DET(MEM)=DET
      DET=DET/DET(MEM)
      DO 70 I=1,M
        DI(I)=FF(I)
70      CONTINUE
      CALL PART(M)
      CALL REDUCE(M)
      RETURN
60      DET=DET/DET(MEM)
      IF (DET.LE.TOL2) GO TO 50
      ICNTR=0
      DO 80 I=1,M
        IF (DABS(FF(I)-DI(I)).LE.TOL1) ICNTR=ICNTR+1
80      CONTINUE
        DI(I)=FF(I)
        IF (ICNTR.EQ.M) GO TO 90
        NITER=NITER+1
        IF (NITER.LT.15) GOTO 100
        GO TO 50
90      CONTINUE
        NEW=1
        WRITE(1,A) 'COLUMN CONVERGED FOR MEMBER',MEM,DET
        DO 500 I=1,M/2
          CC      WRITE(2,A) DS(2*I-1),DS(2*I)
          C500     CONTINUE
C----- PARTITIONING OF AK TO OBTAIN INELASTIC STIFFNESS MATRIX
C      CALL PART(M)
C----- REDUCE PARTITIONED MATRIX TO ELIMINATE INTERMEDIATE NODES
C      CALL REDUCE(M)
C
      DEFORM(MEM,1)=DS(2*MMHOLE-1)
      DEFORM(MEM,2)=DS(2*MMHOLE)
      DO 140 I=1,M
        DSM(MEM,I)=DS(I)
        DIM(MEM,I)=FF(I)
140     CONTINUE
      DO 310 I=1,NSEC
        DO 311 J=1,3
          FAM(MEM,I,J)=FAX(I,J)
          DELM(MEM,I,J)=DELX(I,J)
          DO 311 K=1,3

```





```

AK (I, 1) = COEF (5)
AK (I, 3) = COEF (5)
F (I) = COEF (7)
AK (J, M-5) = COEF (8)
AK (J, M-4) = COEF (10)
AK (J, M-3) = COEF (9)
AK (J, M-2) = COEF (11) + COEF (13)
AK (J, M) = COEF (13)
AK (J, 4) = COEF (12)
F (J) = COEF (14)
GOTO 50
90 AK (I, M-3) = COEF (1) * COEF (6)
AK (I, M-2) = COEF (3)
AK (I, M-1) = COEF (1) - COEF (6)
AK (I, M) = COEF (3)
AK (I, 1) = COEF (5)
AK (I, 3) = COEF (5)
F (I) = COEF (7)
AK (J, M-3) = COEF (8)
AK (J, M-2) = COEF (10) + COEF (13)
AK (J, M-1) = COEF (8)
AK (J, M) = COEF (10) - COEF (13)
AK (J, 2) = COEF (12)
AK (J, 4) = COEF (12)
F (J) = COEF (14)
GOTO 50
60 AK (I, 1) = COEF (5)
AK (I, 3) = COEF (5)
AK (I, M-3) = COEF (6)
AK (I, M-1) = COEF (1)
AK (I, J-2) = COEF (3)
AK (I, J-1) = COEF (2)
AK (I, J) = COEF (4)
AK (I, J+1) = COEF (1)
AK (I, J+2) = COEF (3)
F (I) = COEF (7)
AK (J, 2) = COEF (12)
AK (J, 4) = COEF (12)
AK (J, M-2) = COEF (13)
AK (J, M) = COEF (13)
AK (J, J-2) = COEF (8)
AK (J, J-1) = COEF (10)
AK (J, J) = COEF (11)
AK (J, J+1) = COEF (8)
AK (J, J+2) = COEF (10)
F (J) = COEF (14)
50 CONTINUE
C WRITE (I, A) 'OUT ASMBLE'
RETURN
C
C CROSS SECTIONAL TANGENT STIFFNESS ROUTINE
END

```

```

C
SUBROUTINE SECS (DATA, ISEC, UN1, UN2, COEF)
IMPLICIT REAL*8 (A-H, O-Z)
CHARACTER*4 CODE, LOAD, UNLD
DIMENSION FA (3), FB (3), FT (3), S (3, 3), DEL (3), COEF (14), DATA (4)
C -----
C
COMMON/STRGBL/TSOM (10, 15, 400), TSOC (10, 15, 400), SIGM (10, 15, 400)
COMMON/SIG (10, 15, 400)
COMMON/DLSGBL/DISM (10, 30), OSC (10, 30), OJM (10, 30), DIC (10, 30)
COMMON/FRRP/DELTD (17), POLD (17), DELOC (17), POLCC (17)
COMMON/SRGBL/BRK (10, 3), BKY (10, 3), TKS (10, 3), TRY (10, 3)
COMMON/TTBX (10, 2), TETB (10, 2), TETX (10, 2), TETTY (10, 2)
COMMON/PROFBL/ARR (10), ARYA (10), ARYB (10)
COMMON/ARRND (10), ARYND (10), ARYMD (10), ARYND (10)
COMMON/XZYND (10), XZYND (10)
COMMON/XDIPGBL/XD (10), XTF (10), XTM (10), XEBW (10), XEBT (10)
COMMON/XEDM (10), XEDT (10)
COMMON/CRONGBL/SAL (10), SSEGL (10), SUINT (10), SVINT (10), RRC (10)
COMMON/ART (10), SVO (10, 15), SVO (10, 15), FRTU (10), FRTV (10)
COMMON/MATGBL/ME (10), ASIGY (10), SEVBAR (10)
COMMON/AVLGBL/AVRTB (10), XARTD (10), XRVREB (10), XVRCD (10)
COMMON/XCI (10), XCC (10), XCBK (10), XCBY (10), XCTA (10), XCTY (10)
COMMON/DSCRBL/MSECS (10), MNBX (10), MDX (10), MTBX (10), MTDX (10)
COMMON/NXX (10), NTA (10), NUMEL (10), LLS (10)
COMMON/ASKGBL/SKM (10, 15, 3), SKC (10, 15, 3, 3)
COMMON/FAGBL/FAM (10, 15, 3), FAC (10, 15, 3)
COMMON/DELGBL/DELA (10, 15, 3), DELC (10, 15, 3)
COMMON/FLCGBL/JUNLDA (10, 15, 400), JUNLDC (10, 15, 400)
COMMON/CDIST/P1
COMMON/DETCBL/DETI (10)
COMMON/MSKGBL/SEGA (10, 4, 4), SERP (10, 4, 4), CEGK (10, 4, 4), CERP (10, 4, 4)
COMMON/FRGEO/SPRK (8), RREF (8, 2), RREFE (10, 2), RREFD (10, 2), RREFD J (10, 3)
C
C
COMMON/MSKCLL/EGK (4, 4), ERP (4)
COMMON/STRLCLL/TSO (15, 400), TSN (15, 400), SIG (15, 400)
COMMON/DLSCLL/DI (30), FFI (30)
COMMON/SPRCLL/BR (3), BY (3), TX (3), TY (3), TBA (2), TBY (2), TTX (2), TTY (2)
COMMON/PROPLLEL/AR, RIX, RIV, ARND, RIXND, RIVYND, RYND, ZAND, ZYND
COMMON/XDIPLEL/B, D, TF, TM, EBW, EBT, EDW, EDT
COMMON/CRKCLL/AL, SEGL, UINT, VINT, RC, RT, SIGRE, SIGRT
COMMON/VO (15), VO (15), TU, TV
COMMON/MATLCLL/E, SIGY, EYBAR
COMMON/XVALLCLL/RBTB, RBTD, YRCB, YRCD, C1, C2, C6X, C6Y, C7X, C7Y
COMMON/DSECLL/MSEC, NB, NO, MTB, MTD, MK, NT, LLL, MEL
COMMON/ASRCLL/SRX (15, 3, 3)
COMMON/FALLCLL/FAX (15, 3)
COMMON/DELLCLL/DELK (15, 3)
COMMON/FLEGLL/JUNLD (15, 400), JUNLDA (15, 400), UNLDA (15, 400)
COMMON/FLAGS/CODE, LOAD, UNLD, NEW, MEMTRY, LATFIX
COMMON/TDL/TOL1, TOL2, TOL3, TOL4
MON11560
MON11570
MON11580
MON11590
MON11600
MON11610
MON11620
MON11630
MON11640
MON11650
MON11660
MON11670
MON11680
MON11690
MON11700
MON11710
MON11720
MON11730
MON11740
MON11750
MON11760
MON11770
MON11780
MON11790
MON11800
MON11810
MON11820
MON11830
MON11840
MON11850
MON11860
MON11870
MON11880
MON11890
MON11900
MON11910
MON11920
MON11930
MON11940
MON11950
MON11960
MON11970
MON11980
MON11990
MON12000
MON12010
MON12020
MON12030
MON12040
MON12050
MON12060
MON12070
MON12080
MON12090
MON12100

```

```

NON12110
NON12120
NON12130
NON12140
NON12150
NON12160
NON12170
NON12180
NON12190
NON12200
NON12210
NON12220
NON12230
NON12240
NON12250
NON12260
NON12270
NON12280
NON12290
NON12300
NON12310
NON12320
NON12330
NON12340
NON12350
NON12360
NON12370
NON12380
NON12390
NON12400
NON12410
NON12420
NON12430
NON12440
NON12450
NON12460
NON12470
NON12480
NON12490
NON12500
NON12510
NON12520
NON12530
NON12540
NON12550
NON12560
NON12570
NON12580
NON12590
NON12600
NON12610
NON12620
NON12630
NON12640
NON12650

COMMON/DELCL/DET
C
C
COMMON/FRARE/NUMEM, NODES, NSPR, LPATH, NSESTR, NODE IX (17)
COMMON/LDINC/ALFAN, PINC, PLIN, BNINC, BMLIN, BMDT (17), FPID (10)
COMMON/EXTSPR/SPRKT, SPRKZ, SPRK3, SPRK4
COMMON/LOADS/FPB, FBM
COMMON/CTRS/PFCTR (10), BHCTR (10)
C
C
COMMON/TETA/TETA (4)
COMMON/BMLDQ/BBM (10, 4), FP (10), BR (17)
COMMON/GK/FTHK (3, 4), FIMP (3, 2)
COMMON/RELD5/PB, DBA, BBA, BBT, BTY
C
C
COMMON/TLOAD/GP (30), GL (30, 4), PK (30, 30)
COMMON/INEL/PP, PR, BPP, BARE, BVP, BYRE
COMMON/RESTR/ANKB, ANBY, ANTX, ARTY
COMMON/XE/X1, X2, X3, X4
COMMON/FRES/FA, FARE, FYRE
C
C
WRITE (2, 4) 'IN SECS WITH ISEC= ', ISEC
DO 10 I=1, 3
DEL (I)=DELX (ISEC, I)
FA (I)=FAR (ISEC, I)
10 CONTINUE
DO 35 J=1, 3
DO 35 I=1, 3
S (I, J)=SAX (ISEC, I, J)
CONTINUE
DO 83 I=1, NSEL
TSO (ISEC, I)=TSOX (ISEC, I)
SIG (ISEC, I)=SIGX (ISEC, I)
IUNLO (ISEC, I)=IUNLDX (ISEC, I)
CONTINUE
IF (ISEC.EQ.1.OR.ISEC.EQ.MSEC) GOTO 40
UW1=UW1APB/(RYND*RYND)
UW2=UW2APB/(RXND*RXND)
GOTO 50
UW1=0.0
UW2=0.0
ZBAR=(DFLOAT (ISEC-1)) / (DFLOAT (MSEC-1))
UW0=UW0 (ISEC)
UW0=UW0 (ISEC)
FB (I)=FB
FB (2)=ZBAR*(1.0)+DATA (1)+UW2*ZBAR*DATA (2)+UW0*PB/(RXND*RXND)
1-BBX*ZBAR*(BTX+BBX)
FB (3)=(1.0-ZBAR)*DATA (3)-UW1-ZBAR*DATA (4)-UW0*PB/(RYND*RYND)
1-BBY*ZBAR*(BTY+BBY)
WRITE (2, 4) 'FA & FB ', (FA (I), FB (I), I=1, 3)
CALL TANGNT (ISEC, FA, FB, FT, DEL, 5)
IF (DEL.LE.TOL2) GOTO 60
C NEW SPRING ADDITIONS

```

```

NON12660
NON12670
NON12680
NON12690
NON12700
NON12710
NON12720
NON12730
NON12740
NON12750
NON12760
NON12770
NON12780
NON12790
NON12800
NON12810
NON12820
NON12830
NON12840
NON12850
NON12860
NON12870
NON12880
NON12890
NON12900
NON12910
NON12920
NON12930
NON12940
NON12950
NON12960
NON12970
NON12980
NON12990
NON13000
NON13010
NON13020
NON13030
NON13040
NON13050
NON13060
NON13070
NON13080
NON13090
NON13100
NON13110
NON13120
NON13130
NON13140
NON13150
NON13160
NON13170
NON13180
NON13190
NON13200

XX1=0.0
XX2=0.0
XX3=0.0
XX4=0.0
COEF (1)=-S (3, 3)-S (3, 1)*S (1, 3)/S (1, 1)+C2
COEF (2)=-2.0*COEF (1)*PB/(RYND*RYND)
COEF (3)=-S (3, 1)*S (1, 2)/S (1, 1)-S (3, 2)*C1
COEF (4)=-2.0*COEF (3)
COEF (5)=CBY*ANBY*(1.0-ZBAR)
COEF (6)=-CTY*ARTY*ZBAR
IF (X3.GT.TBY (1)) XX3=XX3*(BY (1)-BY (2))*TBY (1)
IF (X4.GT.TTY (1)) XX4=XX4*(TY (1)-TY (2))*TTY (1)
IF (X3.GT.TBY (2)) XX3=XX3*(BY (2)-BY (3))*TBY (2)
IF (X4.GT.TTY (2)) XX4=XX4*(TY (2)-TY (3))*TTY (2)
XX3=CBY*XX3/TU
XX4=CTY*XX4/TU
COEF (7)=-PB*PP*FR)*S (3, 1)/S (1, 1)-FYRE-BYP-UW0*PB/(RYND*RYND)
1-BBY*ZBAR*(BTY+BBY)+(1.0-ZBAR)*XX3-ZBAR*XX4
C
C
LOAD VECTORS GL AND GP FOR ELASTO-PLASTIC SDE
J1=2*1ISEC
I1=J1
GL (1, 1)=ZBAR-1.0
GL (1, 2)=0.0
GL (1, 3)=ZBAR
GL (1, 4)=0.0
GP (1, 1)=-PB*PP*FR)*S (3, 1)/S (1, 1)-FYRE-BYP-UW0*PB/(RYND*RYND)
1-(1.0-ZBAR)*XX3-ZBAR*XX4
C
C
COEF (8)=-S (2, 3)-S (2, 1)*S (1, 3)/S (1, 1)+C2
COEF (9)=-2.0*COEF (8)
COEF (10)=-C1*S (2, 1)*S (1, 2)/S (1, 1)-S (2, 2)
COEF (11)=-2.0*COEF (10)*PB/(RXND*RXND)
COEF (12)=-CBX*AKBX*(1.0-ZBAR)
COEF (13)=-CTX*AKTX*ZBAR
IF (X1.GT.TBX (1)) X1=XX1*(BX (1)-BX (2))*TBX (1)
IF (X2.GT.TBX (1)) X2=XX2*(TX (1)-TX (2))*TBX (1)
IF (X1.GT.TBX (2)) X1=XX1*(BX (2)-BX (3))*TBX (2)
IF (X2.GT.TBX (2)) X2=XX2*(TX (2)-TX (3))*TBX (2)
X1=CBX*XX1/TV
X2=CTX*XX2/TV
COEF (14)=-FXRE*BP-VU0*PB/(RXND*RXND)-S (2, 1)*(PB*PP*FR)/S (1, 1)
1+BBX*ZBAR*(BTX+BBX)-(ZBAR-1.0)*XX1-ZBAR*XX2
C
C
SDE LOAD VECTORS GL AND GP
GL (J, 1)=0.0
GL (J, 2)=1.0-ZBAR
GL (J, 3)=0.0
GL (J, 4)=0.0
GP (J, 1)=-FXRE*BP-VU0*PB/(RXND*RXND)-S (2, 1)*(PB*PP*FR)/S (1, 1)
1-(ZBAR-1.0)*XX1-ZBAR*XX2
C
C
DO 80 I=1, 3

```

FILE: NONPRFRM FORTRAN A OLD DOMINION UNIVERSITY

```

NON13210
NON13220
NON13230
NON13240
NON13250
NON13260
NON13270
NON13280
NON13290
NON13300
NON13310
NON13320
NON13330
NON13340
NON13350
NON13360
NON13370
NON13380
NON13390
NON13400
NON13410
NON13420
NON13430
NON13440
NON13450
NON13460
NON13470
NON13480
NON13490
NON13500
NON13510
NON13520
NON13530
NON13540
NON13550
NON13560
NON13570
NON13580
NON13590
NON13600
NON13610
NON13620
NON13630
NON13640
NON13650
NON13660
NON13670
NON13680
NON13690
NON13700
NON13710
NON13720
NON13730
NON13740
NON13750

FAK(I,SEC,1)=FB(I)
DELX(I,SEC,1)=DEL(I)
DD 80 J=1,3
SRK(I,SEC,1,J)=S(I,J)
CONTINUE
DD 81 I=1,MEL
TSOR(I,SEC,1)=TSO(I,SEC,1)
SIGX(I,SEC,1)=SIG(I,SEC,1)
LUNLX(I,SEC,1)=LUNLD(I,SEC,1)
CONTINUE
RETURN
MEM=-1
CC WRITE(2,*)'LEAVING SECS'
RETURN
END
C
C SUBROUTINE XSECTIONAL EQUILIBRIUM
C
SUBROUTINE TANGMT(I,SEC,FA,FB,FT,DEL,S)
IMPLICIT REAL*8 (A-H,O-Z)
CHARACTER*4 CODE,LOAD,UNLD
DIMENSION FA(3),FT(3),FB(3),DEL(3),S(3,3),SOLMS(3)
-----
COMMON/STRCLC/TSO(15,400),TSK(15,400),SIG(15,400)
1 ,TSO(15,400),SIG(15,400)
COMMON/DISECL/DI(30),FF(30)
COMMON/SPRCLL/BA(3),BY(3),TX(3),TY(3),TBX(2),TBY(2),TTR(2),TTY(2)
COMMON/PROPLC/AR,RTA,RTY,ARND,RIYND,RIYMD,RYMD,ZYMD,ZYND
COMMON/ADIMLCL/B,O,TF,TM,EBW,EBT,EDM,EDT
COMMON/CROKCLL/AL,SEGL,UJINT,VJINT,RC,RT,SIGRC,SIGRT
1 ,UO(15),VO(15),TU,TV
COMMON/MATLCL/E,SIGY,EYBAR
COMMON/VALLCL/VRTB,VRTD,YRCB,YRCD,C1,C2,CBX,CBY,CTR,CTY
COMMON/DSCRCLL/MSEC,MB,MD,MTB,MTD,MR,MT,LL,MEL
COMMON/RSKCLL/SRX(15,3)
COMMON/FALECL/FAK(15,3)
COMMON/DELCLL/DELX(15,3)
COMMON/FLGLCL/LUNLD(15,400),LUNLX(15,400)
COMMON/FLAGL/CL,LOAD,UNLD,MEM,MENTRY,LATF IX
COMMON/TDL/TDL1,TOL2,TOL3,TOL4
COMMON/DETLCL/DET
C
COMMON/INEL/PP,PR,BXP,BARE,BYP,BYRE
COMMON/FRES/FR,FRE,FYRE
C
C
C WRITE(1,*)'IN TANGMT'
LCNT=1
DET=1.0
DD 21 I=1,3
DEL(I)=DEL(I)

```

FILE: NONPRFRM FORTRAN A OLD DOMINION UNIVERSITY

```

NON13760
NON13770
NON13780
NON13790
NON13800
NON13810
NON13820
NON13830
NON13840
NON13850
NON13860
NON13870
NON13880
NON13890
NON13900
NON13910
NON13920
NON13930
NON13940
NON13950
NON13960
NON13970
NON13980
NON13990
NON14000
NON14010
NON14020
NON14030
NON14040
NON14050
NON14060
NON14070
NON14080
NON14090
NON14100
NON14110
NON14120
NON14130
NON14140
NON14150
NON14160
NON14170
NON14180
NON14190
NON14200
NON14210
NON14220
NON14230
NON14240
NON14250
NON14260
NON14270
NON14280
NON14290
NON14300

FT(I)=FA(I)
CONTINUE
21
CONTINUE
20
DD 32 I=1,3
FT(I)=FB(I)-FT(I)
CONTINUE
32
CALL SOLVE(S,FT,SOLMS,DET,3,1)
IF(DET.LE.TOL2) GOTO 70
DD 40 I=1,3
DEL(I)=DEL(I)+SOLMS(I)
CONTINUE
40
CALL ESTIFF(S,DEL1,ISEC)
DD 80 I=1,MEL
TSO(I,SEC,1)=TSM(I,SEC,1)
CONTINUE
80
DD 50 I=1,3
FT(I)=0.0
DD 50 J=1,3
FT(I)=FT(I)+S(I,J)*DEL1(J)
CONTINUE
50
FT(I)=PPFR+FT(I)
FT(2)=BXP+FYRE+FT(2)
FT(3)=BYF+FYRE+FT(3)
LCNT=0
DD 35 I=1,3
IF(DABS(FB(I)-FT(I)).LE.TOL1) LCNT=LCNT+1
CONTINUE
35
IF(LCNT.EQ.3) GOTO 60
LCNT=LCNT+1
IF(LCNT.GE.15) GOTO 70
GOTO 20
DET=0.0
MEM=-1
RETURN
60
DD 65 I=1,3
DEL(I)=DEL(I)
FA(I)=FB(I)
CONTINUE
65
RETURN
END
C
SUBROUTINE ESTIFF(S,DEL,M)
IMPLICIT REAL*8 (A-H,O-Z)
CHARACTER*4 CODE,LOAD,UNLD
DIMENSION S(3,3),DEL(3)
-----
COMMON/STRCLC/TSO(15,400),TSK(15,400),SIG(15,400)
1 ,TSO(15,400),SIG(15,400)
COMMON/PROPLC/AR,RTA,RTY,ARND,RIYND,RIYMD,RYMD,ZYMD,ZYND
COMMON/ADIMLCL/B,O,TF,TM,EBW,EBT,EDM,EDT
COMMON/CROKCLL/AL,SEGL,UJINT,VJINT,RC,RT,SIGRC,SIGRT

```



FILE: NONPRFRM FORTRAN A OLD DOMINION UNIVERSITY

```

1  ,UO (15) ,VO (15) ,TU,TV
COMMON/MATLCL/E,SIGY,EYBAR
COMMON/XVALLCL/XRTB,XRTD,YRCB,YRCD,C1,C2,CBX,CBY,CTX,CTY
COMMON/DSCRLCL/HSEC,NB,NC,MTB,MTD,NK,NT,LL,NEL
COMMON/XSKLCL/SKK (15,3,3)
COMMON/FALCL/FAX (15,3)
COMMON/DELLCL/DELX (15,3)
COMMON/FLGLCL/IUNLD (15,400) ,IUNLDX (15,400)
COMMON/FLAGS/CODE,LOAD,UNLD,NEW,MENTRY,LATFIX
COMMON/TOL/TOL1,TOL2,TOL3,TOL4
COMMON/DETLCL/DET
COMMON/SUMS/SUM,ASUM,BSUM,CSUM,DSUM,ESUM
COMMON/INEL/PP,PR,BXP,BXRE,BYP,BYRE
COMMON/FRES/FR,FKRE,FYRE
C -----
C LCNT1=1
30 CONTINUE
DO 40 I=1,NL
Y=DFLOAT (2*I-1)
Y=1.0-Y*EBT/2.0
IF (IDX.EQ.1.AND.CODE.EQ.'ISEC') Y=YAEBT/2.0
IF (LCNT1.EQ.2) Y=-Y
IF (IDX.EQ.1) T=Y
TY=YADEL2
IF (IDX.EQ.1) TY=-TY
LCNT2=1
20 CONTINUE
DO 50 J=1,MB
X=DFLOAT (2*J-1)
X=X*EBW/2.0
IF (LCNT2.EQ.2) X=-X
IF (IDX.EQ.0) CALL RESX (SIGR,ER,X)
IF (IDX.EQ.1) CALL RESY (SIGR,ER,X)
TX=X*DEL3
IF (IDX.EQ.0) TX=-TX
TSN (M,K)=DEL1+TX+TY+ER
TS=SIG (M,K)+TSN (M,K)-TSO (M,K)
IF (UNLD.ME.'ELAST') TS=TSN (M,K)
IF (UNLD.ME.'ELAS') TS=TSN (M,K)
IF (IDX.EQ.0) GOTO 80
Y=X
X=T
80 CONTINUE
IF (DABS (TS) .LT. EYBAR) GOTO 60
IUNLD (M,K)=1
FCTR=1.0
IF (TS.LT.0.0) FCTR=-1.0
SIG (M,K)=FCTR
PP=PP+EABFCTR
BXP=BXP+YAEABFCTR
BYP=BYP-XAEABFCTR
GOTO 51
60 CONTINUE
KN=KN+1
NON15410
NON15420
NON15430
NON15440
NON15450
NON15460
NON15470
NON15480
NON15490
NON15500
NON15510
NON15520
NON15530
NON15540
NON15550
NON15560
NON15570
NON15580
NON15590
NON15600
NON15610
NON15620
NON15630
NON15640
NON15650
NON15660
NON15670
NON15680
NON15690
NON15700
NON15710
NON15720
NON15730
NON15740
NON15750
NON15760
NON15770
NON15780
NON15790
NON15800
NON15810
NON15820
NON15830
NON15840
NON15850
NON15860
NON15870
NON15880
NON15890
NON15900
NON15910
NON15920
NON15930
NON15940
NON15950

```

FILE: NONPRFRM FORTRAN A OLD DOMINION UNIVERSITY

```

SUM=SUM+EAB
SIG (M,K)=TS
IF (UNLD.EQ.'ELAS')
1 CALL UNLOAD (SIG (M,K) , SIGR,SR,TSN (M,K) ,TSO (M,K) ,IUNLD (M,K))
FR=FR+SIGR+EAB
FKRE=FKRE+SIGR+Y+EAB
FYRE=FYRE-SIGR+X+EAB
PR=PR+(TS-SIGR)*EAB
ASUM=ASUM+Y+EAB
BSUM=BSUM+X+EAB
CSUM=CSUM+X+Y+EAB
DSUM=DSUM+X+X+EAB
ESUM=ESUM+Y+Y+EAB
BXRE=BXRE+(TS-SIGR)*Y+EAB
BYRE=BYRE-(TS-SIGR)*X+EAB
51 CONTINUE
K=K+1
50 CONTINUE
LCNT2=LCNT2+1
IF (LCNT2.LE.2) GOTO 20
40 CONTINUE
LCNT1=LCNT1+1
IF (LCNT1.LE.2) GOTO 30
RETURN
END
C
C UNLOAD SUBROUTINE TO ACCOUNT FOR ELASTIC UNLOADING SIGR
C
SUBROUTINE UNLOAD (SIG,SIGR,SR,TSN,TSO,IUNLD)
IMPLICIT REAL*8 (A-H,O-Z)
IF (DABS (TSN) .LT. DABS (TSO)) GOTO 10
IF (IUNLD.EQ.-1) GOTO 10
IUNLD=1
RETURN
10 CONTINUE
SR=SIG-TSN
IF (DABS (SR) .GE. 1.0) SR=SR/DABS (SR)
SIGR=SIGR+SR
IUNLD=-1
RETURN
END
C
C
C
C
SUBROUTINE RESX (SIGR,EPSR,X)
IMPLICIT REAL*8 (A-H,O-Z)
CHARACTER*4 CODE,LOAD,UNLD
C -----
C COMMON/PROPLCL/AR,RIX,RIY,ARND,RIXND,RIYND,RXND,RVND,ZXND,ZYND
COMMON/XDIMLCL/B,D,TF,TW,EBW,EBT,EDW,EDT
COMMON/CROKCL/AL,SEGL,UINT,VINT,RC,RT,SIGRC,SIGRT
1 ,UO (15) ,VO (15) ,TU,TV
COMMON/MATLCL/E,SIGY,EYBAR
NON15960
NON15970
NON15980
NON15990
NON16000
NON16010
NON16020
NON16030
NON16040
NON16050
NON16060
NON16070
NON16080
NON16090
NON16100
NON16110
NON16120
NON16130
NON16140
NON16150
NON16160
NON16170
NON16180
NON16190
NON16200
NON16210
NON16220
NON16230
NON16240
NON16250
NON16260
NON16270
NON16280
NON16290
NON16300
NON16310
NON16320
NON16330
NON16340
NON16350
NON16360
NON16370
NON16380
NON16390
NON16400
NON16410
NON16420
NON16430
NON16440
NON16450
NON16460
NON16470
NON16480
NON16490
NON16500

```

FILE: NONPRFR FORTRAN A OLD DOMINION UNIVERSITY

```

COMMON/XVALLC/ARTB,ARTD,YRCB,YRCD,C1,C2,CBX,CBY,CTA,CTY
COMMON/FLAGS/CODE,LOAD,UMLD,NEW,MENTRY,LATFIA
COMMON/TOL/TOL1,TOL2,TOL3,TOL4
COMMON/DETCL/DET
C
C-----
IF (RC.NE.O) GOTO 10
SIGR=O.O
EPSR=O.O
RETURN
10 XB=DABS(X)
IF (CODE.EQ.'1SEC') GOTO 20
----- NEW ADDITION FOR CORNER CORRECTION IN RECT. SECTION -----
XRB=(1.0-ARTB-TW/B-YRCB)
IF (XRB-RRB).GT.(YRCB) GOTO 35
SIGR=(XRB-RRB)*ART/ARTB-RC
EPSR=SIGR
RETURN
35 YRB=RB-(XRB*YRCB)
SIGR=RRB*RT/(ARTB+TW/B)
EPSR=SIGR
RETURN
30 SIGR=SIGRC
EPSR=SIGR
RETURN
20 SIGR=RT-XB*(RC+RT)
EPSR=SIGR
RETURN
C
C
SUBROUTINE RESY(SIGR,EPFR,Y)
IMPLICIT REAL*8 (A-H,O-Z)
CHARACTER*4 CODE,LOAD,UMLD
C-----
COMMON/PROPLC/AR,R1X,R1Y,ARND,R1RMD,R1YMD,R1ZMD,ZYMD
COMMON/UMPLC/LB,D,TF,TM,EBM,ERT,EDM,EDT
COMMON/CROKCL/AL,SECL,UMINT,VIMT,RC,RT,SIGRC,SIGRT
1 UN(15),UN(15),TU,TY
COMMON/PATLCL/E,SIGT,EBBAR
COMMON/XVALLC/ARTB,ARTD,YRCB,YRCD,C1,C2,CBX,CBY,CTA,CTY
COMMON/FLAGS/CODE,LOAD,UMLD,NEW,MENTRY,LATFIA
COMMON/TOL/TOL1,TOL2,TOL3,TOL4
COMMON/DETCL/DET
C
C-----
IF (RC.NE.O) GOTO 10
SIGR=O.O
EPSR=O.O
RETURN
10 YD=DABS(Y)
IF (CODE.EQ.'1SEC') GOTO 20
XRD=(1.0-ARTD-TF/D-YRCD)

```

FILE: NONPRFR FORTRAN A OLD DOMINION UNIVERSITY

```

IF (YD.LE.XRD) GOTO 30
IF (YD-RRD).GT.(YRCD) GOTO 35
SIGR=(YD-RRD)*RT/ARTD-RC
EPSR=SIGR
RETURN
35 XRD=YD-(XRD*YRCD)
SIGR=RRD*RT/(ARTD-TF/D)
EPSR=SIGR
RETURN
30 SIGR=SIGRC
EPSR=SIGR
RETURN
20 SIGR=SIGRT
EPSR=SIGR
RETURN
END
C
C
SUBROUTINE RESTRK(D1,D2,D3,D4)
IMPLICIT REAL*8 (A-H,O-Z)
COMMON/SPRLC/LB,X(3),BY(3),TX(3),TY(3),TBR(2),TBY(2),TTX(2),TTY(2)
COMMON/RESTR/ANGL,ARBY,ARTX,ARTY
ANGL=EX(1)
ARBY=BY(1)
ARTX=TX(1)
ARTY=TY(1)
IF (D1.GT.TBR(1)) ARBA=BR(2)
IF (D2.GT.TTX(1)) ARTA=TA(2)
IF (D3.GT.TBY(1)) ARBY=BY(2)
IF (D4.GT.TTY(1)) ARTY=TY(2)
IF (D1.GT.TBR(2)) ARBA=BR(3)
IF (D2.GT.TTX(2)) ARTA=TA(3)
IF (D3.GT.TBY(2)) ARBY=BY(3)
IF (D4.GT.TTY(2)) ARTY=TY(3)
RETURN
END
C
C
SUBROUTINE TO PARTITION THE AN THAT IS PK MATRIX
SUBROUTINE PART(M)
IMPLICIT REAL*8 (A-H,O-Z)
COMMON/TLOAD/GP(30),GL(30,4),PK(30,30)
C-----EXCHANGE COLUMNS-----
AND
C-----EXCHANGE ROWS-----
DO 20 JJ=1,4
J=JJ+4
1=4-JJ
TKP=GP(J)
GP(J)=GP(N-1)
GP(N-1)=TKP
DO 15 K=1,M

```

FILE: NONPRFRM FORTRAN A OLD DOMINION UNIVERSITY

```

TRP=PK(K,J)
PK(K,J)=PK(K,M-I)
PK(K,M-I)=TRP
CONTINUE
DO 15 J=1,M
TRP=PK(K,J)
PK(K,J)=PK(K,M-I,I)
PK(M-I,I)=TRP
CONTINUE
DO 17 I=1,N
TRP=GL(J,I)
GL(J,I)=GL(M-I,I)
GL(M-I,I)=TRP
CONTINUE
20 RETURN
END
C
C SUBROUTINE TO REDUCE THE PK GL & GP MATRICES FOR CONDENSATION OF
C INTERNAL NODES
C
SUBROUTINE REDUC(M)
IMPLICIT REAL*8 (A-H,O-Z)
DIMENSION T11(M,M),T12(M,M),T21(M,M),T22(M,M),T(B,M)
J = T(B,J),TGL(B,M),GGL(B,M),TTL(22,4),TFF(B,I)
M4=4
M8=8
M16=16
CALL REDUCE(T11,T12,T21,T22,T,T,TFF,TGL
,GGL,TTL,M,M4,M8,M16)
RETURN
END
C
C SUBROUTINE REDUCE1(T11,T12,T21,T22,T,T,TFF,TGL
,GGL,TTL,M,M4,M8,M16)
IMPLICIT REAL*8 (A-H,O-Z)
DIMENSION T11(M,M),T12(M,M),T21(M,M),T22(M,M),T(B,M),TFF(MB,1)
2 ,TTL(M,M),GGL(M,M),EGK(M,M)
COMMON/CROKLEL/AL,SEGL,UJMT,VJMT,RC,RT,SIGRC,SIGRT
1 ,UD(15),VO(15),TU,TV
COMMON/TLOAD/GP(30),GL(30,4),PK(30,30)
COMMON/MSKLEL/EGK(4,4),ERP(4)
DO 7 J=1,M4
GGL(I,J)=0.0
TGL(I,J)=0.0
DO 5 I=1,M8
DO 6 J=1,M8
T12(I,J)=0.0
T21(I,J)=0.0
T1J(I,J)=0.0
TJ(I,J)=0.0
TJ(J,I)=0.0

```

FILE: NONPRFRM FORTRAN A OLD DOMINION UNIVERSITY

```

TFF(J,I)=0.0
CONTINUE
DO 5 J=1,M8
T22(I,J)=0.0
CONTINUE
DO 10 I=1,M8
JJ=J*M8
DO 10 J=1,M8
JJ=J*M8
T22(I,J)=PK(I,J)
T2I(J,I)=PK(J,J)
CONTINUE
DO 20 I=1,M8
DO 20 J=1,M8
T(I,J)=0.0
CONTINUE
CALL MATMUL(T12,T22,T,M8,M8,M8)
CALL MATMUL(T,T21,T11,M8,M8,M8)
DO 25 I=1,M8
DO 25 J=1,M8
T11(I,J)=PK(I,J)-T11(I,J)
CONTINUE
DO 30 I=1,M8
SUM=0.0
DO 35 J=1,M8
SUM=SUM+T(I,J)*GP(J,M8)
CONTINUE
TFF(I,I)=GP(I)-SUM
CONTINUE
DO 40 I=1,M4
DO 40 J=1,M4
TTL(I,J)=GL(I+M8,J)
CONTINUE
CALL MATMUL(T,TTL,TGL,M8,M8,M4)
DO 41 I=1,M8
DO 41 J=1,M4
TGL(I,J)=GL(I,J)-TGL(I,J)
CONTINUE
C
C THE FOLLOWING STATEMENTS REDUCE THE MATRICES FURTHER TO OBTAIN THE
C INELASTIC SLOPE-DEFLECTION EQUATIONS AND CORRESPONDING LOAD VECTOR
C
C SOLVE T11 TO FIND THE FLEXIBILITY MATRIX
C
CALL SOLVE(T11,0.0,0.0,DET,M8,0)
CALL MATMUL(T11,TGL,GGL,M8,M8,M4)
CALL MATMUL(T11,TFF,TF,M8,M8,1)
ERP(1)=TUA(TF(3,-)-TF(1,1))
ERP(2)=TVA(TF(4,1)-TF(2,1))

```







```

C----- IN INITIAL ----- NUMREM' ,NUMREM
C WRITE (1,*)
C P1=2.0*ARSIN(1.0/DOB)
C DO 50 I=1,NUMREM
C   SUIRT(I)=SUIRT(I)*SAL(1)+2.0*IB(I)
C   SVINT(I)=SVINT(I)*SAL(1)+2.0*AD(I)
C   LS(I)=24*SECS(I)
C   NHTD=HTDX(I)
C   IF (CODE.EQ.'1SEC') NHTD=HTDX(I)/2
C   NUMEL(I)=(NMX(I)+NTBX(I)+HDX(I)+NHTD)/42
C CONTINUE
C DO 9 M=1,NUMREM
C   MSEC=NSECS(M)
C   KLM=NSEC/2
C   NPDL=KLM+1
C   DO 8 I=1,KLM
C     ZBAR=DFLOAT(I-1)/DFLOAT(MSEC-1)
C     SVO(M,I)=SUIRT(M)*DSIN(P1+ZBAR)
C     SVO(M,I)=SVINT(M)*DSIN(P1+ZBAR)
C     CONTINUE
C     ZBAR=DFLOAT(KLM)/DFLOAT(MSEC-1)
C     SVO(M,KLM+1)=SUIRT(M)*DSIN(P1+ZBAR)
C     SVO(M,KLM+1)=SVINT(M)*DSIN(P1+ZBAR)
C     DO 7 I=KLM+2,MSEC
C       SVO(M,I)=SVO(M,NSEC-I+1)
C     SVO(M,I)=SVO(M,NSEC-I+1)
C     CONTINUE
C DO 1 I=1,NUMREM
C   FRU(I)=0.0
C   FRTV(I)=0.0
C   DET(I)=1.0
C   CONTINUE
C DO 4 J=1,4
C   ERP(J)=0.0
C   SERP(J)=0.0
C   DO 4 K=1,4
C     EGR(J,K)=0.0
C     SEGK(I,J,K)=0.0
C     IF (J.EQ.K) EGR(J,K)=1.0
C     IF (J.EQ.K) SEGK(I,J,K)=1.0
C   CONTINUE
C DO 11 I=1,NUMREM
C   MSC=NSECS(I)
C   ME=NUMEL(I)
C   DO 11 J=1,MSC
C     DO 11 K=1,ME
C       TSON(I,J,K)=TSO(I,K)
C       TSO(I,J,K)=TSO(I,K)
C       SIGM(I,J,K)=SIG(I,K)
C       SIG(I,J,K)=SIG(I,K)
C     CONTINUE
C DO 25 M=1,MSC
C   DO 25 N=1,ME
C     TSON(M,N)=TSO(M,N)
C     TSO(M,N)=TSO(M,N)
C     SIGM(M,N)=SIG(M,N)
C     SIG(M,N)=SIG(M,N)
C     MSC=NSECS(I)
C     ME=NUMEL(I)
C     DO 25 J=1,MSC
C       DO 25 K=1,ME
C         TSON(J,K)=TSO(J,K)
C         TSO(J,K)=TSO(J,K)
C         SIGM(J,K)=SIG(J,K)
C         SIG(J,K)=SIG(J,K)
C     CONTINUE
C DO 20 M=1,ME
C   CONTINUE
C DO 20 N=1,ME
C     RETURN
C   END
C
MON21460 SIGC(I,J,K)=0.0
MON21470 SIGE(I,K)=0.0
MON21480 SIG(L,K)=0.0
MON21490 IURLDR(I,J,K)=1
MON21500 IURLDC(I,J,K)=1
MON21510 IURLDR(J,K)=1
MON21520 IURLDC(J,K)=1
MON21530 CONTINUE
MON21540 DO 3 I=1,NUMREM
MON21550 LSTMP=LS(I)
MON21560 DO 3 L=1,LSTMP
MON21570 DSA(L,L)=0.0
MON21580 DSC(L,L)=0.0
MON21590 DIPR(L,L)=0.0
MON21600 DIC(L,L)=0.0
MON21610 CONTINUE
MON21620 DO 22 I=1,NUMREM
MON21630 MSC=NSECS(I)
MON21640 DO 22 J=1,MSC
MON21650 DO 22 K=1,3
MON21660 FAN(I,J,K)=0.0
MON21670 FAC(I,J,K)=0.0
MON21680 FAR(I,J,K)=0.0
MON21690 DELC(I,J,K)=0.0
MON21700 DELC(J,K)=0.0
MON21710 DELK(J,K)=0.0
MON21720 DO 22 L=1,3
MON21730 SKX(J,K,L)=0.0
MON21740 SKR(I,J,K,L)=0.0
MON21750 SKC(I,J,K,L)=0.0
MON21760 IF (K.NE.L) GOTO 22
MON21770 SKX(J,K,L)=1.0
MON21780 SKR(I,J,K,L)=1.0
MON21790 SKC(I,J,K,L)=1.0
MON21800 CONTINUE
MON21810 DO 20 M=1,NUMREM
MON21820 CALL READIN(M)
MON21830 CALL PROPS(M)
MON21840 IF (DABS(MRC(M)) .GT. .TOL2) CALL SIGMA(M)
MON21850 MSC=NSECS(I)
MON21860 ME=NUMEL(I)
MON21870 DO 25 J=1,MSC
MON21880 DO 25 K=1,ME
MON21890 TSON(M,J,K)=TSO(I,K)
MON21900 TSO(M,J,K)=TSO(I,K)
MON21910 SIGM(M,J,K)=SIG(I,K)
MON21920 SIG(M,J,K)=SIG(I,K)
MON21930 CONTINUE
MON21940 DO 25 M=1,MSC
MON21950 DO 25 N=1,ME
MON21960 TSON(M,N)=TSO(M,N)
MON21970 TSO(M,N)=TSO(M,N)
MON21980 SIGM(M,N)=SIG(M,N)
MON21990 SIG(M,N)=SIG(M,N)
MON22000 CONTINUE

```

```

MON20910
MON20920
MON20930
MON20940
MON20950
MON20960
MON20970
MON20980
MON20990
MON21000
MON21010
MON21020
MON21030
MON21040
MON21050
MON21060
MON21070
MON21080
MON21090
MON21100
MON21110
MON21120
MON21130
MON21140
MON21150
MON21160
MON21170
MON21180
MON21190
MON21200
MON21210
MON21220
MON21230
MON21240
MON21250
MON21260
MON21270
MON21280
MON21290
MON21300
MON21310
MON21320
MON21330
MON21340
MON21350
MON21360
MON21370
MON21380
MON21390
MON21400
MON21410
MON21420
MON21430
MON21440
MON21450

```

FILE: NONPRFRM FORTRAN A OLD DOMINION UNIVERSITY

```

SUBROUTINE PROPS(MEM)
IMPLICIT REAL*8 (A-H,O-Z)
CHARACTER*4 CODE,LOAD,UNLD
-----
COMMON/STRGBL/TSOK(10,15,400),TSOC(10,15,400),SIGR(10,15,400)
1 .SIGR(10,15,400)
COMMON/DISGBL/DSR(10,30),DSC(10,30),DJR(10,30),DIC(10,30)
COMMON/FRDP/DELOC(17),POLD(17),DELOC(17),POLDC(17)
COMMON/SPRGL/BRK(10,3),BKY(10,3),TRX(10,3),TKY(10,3)
1 .TEYB(10,2),TETBY(10,2),TETTX(10,2),TETTY(10,2)
COMMON/PROGGL/AR(10),ARIX(10),ARIY(10)
1 .ARMO(10),ARRAND(10),ARRYND(10),ARRND(10),XRYND(10)
2 .ZZAND(10),XZYND(10)
COMMON/ADIMGBL/AB(10),AD(10),XTF(10),XTM(10),XEBW(10),XEBT(10)
1 .XEDW(10),XEDT(10)
COMMON/CRKGBL/SAL(10),SSEGL(10),SUIMT(10),SVIMT(10),ARC(10)
1 .ART(10),SUO(10,15),SVO(10,15),FRTU(10),FRTV(10)
COMMON/MATGBL/AE(10),ASIGY(10),SEYBAR(10)
COMMON/ZVALGBL/ZARTB(10),ZARTD(10),ZYRGB(10),ZYRCO(10)
1 .XCI(10),XCI(10),XCBK(10),XCBY(10),XCTA(10),XCTY(10)
COMMON/OSRGBL/MSSEGS(10),MNB(10),MNB(10),MTBK(10),MTDX(10)
1 .MKE(10),MTX(10),MUREL(10),LS(10)
COMMON/ASRGBL/SKR(10,15,3),SKC(10,15,3,3)
COMMON/FAGBL/FAR(10,15,3),FAC(10,15,3)
COMMON/DEGLBL/DELA(10,15,3),DELC(10,15,3)
COMMON/FELGBL/FUMLDR(10,15,400),FUMLUC(10,15,400)
COMMON/COMST/PI
COMMON/DETBGL/DETI(10)
COMMON/MSKGBL/SEBK(10,4,4),SERP(10,4),CEGK(10,4,4),CERP(10,4)
COMMON/FRCEO/SPRK(B),KREF(B,2),MEREFF(10,2),MEMID(10),MEMADJ(10,3)
-----
COMMON/ASKLCL/EGR(N,4),ERP(N)
COMMON/STRLCL/TSO(15,400),TSM(15,400),SIG(15,400)
1 .TSOK(15,400),SIGR(15,400)
COMMON/DISLCL/DI(30),FFI(30)
COMMON/SPRCLL/BR(3),BY(3),TX(3),TY(3),TBY(2),TBY(2),TTY(2)
COMMON/PROPLCL/AR,RIX,RIY,ARMO,RIKND,RIYND,RRND,ZYND,ZYND
COMMON/ADIMBL/B,D,TF,TW,EBW,EDT,EDM,EDT
COMMON/CRKCLL/AL,SEGL,UJINT,VINT,RC,RT,SIGRC,SIGRT
1 .JUD(15),VO(15),TU,TY
COMMON/MATLCL/E,SIGY,EYBAR
COMMON/ZVALLCL/ARTB,ARTD,YRCB,YRCD,C1,C2,CBK,CBY,CTX,CTY
COMMON/OSRCLL/MSSE,MW,MD,MTB,MTD,MK,MT,LL,MEL
COMMON/ASKCLL/SKR(15,3,3)
COMMON/FELCLL/FAR(15,2)
COMMON/DELLCL/DELA(15,3)
COMMON/FELGCLL/FUMLD(15,400),FUMLDX(15,400)
COMMON/FLAGS/CODE,LOAD,UNLD,MEM,MENTRY,LATI,IX
COMMON/TOL/TOL1,TOL2,TOL3,TOL4
COMMON/DETLCL/DET

```

FILE: NONPRFRM FORTRAN A OLD DOMINION UNIVERSITY

```

COMMON/FRAME/NUMBRM,MODES,MSPR,LPATH,NRESTR,MODFIX(17)
COMMON/LOADING/ALFAR,PINE,PLIM,BHINC,BHLM,OMRODT(17),FPID(10)
COMMON/LETSPR/SPRK1,SPRK2,SPRK3,SPRK4
COMMON/LOADS/FPB,FBA
COMMON/FCTMS/PTSTR(10),BMECTR(10)
-----
COMMON/TETA/TETA(N)
COMMON/BNLOAD/BNR(10,4),FP(10),BM(17)
COMMON/GN/FRK(3,4),FRMP(3,2)
COMMON/AELOADS/PB,GBA,GBY,BTX,BTY
-----
IF (CODE.EQ.'ISEC') RT=RC*RT/((B*F+(D-2.0*ATF)*M)
SIGRC=RC
SIGRT=RT
SEGL=MSGL-1.0
SEGL=AL/SEGL
TU=B/(4.0*SEGL)
TV=D/(4.0*SEGL)
T=TW
IF (CODE.EQ.'ISEC') T=TW/2.0
WH=B-TW
IF (CODE.EQ.'ISEC') WH=TW/2.0
AR=AR0-(D-2.0*ATF)*B*(B-2.0*AT)
RIK=2.04*(B*ATF+3/12.0)*B*RTF4*(0.5*(D-TI))+2*TA*(D-2.0*ATF)**3/12.0)
RIY=2.04*(B*ATF+3/12.0)*B*RTF4*(0.5*(D-TI))+2*TA*(D-2.0*ATF)**3/12.0)
I=TF*B*WJ/12.0)
C1=E/(4.0*SIGY*SEGL*SEGL)
C2=B*BRAC1
C1=D*DAE1
C2=B*BAE/(4.0*SIGY*SEGL*SEGL)
C3=B*BAE/(4.0*SIGY*SEGL*SEGL)
C4=B*BAE/(4.0*SIGY*SEGL*SEGL)
C5=B*BAE/(4.0*SIGY*SEGL*SEGL)
C6=B*BAE/(4.0*SIGY*SEGL*SEGL)
C7=B*BAE/(4.0*SIGY*SEGL*SEGL)
C8=B*BAE/(4.0*SIGY*SEGL*SEGL)
C9=B*BAE/(4.0*SIGY*SEGL*SEGL)
C10=B*BAE/(4.0*SIGY*SEGL*SEGL)
C11=B*BAE/(4.0*SIGY*SEGL*SEGL)
C12=B*BAE/(4.0*SIGY*SEGL*SEGL)
C13=B*BAE/(4.0*SIGY*SEGL*SEGL)
C14=B*BAE/(4.0*SIGY*SEGL*SEGL)
C15=B*BAE/(4.0*SIGY*SEGL*SEGL)
C16=B*BAE/(4.0*SIGY*SEGL*SEGL)
C17=B*BAE/(4.0*SIGY*SEGL*SEGL)
C18=B*BAE/(4.0*SIGY*SEGL*SEGL)
C19=B*BAE/(4.0*SIGY*SEGL*SEGL)
C20=B*BAE/(4.0*SIGY*SEGL*SEGL)
C21=B*BAE/(4.0*SIGY*SEGL*SEGL)
C22=B*BAE/(4.0*SIGY*SEGL*SEGL)
C23=B*BAE/(4.0*SIGY*SEGL*SEGL)
C24=B*BAE/(4.0*SIGY*SEGL*SEGL)
C25=B*BAE/(4.0*SIGY*SEGL*SEGL)
C26=B*BAE/(4.0*SIGY*SEGL*SEGL)
C27=B*BAE/(4.0*SIGY*SEGL*SEGL)
C28=B*BAE/(4.0*SIGY*SEGL*SEGL)
C29=B*BAE/(4.0*SIGY*SEGL*SEGL)
C30=B*BAE/(4.0*SIGY*SEGL*SEGL)
C31=B*BAE/(4.0*SIGY*SEGL*SEGL)
C32=B*BAE/(4.0*SIGY*SEGL*SEGL)
C33=B*BAE/(4.0*SIGY*SEGL*SEGL)
C34=B*BAE/(4.0*SIGY*SEGL*SEGL)
C35=B*BAE/(4.0*SIGY*SEGL*SEGL)
C36=B*BAE/(4.0*SIGY*SEGL*SEGL)
C37=B*BAE/(4.0*SIGY*SEGL*SEGL)
C38=B*BAE/(4.0*SIGY*SEGL*SEGL)
C39=B*BAE/(4.0*SIGY*SEGL*SEGL)
C40=B*BAE/(4.0*SIGY*SEGL*SEGL)
C41=B*BAE/(4.0*SIGY*SEGL*SEGL)
C42=B*BAE/(4.0*SIGY*SEGL*SEGL)
C43=B*BAE/(4.0*SIGY*SEGL*SEGL)
C44=B*BAE/(4.0*SIGY*SEGL*SEGL)
C45=B*BAE/(4.0*SIGY*SEGL*SEGL)
C46=B*BAE/(4.0*SIGY*SEGL*SEGL)
C47=B*BAE/(4.0*SIGY*SEGL*SEGL)
C48=B*BAE/(4.0*SIGY*SEGL*SEGL)
C49=B*BAE/(4.0*SIGY*SEGL*SEGL)
C50=B*BAE/(4.0*SIGY*SEGL*SEGL)
C51=B*BAE/(4.0*SIGY*SEGL*SEGL)
C52=B*BAE/(4.0*SIGY*SEGL*SEGL)
C53=B*BAE/(4.0*SIGY*SEGL*SEGL)
C54=B*BAE/(4.0*SIGY*SEGL*SEGL)
C55=B*BAE/(4.0*SIGY*SEGL*SEGL)
C56=B*BAE/(4.0*SIGY*SEGL*SEGL)
C57=B*BAE/(4.0*SIGY*SEGL*SEGL)
C58=B*BAE/(4.0*SIGY*SEGL*SEGL)
C59=B*BAE/(4.0*SIGY*SEGL*SEGL)
C60=B*BAE/(4.0*SIGY*SEGL*SEGL)
C61=B*BAE/(4.0*SIGY*SEGL*SEGL)
C62=B*BAE/(4.0*SIGY*SEGL*SEGL)
C63=B*BAE/(4.0*SIGY*SEGL*SEGL)
C64=B*BAE/(4.0*SIGY*SEGL*SEGL)
C65=B*BAE/(4.0*SIGY*SEGL*SEGL)
C66=B*BAE/(4.0*SIGY*SEGL*SEGL)
C67=B*BAE/(4.0*SIGY*SEGL*SEGL)
C68=B*BAE/(4.0*SIGY*SEGL*SEGL)
C69=B*BAE/(4.0*SIGY*SEGL*SEGL)
C70=B*BAE/(4.0*SIGY*SEGL*SEGL)
C71=B*BAE/(4.0*SIGY*SEGL*SEGL)
C72=B*BAE/(4.0*SIGY*SEGL*SEGL)
C73=B*BAE/(4.0*SIGY*SEGL*SEGL)
C74=B*BAE/(4.0*SIGY*SEGL*SEGL)
C75=B*BAE/(4.0*SIGY*SEGL*SEGL)
C76=B*BAE/(4.0*SIGY*SEGL*SEGL)
C77=B*BAE/(4.0*SIGY*SEGL*SEGL)
C78=B*BAE/(4.0*SIGY*SEGL*SEGL)
C79=B*BAE/(4.0*SIGY*SEGL*SEGL)
C80=B*BAE/(4.0*SIGY*SEGL*SEGL)
C81=B*BAE/(4.0*SIGY*SEGL*SEGL)
C82=B*BAE/(4.0*SIGY*SEGL*SEGL)
C83=B*BAE/(4.0*SIGY*SEGL*SEGL)
C84=B*BAE/(4.0*SIGY*SEGL*SEGL)
C85=B*BAE/(4.0*SIGY*SEGL*SEGL)
C86=B*BAE/(4.0*SIGY*SEGL*SEGL)
C87=B*BAE/(4.0*SIGY*SEGL*SEGL)
C88=B*BAE/(4.0*SIGY*SEGL*SEGL)
C89=B*BAE/(4.0*SIGY*SEGL*SEGL)
C90=B*BAE/(4.0*SIGY*SEGL*SEGL)
C91=B*BAE/(4.0*SIGY*SEGL*SEGL)
C92=B*BAE/(4.0*SIGY*SEGL*SEGL)
C93=B*BAE/(4.0*SIGY*SEGL*SEGL)
C94=B*BAE/(4.0*SIGY*SEGL*SEGL)
C95=B*BAE/(4.0*SIGY*SEGL*SEGL)
C96=B*BAE/(4.0*SIGY*SEGL*SEGL)
C97=B*BAE/(4.0*SIGY*SEGL*SEGL)
C98=B*BAE/(4.0*SIGY*SEGL*SEGL)
C99=B*BAE/(4.0*SIGY*SEGL*SEGL)
C100=B*BAE/(4.0*SIGY*SEGL*SEGL)

```

FILE: NONPFRM FORTRAN A OLD DOMINION UNIVERSITY

```

TXT=NB
EDW=2.0/TXT
TXT=MTB
EBT=2.0ATF/(DATXT)
TXT=MTD
EDW=2.0ATW/(BATXT)
TXT=MD
EDT=2.0A(D-2.0ATF)/(DATXT)
C WRITE(1,4) 'EDW=',EDW,' EBT=',EBT,' EDW=',EDW,' EDT=',EDT
  IF (RT.EQ.0.0.OR.CODE.EQ.'ISEC') GOTO 10
  XRTB=RC*RT*(B+D-2.0AT)/(2.0A(RT+RC)**2)
  XRTD=2.0AXRTB/D
  XRTB=2.0AXRTB/B
  YRCB=XRTB*RC/RT
  YRCD=XRTD*RC/RT
  GOTO 20
10 CONTINUE
  IF (RT.EQ.0.0) GOTO 30
  XRTB=RC/(RC+RT)
  YRCB=XRTB*RT/RC
  YRCD=(D-2.0ATF)/D
  XRTD=0.0
  GOTO 20
30 CONTINUE
  XRTB=0.0
  XRTD=0.0
  YRCB=0.0
  YRCD=0.0
20 CONTINUE
  PFCTR(MEM)=SIGY*AR
  IF (MEMID(MEM).EQ.0) BMFCTR(MEM)=2.0ARIYASIGY/B
  IF (MEMID(MEM).EQ.1) BMFCTR(MEM)=2.0ARIASIGY/D
C WRITE(1,4) 'XR YR S',XRTB,XRTD,YRCB,YRCD
  CALL ASSIGN(MEM)
  RETURN
  END
C
C
C SUBROUTINE ASSIGN(M)
  IMPLICIT REAL*8 (A-H,O-Z)
  CHARACTER*4 CODE,LOAD,UNLD
C -----
C
COMMON/PROPGBL/XAR(10),XRIX(10),XRIY(10)
1 ,XARN(10),XRIXND(10),XRIYND(10),XARN(10),XRYND(10)
2 ,XRXND(10),XZYND(10)
COMMON/XDIMGBL/XB(10),XD(10),XTF(10),XTW(10),XEBW(10),XEBT(10)
1 ,XEDW(10),XEDT(10)
COMMON/CROKGBL/SAL(10),SSEGL(10),SUINT(10),SVINT(10),XRC(10)
1 ,XRT(10),SUO(10,15),SVD(10,15),FRTU(10),FRTV(10)
COMMON/XVALGBL/XXRTB(10),XXRTD(10),XYRCB(10),XYRCD(10)
1 ,XC1(10),XC2(10),XCBX(10),XCBY(10),XCTX(10),XCTY(10)
COMMON/DSCRGBL/NSECS(10),NBX(10),NDX(10),MTBX(10),MTDX(10)
1 ,NXX(10),NTX(10),NMEL(10),LS(10)
NON23110
NON23120
NON23130
NON23140
NON23150
NON23160
NON23170
NON23180
NON23190
NON23200
NON23210
NON23220
NON23230
NON23240
NON23250
NON23260
NON23270
NON23280
NON23290
NON23300
NON23310
NON23320
NON23330
NON23340
NON23350
NON23360
NON23370
NON23380
NON23390
NON23400
NON23410
NON23420
NON23430
NON23440
NON23450
NON23460
NON23470
NON23480
NON23490
NON23500
NON23510
NON23520
NON23530
NON23540
NON23550
NON23560
NON23570
NON23580
NON23590
NON23600
NON23610
NON23620
NON23630
NON23640
NON23650

```

FILE: NONPFRM FORTRAN A OLD DOMINION UNIVERSITY

```

C
COMMON/PROPLCL/AR,RIX,RIY,ARN,RIXND,RIYND,RXND,RYND,ZXND,ZYND
COMMON/XDMLCL/B,D,TF,TW,EBW,EBT,EDW,EDT
COMMON/CROKCL/AL,SEC1,UINT,VINT,RC,RT,SIGRC,SIGRT
1 ,UO(15),VO(15),TU,TV
COMMON/XVALCL/XRTB,XRTD,YRCB,YRCD,C1,C2,CBX,CBY,CTX,CTY
COMMON/DSCRLCL/NSEC,NB,ND,MTB,MTD,NX,NT,LL,NEL
C -----
NON23660
NON23670
NON23680
NON23690
NON23700
NON23710
NON23720
NON23730
NON23740
NON23750
NON23760
NON23770
NON23780
NON23790
NON23800
NON23810
NON23820
NON23830
NON23840
NON23850
NON23860
NON23870
NON23880
NON23890
NON23900
NON23910
NON23920
NON23930
NON23940
NON23950
NON23960
NON23970
NON23980
NON23990
NON24000
NON24010
NON24020
NON24030
NON24040
NON24050
NON24060
NON24070
NON24080
NON24090
NON24100
NON24110
NON24120
NON24130
NON24140
NON24150
NON24160
NON24170
NON24180
NON24190
NON24200
C
C
C SUBROUTINE SIGMA(MEM)
  IMPLICIT REAL*8 (A-H,O-Z)
  CHARACTER*4 CODE,LOAD,UNLD
C -----
C
COMMON/STRGBL/TSOM(10,15,400),TSOC(10,15,400),SIGM(10,15,400)
1 ,SIGC(10,15,400)
COMMON/DISGBL/DSM(10,30),DSC(10,30),DIM(10,30),DIC(10,30)
COMMON/FROF/DELOLQ(17),POLD(17),DELOLOC(17),POLDC(17)
COMMON/SPRGBL/BKX(10,3),BKY(10,3),TKX(10,3),TKY(10,3)
1 ,TETBX(10,2),TETBY(10,2),TETTX(10,2),TETTY(10,2)
COMMON/PROPGBL/XAR(10),XRIX(10),XRIY(10)
1 ,XARN(10),XRIXND(10),XRIYND(10),XRXND(10),XRYND(10)

```



FILE: NONPRFRM FORTRAN A OLD DOMINION UNIVERSITY

```

COMMON/SPRCLL/BR(3),BY(3),TX(3),TBY(2),TBY(2),TTX(2),TTY(2)
COMMON/PROPLC/AR,RIK,RIY,ARND,RIYND,RYND,ZAND,ZYND
COMMON/ADINCL/AD,TE,TH,EDW,EBT,EDM,EDT
COMMON/CRONCL/AL,SEGL,UINT,VINT,RC,RT,SIGRC,SIGRT
  /UO(15),VO(15),TV
COMMON/RATLCL/E,SIGT,EYBAR
COMMON/AVALLC/AR,RTB,ARTD,YRCB,YRCD,C1,C2,CBA,CBY,CTA,CTY
COMMON/PSNCL/INSEC,MB,MD,MTB,MTD,MR,MT,LL,NEL
COMMON/SI/SLCL/SR(15,3,3)
COMMON/ALCL/FAK(15,3)
COMMON/ELCL/DELK(15,3)
COMMON/FLGLC/UNLQ(15,400),IUNLQ(15,400)
COMMON/FLAGS/CODE,LOAD,UNLD,HEM,MENTRY,LATFX
COMMON/TOL/TOL1,TOL2,TOL3,TOL4
COMMON/DETLCL/DET

C
C
COMMON/FRAME/NUMBER,MODES,NSPA,LPATH,MRESTR,MODFIX(17)
COMMON/LDINC/ALFAM,PINC,PLI,PMIME,BNLI,M,BNROT(17),FPIQ(10)
COMMON/EXTSPR/SPR1,SPR2,SPR3,SPR4
COMMON/LOADS/FPB,FBM
COMMON/FEINS/FECTR(10),BNECTR(10)

C
C
COMMON/ZETA/ZETA(4)
COMMON/BNLOAD/BNR(10,4),FP(10),BR(17)
COMMON/CR/THK(3,4),FIMP(3,2)
COMMON/RELOADS/PB,DBA,BBY,BTX,BTY

C
C
LCMT1=1
DO 30 CONTINUE
  DO 40 I=1,NL
    Y=DFLOAT(2#I-1)
    Y=1.0-Y*EBT/2.0
    IF (LDX.EQ.1.AND.CODE.EQ.'1SEC') Y=Y*EBT/2.0
    IF (LCMT1.EQ.2) Y=Y
  30 CONTINUE
  DO 50 J=1,MB
    X=DFLOAT(2#J-1)
    X=X*REBW/2.0
    IF (LCMT2.EQ.2) X=X
    IF (LDX.EQ.0) CALL RESX(SIGR,ER,X)
    IF (LDX.EQ.1) CALL RESY(SIGR,ER,X)
    SIG(M,N)=SIGR
    TSD(M,N)=ER
    K=K+1
  50 CONTINUE
  LCMT2=LCMT2+1
  IF (LCMT2.LE.2) GOTO 20
  40 CONTINUE
  LCMT1=LCMT1+1
  IF (LCMT1.LE.2) GOTO 30

```

FILE: NONPRFRM FORTRAN A OLD DOMINION UNIVERSITY

```

RETURN
END

C
SUBROUTINE READIN(M)
  IMPLICIT REAL*8 (A-H,O-Z)
  CHARACTER*8 CODE,LOAD,UNLD
  COMMON/RESTR/ANBR,ANBY,ANX,ANTY

C
C
C
COMMON/STRGBL/TSOM(10,15,400),TSOC(10,15,400),SIGN(10,15,400)
  /SIEG(10,15,400)
COMMON/DI/SGBL/DSM(10,30),DSC(10,30),DIA(10,30),D1C(10,30)
COMMON/FRDP/DELD(17),POLD(17),DELODC(17),POLDC(17)
COMMON/SPRCL/BRK(10,3),BRK(10,3),TKX(10,3),TKY(10,3)
  /TETB(10,2),TETBY(10,2),TETTX(10,2),TETTY(10,2)
COMMON/PROPGL/KAAR(10),KRIK(10),KRIY(10)
  /KARND(10),KARND2(10),KRIYND(10),KARND(10),KRYND(10)
  /KZAND(10),KZYND(10)
COMMON/ADINCL/AR(10),AD(10),ATF(10),ATW(10),KEBW(10),KEBT(10)
  /XEDW(10),KEBT(10)
COMMON/CRONCL/SAL(10),SSEGL(10),SVINT(10),SVINT(10),ARC(10)
  /RBT(10),SVD(10,15),SVO(10,15),FRTV(10),FRTV(10)
COMMON/RATLCL/RE(10),RESY(10),SEYBAR(10)
COMMON/AVALLC/AR,RTB,ARTD,YRCB(10),YRCD(10)
  /ACT(10),AC2(10),ACR(10),ACBT(10),ACTA(10),ACTY(10)
COMMON/OSCRCL/INSEC(10),MBA(10),MDX(10),MTB(10),MTD(10),MTX(10)
  /MKA(10),MTX(10),MUNEL(10),LS(10)
COMMON/ASKGBL/SRM(10,15,3,3),SKC(10,15,3,3)
COMMON/FAGBL/FAK(10,15,3),FAC(10,15,3)
COMMON/DEGLC/DELM(10,15,3),DELC(10,15,3)
COMMON/FLGBL/UNLQ(10,15,400),IUNLQ(10,15,400)
COMMON/CONST/PI
COMMON/DETLCL/DETT(10)
COMMON/MSRGL/SECK(10,4,4),SERP(10,4,4),CECK(10,4,4),CERP(10,4,4)
COMMON/FRGEO/SPR(8),KREF(8,2),MREF(10,2),MEMID(10),MEMADJ(10,3)

C
C
COMMON/ASLCL/EGR(4,4),ERP(4)

C
COMMON/STRCL/TSO(15,400),TSN(15,400),SIG(15,400)
  /TSOX(15,400),SIGR(15,400)
COMMON/DI/SLCL/BI(30),FFI(30)
COMMON/SPRCL/BR(3),BY(3),TX(3),TBY(2),TBY(2),TTX(2),TTY(2)
COMMON/PROPLC/AR,RIK,RIY,ARND,RIYND,RYND,ZAND,ZYND
COMMON/ADINCL/AD,TE,TH,EDW,EBT,EDM,EDT
COMMON/CRONCL/AL,SEGL,UINT,VINT,RC,RT,SIGRC,SIGRT
  /UO(15),VO(15),TV
COMMON/RATLCL/E,SIGT,EYBAR
COMMON/AVALLC/AR,RTB,ARTD,YRCB,YRCD,C1,C2,CBA,CBY,CTA,CTY
COMMON/OSCRCL/INSEC,MB,MD,MTB,MTD,MR,MT,LL,NEL
COMMON/ASLCL/SR(15,3,3)
COMMON/ALCL/FAK(15,3)
COMMON/DETLCL/DELK(15,3)

```

FILE: MONPRFRM FORTRAN A OLD DOMINION UNIVERSITY

```

COMMON/FLGCL/LUNLD(15,400),LUNLDX(15,400)
COMMON/FLGCS/CODE,LOAD,UMLD,NEW,MENTRY,LATFIX
COMMON/TOL/TOL1,TOL2,TOL3,TOL4
COMMON/DETCLL/DET
C
C
COMMON/FRAME/NUMKFR,MODES,NSPR,LPATH,NRESTR,MODFIX(17)
COMMON/LDINC/ALYAR,PLINC,PLIAR,BRINC,BNLIYR,BMROT(17),FPIID(10)
COMMON/EXTSPR/SPRK1,SPRK2,SPRK3,SPRK4
COMMON/LOADS/FPB,FBR
COMMON/ECTRS/FFCTR(10),BRFCTR(10)
C
C
COMMON/TETA/TETA(N)
COMMON/BLOAD/BBR(10,4),FP(10),BM(17)
COMMON/SK/FINK(3,4),FHP(3,2)
COMMON/AEALDS/PB,BDX,BBY,BTX,BTY
C
C
B=XB(N)
D=XD(N)
TF=XTF(N)
TW=XTW(N)
AL=SAL(N)
U=U(SUJINT(N))
V=V(SVJINT(N))
RC=RC(N)
BT=BT(N)
SIGRC=RC
SIGBT=BT
E=XE(N)
EYBAR=SEYBAR(N)
NSEC=NSECS(N)
ND=NDX(N)
NTD=NTDX(N)
NR=NRX(N)
NT=NTX(N)
NEL=NUEL(N)
LL=LLS(N)
RETURN
END
C
C
SUBROUTINE SOLVE(A,B,SOLNS,DET,M,ISOL)
IMPLICIT REAL*8(A-H,O-Z)
DIMENSION A(M,M),B(M),SOLNS(M),Y(30)
DIMENSION IROM(30),JCOL(30),JORD(30)
COMMON/FRAME/NUMKFR,MODES,NSPR,LPATH,NRESTR,MODFIX(17)
COMMON/TOL/TOL1,TOL2,TOL3,TOL4
DET=1.0

```

FILE: MONPRFRM FORTRAN A OLD DOMINION UNIVERSITY

```

IF(M.EQ.MODES)DET=1.0E-60
DO 10 K=1,M
  KRI=K-1
  C SEARCH FOR PIVOT
  PIV=0.0
  DO 11 I=1,M
    DO 11 J=1,M
      IF(K.EQ.I)GOTO 9
      DO B ISCAM=I,KRI
        DO B JSCAM=I,KRI
          IF(I.EQ.IROM(IJSCAM))GOTO 11
          IF(J.EQ.JCOL(IJSCAM))GOTO 11
        CONTINUE
      IF(DABS(A(I,J)).LE.DABS(PIV))GOTO 11
      PIV=A(I,J)
      IROM(K)=I
      JCOL(K)=J
    CONTINUE
  IF(DABS(PIV).GT.TOL2)GOTO 13
  DET=0.0
  GOTO 40
C RETURN
13 IROMK=IROM(K)
  JCOLK=JCOL(K)
  DET=DETA*PIV
  DO 14 J=1,M
    A(IROMK,J)=A(IROMK,J)/PIV
  CONTINUE
  IF(150L.EQ.1)B(IROMK)=B(IROMK)/PIV
  A(IROMK,JCOLK)=1.0/PIV
  DO 15 I=1,M
    AIJCK=A(I,JCOLK)
    AIJCK=A(I,JCOLK)GOTO 19
  IF(I.EQ.IROMK)=AIJCK/PIV
  DO 17 J=1,M
    IF(J.NE.JCOLK)A(I,J)=AIJCK*A(IROMK,J)
  CONTINUE
  IF(150L.EQ.1)B(I)=B(I)-AIJCK*B(IROMK,J)
  CONTINUE
19 CONTINUE
18 IF(150L.EQ.1)B(I)=B(I)-AIJCK*B(IROMK)
CONTINUE
IF(150L.EQ.0)GOTO 35
DO 20 I=1,M
  IROMI=IROM(I)
  JCOLI=JCOL(I)
  JORD(IROMI)=JCOLI
  SOLNS(JCOLI)=B(IROMI)
CONTINUE
20 CONTINUE
25 IATCH=0
  KRI=K-1
  DO 22 I=1,M
    IPI=I+1
    DO 22 J=IPI,M
      IF(JORD(IJ).GE.JORD(I))GOTO 22
      JTEMP=JORD(J)

```



FILE: NOMPRFRM FORTRAN A OLD DOMINION UNIVERSITY

```

JORD(J)=JORD(I)
JORD(I)=JTEMP
INTCH=INTCH+1
CONTINUE
IF ( (INTCH/2)*2.NE.INTCH ) DET=-DET
DO 28 J=1,M
DO 27 I=1,M
IROWI=IROW(I)
JCOLI=JCOL(I)
Y(JCOLI)=A(IROWI,J)
CONTINUE
DO 28 I=1,M
A(I,J)=Y(I)
DO 29 J=1,M
IROWJ=IROW(J)
JCOLJ=JCOL(J)
Y(IROWJ)=A(I,JCOLJ)
DO 30 J=1,M
A(I,J)=Y(J)
CONTINUE
RETURN
END
C SUBROUTINE MATRIX MULTIPLICATION
C
SUBROUTINE MATMUL(A,B,C,I1,M,N)
IMPLICIT REAL*8 (A-H,O-Z)
DIMENSION A(L,M),B(M,N),C(L,N)
DO 15 I=1,L
DO 15 K=1,N
SUM=0.0
DO 16 J=1,M
SUM=SUM+A(I,J)*B(J,K)
CONTINUE
C(I,K)=SUM
CONTINUE
RETURN
END
16
15
```

## VITA AUCTORES

Name: Siva Prasad Darbhamulla  
Born: February 20, 1955  
Place of birth: Titilagarh, India.

Born to Sastry and Jayalaxmi, the author grew up in India with basic education from the city of Visakhapatnam. He received his Baccalaureate degree with honors in Civil Engineering from Andhra University College of Engineering in May 1977. He was the winner of university gold medals and cash prizes for excellence in academic performance. He also served on academic committees and student body in Andhra University. The author continued his education, receiving a Master's degree from the Indian Institute of Technology, Kanpur, India in August 1979. Selected through a national level competitive examination, the author served as an Assistant Engineer (Indian Railway Service of Engineers) for three years in India. Intrigued and persuaded by the complex engineering phenomena, he opted to further his education and commenced a doctoral degree program at Old Dominion University, Norfolk, Virginia, USA in August 1983. The author has two journal papers and a number of conference papers to his credit. The present dissertation research is titled "Nonproportionally Loaded Steel Beam-Columns and Flexibly-Connected Nonsway Frames." He is married to a lovely lady Jan. The author is a member of Chi Epsilon, Phi Kappa Phi, American Society of Civil Engineers (ASCE), and Structural Stability Research Council (SSRC). He is also member of Task Group 3 of SSRC.

### PUBLICATIONS AND PRESENTATIONS:

1. Darbhamulla, S.P., "Optimal Design of Tee-Beam -- A Limit State Approach," *A thesis submitted to the faculty of the Indian Institute Technology, Kanpur, in partial fulfillment of the requirements for the degree of Master of Technology*, Kanpur, India, August, 1979.
2. Darbhamulla, S.P., Razzaq, Z., and Storaasli O.O., "Concurrent Processing for Nonlinear Analysis of Hollow Rectangular Structural Sections," presented in Orlando, Florida, *Proceedings, 26th Structures, Structural Dynamics and Materials Conference, AIAA/ASME/ASCE/AHS*, April, 1985.
3. Darbhamulla, S.P., Razzaq, Z., and Storaasli O.O., "Concurrent Processing in Nonlinear Structural Stability," presented in San Antonio, Texas, *Proceedings, 27th Structures, Structural Dynamics and Materials Conference, AIAA/ASME/ASCE/AHS*, May, 1986.
4. Razzaq, Z., and Darbhamulla, S.P., "Restraint Modelling Effect on Beam-Column Strength," presented in Washington, D.C., *Proceedings, Structural Stability Research Council, Lehigh University, Bethlehem, Pennsylvania*, 1986.
5. Razzaq, Z., and Darbhamulla, S.P., "Nonproportionally Loaded Elasto-Plastic Steel Beam-Columns Restrained Partially," presented in Budva, Yugoslavia, *International Conference on Steel Structures*, September, 1986.

6. Darbhamulla, S.P., Razzaq, Z., and Storaasli O.O., "Concurrent Processing for Nonlinear Analysis of Hollow Rectangular Structural Sections," *Engineering with Computers: An International Journal for Computer-Aided Mechanical and Structural Engineering*, Springer-Verlag New York Inc., 2, 1987.
7. Razzaq, Z., and Darbhamulla, S.P., "Behavior and Strength of Nonproportionally Loaded Imperfect Beam-Columns Restrained Partially," presented in Houston, Texas, *Proceedings, Structural Stability Research Council, Lehigh University, Bethlehem, Pennsylvania*, 1987.
8. Razzaq, Z., Prasad, V., and Darbhamulla, S.P., "Two-Dimensional Finite Element Analysis of Rectangular Panel with Hole using NICE/SPAR," *STAR Journal*, NASA NAG1-438 (28p), Abstract #N87-27217, Vol. 25, No. 21, November, 1987.
9. Razzaq, Z., and Darbhamulla, S.P., "Imperfect Rectangular Beam-Columns with Nonproportional Biaxial Loads," presented in Minneapolis, Minnesota, *Proceedings, Structural Stability Research Council, Lehigh University, Bethlehem, Pennsylvania*, 1988.
10. Darbhamulla, S.P., Razzaq, Z., and Storaasli O.O., "Concurrent Processing in Nonlinear Column Stability," *Engineering with Computers: An International Journal for Computer-Aided Mechanical and Structural Engineering*, Springer-Verlag New York Inc., 4, 1988.
11. Darbhamulla, S.P., and Razzaq, Z., "Portal Frame Stability with Nonproportional Loads," presented in San Francisco, California, at the *7th Structures Congress, ASCE*, May, 1989.